Electrochemical Routes for the Valorization of Biomass-Derived Feedstocks: From Chemistry to Application

Francisco W. S. Lucas^{1,2}, R. Gary Grim³, Sean A. Tacey³, Courtney Downes³,

Joseph Hasse^{1,2}, Alex M. Roman^{1,2}, Carrie A. Farberow³, Joshua A.

Schaidle^{3*}, Adam Holewinski^{1,2*}

¹Department of Chemical and Biological Engineering, University of Colorado, Boulder, CO 80303, United States; ²Renewable and Sustainable Energy Institute, University of Colorado, Boulder, CO 80303, United States; ³Catalytic Carbon Transformation and Scale-up Center, National Renewable Energy Laboratory, Golden, CO 80401, United States.

Corresponding Authors

Adam Holewinski – Renewable and Sustainable Energy Institute & Department of Chemical and Biological Engineering, University of Colorado, Boulder, CO 80303, United States; orcid.org/0000-0001-8307-5881; Phone: +1 303 492-3153; e-mail: adam.holewinski@colorado.edu

Joshua A. Schaidle – Catalytic Carbon Transformation and Scale-up Center, National Renewable Energy Laboratory, Golden, CO 80401, United States; orcid.org/0000-0003-2189-5678; Phone: +1 303 384-7823; e-mail: joshua.schaidle@nrel.gov

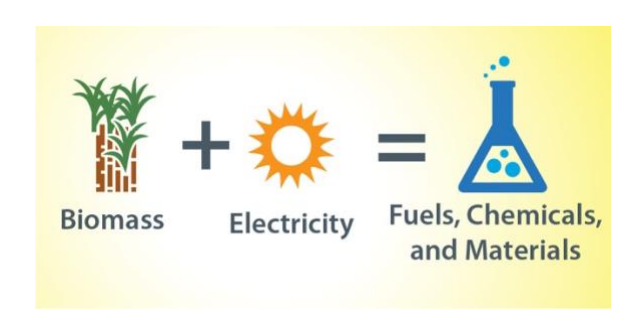
1

Authors' ORCID: F.W.S.L. (0000-0002-4637-8469), R.G.G. (0000-0002-1154-7795), J.C.H. (0000-0002-0580-1355), C.D. (0000-0001-8631-1579), S.A.T. (0000-0001-7833-6901), C.A.F. (0000-0002-3753-962X), J.A.S. (0000-0003-2189-5678), and A.H. (0000-0001-8307-5881)

ABSTRACT

The drive to reduce consumption of fossil resources, coupled with expanding capacity for renewable electricity, invites the exploration of new routes to utilize this energy for the sustainable production of fuels, chemicals, and materials. Biomass represents a possible source of platform precursors for such commodities due to its inherent ability to fix CO₂ in the form of multi-carbon organic molecules. Electrochemical methods for the valorization of biomass are thus intriguing, but there is a need to objectively evaluate this field and define the opportunity space by identifying pathways suited to electrochemistry. In this contribution we offer a comprehensive, critical review of recent advances in low-temperature (liquid phase), electrochemical reduction and oxidation of biomass-derived intermediates (polyols, furans, carboxylic acids, amino acids, and lignin), with emphasis on identifying the state of the art for each documented reaction. Progress in modeling efforts is also reviewed. We further suggest a number of possible reactions that have not yet been explored but which are expected to proceed based on established routes to transform specific functional groups. We conclude with a critical discussion of technological challenges for scaleup, fundamental research needs, process intensification opportunities (e.g., by pairing compatible oxidations and reductions), and new benchmarking standards that will be necessary to accelerate progress toward application in this still-nascent field.

TOC GRAPHIC



- 1. Overview
- 2. Biomass deconstruction and the generation of primary building blocks
 - 2.1. Composition and availability of raw feedstocks
 - 2.2. Deconstruction and conventional biorefining
- 3. Demonstrated electrochemical routes for conversion of intermediates to platform chemicals and products
 - 3.1. Polyols
 - 3.1.1. Glycerol
 - 3.1.2. C5 and C6 polyols
 - 3.2. Furans
 - 3.2.1. 5-HMF
 - 3.2.2. Furfural
 - 3.3. Carboxylic acids (CAs)
 - 3.3.1 Saturated CAs
 - 3.3.2 Unsaturated CAs and fatty acids
 - 3.4. Amino Acids
 - 3.4.1 Carboxyl and amine group chemistry
 - 3.4.2 R-group transformations
 - 3.5. Lignin
 - 3.5.1 Electrochemical depolymerization of lignin
 - 3.5.2 Electro-hydrogenation and deoxygenation of lignin-derived aromatics
- 4. Computational methodologies to model electrocatalytic environments
 - 4.1. Computational frameworks for the electrochemical environment
 - 4.2. Modeling large reaction networks
 - 4.3. Multiscale modeling of electrochemical systems
- 5. Critical discussions
 - 5.1. Opportunities precedented by electrochemistry of analogues
 - 5.1.1 Reduction and oxidation of esters derived from biomolecules
 - 5.1.2 CO₂ coupling to organic functional groups

- 5.2. Benchmarking and protocols for comparing data
 - 5.2.1. Establishing mass and energy balances
 - 5.2.2. Cell validation and consistency of reaction conditions
 - 5.2.3. Catalyst reporting conventions
- 5.3. Fundamental research needs
- 5.4. Economic, logistic, and technical considerations
- 5.4.1 Production scale and energy needs for biofuels and bioproducts
 - 5.4.2. Process intensification and half-reaction pairing
 - 5.4.3. Top technical challenges
- 6. Prospects

References

1. Overview

Environmental, economic, and societal issues related to fossil resource usage are driving the scientific community toward a search for sustainable and renewable sources of energy and chemicals. Sources of renewable electricity such as solar, wind, hydroelectric, tidal, and geothermal energy have attracted widespread attention, with many of these production methods becoming economically competitive with conventional power generation. While the intermittency of these resources has prompted the need for primary, reversible storage on the grid itself,² secondary storage in the form of fuels, chemicals, and materials may also be a means to displace carbon-intensive production processes and maximize the utilization of renewable power. While much remains to be determined regarding supply and integration, it is in this context that electrochemical synthesis routes should be evaluated as possible components of a renewable energy and commodity production infrastructure. This article aims to critically review the emerging field of electrochemical synthesis involving renewable feedstocks beyond the commonly discussed targets of water electrolysis and CO₂ reduction. In particular, the focus will be on the intersection of electrosynthesis with the vast inventory of renewable carbon found in the form of biomass. Figure 1 illustrates the relationship between these themes.

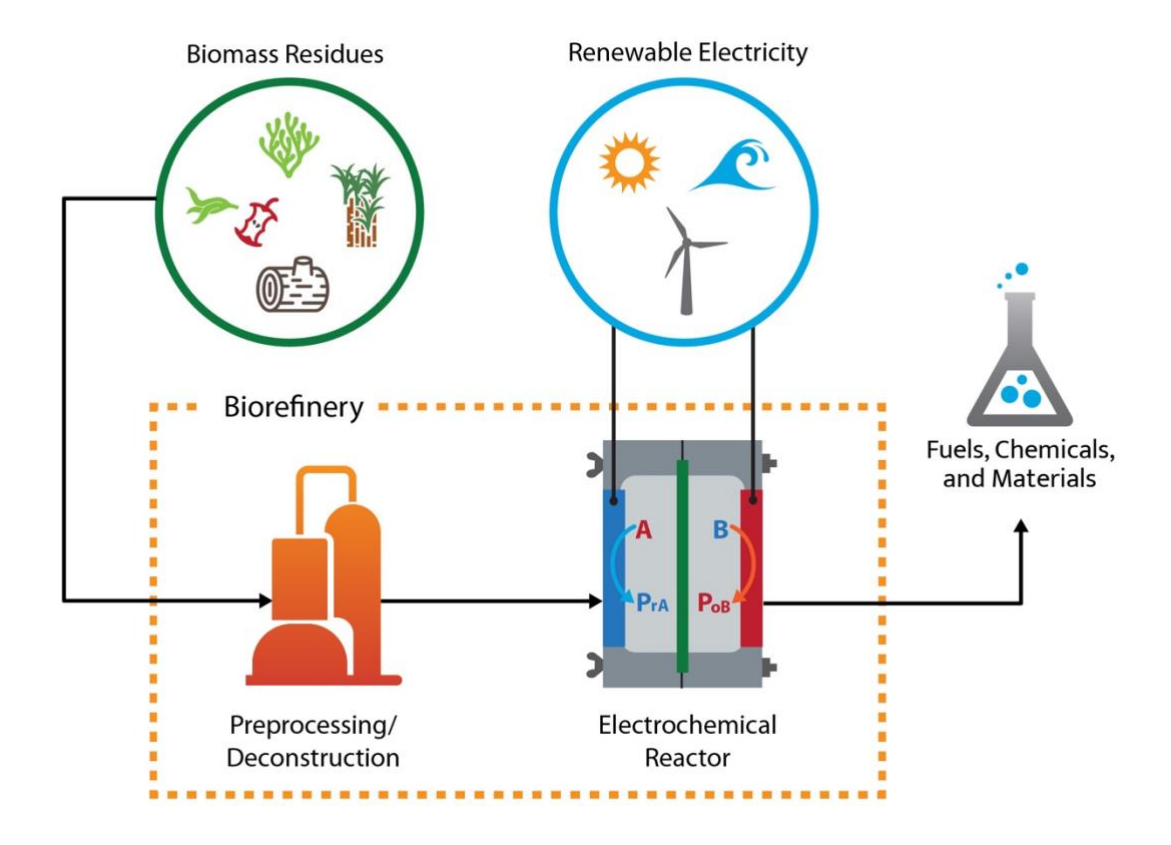


Figure 1. Biorefining with renewable electricity. While electrochemical valorization will not be the exclusive method of feedstock treatment, a large number of intermediates and products can be accessed using electricity. In the electrochemical reactor "A" and "B" represent biomass-derived compounds that are upgraded by forming either reduction products (blue arrow, P_{rA}) or oxidation products (red arrow, P_{rB}).

Biomass has the potential to be a sustainable platform to produce a significant fraction of liquid and gaseous fuels and other carbon-based chemicals and intermediates.^{3–5} Analysis by the US Department of Energy (DOE) has shown that the country could sustainably produce on the order of 1 billion tons of dry biomass annually (1 Gt/y), translating to roughly 25 % of domestic transportation fuel use with residual material for 20 Mt/y renewable chemicals and materials.⁶ Combined with light-vehicle electrification, biofuels could thus play a major role in decarbonization

of the transportation sector.⁵ Of note, the methods of biomass production rely heavily on sustainable, "2nd generation" energy crops⁷ that remove the competition for arable land with food sources.⁸ Beyond just dedicated crops, it is estimated that the global generation of biomass waste, including residues from industries of biomass-based materials production (e.g., logging, pulp and paper industry), as well as production, processing, retail, and consumption of human food and animal feed, is 100 – 140 gigatons/year (Gt/v).^{3,9} Assuming an inherent carbon content of approximately 50 wt. %, 140 Gt/y of biomass (i.e., 70 Gt/y carbon) has the potential to satisfy the entire global demand for gasoline, diesel, and jet fuel by factors of 45, 63, and 185 times over, respectively. 10,11 Demands for ethylene and propylene—the top two carbonaceous industrial chemicals by volume at ~150 Mt/y and ~120 Mt/y respectively—could be met by almost 300 times over. 12 It is therefore sensible, if not imperative, to develop environmentally friendly and economically viable processes for biomass valorization, thus enabling a transition to a circular carbon economy. Electrochemistry poses a number of possible advantages for chemical conversion, and biomass valorization in particular. These include (i) amenability to operate directly on aqueous feedstocks, (ii) generation of oxidative or reducing equivalents without external (wasteful, possibly toxic) reagents, and (iii) operability near ambient conditions, which also facilitates (iv) smaller (possibly highly distributed) scale, intermittent processing with diminished reliance on heat recovery. In general, the macroscopic conditions of electrochemistry are mild (low voltages, room temperature and pressure) while, only at the electrode/solution interface, the energetic conditions are very intense (e.g., the electric field at this interface is typically $10^6 - 10^7$ V/cm), enabling access to difficult chemical transformations

without imposing harsh protocols. ^{13–15} It is thus also possible to generate a wide variety of reactive intermediates *in situ* (free radicals, ionic radicals, carbocations, carbanions) yielding different products or selectivity distributions than may be achieved within typically-accessible temperatures and pressures. ^{13–16} Due to these advantages over some conventional synthetic methods, there are several commercial organic synthesis processes already being performed with electrochemistry. The most successful is the manufacture of adiponitrile from acrylonitrile—which has been employed by Solutia in Decatur (Alabama, US), Asahi Chemical (Nobeoka, Japan), and by BASF (Seal Sands, UK)—but other examples include the production of acetoin from butanone (BASF), L-cysteine from L-cystine (Wacker Chemie AG), 2,5-Dimethoxy-2,5-dihydrofuran from furan (BASF), perfluorinated hydrocarbons from alkyl substrates (3M, Bayer, Clariant), and succinic acid from maleic acid (CERCI, India), amongst others. ¹⁷

Despite the aforementioned advantages, electrochemical biomass upgrading is at an early-stage of development, facing both technical and market challenges. Throughout this review, we will comprehensively address the technical challenges, but we highlight one of the major market challenges here. Specifically, although the levelized cost of electricity for renewable energy sources has fallen dramatically over the past decade, ¹⁸ the cost per unit energy of renewables in most cases still far exceeds that of natural gas (~\$3/MMBTU in the US) as shown in Figure 2. At current average global rates for solar and onshore wind of \$0.05 - \$0.06/kWh, ^{18,19} the price per unit energy of electricity is approximately a factor of 6x greater than that of natural gas. Further, even at a rate of \$0.02/kWh, representative of a curtailed or low-cost renewable case, ²⁰ the cost of energy is still higher by a factor of 2x relative to

conventional natural gas in the US. Thus, solely switching energy inputs from heat and pressure to renewable electricity is unlikely to shift the economics of chemicals production in favor of electrochemical conversion, albeit this analysis does not take into account carbon credits or other low-carbon policies. Rather, accompanying transformational research is also needed to develop these nascent technologies before challenging incumbent practices.

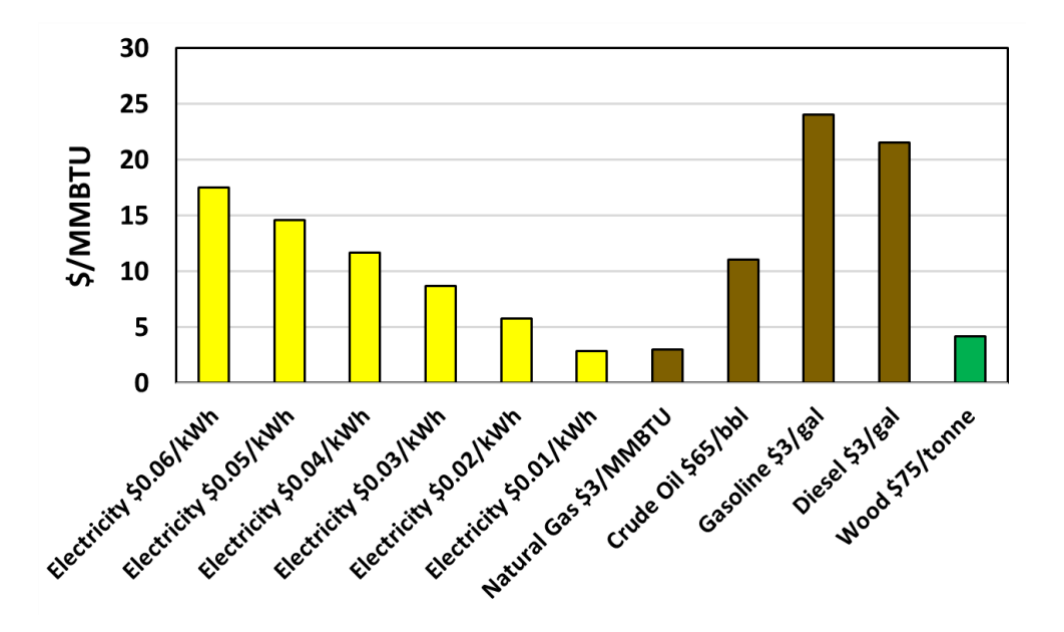


Figure 2. Normalized cost of energy across common renewable and fossil sources.

This review seeks to define the opportunity space for electrochemical valorization of biomass-derived intermediates by discussing opportunities and challenges across various electrochemistry-based approaches for conversion of major biomass-derived constituents (i.e., polyols, furans, carboxylic acids, amino acids, and lignin-derived aromatics) into value-added chemicals and fuels. The current state of existing chemistries is reviewed, followed later by a forward-looking assessment of underexplored and completely unexplored electrochemical routes

that should be possible based on precedented analogs. We couple this with a review on predictive modeling approaches, owing to the fact that solvation, applied potential and fields, and the size of biomass-derived molecules can significantly increase computational complexity and cost. With scalable applications in mind, we close with critical discussions of benchmarking standards, fundamental research needs, and economic, logistical, and technical challenges for the eventual implementation of electrochemical processes powered by renewables.

Our overarching goal is to comprehensively organize the field of electrosynthesis for bio-based fuels and chemicals, and to stimulate the development and research of new processes. The format will thus deviate slightly from a standard review; we attempt to provide comprehensive citations, but only discuss in detail studies that exemplify particular chemistries and represent the stateof-the-art for a given reaction, based on record faradaic efficiencies and yields. While certain sub-fields such as electrochemical hydrogenation (ECH) for fuels have recently begun to discuss benchmarking standards, 21 many of the works cited here have not involved well-defined conditions with both potential and current density known throughout the course of reaction, systematic characterization of materials and reaction kinetics as a function of the conditions, or closure of both mole and electron balances. Where possible, comparison tables present conversions of reported data to place results in terms of current densities on the same potential scale (reversible hydrogen potential scale) and also note turnover frequencies (TOF) for catalytic processes where available. The challenges in drawing comparison on equal bases in some cases underscores the need for improved benchmarking and motivates the critical discussion on best practices, which need to become

standardized in a manner similar to what has been established for simpler systems such as water electrolyzers or fuel cells.^{22,23}

Regarding scope, we note that broad statistics regarding biomass resource availability and market sizes for key products will be referred to when relevant, but no in-depth technoeconomic analysis will be given—the technologies in discussion are too nascent to speculate realistic costs. Themes such as the carbon dioxide reduction reaction (CO₂RR) have already been extensively reviewed 12,24-27 and given technoeconomic analyses, 28-32 and are thus also not reviewed in this study. CO₂ chemistry will be addressed in cases where there is an organic co-reactant, e.g., coupling chemistry, or in the context of pairing for electrolyzers running opposite organic molecule oxidation reactions (OOR).33 Other topics that will not be reviewed include the end-uses of biomass-derived fuels (e.g., direct alcohol fuel cells)^{34–36} and biologically-assisted conversion methods (e.g., electro-fermentation or other uses of electrolyses to promote growth of synthetically-capable micro-organisms).³⁷ It is also pertinent to mention here that the electrochemical valorization of a handful of biomass-related compounds—in particular glycerol oxidation, hydrogenation reactions, 21 and a number of pathways for furfural and 5-(hydroxymethyl)furfural have been discussed in more focused reviews, 35,38-40 though not in the context of full utilization of biomass. Due to the focus on organizing the field and aggregating the current-state-of-the-art, these chemistries are still discussed here, but readers may find additional detail on cited works in the respective reviews.

2. Biomass deconstruction and the generation of primary building blocks

2.1. Composition and availability of raw feedstocks

The chemical composition of biomass is diverse and can vary dramatically depending on the source. Even amongst vegetal (non-animal) sources such as agricultural residues, produce food waste, and dedicated energy crops, the composition is variable. On a dry basis, vegetal biomass is on average composed of 47 – 51 wt. % carbon, 5.8 – 6.0 wt. % hydrogen, and 41 – 43 wt. % oxygen, as well as other components like sulfur (< 0.15 wt. %) and ash (mainly inorganics such as Ca, Mg, Si, K, Na, and trace metals, totaling < 10 wt. %).^{41,42} The high oxygen to carbon ratio (O/C ratio), besides the high moisture content, gives biomass a lower calorific value in comparison with petroleum-derived compounds (about 10 – 40% lower).⁴³ The composition can be more specifically classified into polysaccharides, lignin, lipids, and proteins (Figure 3).⁹ Other fine chemicals (some with pharmaceutical uses) can also be present in a lower quantity such as polyphenols, flavonoids, carotenoids, terpenoids, cinnamic acid derivatives, and secoiridoids, among others.⁹

Lignocellulosic biomass—represented by hardwoods, softwoods, short rotation crops (SRC), short rotation forestry (SRF), and agricultural biomass— is the most abundant and cheapest source of biomass. It is composed of cellulose (25 – 55 % wt.), hemicellulose (10 – 50 % wt.), and lignin (6 – 30 % wt.). ^{44,45} Cellulose is a crystalline biopolymer mainly composed of disaccharide cellobioses (made of glucose units), representing about half of the organic carbon in the biosphere. Hemicellulose is an amorphous polymer composed of several heteropolymers (xylan, galactomannan, glucuronoxylan, arabinoxylan, glucomannan, and

xyloglucan), which are the source of arabinose and xylose (pentoses); galactose, glucose and mannose (hexoses); and acetylated sugars (some chemical structures are presented in Scheme 1). Lastly, lignin, the most complex and recalcitrant biopolymer, is composed of three different phenylpropene monomeric units: *p*-coumaryl, coniferyl, and sinapyl alcohols (chemical structures are shown later in Scheme 14).^{4,44}

A variety of lipids—mainly composed of saturated and unsaturated fatty acids and glycerides—can also be extracted from biomass and are most often converted into biodiesel (generally methyl or ethyl esters of fatty acids, *via* esterification or transesterification), with glycerol being a major byproduct. 46–50 For many years, almost all bio-lipids for fuel production (> 90%) were produced from edible plant oils (rapeseed, palm, and soybean). However, competition with food production has stimulated the use of other biomass sources, such as oil-rich energy crops (*Jatropha*, *Pongamia*, jojoba, linseed, and cottonseed), inedible animal fat wastes (tallow, lard, oils from fish viscera), and waste from edible oils from cooking or frying foods. Other promising sources of lipids (as well as sugars) are algae and oleaginous microorganisms (3rd generation biofuels), and their genetically-modified or engineered analogs (4th generation), 46–50 which may be composed of 30 – 70 wt. % lipids (dry basis) with a potential generation of 6,275 – 14,635 gal lipids per acre, (10 – 24x higher than palm, the most efficient oil crop). 47

Lastly, extending further into animal and food production byproducts and waste, biomass can also be a source of proteins,^{51–53} which are composed of essential amino acids (e-AAs) and non-essential amino acids (ne-AAs, cf. structures in Scheme 10). In comparison to lignocellulose and lipids, this fraction of biomass

has not received as much research attention, but amino acids can be a feedstock for a number of high-value polymers and chemicals.⁵³ In most cases, the extractable AAs show insufficient nutritional quality (low e-AA content) or cannot be cost-effectively converted into food/feed supplements (due to biologic contamination, toxicity, or legislative issues⁵⁴). Ideally, with development of efficient and cheap separation methods, the e-AAs would be diverted for food or animal feed, while the ne-AAs (and non-food/feed grade e-AAs) would be converted into bulk chemicals.^{55–58}

In addition to previously mentioned estimates for growth capacity for various dedicated energy crops, many existing waste sources are well documented and are summarized in Table 1.

Table 1. Quantity of biomass-derived residues produced by classes.

Lignocellulose residues			
Rice husk and straw	Global production of ~0.84 Gt/y (80 % not		
	currently utilized) ^{9,59}		
Sugarcane bagasse	Global production of ~0.18 - 0.22 Gt/y (primari		
	burned for low-value energy production)9,52		
Lignin residues			
Extracted lignin	Globally, >50 Mt/y from the paper and pulp		
	industry (~98% burned as a low-value fuel).60		
	US bioethanol industry estimated to generate		
	~60 Mt/y lignin waste by 2022.61		
Lipid residues			
Waste from cooking oils	>10 Mt/y in US ⁶²		
Total animal fat waste	4.35 Gt/y in US ⁴⁸		
Protein residues			

	Global production >1700 billion liters expected in				
Vinasses	2024 ⁶³ (ex.: sugar beet vinasse has 15 – 30 wt.				
	% protein, dry basis, >79 wt. % ne-AA ⁶⁴)				
Dried distiller grains with	US bioethanol industry produces >44 Mt of				
Dried distiller grains with	DDGS ⁶⁵ (contains 20 – 40 wt. % proteins, dry				
solubles (DDGS)	basis, >70 wt. % ne-AAs ⁶⁴)				
	In 2011, China alone produced 0.32 Mt (20 – 30				
Tea leaf waste	wt. % of proteins, dry basis, containing >50 wt.				
	% ne-AA) ⁶⁶				
Davidan da ada ava	Global generation ~5 Mt/y (80 – 90 wt. % crude				
Poultry feathers	proteins, dry basis, > 60 wt. % ne-AAs). ^{64,67}				
Food waste	~1.3 Gt/y ^{53,54,59} (1/3 total global production,				
i oou wasie	includes all edible carbohydrate, lipid, & protein)				

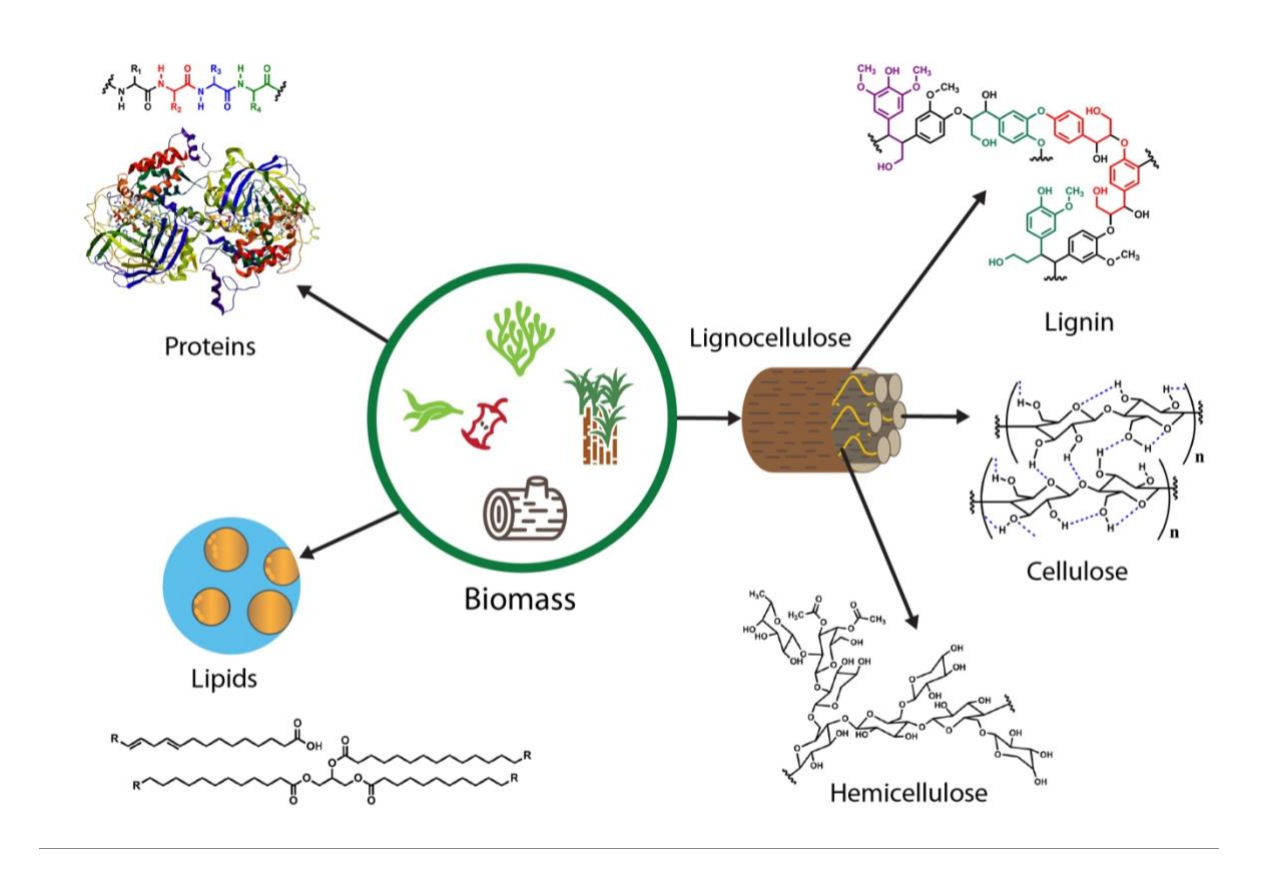


Figure 3: Biomass as a source of lipids, proteins, and lignocellulose (cellulose, hemicellulose, and lignin), possible precursors to fuels, chemicals, and materials.

2.2. Deconstruction and conventional biorefining

The concept of "biorefining" refers to the integrated process of deconstructing, separating, and converting biomass elements into higher-value products (as represented in Figure 4).⁶⁸ This section highlights the main methods for primary component and intermediate building block production. It is not the aim of this work to present a review of all biorefinery processes for biomass deconstruction since several articles and books can be found on this topic.^{9,68–72} However, it is a pertinent context to outline the pathways required to generate key molecule classes and species that may be valorized with electrochemistry. Processes mentioned here are also summarized in Scheme 1.

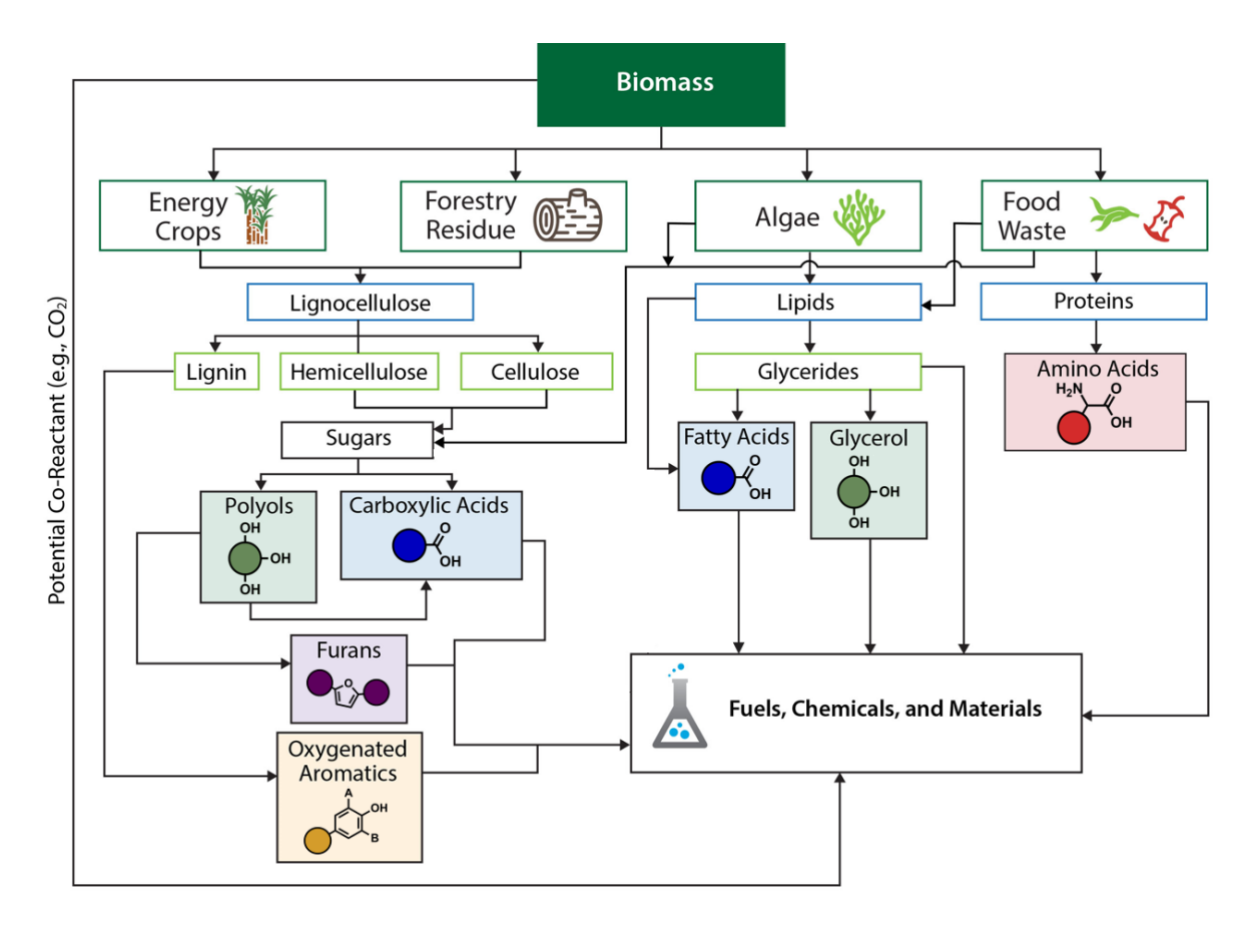


Figure 4: Biorefining overview. Lignocellulose-, lipid- and protein-rich sources of biomass—as exemplified by energy crops and forestry residues, algae, and food waste, respectively—can be deconstructed to produce a variety of chemical intermediates for synthesis of value-added products. Colored circles in each highlighted chemical class represent variable moieties attached to the defining functional group.

Of the methods for the initial decomposition of biomass, pyrolysis is the oldest and simplest technique. Pyrolysis involves the heating of biomass in an inert environment until chemical breakdown occurs. There are three major regimes of pyrolysis based on heating and feed rates, operating temperature, and residence time. "Slow pyrolysis" uses the lowest temperatures (300 – 700 °C), takes the longest time, and generates the most solid biochar. "Fast pyrolysis" operates in a medium

temperature range (450 – 650 °C) and generates a higher fraction of liquid products (bio-oil). Lastly, in "flash pyrolysis", high operating temperatures (800 – 1000 °C) require less residence time and generate more gaseous and aerosol products that can then be condensed or otherwise collected.⁷⁰ Varying the time and the temperature thus results in a variety of different products, which include charcoal, bio-oil, depolymerized products such as levoglucosan, volatile furans, such as 5hydroxymethylfurfural (HMF) and furfural, and syngas.^{73,75} In this context, the bio-oil (pyrolysis oil) fraction is a source of a wide variety of chemicals. This liquid mixture is composed of 15 - 30 wt. % water, oxygenated organic compounds such as phenolics (up to 40 wt. % total, including quaiacols, syringols and other lignin-derived aromatics), carboxylic acids (up to 30 wt. % total), alcohols (up to 5 wt. % total), furans (up to 15 wt. % total), sugars (up to 15 wt. % total), and other short-chain oxygenated molecules. The most abundant single chemicals present in bio-oil are hydroxyacetaldehyde (up to 10 wt. %), acetic acid (~5 wt. %), and formic acid (~3 wt. %); these acids and the phenolic compounds give this mixture a low pH (2.0 -3.0). In general the high oxygen/carbon ratio, 0.6 – 0.7 (wt.), of these mixtures also makes the majority water-soluble.^{72,76}

A variant on pyrolysis, gasification essentially involves treatment at very high temperatures (generally, > 1000 °C) with some amount of oxidizer (air or pure oxygen) added to achieve partial oxidation of the biomass. This partial oxidation is used to obtain the necessary thermal energy to drive organic degradation to completion. Gasification naturally results in primarily gaseous products, specifically syngas containing hydrogen, carbon monoxide, carbon dioxide, light hydrocarbons, and some heavier hydrocarbons that can be condensed out.^{74,77–79}

Hydrothermal liquefaction (HTL) and aqueous phase reforming (APR) are also thermochemical degradation methods for biomass processing. As a brief overview, liquefaction is thermal degradation done in either a sub- or supercritical water environment, at temperature ranges of 200 – 700 °C and high pressures (3 – 30 MPa).⁷⁰ Catalysts are also generally used in HTL, with acids, bases and transition metals all being common and giving differences in product distributions.^{80–82} Similar to HTL, APR occurs in a liquid environment; however, operations occur at lower temperatures and pressures and generally produce gaseous products. Original APR systems focused on producing hydrogen using platinum catalysts, but additional work has been done to produce various other small carbon products such as alkanes (C1-C6), alcohols, and other chemically functionalized products. Product specificity is determined by choice of feedstock, reaction conditions, and catalyst.^{83–85} In either case, these thermal degradation methods often need additional purification steps for the liquid products.

Another common chemical method of biomass deconstruction is through hydrolysis. This approach involves more mild conditions than pyrolysis and generally uses either an acidic or a basic catalyst (also in some cases enzymes). ^{86,87} Specific conditions and product distributions have been well described elsewhere ^{87–90} but are highlighted here. Notably, hydrolysis conditions often can promote further dehydration and isomerization reactions. The end products are inherently aqueous, although sometimes organic co-solvents are used (usually for extraction of glycerides and fatty acids). ⁴⁸ Polyols (sugars), furans (HMF, and furfural), and some carboxylic acids (e.g., formic, acetic, and levulinic acids) can be easily obtained from hemicellulose and cellulose hydrolysis (generally using 0.2 – 40 wt. % NaOH or

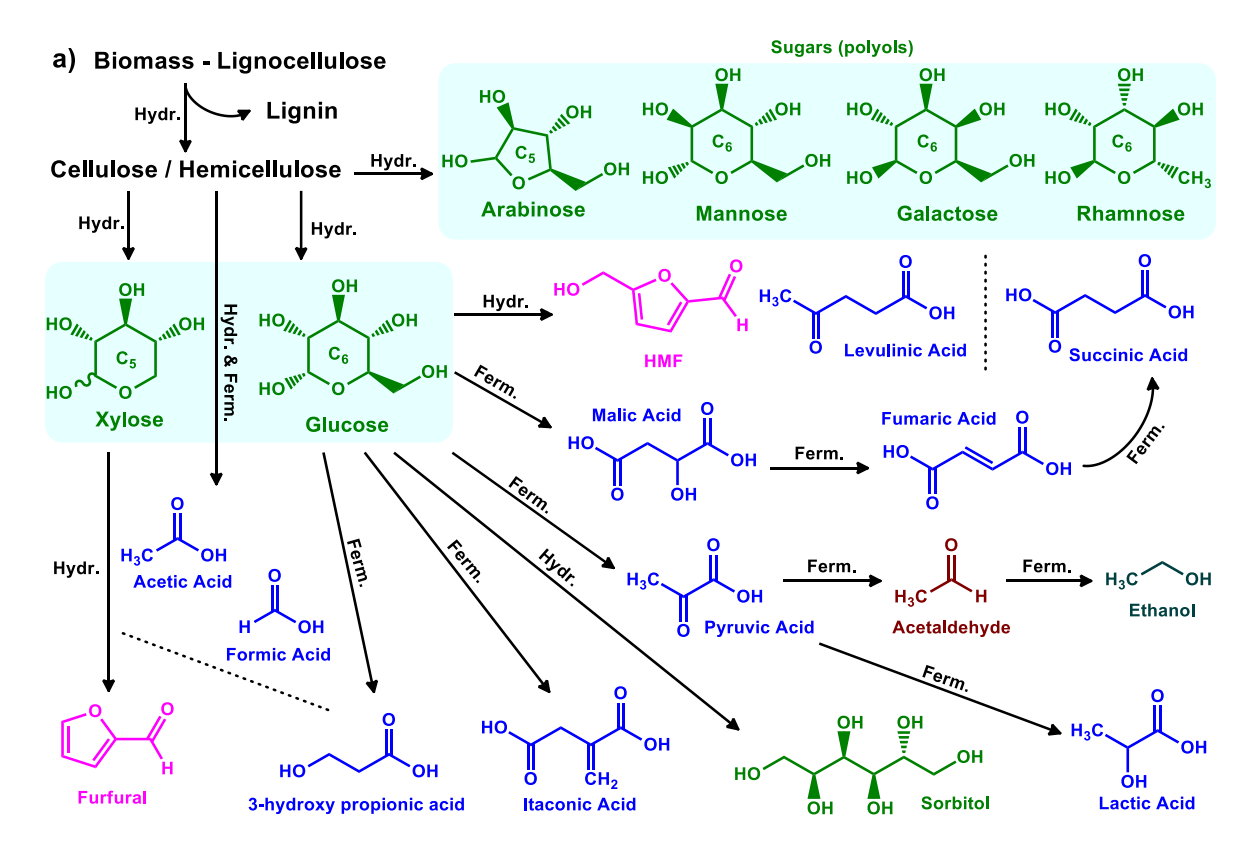
H₂SO₄)⁷², while lignin is more resistant to this method of deconstruction. ^{44,68,72,91} Xylose is primarily used to produce furfural, furfuryl alcohol, and light carboxylic acids (e.g., formic and acetic acid) and alcohols through hydrolysis (often by continued reaction during the primary treatment) and/or by fermentation. ⁹² Some other polyols, such as ring-opened derivatives of arabinose and xylose, are also produced at medium-scale, including xylitol, arabinitol, and xylaric acid. ^{44,45} Lastly, amino acids can also be extracted from protein-rich biomass hydrolysis; alkali-catalyzed or subcritical conditions are generally better for breakdown of cell wall structure (releasing the proteins) and protein solubility. ^{53,93}

Fermentation and other biological processes are also used to transform lignocellulosic biomass to platform-level chemicals. This method frequently has high selectivity towards the specific product that the organism has been engineered to produce. Operating conditions generally involve a sugar feedstock in an aqueous environment at near-neutral conditions. 9,94–97 However, these biological processes have much longer completion times than their thermal degradation or chemical transformation counterparts. Still, some of the most well-developed technologies for lignocellulosic biomass valorization are the production of bio-ethanol and the fermentation of glucose to lactic acid. 72,91 Other medium-TRL (technology readiness level) approaches are the microbial production of succinic acid. (it is expected that bio-based succinic acid production will gain a cost advantage over petroleum-based processes in the near future. (as well as itaconic, maleic, fumaric, and other acids. (as well as itaconic, maleic, fumaric, and other acids. (as well as itaconic, maleic, fumaric, and other acids. (as well as itaconic).

Beside the chemical, thermochemical and biochemical processes to deconstruct biomass into smaller bio-structures and molecules, some components

can be separated from biomass by physical methods, solvent extraction, or steam distillation. This is the case for lipids including fatty acids, glycerides, and essential oils, amongst other components that are generally insoluble in water.⁴⁸

Scheme 1 summarizes the common routes for chemicals production from biomass deconstruction. Of particular interest, the US DOE has identified 12 sugarderived building blocks (obtainable from cellulose and hemicellulose) that can be used to produce commodities or be converted into novel chemical classes. These platform compounds include aspartic acid, glucaric acid, glutamic acid, itaconic acid, levulinic acid, 3-hydroxypropionic acid, 1,4-diacids (fumaric, malic, and succinic), 2,5-furan dicarboxylic acid (associated with furfural and 5-hydroxymethylfurfural), 3-hydroxybutyrolactone, glycerol, sorbitol, and arabinitol/xylitol.⁹



Scheme 1. a) Deconstruction of hemicellulose and cellulose to pentoses (C_5) and hexoses (C_6). Major paths to building block production from glucose and xylose are shown, but other sugars can also be used for the generation of many of these compounds. **b)** Deconstruction of biomass to glycerides, fatty acids, amino acids, bio-gas, biochar, and bio-oil. The processes of deconstruction are exemplified by hydrolysis (Hydr.), fermentation (Ferm.), pyrolysis/gasification (Pyrol. / Gas.), and physical extraction (Physc. Extrac.).

After deconstruction steps, the focus moves to specific chemical production (valorization) routes, separation, and purification steps. The associated processes are evaluated by their ability to increase rates, decrease energy consumption, and broadly add value to the initial intermediates available. In this context, the integration of electrochemical processes into a biorefinery to further valorize some of these products is a promising approach. Most of the deconstruction processes generate liquid water-soluble mixtures (bio-oils, hydrolysates, fermentation broths)⁷² which are

in principle compatible with electrochemical valorization. Hydrolysates in particular have a high concentration of acids or bases, which may even prevent the need for addition of extra supporting electrolyte. This said, electrochemical processes can also be performed in organic solvents, but the key point is the (ideally) diminished need to pre-separate the reactants. In spite of these perceived benefits, the presence of organic and inorganic components such as biochar, cellular matter (in fermentation), and ash (CaO, MgO, SiO₂, K- and Na- salts, and metals such as Fe, AI, and Zn),^{9,68–72} also must be evaluated as these can be sources of electrode fouling. Physical separations such as filtration may permit a large fraction of these components to be removed, but further evaluation of their influences will be a technical challenge in any scale up and is addressed further in Section 5.4.3.

3. Demonstrated electrochemical routes for conversion of intermediates to platform chemicals and products

Once broken down into constituent small molecules, a variety of chemistries can be attempted to install or remove functional groups as desired (the upgrading process). The general classes of reactions most commonly needed are i) dehydration, ii) hydrodeoxygenation, iii) hydrogenolysis, iv) decarboxylation, v) deoxydehydration, vi) condensation, among others. Thermally-driven mechanisms to these various pathways have been long studied, 68,99 but in some cases may be achievable with electrochemistry. To aid in the discussion, we first identify some relevant nomenclature and general reaction schemes possible for electrochemical charge transfer processes.

Shifting focus to the electrochemical reaction itself, the charge transfer (CT) process can occur between the reactant and the electrode surface directly (direct electrolysis), or by a solution-phase redox mediator (indirect electrolysis), as exemplified in Figure 5. In direct electrolysis, the reactive species can be formed by catalytic interactions of the electrode that form adsorbates (inner sphere electron transfer) or by direct CT to solution-phase forming solvated radicals (outer sphere transfer). This division tends to separate the traditional fields of electro-organic chemistry and electrocatalysis; in the present suite of reactive molecules, principles from both must be considered. Indirect electrolyses also generally involve outer sphere electron transfer to the mediators and allow exploiting highly tailored molecular redox catalysts. These can circumvent problems such as electrode deactivation or poor selectivity, though they can add complexity with separations and stability of the mediator itself. 13-16 In many cases with large, multistep transformations, electrochemical reactions of all types can also involve both chemical and electrochemical steps. Thus, various transformations can be described by kinetic sequences defined by their reaction sequences for example, electrochemical-electrochemical (sequential charge transfer processes, electrochemical-chemical (EC), chemical-electrochemical (CE). and electrochemical-chemical-electrochemical (ECE).

For direct charge transfer processes in aqueous medium –the most common scenario for biomass-based molecule transformations— water molecules can be activated at a solid electrode surface and react with electrochemically-activated organic substrates (usually co-adsorbed onto the electrode from solution). Alternatively, solution-phase radicals may be formed from the organic. In the case

of inner-sphere surface mediation, activated oxygen (adsorbed hydroxide or hydroxyl species, via H₂O or OH⁻ oxidation) or hydrogen (via H₂O or H⁺ reduction) may be added to an adsorbed organic in a surface step, or by concerted or sequential electron transfer directly from solution (Figure 5). Surface interactions may also facilitate coupling or scission of bonds within the organic. In comparison, starting with outer-sphere electron transfer (a chemical step/equilibrium may happen before the CT), the transfer of one electron from/to the electrode (or mediator) to/from the substrate molecule generates a reactive radical anion/cation, which can undergo chemical transformations such as cleavage (generating free-radicals and anions/cations), elimination, and acid/base reaction, as schematized in Figure 5. This figure exemplifies the electrochemical transformation of an organic molecule (R-X) that has a specific function "X" (e.g., alkenyl, hydroxyl, carbonyl, aldehyde, carboxyl, and amino groups). After CT and cleavage steps, the main chain (R) can be in radical or anion/cation forms. The radical can dimerize or be further reduced/oxidized to an anion/cation. Anions can react with electrophiles present in the reaction medium (including protons from protic solvent, acid-base reaction), while cations can undergo a proton elimination to generate olefins or react with nucleophiles. Some of these routes may also occur in conjunction with surface reactions for example, radical species can adsorb to the electrode and participate in dimerization reactions or react with other adsorbed species. In some cases, polymerization may even occur, and this can represent a particular challenge for sustained direct CT processes and heterogeneous catalysis.

Having this background in mind, different opportunities for the electrochemical valorization of biomass are organized by organic classes—polyols,

furans, carboxylic acids, lignin-derived aromatics, and amino acids—in the following sections. The convention will be that all schemes show chemical steps represented by black arrows and electrochemical steps by red and blue arrows for oxidation and reduction paths, respectively.

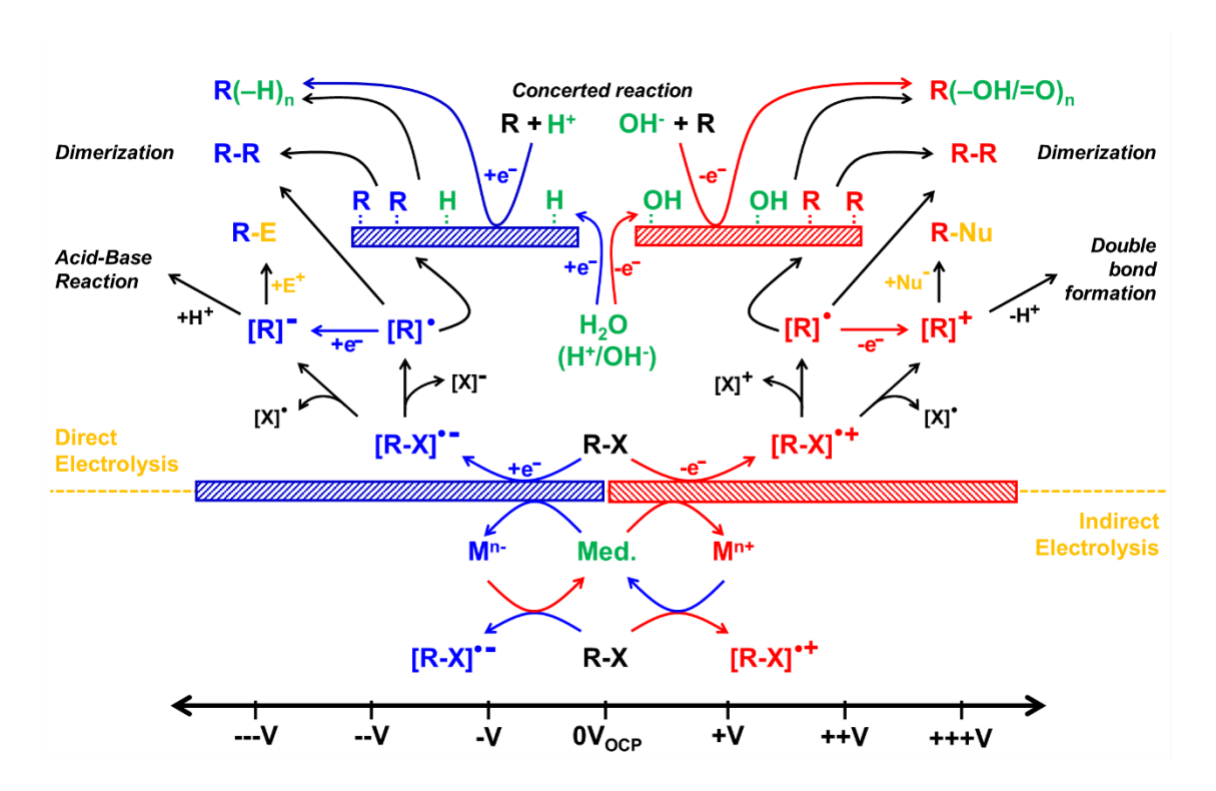


Figure 5. Schematic illustration of some initial steps in generalized electrochemical reactions. Black arrows represent chemical steps, while red and blue arrows represent electrochemical oxidation and reduction steps, respectively; this convention is used in all subsequent figures. "X" represents the more electroactive molecule moiety and its main chain (R), while "E" and "Nu" are electrophile and nucleophile species, and "Med." is an electrochemical mediator with reduced (Medⁿ⁻) and oxidized (Medⁿ⁺) forms, respectively. Adapted idea from Frontana-Uribe and coauthors.¹³

3.1. Polyols

3.1.1. Glycerol

Glycerol is the main byproduct of biodiesel production. ^{100,101} A forecast report based on statistical data from the Organization for Economic Cooperation and Development (OECD) pointed out that global glycerol production was 3.6 billion liters in 2016, with projection to reach 4.0 billion liters/year by 2026. ¹⁰² The glycerol oxidation reaction (GOR) is the most studied amongst all biomass-derived polyols. ^{103,104,113–118,105–112} Tuning of selectivity for this reaction toward specific products has been demonstrated through choice of catalyst, potential, and reaction medium, amongst other reaction parameters. Scheme 2a and Table 2 summarize each major GOR product that has been reported, along with record selectivity/yield. Readers may be reminded that due to the absence of widely observed benchmarking standards, reported performance is not always directly comparable. Nonetheless, the documented state-of-the-art is a noteworthy basis for future work aiming to tune selectivities and rates for various reaction paths.

In the GOR, lactic acid (structure 1m) can be produced with high selectivity and faradaic efficiency (73% and >86%, respectively) on AuPt alloys electrodes, ¹⁰⁵ while dihydroxyacetone (1,3-dihydroxypropan-2-one, DHA, structure 1h) can be obtained with both selectivity and faradaic efficiency close to 100% on Bi-modified Pt electrodes. ¹⁰⁶ Noteworthy activity towards this product has also been obtained on PtSb/C catalysts (yield and glycerol conversion of 61.4% and 90.3%, respectively) ¹¹¹, PtAg skeletons (selectivity of 82.6%) ¹¹⁴, and P-doped Pd/carbonnanotubes (selectivity of 90.8%). ¹¹⁹ Indirect electrolysis of glycerol mediated by TEMPO (2,2,6,6-tetramethylpiperidine-1-oxyl) also showed selectivity towards DHA but with lower yield (30%). ^{120,121} DHA is the most valuable product of the GOR, costing \$150/kg (crude and refined glycerol cost \$0.11 and \$0.66/kg,

respectively).¹²² Currently, commercial production of this compound is principally performed *via* slow fermentation.¹²³ Additional details on various GOR studies and proposed mechanisms on different electrocatalytic surfaces have been published in other reviews.^{38,39,109,112,118,124–127} Key results are compiled in Table 2 except for acetic acid, which have shown very low yields (<< 10 %).^{103,104,113–116,128,129,105–112} Engineering selectivity to acetic acid with improved electrocatalysts and electrolysis conditions could be quite valuable, as this product has a large market size (\$ 8.9 billion in 2019,¹³⁰ > 9 Mt in 2020¹³¹), albeit with competitive incumbent production technologies.

Another approach to access the production of important feedstocks from biomass-derived molecules is to chemically convert primary molecules into secondary platforms that can be further electrochemically valorized. This approach is exemplified in Schemes 2b and c, where glycerol is dehydrated to hydroxyacetone (acetol, 1-hydroxypropan-2-one, Scheme 2, structure 10), which can be further electrochemically converted into 1,2-propanediol (propylene glycol, Scheme 2b, structure 1p), or acetone and 2-propanol (Scheme 2c, structures 1q and r, respectively). 132 The process of glycerol dehydration to acetol can in principle be easily coupled to an electrochemical reactor. The initial chemical process can be performed in both semi-batch reactive-distillation (conversion and selectivity higher than 90% were demonstrated on copper-chromite catalysts at 240°C and 98 kPa¹³³-¹³⁵), and in vapor phase heterogeneous reaction (selectivity of 96% was shown on Cu-SiO₂ catalyst, despite lower conversion ~66%¹³⁶), where the product can be directly condensed into an electrochemical reactor, possibly without purification steps, depending on final product needs. The subproducts of glycerol dehydration

such as formic acid, acetaldehyde, and acrylic acid do not significantly interfere in the electrochemical-conversion of hydroxyacetone, though some will be simultaneously converted (acetaldehyde and acrylic acid would be converted into ethanol and propanoic acid, respectively). It is also important to comment that the conversion of acetol into 1,2-propanediol is mostly performed under thermochemical conditions at temperatures higher than 200 °C and hydrogen pressures up to 2 MPa, which highlights the possible advantage of an electrochemical process. This diol is largely used as a solvent and in the manufacture of food additives, polymers, resins, functional fluids, perfumes, cosmetics; it has an annual consumption >20 Mt. 138

One of the biggest challenges of GOR—and oxidation reactions of other polyols— is the surface poisoning of some electrocatalysts by strongly adsorbed acyl and CO species. 139,140 This kind of poisoning has also been a technological problem for methanol and ethanol oxidation in proton exchange membrane fuel cells (PEMFC) and can be overcome/minimized with the same strategies applied in those fields. One of these strategies is catalyst engineering, such as the use of alloys and/or bifunctional materials composed of active elements mixed with poisoning-tolerant materials (generally, oxophilic elements). These include PtRh, PtRhFe, PtNi, and PtCo alloys where Pt is the main active metal, and Rh, Fe, Ni, or Co inhibit the poisoning process or promote the degradation of poisoning species. 141–143

Scheme 2. a) Electrooxidation of glycerol to produce value-added chemicals.^{103–105} Electrochemical conversion of acetol, a glycerol dehydration product, into **b)** 1,2-propanediol and **c)** acetone and 2-propanol.¹³² Black, red and blue arrows represent chemical, and electrochemical oxidation and reduction steps, respectively.

Table 2. Record efficiencies* for production of major compounds from the electrochemical oxidation of glycerol.

Entry	Product	Y% (X%)&	F.E.	Electrochemical parameters	Ref.
1	Glyceraldehyde (1b)	100% (U.D.)	100%	$+0.05 - 0.1 \text{ mA cm}^{-2}$, $+0.4 \text{ V}^{@-1}$ in $0.5 \text{ M H}_2\text{SO}_4$ on Pt/C-black	106
2	Glyceric acid (1c)	87% (92%)	U.D.	+1.1 V ^{@-1} in 0.5 M H ₂ SO ₄ (TOF: 305 h ⁻¹) at 60 °C on 20 wt. % Pt/C	107
3	Formic acid (1d)	90% (47%)	U.D.	+1.55 V ^{@-1} in 1.0 M KOH at 50 ^o C on Ni	113
4	Glycolic acid (1e)	85% (50%)	U.D.	+1.6 V ^{@-1} in 2.0 M KOH on Au/carbon nanotube	110
5	Oxalic acid (1f)	45% (90%)	35%	+0.73 V ^{@-1} for 24h (~40 mA cm ⁻²) in 4.0 M KOH at 90°C on Au ₃ Ag/C	129
6	Tartronic acid (1g)#	79% (35%)	U.D.	+0.35 V ^{@-1} in 2.0 M KOH at 50 °C on 40 wt. % Au/C	108
7	1,3- dihydroxypropan-2- one (1h)	100% (U.D.)	100%	$0.05-0.1$ mA cm $^{-2}$, +0.5 $-$ 0.6 $V^{@-1}$ in 0.5 M H $_2$ SO $_4$ on Bimodified Pt	106
8	2-oxomalonic acid (1j)	57% (80%)	U.D.	0.65 V ^{@-1} in 2.0 M KOH at 50 °C on 40 wt. % Au/C	108
9	Lactic acid (1m)	73% (73%)	86 – 99%	0.45 V ^{@-1} in 1 M KOH on AuPt alloy (15% Pt _{surf})	105

10	1,2-propanediol (1p) from Acetol (1o)	90% (U.D.)	64%	-1.8 V ^{@-2} (or -1.19 V ^{@-1}) in 0.5 M phosphate buffer (pH 7), production rate of 616 mmol h ⁻¹	132
				¹ m ⁻² on Cu	
				-1.8 V ^{@-2} (or -1.19 V ^{@-1}) in 0.5	
11	Acetone (1q) from	55%	30%	M phosphate buffer (pH 7),	132
	Acetol (1o)\$	(U.D.)		production rate of ~110 mmol	
				h ⁻¹ m ⁻² on Pb	
12	2-propanol (1r) from	87%	26%	-1.8 V ^{@-2} (or -1.19 V ^{@-1}) in 0.5	132
	Acetone (1q)	(81%)		M NaCl/HCl (pH 2) on Fe	132

*Record performance for production of a specific compound was chosen based on highest faradaic efficiency (F.E.) to the primary product, followed by yield. Only products with yields higher than 20% shown. &Yield [Y%] (conversion [X%]). U.D. = Unavailable data. Reference electrodes: @-1 reversible hydrogen electrode (RHE), @-2 Ag/AgCl_(sat. KCl).*A higher yield of 95.3% was demonstrated on Pt/Carbon-nanotube electrodes in 0.5 NaOH solution, but glycerol conversion was not shown. 115 \$A higher yield of 75% was shown on Zn electrode in 0.5 M NaHSO₄, but the faradaic efficiency was just 5%. 132

3.1.2. C5 and C6 polyols

The electrochemical oxidation of C5 and C6 polyols also follows a glycerol-like path^{103,104} producing various chemical derivatives. Scheme 3 (a and b) shows routes for the electrochemical oxidation of xylose^{144,145} and glucose,¹⁴⁶ respectively; these also represent the trends observed for galactose¹⁴⁷ and mannose.¹⁴⁸ Analysis of the surface adsorbed intermediates by *in situ* FTIR spectroscopy^{149–153} and the product distribution as a function of time shows that the aldehyde group, in the case

of aldoses, is the first part of the molecule to be oxidized, producing carboxylic acids (e.g., products 2b and 3b in Scheme 3) with good selectivity. In sequence, the terminal hydroxyl group is oxidized to an aldehyde, and then carboxylic acid. The next oxidation step for producing shorter molecules is C-C bond cleavage. 144–146,154 Molecules such as glycolic acid (compound 1e), glyceric acid (1c), formic acid (1d), oxalic acid (1f) and tartronic acid (1g) are products also observed in the GOR. 144–146,154 Acyl- species and CO are further relevant as strongly adsorbed poisoning species 149–153 that may promote electrode deactivation during electrolysis. Derivatives of the above monosaccharides, as well as di-, oligo-, and polysaccharides, can also be converted into uronic acids (oxidation at the primary hydroxyl groups) *via* indirect electrolysis mediated by TEMPO with > 99 % yields. 121,155

Some of the above-mentioned polyols (those with ketone or aldehyde secondary functions) can also undergo electrocatalytic hydrogenation (ECH) and hydrodeoxygenation (ECHDO); 153,156–158 for example, glucose and fructose ECHDO can yield sorbitol and mannitol, respectively. 156,159 This is of particular interest as sorbitol is one of the DOE's top 12 biomass sugar-derived platform chemicals, with wide uses in production of food, drugs, cosmetics, and several commodities. 153,156–158 In a recent study, Koper and Kwon 156 evaluated the ECHDO of glucose to sorbitol on a wide range of metals, observing the highest selectivity and yield for Pb and Bi electrodes. They also observed the formation of 2-deoxysorbitol (with selectivity > 90%) on a Sn electrode, where a likely mechanism involves the ECHDO of fructose formed from the *in-situ* mutarotation of glucose (since the pH close to the electrode tends to become alkaline during the electrolysis, favoring this isomerization). 156

Another interesting ECHDO work was published by Schröder and coauthors, where xylitol was converted into γ-valerolactone *via in-situ*, sequential, electrochemical-oxidation and ECHDO (tandem paired electrolysis).¹⁶⁰

Table 3 shows the record selectivity/yield for the different products of electrochemical polyol transformations. It should be noted that there are no current studies on other important polyols and derivatives that can be produced from biomass, such as isosorbide, erythritol, mannitol, sorbitol, xylitol, arabinitol, α -ketoglucarates, and 2-ketogluconic acid, among others. Thus, there may be a range of unexploited opportunities for the electrochemical production of valuable building blocks from these polyols.

Scheme 3. Electrooxidation of polyols follows pathways similar to glycerol^{103–105} to produce value-added chemicals. **a)** Electrooxidation of xylose (adapted from Coutanceau and coauthors, ¹⁶³ and Fonseca and coauthors ¹⁴⁵). **b)** Electrochemical oxidation of glucose (adapted from Yu and coauthors). ¹⁴⁶ The shorter chain products shown in (a) are also observed for glucose oxidation. ^{161,162}

Table 3. Record performance* for production of major compounds from the electrochemical valorization of carbohydrates.

Entry	Polyols	Products	Y% (X%) ^{&}	F.E.	Electrochemical parameters	Ref.
1	Xylose	Xylonic acid	>92% (52%)	> 80%	+0.4 V [#] in 0.1 M NaOH on Pd ₃ Au ₇ /C (ECSA: 33 m ² g _{metal} -1)	163
2	Xylose	Xylitol	>90% (>90%)	> 80%	10 mA cm ⁻² , -1.10 V ^{@-3} (-0.44 V ^{@-1}) in 0.1 M Na ₂ SO ₄ on MoFe _{3-x} Pt _x	144
3	Xylose	δ-valerolactone	Tandem paired electrolysis: U.D. (U.D.)	18%.	Undivided cell with Pb (cathode) at -1.80 V ^{@-2} (-1.54 V ^{@-1}) and RuO _x -TiO ₂ DSA [®] (anode), in 1.0 M HCI	160
4	Galactose	Galactonic acid	93% (87%)	U.D.	+1.50 V ^{@-3} (+2.46 V ^{@-1}) in 0.1 M NaOH on	147
5	Glucose	Gluconic acid	>84 % (69%)	> 60%	+0.40 V [#] in 0.1 M NaOH on Pd ₃ Au ₇ /C (ECSA: 33 m ² g _{metal} ⁻¹)	163
6	Glucose	Glucaric acid	>71% (>91%) /	>73%	18 – 90 mA cm ⁻² (TOF : 0.03 – 0.16 s ⁻¹), +1.3 V ^{@-1} in 1 M KOH on NiFe ₂ O ₄	146
7	Mannose	Mannonic acid	50 % (80%)	U.D.	+1.5 V ^{@-3} (+2.46 V ^{@-1}) in 0.1 M NaOH on	148

8	Gluconic acid	Arabinose	Cathodic: 90 – 98%; Anodic: 47 – 94% (U.D.)	Cathodic: 5 – 39%; Anodic: 83 –88%	LPE on graphite, 1.1 mA in 0.2 M Na- acetate/acetic acid buffer + 0.05 M FeCl ₃ (cathodic mediator)	164
9	Glucose	Sorbitol (cathodic) and gluconic acid (anodic)	Cathodic: 100% (22%); Anodic: 100% (22%)	Cathodic: 100%; Anodic: 100%	DPE in an undivided packed-bed flow reactor with Raney Ni (cathode) and graphite (anode), 250 mA in 0.4 M CaBr ₂ (pH 5 – 7) at 60°C	157

^{*}Record performance for production of a specific compound was chosen based on highest faradaic efficiency to the primary product, followed by yield. Only products with yields higher than 20% shown. &Yield [Y%] (conversion [X%]). # Cell voltage with HER on Pt as the coupled cathodic reaction. Reference electrodes: @-1 reversible hydrogen electrode (RHE), @-2 Ag/AgCl_(sat. KCl), @-3 saturated calomel electrode (SCE). U.D. = Unavailable data. LPE = Linear paired electrolysis. DPE = Divergent paired electrolysis. DSA® = Dimensionally stable anode.

3.2. Furans

3.2.1. Hydroxymethyl Furfural (HMF)

Often referred to as the sleeping giants of renewable intermediates, furfural and 5-hydroxymethyl furfural (HMF) have garnered much attention due to their position as a platform to various monomers, flavorants, pharmaceutical feedstocks, and fuels. 44,165,166 In particular, the HMF oxidation product 2,5-furandicarboxylic acid (FDCA) has been proposed as a viable bio-renewable replacement for terephthalic acid in polymers. Polyethylene furoate (PEF) has been shown to have superior barrier properties for common gases and comparable mechanical properties to polyethylene terephthalate (PET),44 currently produced at 50Mt/y scale.167 Oxidation of HMF to FDCA is also one of the most technologically validated amongst the various electrochemical routes discussed in this review. 168 As illustrated in Scheme 4, this reaction can proceed through the oxidation of the alcohol group to make 2,5diformylfuran (DFF) or the oxidation of the aldehyde group to 5-hydroxymethyl-2furan carboxylic acid (HFCA). From either of these products, 5-formyl-2-furan carboxylic acid (FFCA) is formed before the remaining aldehyde is oxidized further to make FDCA¹⁶⁹.

Many electron efficient and selective catalysts have been developed to produce FDCA. Notably, Liu et al.¹⁷⁰ developed a NiFe doped layered doubled hydroxide capable of achieving a 98% yield with 99.4% faradaic efficiency in alkaline conditions with 10 mM HMF. These non-precious metal catalysts were also stable, showing just a 5% loss in conversion while retaining identical Faradaic efficiencies over four cycles with concentrations up to 100 mM HMF. You et al. developed a series of Ni,¹⁷¹ Ni₂S₃,¹⁷² and Ni₂P¹⁷³ catalysts in a series of papers that achieved

95%, 98%, and 100% yields in 1.0 M KOH with 10 mM HMF with >98% faradaic efficiencies in all cases. All of these Ni-based catalysts showed evidence of oxidizing HMF to FDCA through HFCA, showing a greater proclivity for the oxidation of the aldehyde over the alcohol. These catalysts as well as the other catalysts discussed in this section have been summarized in Table 4 below.

Homogeneous redox mediators have also been developed to oxidize HMF; this approach is particularly advantageous for stopping oxidation at the dialdehyde, DFF. Kasparova et al., ¹⁷⁴ have utilized 4-acetylamino-2,2,6,6-tetramethylpiperidine-1-oxyl (4-AcNH-TEMPO), to oxidize HMF to DFF in a two-phase, double mediator system containing aqueous NaHCO₃, KI and CH₂Cl₂. The preferential oxidation of iodine anions on the platinum working electrodes occurs at lower potentials than nonselective HMF oxidation, whereby the I2 formed then reacts with 4-AcNH-TEMPO to form 4-AcNH-TEMPO+, which then oxidizes the HMF. The organic phase is purposed to limit the further oxidation of DFF by limiting the concentration in the aqueous phase. Further pulse-electrolysis was found to limit accumulation and increase current density. It is also noteworthy that all the above-mentioned electrolyses (heterogeneous and homogeneous) have been carried out in strong basic media, indirectly showcasing the challenge oxidizing HMF in acid presents due to the precipitation of FDCA at very low pH (which may foul the electrode). 175 However, this high pH constraint creates carbon balance and selectivity problems since HMF is not chemically stable under aqueous alkaline conditions. It can humins¹⁷⁶ undergo base-catalyzed conversion into and Cannizzaro disproportionation into alcohol and carboxylic acid mixtures;¹⁷⁷ these reactions are also faster and more problematic under higher initial concentrations of HMF.

Therefore, we emphasize here that evaluation of optimal base concentration—as well as the chemical nature of this base and the initial concentration of HMF—may be an important step for improvement of this technology, increasing the total yield without compromising the selectivity and activity.

Reduction of HMF is also of value and is generally accepted to begin with the production of 2,5-dihyroxymethylfuran (DHMF), which can be used as a monomer in the production of various polymers. Roylance et al. ¹⁷⁸ have shown that DHMF can be produced at relatively low overpotentials (-0.36 V vs. RHE) with greater than 98% yield and faradaic efficiency using silver electrodes. This was demonstrated in a batch cell with slightly basic conditions (pH 9.2) and 0.02 M HMF. Further reduction of the ring results in 2,5-dihydroxymethyl-tetrahydrofuran, which is another monomer unit for polymer synthesis. Alternatively, full reduction of the functional groups at the 2- and 5- positions results in 2,5-dimethylfuran. This product, as well as the fully-reduced 2,5-dimethyl-tetrahydrofuran, have been considered as drop-in fuel additives ¹⁶⁹. These pathways are summarized in Scheme 4.

Alternatively, reductive ring opening has been demonstrated, with a path to 2,5-hexanedione (a precursor to para-xylene and methyl cyclopentane) shown by Roylance et al.¹⁷⁹ They achieved 81.6% yield from HMF on Zn electrodes with 72.4% Faradaic efficiency by using an undivided three-electrode cell in acidic conditions. The overall reaction is composed of electrochemical hydrogenolysis and chemical Clemmensen reduction alongside a ring-opening step, and it can be contrasted with thermochemical production by hydration of 2,5-dimethylfuran.¹⁸⁰ Other ring-opening reductive paths of HMF to 1,6-hexanediol (a polycaprolactone precursor¹⁸¹) have

been developed in thermochemical systems but have not yet been realized with electrochemistry.

Finally, paired cell electrolyses involving both oxidation and reduction of HMF have been developed to demonstrate a possible means of process intensification. Chadderdon et al. 182 used an H-cell with 20 mM HMF to simultaneously produce FDCA and 2,5-dihydroxymethylfurfural (DHMF). The reduction to DHMF was accomplished with an Ag cathode held at -1.2 V vs. Ag/AgCl in slightly basic conditions (pH 9.2). The anode was a carbon felt, and due to the inability to control both the cathodic and anodic potentials at the same time, 2,2,6,6-tetramethylpiperidine-1-oxyl (TEMPO) was used as an oxidizing mediator as it is insensitive to the anodic potential. A stoichiometrically equivalent amount of FDCA (10mM) was thus produced by the anode (*via* TEMPO), with DFF as the apparent intermediate. Overall, faradaic efficiencies of 90% and 97% along with yields of 85% and 98% were achieved for DHMF and FDCA respectively.

Scheme 4. Electrochemical oxidation (above) and reduction (below) of HMF to various fuels and chemicals.

3.2.2. Furfural

Similar to HMF, there are both oxidative and reductive routes to valorization of furfural (FF). One of the primary targets for oxidation of furfural is furoic acid, which in addition to its niche applications is proposed as a platform to synthesize FDCA *via* carboxylation.¹⁸³ The path to FDCA is suggested because furfural is presently recovered in higher yields than HMF during biomass deconstruction, and it is already produced with a global capacity of over 300 kt/y.^{165,184} Parpot et. al.¹⁸⁵ showed that an 80% yield of furoic acid could be achieved on Ni electrodes under basic conditions using a separated three-electrode batch cell. Despite being in base medium, where the solution phase Cannizzaro reaction is known to occur, no furfuryl alcohol was detected in product analysis. Oxidation in acidic environments has also recently

been explored on noble metal electrodes; it is found that decarbonylation of furfural and consequent CO poisoning is a limiting process on Pt, while desorption of self-assembled adsorbed furoate limits rates significantly on Au. 186,187 High conversions, however, are only achievable at potentials above ~1.2 V vs. RHE, where selectivity becomes poor. Subsequent carboxylation of furoic acid to FDCA has not been demonstrated electrochemically, but initial technoeconomic analyses have found the carboxylation by other routes to be scalable. 188,189

The next most sought oxidation product of furfural is maleic acid (again most relevant to polymers). Maleic acid can be produced through further oxidation of furoic acid, with 2-furanol and 2,5-hydroxyfuranone reported as intermediates (Scheme 5).^{169,187} Kubota et al.¹⁹⁰ have demonstrated that a 65.1% selectivity to maleic acid can be achieved in acidic conditions at 2 V vs. RHE on a PbO₂ electrode with 10 mM furfural. 2-furanone was noted as a detected intermediate in this system. Additional routes to produce maleic acid have been developed by Thiyagaranjan et al.¹⁹¹ using a combination of photo and electrochemistry. Furfural was initially oxidized using singlet oxygen generated by methylene blue to produce 2,5-hydroxyfuranone. Then, utilizing 4-AcNH-TEMPO, 2,5-hydroxyfuranone was further oxidized to maleic acid in 0.5 M H₂SO₄ with 97% yield. It should be noted that many other oxidative products such as furan and succinic acid exist and have been explored in other systems (e.g. thermochemical oxidation)^{44,165,192} but are not documented as direct electrochemical products.

Reduction of furfural usually first yields furfuryl alcohol, ¹⁹³ which can undergo acid-catalyzed dehydration synthesis to form furan resins, used in composites, cements, adhesives, and coatings. Yields of ~86% furfural alcohol have been

demonstrated by Wang et al. 194 using lanthanum doped titanium oxide electrodes in a typical three-electrode cell. The cell was maintained at 25°C with 0.1 M FF and 0.1 M tetrabutylammonium bromide in water at a constant current density of 50 mA cm⁻¹ 2. Furfuryl alcohol can also be further reduced to 2-methylfuran, which is a potential drop in fuel additive. 38,169 Jung et al. 195 investigated the effects of pH, cosolvent ratio and current densities on the galvanostatic reduction of furfural to furfuryl alcohol and 2-methylfuran on copper electrodes in a typical three electrode cell. They found that furfuryl alcohol was the primary product in mildly acidic electrolytes (0.2 M NH₄Cl) while both products were observed at lower pH's (0.1 – 0.5 M H₂SO₄). They further found that increasing current density increased yield and selectivity to these two species but did not affect the ratio of furfuryl alcohol to 2-methylfuran. Upon varying acetonitrile cosolvent between 20-80 vol.%, no clear correlation between solvent ratio and product distribution was observed. In an additional work by Jung et al., 196 high surface area copper electrodes were investigated in comparison with copper foil electrodes. The engineered high surface area Cu was able to achieve >94% faradaic efficiency at -0.5 V vs. RHE. Notably, this performance also included a 240% increase in production rate towards furfuryl alcohol and 2-methylfuran compared to the Cu foil. At larger potentials (-0.65 V and -0.8 V), the high surface area copper maintained a more than 200% increase in production rate towards 2methylfuran, the dominant product, although the faradaic efficiency suffered (64% at -0.65 V).

Reductive ring-opening of FF can also produce 1,5-pentanediol, a monomer unit. Parpot et al. reported this product, as well as the furfural dimer hydrofuroin, on Pb electrodes when obtaining a 70% selectivity towards furfuryl alcohol at -1.26 V

vs. RHE.¹⁹⁷ In contrast, Parpot reported dimerization as the majority path on copper electrodes. In another work, Zhao et al.¹⁹⁸ also showed 1,5 pentanediol and hydrofuroin products, in this case at -1.2 V vs SCE on Cu electrodes in 0.1 M NaOH, consistent with Parpot's results. Additional experiments by Zhao on Pb electrodes at -1.1 V vs. SCE resulted in hydrofuroin being the major product, as opposed to furfuryl alcohol. Neither pentanediol nor hydrofuroin were quantified in these works, though Zhao et al. did report that Pt catalysts supported on activated carbon fiber in 0.1M H₂SO₄ could give 99% selectivity towards furfuryl alcohol, with 82% conversion.¹⁹⁸ Chadderdon et al.¹⁹³ also studied furfural EC reduction and obtained the dimerized product (hydrofuroin) on copper electrodes in a variety of acidic pH's and with surface modification by self-assembled monolayer (SAM) additives. They found that while 2-methylfuran and furfuryl alcohol yields changed with SAM modification, the dimerization product stayed relatively constant, implying that the first electron transfer is an outer-sphere process.

Similar to HMF, FF electrolysis at high pHs and initial FF concentrations can cause total yield and selectivity losses related to homogenous base-catalyzed humin/polymer formation¹⁷⁶ and Cannizzaro disproportionation¹⁷⁷ side reactions. On the other hand, very acidic media can also catalyze the polymerization of FF and furfuryl alcohol (one of the reduction products).¹⁹⁹ As emphasized before, performance advances for this process will not only be achieved by electrode engineering (improving catalyst poisoning tolerance) but also by the optimization of initial concentrations of base and FF²⁰⁰ or other electrolyte components to inhibit undesired homogeneous side reactions.

Additional details and assessment of the trends in furfural and HMF conversion studies discussed here can be found in focused reviews on electrochemical conversion of furanics. 38,39,169,201 Broader uses and accessible derivatives of these compounds by thermochemical or biological routes can also be found in appropriate sources. 202–206169,201,202

Scheme 5. Electrochemical oxidation and reduction of furfural to various value-added chemicals.

Table 4. Record efficiencies* for production of major compounds from the electrochemical valorization of furans.

Entry	Furan	Products	Y% (X%)&	F.E	Electrochemical parameters	Ref.
1	FF	2-methylfuran	U.D. (U.D.)	80%	-10 mA cm ⁻² in 0.5 M H ₂ SO ₄ on Cu in an H cell held at 8 °C with an acetonitrile trap	207
2	FF	2-methylfuran	U.D. (64%)	65%	-0.65 V ^{@-2} (-0.42 V ^{@-1}) in 0.1 M H ₂ SO ₄ with 20% acetonitrile on high surface area Cu	196
3	FF	Furfuryl alcohol	86% (U.D.)	89%	+3.5 – +4.8V ^{@-3} , -50 mA cm ⁻² in 0.1 M tetrabutylammonium bromide in DMF on La-doped TiO ₂	194
4	FF	Furfuryl alcohol	99% (82%)	78%	-0.5 V ^{@-3} (-0.2 V ^{@-1}) in 0.1 M H ₂ SO ₄ on 3% Pt supported on activated carbon fibers	198
5	HMF	2,5 dihydroxymethyl Furan	99% (0.51%)	98%	-1.3 V ^{@-2} (-0.57 V ^{@-1}) in 0.5 M Borate Buffer (pH 9) on Ag	178

6	FF	Furoic Acid	80% (>90%)	80%	0.8 mA cm ⁻² in 0.5 M NaOH on Ni	185
7	HMF	Furan Dicarboxylic Acid	98% (99%)	99%	+1.23 V ^{@-1} in 1 M KOH on NiFe Layered Double Hydroxide	170
8	НМЕ	Furan Dicarboxylic Acid	100% (100%)	100%	1.42 V ^{@-1} with >200 mA cm ⁻² in 1 M KOH on Ni₂P	173
9	HMF	Furan Dicarboxylic Acid	98% (100%)	100%	1.42 V ^{@-1} with >200 mA cm ⁻² in 1 M KOH on Ni ₂ S ₃	172
10	HMF	Furan Dicarboxylic Acid	95% (>98%)	98%	1.42 V ^{@-1} with >200 mA cm ⁻² in 1 M KOH on Ni	171
11	НМЕ	2,5-diformylfuran	65% (92%)	U.D.	80 mA cm ⁻² in 50 mL CH ₂ Cl ₂ /100 mL 20 mM KI 50 mM NaHCO ₃	174
12	НМЕ	Furan Dicarboxylic Acid / 2,5- dihydroxymethylfurfural	Cathodic:98% (U.D); Anodic: 87% (U.D.);	Cathodic: 97% Anodic: 90%	-1.2 V ^{@-3} (-0.41 V ^{@-1}) / 0.5 M NaBO ₃ (pH 9.2)	182

13	FF	Maleic Acid	97% (>99%)	/ U.D.	0.8 V ^{@-3} (-0.556 V ^{@-1}) / 0.5 M H ₂ SO ₄	191
14	FF	Maleic Acid	65% (>99.9%).	U.D	+2.0 V ^{@-2} (+2.2 V ^{@-1}) in 0.1 M H ₂ SO ₄ on PbO ₂	190
15	НМЕ	2,5-Hexanediol	82% (1.5%)	72%	-1.2 V ^{@-2} (-0.885 V ^{@-1}) with 14.4 mA cm ⁻² in 0.2 M K ₂ SO ₄ /H ₂ SO ₄ (pH 2) on Zn	179

^{*}Record performance for production of a specific compound was chosen based on highest faradaic efficiency (F.E.) to the primary product, followed by selectivity and conversion. Only products with yields higher than 20% shown. *Yield [Y%] (conversion [X%]). Reference electrodes: *@-1* reversible hydrogen electrode (RHE), *@-2* Ag/AgCl(sat. KCI), *@-3* saturated calomel electrode (SCE). U.D. = Unavailable data.

3.3. Carboxylic acids (CAs)

Usable biomass-derived carboxylic acids (CAs) include i) short-chain carboxylic acids (SCCAs, C₁ – C₅) —formic acid, acetic acid, lactic acid (secondary function: alcohol), propanoic acid, 3-hydroxypropanoic acid (3-HPA, secondary function: alcohol), butanoic acid, succinic acid (diacid), malic acid (diacid, secondary function: alcohol), fumaric acid (monounsaturated diacid), pentanoic acid, itaconic acid (monounsaturated diacid), levulinic acid (secondary function: ketone), and others; ii) medium-chain CAs (MCCAs, $C_6 - C_{12}$) —hexanoic acid (caproic acid), muconic acid (diunsaturated diacid), octanoic acid (caprylic acid), and others; and iii) fatty acids (>C₁₂) generally used for bio-diesel production. Most of these SCCAs and MCCAs are produced from the fermentation of sugars, while the fatty acids are present in the lipidic fraction of biomass. The SCCAs are largely soluble in fermentation broths, making the subsequent separation/extraction process difficult. In contrast, MCCAs have low solubility in the media, forming an oily phase that makes the separation easier.²⁰⁸Amongst these compounds, levulinic acid (LA) has been highlighted in particular as a promising feedstock for fuel production, as it can be converted into hydrocarbons as well as valeric esters, which have been proposed as future transportation biofuels.²⁰⁹ LA is produced at large scale from the hydrolysis of lignocellulose in dilute sulfuric acid.²¹⁰

3.3.1. Saturated CAs

Electrochemical oxidation of carboxylic acids is a well-known process and one of the oldest electro-organic reactions studied, first demonstrated in 1849 by Kolbe. 13,14,16,211–214 The oxidation of carboxyl group occurs *via* one or two electrons,

followed by CO₂ evolution, forming a radical or a carbenium ion as intermediates. respectively. In general, the one-electron route is favored on platinum and platinum alloys electrodes, while the two-electron route is more prominent on carbonaceous electrodes, such as graphite. The radical promptly dimerizes on the electrode surface (Kolbe path or Kolbe electrolysis); for example, octane-2,7-dione is formed from Kolbe electrolysis of levulinic acid (LA) (Scheme 6 - Path 1). In turn, the carbenium ion follows stability and reactivity trends common for this kind of intermediate; it can undergo a proton elimination, generating alkenes (for example, but-3-en-2-one from LA oxidation, Scheme 6 - Path 3), or a nucleophilic attack (Hofer-Moest route, Scheme 6 - Path 2). Therefore, the Hofer-Moest route can be used for producing alcohols (using H₂O or OH as nucleophile), ethers (using alcohols or alkoxides as a nucleophile), or esters (using CAs or carboxylates as a nucleophile), which are directly usable as bio-fuels and bio-fuel additives. 209,215 It has been demonstrated that oxidation of LA via two electrons can produce 3-buten-2one (proton elimination with a selectivity of 45%), and 4-hydroxy-2-butanone (selectivity of 20%).²¹⁶ The etherification products, 4-methoxy-2-butanone and 4ethoxy-2-butanone, have been also confirmed from the reaction in methanol and ethanol, respectively.²¹⁶ The formation of an ester *via* Hofer-Moest route has also been observed in the electro-oxidation of valeric acid (VA, the main product of electrochemical hydrodeoxygenation of LA). In this case, the VA (or the valerate ion) also acted as the nucleophile, producing n-butyl valerate, a promising bio-diesel additive, 209,215 with selectivity close to 30% (Scheme 7).217 Kolbe electrolysis can also be used for promoting cross-coupling of radicals derived from the oxidation of different CAs; for example, Palkovits and co-authors produced branched and longchained alkanes (fuel molecules) through Kolbe electrolysis of mixtures composed of succinic acid, methylsuccinic acid (obtained from itaconic acid) and isovaleric acid derivates with faradaic efficiencies close to 50%.²¹⁸

Scheme 6. Electro-oxidation of levulinic acid via Kolbe and non-Kolbe electrolysis.^{216,217,219} The oxidation products can be electrochemically reduced to several value-added chemicals.

In contrast to oxidations, the ECH and ECHDO of the carboxylic moiety have proven much harder to achieve with appreciable yield. However, many saturated CAs have secondary organic functions, such as ketone, aldehyde and alcohol, that can undergo ECH / ECHDO. Several α -oxo/aldo acids (e.g. glyoxylic acid, pyruvic acid, 2-oxopentaoic acid, and α -ketoglutaric acid) can be electrochemically reduced to α -hydroxy acids with good yields. The ECHDO of the LA ketone fragment produces valeric acid and γ -valerolactone, with the selectivity of these products strongly depending on the overpotential and pH of the supporting electrolyte

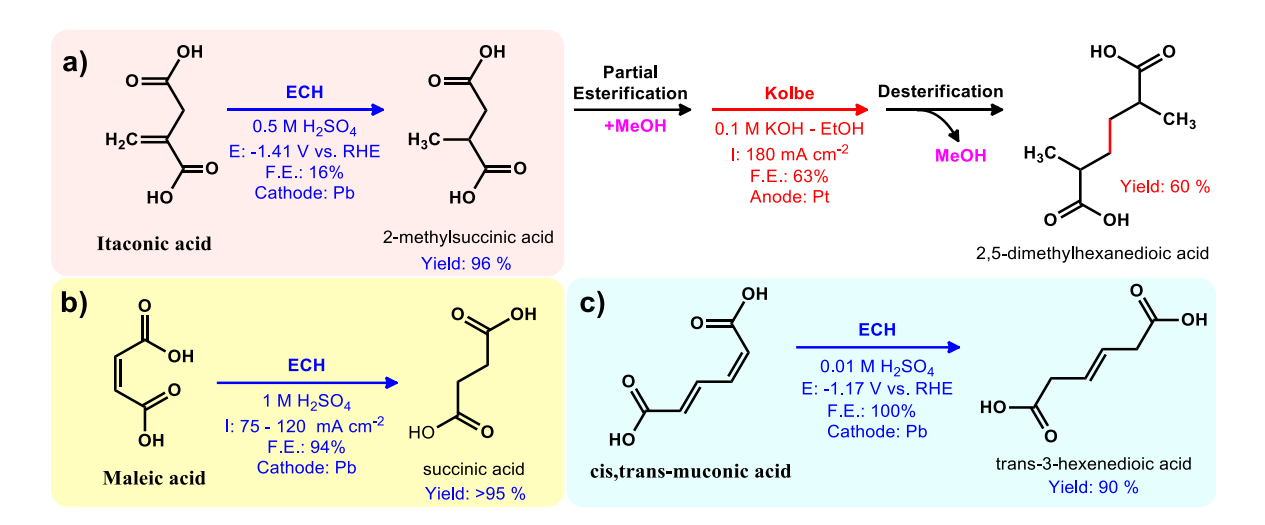
(Scheme 7).^{210,216,217,221,222} The selectivity has been demonstrated at over 90% for valeric acid in very acidic medium at high overpotential, while nearly 100% to γ-valerolactone was found at neutral pH at low overpotential.²¹⁰ Comparing with the thermochemical route, the multiple-step reaction to convert LA into γ-valerolactone is generally carried out at high temperatures and hydrogen pressures, using noble metal based catalysts such as Pt, Ru, and Pd.^{209,223}

Some secondary products from electrochemical transformation of CAs can also undergo ECH / ECHDO. For example, 4-hydroxy-2-butanone (Hofer-Moest product of LA oxidation, Scheme 6 – Path 2) has been reduced over Pb in 0.5 M H₂SO₄ to produce 1-butanol (selectivity over 75%), and over Fe in 0.5 M KH₂PO₄/K₂HPO₄ (pH 7) to form 1,3-butanodiol (yield of 34%).⁷¹ In general, ketones are more easily deoxygenated under ECH conditions than converted to secondary alcohols.^{13,14,16,211,212}

Scheme 7. Electrochemical reduction of levulinic acid can produce γ-valerolactone and valeric acid as the main products.^{210,216,217,221,222} Valeric acid can be electro-oxidized to produce octane, n-butanol, 1-butene and n-butyl valerate.^{216,217,221}

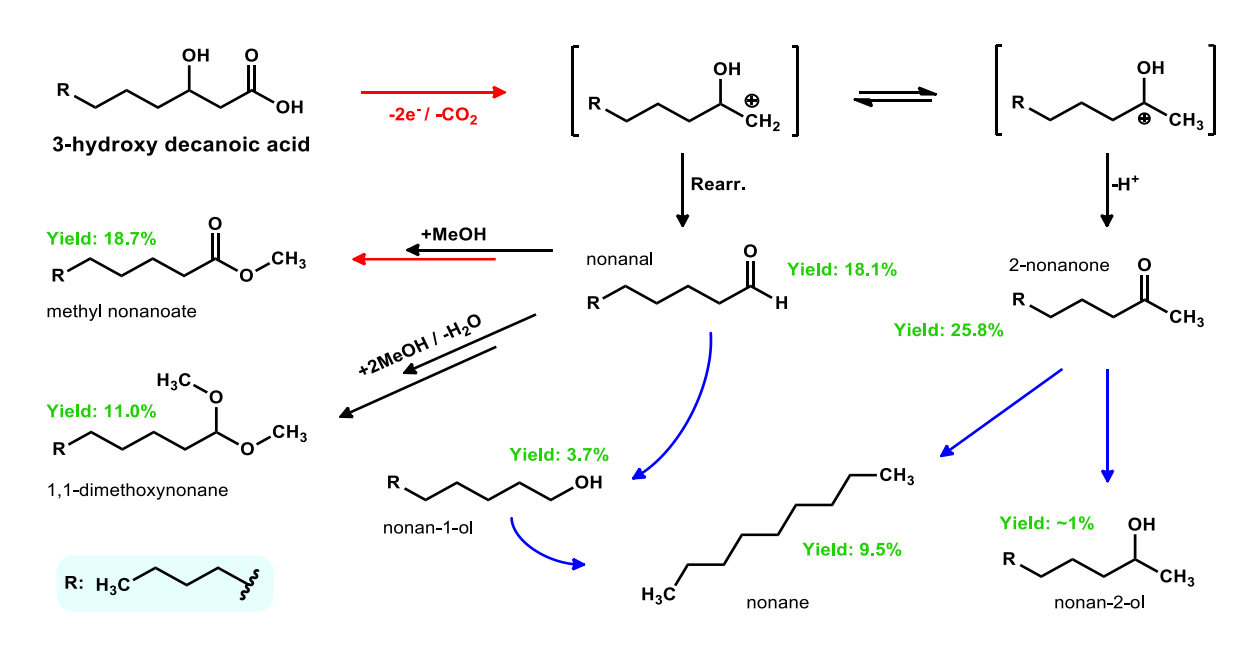
3.3.2. Unsaturated CAs and fatty acids

For unsaturated acids, the ECH of the alkenyl group can be performed with excellent yields. Palkovits and coauthors²²⁴ showed the conversion of itaconic acid (IA) to 2-methylsuccinic acid (MsA) at yield and conversion of 96% on Pb in 0.5 M H₂SO₄ (Scheme 8a). They also demonstrated that it is possible to electrochemically produce MsA (with a yield of 60%) directly from the fermentation broth containing IA, despite the presence of high glucose concentrations and several salts (biomass subproducts).²²⁴ To extend the discussion about these compounds, in another work published by Hancock and Linstead, 225 it was demonstrated that MsA can also be electro-oxidized via Kolbe electrolysis to produce 2,5-dimethylhexenedioic acid (Scheme 8a); good yields were achieved by protecting one of the carboxylic function via esterification. In a patent submitted by Yunfang Gao, the ECH of maleic acid into succinic acid was demonstrated on Pb cathodes at high reaction rates (current density of 75 - 120 mA cm⁻² and faradaic efficiency of 94 - 95%) and low cell voltages, 1.38 - 1.64 V (Scheme 8b).²²⁶ Several other patents also have demonstrated the feasibility of the ECH of maleic acids to produce succinic acid.²²⁷ ²³¹ Other work by Tessonnier and coworkers demonstrated a diastereoselective ECH of cis,trans-muconic acid to trans-3-hexenedioic acid²³² with a yield of 90% and Faradaic efficiency of 100% (Scheme 8c).



Scheme 8. a) ECH of itaconic acid to produce 2-methylsuccinic acid,²²⁴ which can be electro-oxidized via Kolbe electrolysis to produce 2,5-dimethylhexenedioic acid.²²⁵ b) ECH of maleic acid into succinic acid,²²⁶ and **c)** Diastereoselective ECH of cis,trans-muconic acid to trans-3-hexenedioic acid.²³²

Under similar electrochemical conditions to that of the oxidization of saturated CAs, fatty acids can also be oxidized to produce fuel compounds. For example, Palkovits and coauthors showed the electrooxidation of 3-hydroxy decanoic acid (3-HDA), a fatty acid derivable from glucose or xylose waste-streams. ²³³ This reaction was performed in an undivided cell on a carbon anode, which promotes the CA oxidation *via* non-Kolbe paths. A mixture of C₉ molecules was produced, as shown in Scheme 9, which can be used as drop-in oxygenate diesel fuel, since these long-chain low-oxygenate molecules (such as alcohols or ethers) have high cetane number, but reduced sooting propensity (related to lower smoke emission) compared to some petroleum-derived fuels.



Scheme 9. EC-transformation of 3-hydroxy decanoic acid, a compound derived from glucose and xylose waste streams.

Using the example of electrochemical valorization of LA and other CAs shown in this section, it is interesting to point out the vast number of value-added chemicals that can be electrocatalytically produced from biomass-derived CAs. In many cases, high selectivity towards a specific product can be achieved through the correct choice of electrocatalyst, reactional medium, and other electrochemical parameters. Fuel, fuel additives, and lubricants such as long-chain alkanes (ex. octane, Scheme 6 - Path 1 and Scheme 7, and nonane Scheme 9), bio-ethers and bio-alcohol²¹⁵ (Scheme 6 - Path 2, and Scheme 9), and bio-esters²⁰⁹ (e.g. n-butyl valerate, Scheme 7, methyl nonanoate, Scheme 9) may all be generated. The conversion of CAs into other platform chemicals such as diols, ketols, and aldols can also be performed by electrocatalysis. These feedstocks are useful to produce biopolymers, drugs, food, and cosmetics additives, among other applications. With the exception of perhaps

LA, the full range of accessible products from biomass-derived CAs is still largely unestablished.

To summarize reactivity trends, it is noteworthy that CAs are much more chemically stable under strong alkaline and acid conditions than furans, allowing wide flexibility for reaction at different pH conditions. Faradaic efficiencies for CA oxidation are generally higher at high pH because deprotonated species are more easily oxidized than neutral ones, decreasing competition from OER. On the other hand, CA reduction (secondary functional group reduction) is generally more efficient at acidic pH (below pKa) since the deprotonated conjugate bases can be repelled by electrodes under cathodic polarization (negative of pzc). These reductions are often most selective on electrodes that present high overpotentials for HER (e.g. Pb, In, Cd²²²). In this context, CA valorization opportunities can be improved by identifying electrodes and conditions that suppress the OER and HER side reactions over wider pH windows, as well as by minimizing unwanted electrostatic effects (e.g. by improving screening). Aqueous solubility may also be a challenge for some MCCAs and fatty acids due to salting out (pH > pKa) and hydrophobicity (pH < pKa) effects, and thus understanding the roles of organic cosolvents will also be valuable.

Table 5 shows the highest recorded performance metrics for electrochemical valorization of biomass-derived CAs and derivatives discussed in this section.

Table 5. Record efficiencies* for production of some compounds from the electrochemical valorization of biomass-derived carboxylic acids.

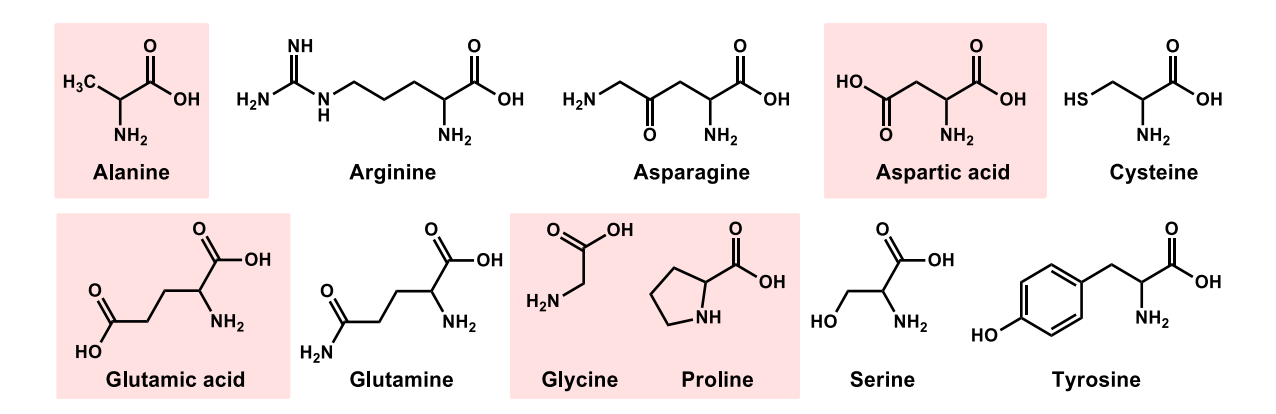
Entry	CAs	Products	Y% (X%)&	F.E.	Electrochemical parameters	Ref.
1	Levulinic acid	Valeric acid	> 86% (78%)	65%	-1.8 V ^{@-2} in 0.5 M H ₂ SO ₄ on Pb	216
2	Levulinic acid	γ-valerolactone	100% (U.D.)	79%	13.5 mA cm ⁻² , -2.15 V [@] -3 in [Bmim]BF ₄ (1.8 wt. %)–MeCN–H ₂ O (1.8 wt. %) on PbS	234
3	Levulinic acid	2,7-octanedione	47% (60%)	86%	5 V# in Methanol on Pt	216
4	2,7-octanedione	n-octane	27% (U.D.)	11%	$20-40$ mA cm $^{\text{-}2}$ / -1.8 V $^{\text{@-}2}$ in 0.5 M H_2SO_4 on $$Pb$$	217
5	Levulinic acid	4-hydroxy-2- butanone	20% (57%)	5%	6 V# in 0.2 M NaOH on C	216
6	4-hydroxy-2- butanone	1-butanol	75% (100%)	29%	-1.5 V ^{@-2} in 0.5 M H ₂ SO ₄ on Pb	216
7	Levulinic acid	3-buten-2-one	45% (74%)	24%	+1 - +3 V ^{@-2} in 0.1 M NaOH on C	216
8	Levulinic acid	5-acetyl-2,9- decanedione	~20% (U.D.)	35%	250 – 400 mA cm ⁻² , +60 – +100 V [#] in 0.01 M NaOH Methanol/H ₂ O on Pt	235
9	Valeric acid	n-octane	52% (U.D.)	66%	$40 - 50 \text{ mA cm}^{-2}$, +3.5 V ^{@-2} in 1 KHCO ₃ (pH 5.5) on Pt sheet	217
10	Lactic acid	Lactaldehyde	80% (91%)	I.D.	100 mA, -0.4 V ^{@-2} in 0.01 M HCl, at 70 °C on 5% Ru/C supported on RVC.	236
11	Pyruvic acid	Lactic acid	100% (90%)	56%	~38 mA cm 2 , -1.5 V $^{@-1}$ in 0.5M H $_2$ SO $_4$ on Pb	210

12	Itaconic acid	Methylsuccinic acid	96% (96%)	16%	-1.41 V ^{@-1} in 0.5 H ₂ SO ₄ on Pb	224	
13	Methylsuccinic	2,5-dimethyladipic	60% (85%)	63%	180 mA cm ⁻² in 1 M KOH Methanol on Pt	225	
13	acid ⁺	acid	00 % (03 %)	0376	100 IIIA GIII III I IVI KOH METILAHOI OH PT		
14	Maleic acid	Succinic acid	95% (U.D.)	94 –	75 – 120 mA cm ⁻² , +1.38 – +1.64 V [#] in 1.0 M	226	
14	Waleic acid	Succinic acid	93 % (O.D.)	95%	H₂SO₄ on Pb		
15	Muconic acid	trans-3-hexenedioic	90% (60%) /	60 –	-1.17 V ^{@-1} (TOF : 3.5 - 5.6 s ⁻¹) in 0.01 M	232	
15	Widconic acid	acid	90 /6 (00 /6) /	100%	H₂SO₄ (+ 1% formic acid) on Pb		

^{*}Record performance for production of a specific compound was chosen based on highest faradaic efficiency (F.E.) to the primary product, followed by selectivity/yield and conversion. Only products with yields higher than 20% shown. [&]Yield [Y%] - selectivity [S%] (conversion [X%]). Reference electrodes: [@]-¹ reversible hydrogen electrode (RHE), [@]-² Ag/AgCl_(sat. KCl), [@]-³ Ag/Ag+ in [Bmim]BF₄(1.8 wt%)–MeCN–H₂O (1.8 wt%). [#]Cell voltage. U.D. = Unavailable data. I.D. = inconclusive data. [†]Itaconate-derived methylsuccinic acid, the electrochemical route for dimethyl-adipic acid production was performed with selective esterification of one or both carboxylic acids. ²²⁵ RVC = reticulated vitreous carbon.

3.4. Amino Acids

As mentioned above, a variety of amino acids (AAs) can be economically obtained from the hydrolysis of many plants and animal waste-proteins.⁵² They are potential feedstock for nitrogen-based molecules, which are present in the overwhelming majority of drug molecules, food additives, agrochemicals, and functional materials. According to a report by Grand View Research Incorporation, ²³⁷ the global market size for N-containing molecules is expected to reach US\$ 29.3 billion by 2025, with a compound annual growth rate (CAGR) of 8.3%. This fast growth will be stimulated principally by the personal care, water treatment, and building and construction industries.²³⁷ The industrial production of these Ncompounds involves, in general, the use of high-pressure NH₃, a reagent mainly produced via the energy- and capital-intensive Haber-Bosch process using nonrenewable sources of hydrogen gas.²³⁸ Therefore, environmentally-friendly routes for the production of N-containing building blocks from protein-rich biomass wastes (which are often unsuitable for food/feed production due to poor nutritional quality, biologic contamination, toxicity, or legislative issues⁵²) are desirable. In this context, the electrochemical-valorization of non-essential AAs (ne-AAs) could be a sustainable way to achieve this industrial need. For reference, the eleven ne-AAs are: alanine, arginine, asparagine, aspartic acid, cysteine, glutamic acid, glutamine, glycine, proline, serine, and tyrosine (Scheme 10). There are guidelines and recommendations for arginine, cysteine, and tyrosine dietary supplementation ('semi-essential AA'), and glutamic acid is often used in food and flavor enhancers.⁵¹



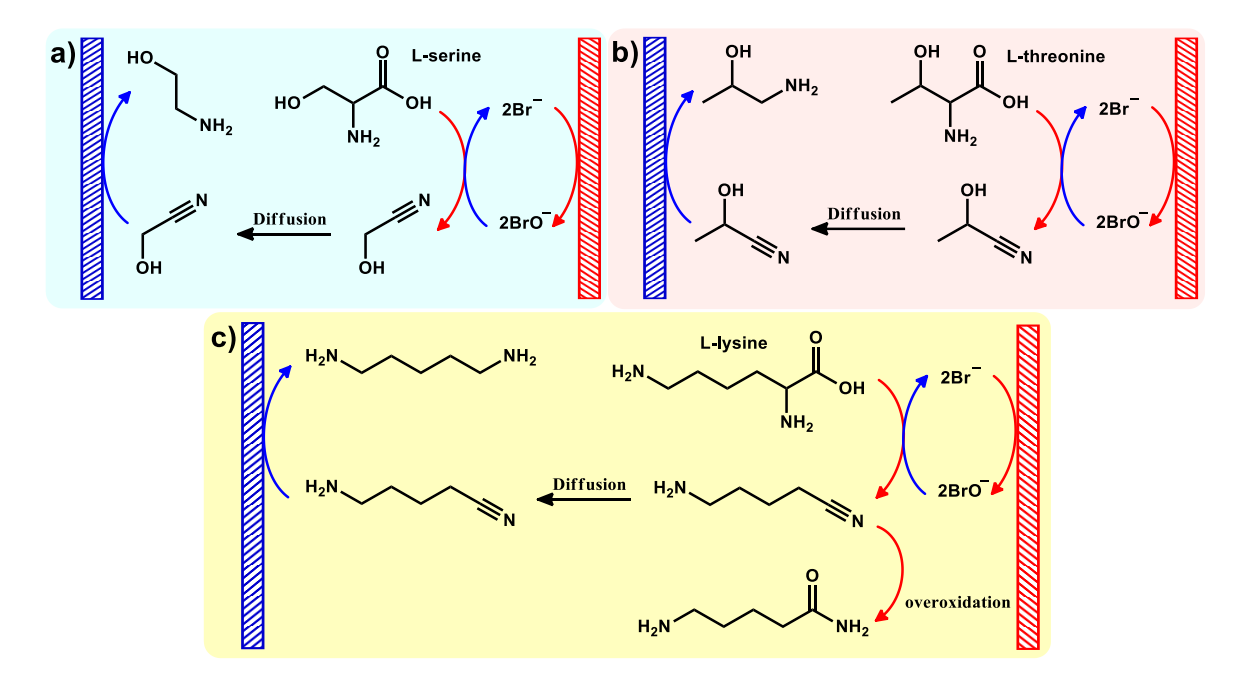
Scheme 10. Non-essential (and semi-essential) amino acids. Those in red shading are just composed of amine and carboxyl functions.

3.4.1. Carboxyl and amine group chemistry

In general, the electrochemical behavior of AAs follows the common paths of CAs and amines since these are the main functionalities of the molecules. 14,15,239–243 Oxidative decarboxylation to form nitriles with or without subsequent nitrile reduction to form primary amines are the most studied and potentially valuable electrochemical technologies to date. Nitriles can be easily isolated from other biomass constituents present in protein hydrolysates by distillation or extraction. 53 Conventional methods of AA conversion into nitriles are hypohalite-mediated, using unstable (e.g., NaOBr²⁴⁴) or expensive and toxic organic precursors (e.g., *o*-iodoxybenzoic acid, 245 trichloroisocyanuric acid, 246 N-bromosuccinimide, 247 or chloramine-T²⁴⁸). Methods to avoid hypohalite precursors, using noble-metal catalysts (Ru-based) have limited substrate scope (only AAs with aliphatic or acidic chains). 249 Conversion AA into primary amines is mainly performed *via* enzymatic 250,251 or chemocatalytic decarboxylation. This latter step is often still performed in toxic organic solvents (e.g., nitrobenzene²⁵², chloroethane²⁵³), at high temperatures (120 – 270 °C), with large

excess of decarboxylating agent (aldehyde and ketone to form Schiff-base adduct²⁵⁴) or with noble-metal catalysts (e.g., Pd-based materials^{255,256}).

In the electrochemical environment, non-branched α-carboxylic acids with primary amines are generally oxidized to nitriles via decarboxylation. Higher selectivity and F.E. are often achieved using halide mediators rather than performing direct electrolysis. Bromide salts have generally been found more optimal than iodides and chlorides, since I generates a weaker oxidant mediator, and the mediation efficiency of Cl⁻ is suppressed by competition with H₂O oxidation. 14,15,239– ^{243,257,258} As an example, De Vos and co-authors showed bromide-mediated electrochemical conversion of fourteen AAs into nitriles with excellent yields (77 -94%) and moderate faradaic efficiencies (51 – 63%).²⁵⁸ For some AAs, the formed nitriles were sequentially reduced to amines at the counter electrode (Ni cathode) —a kind of tandem paired electrolysis that will be further discussed in Section 5.4.2.²⁵⁸ Scheme 11 shows the sequential conversion of L-serine, L-threonine, and L-lysine into their respective amines, via nitriles. For L-lysine, the formation of the amide (which is a product of nitrile oxidation) was also observed at a yield of 97% when more charge was supplied after full conversion of L-lysine.²⁵⁸



Scheme 11. Bromide-mediated electrochemical conversion of (a) L-serine, (b) L-threonine, and (c) L-lysine into Glycolonitrile, Lactonitrile, and 5-aminopentanenitrile (and overoxidation product, 5-aminopentanamide), respectively. Also shown is the sequential reduction of the respective nitriles into ethanolamine, 1-amino-2-propanol, and 1,5-pentanediamine. Scheme adapted from De Vos and co-authors.²⁵⁸

Amongst all AAs, glutamic acid (a ne-AA) is one of the most abundant; it can be economically derived from the hydrolysis of many vegetal and animal waste-proteins. For example, proteins extracted from sugar beet vinasses by acid hydrolysis contain ~55 wt. % glutamic acid. Hydrolysis of the waste stream proteins can further convert glutamine into glutamic acid, increasing its concentration.⁵² This is of perhaps most interest as an alternative feedstock to form adiponitrile, a precursor of Nylon-6,6 produced at ~5 Mt/y.²⁴² The current industrial route to this product involves ammoxidation of propylene to form acrylonitrile, followed by coupling (often electrochemical hydrodimerization) to yield adiponitrile.²⁵⁹ A

complete electrochemical path is shown in Scheme 12, where glutamic acid is first oxidized *via* bromide-mediation to 3-cyanopropanoic acid (one of the carboxylic acids was protected by esterification to improve the selectivity). In this example, the subsequent cyano-ester (methyl 3-cyanopropanoate) was deprotected (recovering the carboxyl function) and oxidized *via* Kolbe route to form adiponitrile.

Scheme 12. EC-conversion of glutamic acid in adiponitrile. Scheme adapted from Fu and coauthors²⁴² and Baran and coauthors¹⁶.

3.4.2. R-group transformations

Groups such as thiol (present in cysteine), thioether (present in methionine), phenol (present in tyrosine), and guanidine (arginine) may be oxidized to sulfonic acids (*via* disulfide), sulfone/sulfoxides, quinones,^{260,261} and urea-derivates, respectively.^{13,14,16,211–213,258} For halide-mediated electrolysis, the aromatic ring of some AAs (tyrosine, tryptophan, phenylalanine, and histidine) can also be halogenated.²⁵⁸ As an example of R-group transformation, Scheme 13 shows the divergent paired electrolysis of L-cystine, where the oxidation and reduction products are L-cysteic acid and L-cysteine, respectively.^{262,263} The non-paired conversion of

L-cystine into L-cysteine has also been studied by several researchers, and the main results were organized in one publication by Walsh and co-authors.²⁶²

Scheme 13. Divergent paired electrolysis of L-cystine for producing L-cysteic acid (anodic faradaic efficiency of 98%) and L-cysteine (cathodic faradaic efficiency of 85%).²³⁹

Table 6 shows some opportunities for production of fine and bulk chemicals from electrochemical valorization of AAs. Some of these chemicals are: adiponitrile (a polyamide precursor²⁴²), glycolonitrile (a precursor of ethylenediaminetetraacetic acid—EDTA— an important chelating agent²⁶⁴), ethanolamine (global production 0.5 Mt/y, precursor of herbicides, detergent, plastics, etc.), and N-methylpyrrolidone (also known as γ-butyrolactam, used as a precursor of poly(vinylpyrrolidone), a specialty polymer applied in the cosmetic and medical sectors, with a market size ~100 kt/yr).²⁶⁵

Table 6. Record efficiencies* for production of major compounds from the electrochemical valorization of amino acids.

Entry	AAs	Products	Y% [S%] (X%)&	F.E.	Electrochemical parameters	Ref.
1	L-glutamic acid [@]	3-cyanopropanoic acid	91% (91%)	76%	80 mA cm ⁻² , +5 - +10 V [#] in MeOH/H ₂ O (4/1, v/v) and 0.4 mM NaBr (as anodic mediator) at 0 °C on Pt	242
2	3- cyanopropanoic acid	adiponitrile	78% (78%)	29%	180 mA cm ⁻² , +7 – +15 V [#] in 0.3 M KOH MeOH/acetone (1/1, v/v) at 60 °C on Pt	242
3	L-cystine	L-cysteic acid (anodic) and L-cysteine (cathodic)	Anodic: 98% (95%); Cathodic: 85% (85%)	Anodic: 97%. Cathodic: 90%	Divergent paired electrolysis on graphite electrodes, 70 mA cm ⁻² in 0.6 M HCl and 10 mM HBr (as anodic mediator) at 40 °C	239
4	L-cystine	L-cysteine	94% (100%)	92%	500 mA cm ⁻² , parallel plate reactor with catholyte and anolyte separated by Nafion-324 [®] membrane, porous reticulated carbon cathode, in 2.0 M HCl at 30-40°C	262,266
5	L- phenylalanine	benzyl cyanide	93% (U.D.)	62%	10 mA cm ⁻² , in MeOH/H ₂ O (13/1, v/v) and 0.15 M NH ₄ Br (as anodic	258

					mediator) at 0 °C on Pt anode (Ni cathode)	
6	L-isoleucine	2-methylbutyronitrile	86% (U.D.)	57%	10 mA cm ⁻² , in MeOH/H ₂ O (13/1, v/v) and 0.15 M NH ₄ Br (as anodic mediator) at 0 °C on Pt anode (Ni cathode)	258
7	L-alanine	Acetonitrile	94% (U.D.)	63%	10 mA cm ⁻² , in MeOH/H ₂ O (13/1, v/v) and 0.15 M NH ₄ Br (as anodic mediator) at 0 °C on Pt anode (Ni cathode)	258
8	L-valine	Isobutyronitrile	91% (U.D.)	61%	10 mA cm ⁻² , in MeOH/H ₂ O (13/1, v/v) and 0.15 M NH ₄ Br (as anodic mediator) at 0 °C on Pt anode (Ni cathode)	258
9	L-leucine	Isovaleronitrile	89% (U.D.)	59%	10 mA cm ⁻² , in MeOH/H₂O (13/1, v/v) and 0.15 M NH₄Br (as anodic mediator) at 0 °C on Pt anode (Ni cathode)	258
10	L-serine	Glycolonitrile (GN) and Ethanolamine (EAM)	Pt-cathode: 82% [GN:EAM = 100:0] (U.D.);	Pt-cathode: 55%. Ni-cathode: 54%	10 mA cm ⁻² , in MeOH/H ₂ O (13/1, v/v) and 0.15 M NH ₄ Br (as anodic mediator) at 0 °C on Pt anode	258

			Ni-cathode: 81%			
			[GN:EAM =			
			80:20] (U.D.)			
11	L-threonine	Lactonitrile (LN) and 1- amino-2-propanol (APL)	Pt-cathode: 80% [LN:APL = 100:0] (U.D.); Ni-cathode: 77 % [LN:APL = 86:14] (U.D.)	Pt-cathode: 53%. Ni-cathode: 51%	10 mA cm ⁻² , in MeOH/H₂O (13/1, v/v) and 0.15 M NH₄Br (as anodic mediator) at 0 °C on Pt anode	258
12	L-Glutamine	3-cyanopropionamide	In MeOH/H ₂ O (13/1, v/v): 85% (U.D.); In H ₂ O: 83% (U.D.)	In MeOH/H ₂ O (13/1, v/v): 57%. In H ₂ O: 55%.	10 mA cm ⁻² , 0.15 M NH₄Br (as anodic mediator) at 0 °C on Pt anode (Ni cathode)	258
13	L-asparagine	acetamide	86% (100%)	U.D.	+2.5 V [#] for 15h, in H ₂ O and 0.15 M NH ₄ Br (as anodic mediator) at 0 °C on Pt anode (Ni cathode)	258
14	L-aspartic acid	3-cyanopropionic acid	In MeOH/H ₂ O (13/1, v/v): 80% (U.D.); In H ₂ O: 91% (U.D.)	In MeOH/H ₂ O (13/1, v/v): 53%. In H ₂ O: 61%.	10 mA cm ⁻² , 0.15 M NH₄Br (as anodic mediator) at 0 °C on Pt anode (Ni cathode)	258

15	L-proline	2-pyrrolidone	91% (100%)	U.D.	+2.5 V [#] for 15h, in H ₂ O and 37.5 mM NH ₄ Br (as anodic mediator) at 0 °C on Pt anode (Ni cathode)	258
16	L-lysine	5-aminopentanenitrile (APN) / 1,5- pentanediamine (PDA)	Pt-cathode: 93 % [APN:PDA = 80:20] (U.D.); Ni-cathode: 92 % [APN:PDA = 35:65] (U.D.)	Pt-cathode: 62%. Ni-cathode: 61%	10 mA cm ⁻² , H ₂ O and 0.15 M NH ₄ Br (as anodic mediator) at 0 ⁰ C on Pt anode	258
17	L-lysine	5-aminopentanamide	97% (100%)	U.D.	+2.5 V* for 15h, in H ₂ O and 0.15 M NH ₄ Br (as anodic mediator) at 0 °C on Pt anode (Ni anode)	258
18	L- arginine	N-(3-cyanopropyl)- guanidine	91% (U.D.)	U.D.	10 mA cm ⁻² , in MeOH/H ₂ O (13/1, v/v) and 0.15 M NH ₄ Br (as anodic mediator) at 0 °C on Pt anode (Ni cathode)	258

^{*}Record performance for production of a specific compound was chosen based on highest faradaic efficiency to the primary product, followed by selectivity and conversion. Only products with yields higher than 20% shown. *Yield [Y%] -selectivity [S%] (conversion [X%]). * L-glutamic acid was partially esterified to improve the selectivity. * Cell voltage with HER on Pt as the cathodic reaction. U.D. = Unavailable data.

3.5 Lignin

3.5.1. Electrochemical depolymerization of lignin

Lignin has the potential to be a renewable source for a plethora of aromatic compounds. However, the production of value-added commodity chemicals *via* lignin depolymerization remains a major challenge because this biopolymer is by far the most recalcitrant component of biomass. The structure is formed by a heterogeneous and complex 3D network composed of diverse linkages between monomeric units (β-O-4, β-5, β-1, 5-5, 4-O-5, α-O-4, and β-β, as seen in Scheme 14), which render it practically invulnerable to simple hydrolytic cleavage. ²⁶⁷ Because of this structural integrity, lignin remains intact after extraction of cellulose, hemicellulose, and other hydrolysable components of biomass sources. Depending on the chemical pretreatment method used, lignin extracts have been classified into four principal categories: kraft lignin (treatment with NaOH and Na₂S, the common treatment in the pulping industry), soda lignin (alkali lignin, treatment with S-free NaOH), lignosulfonates (treatment with aqueous SO₂, acid extract), and organosolv lignin (extraction with ethanol-water). ²⁶⁷

Over the past few decades, approaches to valorize lignin have included microbial-enzymatic, ²⁶⁸ thermochemical (including pyrolysis, ²⁶⁹ hydrothermal, ²⁷⁰ including microwave-assisted methods, ^{271,272} etc), photochemical, ^{273,274} electrochemical, ^{275,276,285,277–284} and electrochemical-photoredox ²⁸⁶. Generally, the thermochemical methods are performed at high temperatures and pressures, combined with metallic catalysts (ruthenium-, iron-, copper-, and vanadium-based catalyst). Problems with catalyst recovery and poisoning are the main bottlenecks to achieve a sustainable and economically viable thermochemical process. In contrast,

the electrochemical oxidative depolymerization (ECOD) of waste stream lignin has been considered a promising technology for the production of aromatic fine chemicals due to its environmental-friendly characteristics, and apparent robustness and scalability.^{275,276,285,277–284}

Scheme 14. Major products from lignin-depolymerization. The varied methoxyphenolic subunits and cross-linking modes of the lignin are also illustrated.

In this context, many works have outlined different thermochemical and biochemical approaches for lignin valorization;^{267–274,287} however, just in 2018, a review about lignin ECOD was published by Zirbes and Waldvogel.²⁷⁹ Therefore, in this section, we will present only the main advances of this field published over the

last 5 years as well as some novel methodologies that were not cited in that mentioned review, summarizing key information about these works in Table 7.

Overoxidation and repolymerization of monomers are some of the main problems found in lignin ECOD, as observed in many publications.^{275–279} To overcome these issues, some authors have proposed methodologies to remove the low molecular weight depolymerization products from the reaction medium as soon as they are formed, such as the integration of polymeric nanofiltration membranes for continuous permeation of these monomers, 275,276 the use of resins, 277 or emulsions to extract these products.²⁷⁸ Waldvogel and coworkers²⁷⁷ demonstrated the highly selective production of vanillin from Kraft lignin ECOD coupled to the separation of this product with a strongly basic anion exchange resin (Table 7, Work 11). They tested several commercially available resins; the best results were achieved with polystyrene divinylbenzene-tetraalkylammonium, where more than 90% of dissolved vanillin was removed from the reaction medium, inhibiting the overoxidation of this molecule. Vanillin was afterward recovered from the resin by the simple use of a biocompatible acidic eluent consisting of EtOAc/AcOH (8:2), which can also be recovered by distillation. This elegant approach also solves challenges related to the purification/extraction of the depolymerization products from the reaction medium; traditional methods generally involve precipitation of remaining lignin with an excess of acid and subsequent liquid-liquid extraction of the low molecular weight products with dichloromethane, a non environmentally friendly solvent.²⁷⁷ Wessling and coauthors²⁷⁸ demonstrated another interesting methodology for inhibiting the overoxidation of lignin monomers (Table 7, Work 6). They proposed the use of an emulsion as supporting electrolyte; the organic solvent (extractant phase) removes these products *in situ*, as soon as they are produced, from the aqueous phase. This emulsion was composed of H₂O (10 g L⁻¹ Kraft lignin), deep eutectic solvent (choline chloride:ethylene glycol, in the molar proportion of 1:2), and methyl isobutyl ketone (extractant solvent) in the volumetric proportion of 1:3:6. They showed that the average of the total molecular weight decreases 75% and 90% after 1h electrolysis on Ni anodes at cell voltages of 2.5 and 3.5 V, respectively. However, they did not show identification or quantification of the depolymerization products.²⁷⁸

Lignin ECOD results have also been obtained using ionic liquids (ILs), which have a relatively wide electrochemical stability window and thus can improve Faradaic efficiency by decreasing parasitic water electrolysis. Some ILs can be efficiently reused without purification (after extraction of ECOD products) and have also shown a superior capacity to solubilize this biopolymer. 288 Volmer and coauthors²⁸⁸ (Table 7, Work 7) studied the lignin ECOD with reticulated vitreous carbon foam electrodes and using two different ILs, 1-ethyl-3-methylimidazolium trifluoromethanesulfonate ([emim][OTf]) and triethylammonium methanesulfonate (TMS). They demonstrated the participation of electrogenerated H₂O₂ or hydroxyl radicals (from the oxidation of intentionally added H2O) as both auxiliary oxidant and radical scavenger (as also observed in other works²⁸⁹⁻²⁹²), which inhibits the repolymerization of monomers under oxidative pathways. TMS and [emim][OTf] showed maximum lignin decomposition rates of 22–31 and 19–23 wt%, respectively. Several depolymerization products were identified, the main components being: acetovanillone (relative yield: 12.03%), homovanillic acid (34.68%) and vanillic acid (6.09%) for electrolysis in [emim][OTf]; and homovanillic acid (25.24%), vanillic acid

(14.52%), and 3,4-dihydroxybenzaldehyde (11.8%) for electrolysis in TMS. Interestingly, they also observed the formation of polycyclic hydrocarbons likely due to side repolymerization of mono-aromatic monomers followed by dehydroxylation or demethoxylation reactions.²⁸⁸ Lastly, the ILs were virtually fully recovered after liquid-liquid extraction of the ECOD products. In another work (Table 7, Work 8), they also demonstrated dood results in triethylammonium methanesulfonate [Et₃NH][MeSO₃] with different dimensionally stable anodes (DSAs, Ru_{0.4}Ir_{0.6}O_x, $Ru_{0.2}Mn_{0.2}Ir_{0.6}O_x$, $Ru_{0.2}Pd_{0.2}Ir_{0.6}O_x$, $Ru_{0.2}V_{0.2}Ir_{0.6}O_x$, and $Ru_{0.2}Ti_{0.2}Ir_{0.6}O_x$). ²⁹³ It was shown that the distribution of the products was affected by the electrode composition, where the p-coumaric acid was the main product obtained with Ru_{0.2}Mn_{0.2}Ir_{0.6}O_x electrode while 4-hydroxy-3,5-dimethoxy cinnamaldehyde, 4hydroxy-3,5-dimethoxy acetophenone, and vanillin were the principal compounds generated on $Ru_{0.2}Pd_{0.2}Ir_{0.6}O_x$, $Ru_{0.2}V_{0.2}Ir_{0.6}O_x$, and $Ru_{0.2}Ti_{0.2}Ir_{0.6}O_x$, respectively. Among the evaluated electrodes, the total yield of degradation-products was maximum for the Ru_{0.2}Mn_{0.2}Ir_{0.6}O_x electrode (11.5 wt% after 3h electrolysis), which also showed the highest production of alkylphenolic compounds (20.5% of the total depolymerization products).²⁹³ In the same context, Wessling and coworkers²⁹⁴ studied the applicability of two deep eutectic solvents (DESs) as supporting electrolyte for the depolymerization reaction since DESs have electrochemical properties compared to ILs (Table 7, Work 5).²⁹⁴ Mixtures of choline chloride with urea (urea-ChCl) and with ethylene glycol (EtGly-ChCl) in the proportion of 1:2 (mol/mol) were studied. EtGly-ChCl with 10% (mol) of water showed better lignin solubility and conductivity in comparison with urea-ChCl, and the dry solvents. The maximum depolymerization rate of 80 wt% was achieved at a cell voltage of 1.0 V in

EtGly–ChCl–H₂O. The total yield of monomers was close to 2 wt. % (relative to the starting quantity of lignin), and the main identified compounds were guaiacol (relative yield: 30–38%), vanillin (relative yield: 34–37%), acetovanillone (relative yield: 9%), and syringaldehyde (relative yield: 12%).²⁹⁴

Several authors also studied the ECOD of lignin model molecules, ^{286,290,292} which can represent some specific linkages present in real lignin but do not show some of the most technologically challenging limitations of this macro-molecule such as low solubility in pH below 9, low diffusion coefficients (which limit the direct electrolysis) and the general recalcitrance.

In summary, this process can be less energy-intensive than thermochemical alternatives; however, it still shows low yields and selectivity towards value-added products. Unfortunately, most works in this field have not yet demonstrated concepts for downstream processing of the depolymerization products, which is imperative for industrial applicability.

Table 7. Summary of major studies on electrochemical depolymerization of lignin published over the last 5 years.

Work	Electrodes / Substrate / Reaction conditions / Reference	Depolymerization results	
1	NiSn alloys anodes / 10 g L ⁻¹ lignin dissolved in 1 M aqueous NaOH / Continuous-flow reactor, divided by an anion exchange membrane, at optimized potential of 1.4 V [®] (3 mA cm ⁻²) on	Simultaneous lignin depolymerization and production of H ₂ . Vanillin was the only monomer quantified, showing a max production rate of ~0.3 g/kg of lignin per min. H ₂ evolution	
	Ni _{0.7} Sn _{0.2} anode / Staser and coauthors (2020) ²⁸²	showed F.E. close to 100%.	
2	Nickel cathode and Pb/PbO ₂ anode / 40 g L ⁻¹ cornstalk lignin dissolved in 1 M aqueous NaOH / Undivided batch reactor used, with optimized applied current density of 30 mA cm ⁻² and at 35°C / Li and coauthors (2020) ²⁹⁵	ECOD rate reached 78.7% after 12h electrolysis. Eight products of ECOD and cathodic hydrodeoxygenation (such as toluene and xylenes) were identified (yields up to 3.6 wt. %). Five unidentified products also observed. Cell voltage not given.	
3	Ti, Ti/Fe, Ti/Cu, and Ti/Cu/Sn cathodes, and Ti/SnO $_2$ – Sb $_2$ O $_3$ /PbO $_2$ anode / 40 g L $^{-1}$ rice straw lignin dissolved in 1 M aqueous NaOH / Undivided batch reactor used, with applied current densities between 10 – 60 mA cm $^{-2}$ and temperature range 25 – 65 $^{\circ}$ C; best performances at 30 – 40 mA cm $^{-2}$ and 35 $^{\circ}$ C / Li and coauthors (2018) 296	Total yield of monomers (sixteen different molecules) was 3.3 wt. %. The most hydrodeoxygenation products were seen with Ti/Fe cathode (total yield up to 0.3 wt. %), while max production of oxidation products was with Ti and Ti/Cu/Sn cathodes (total yield up to 2.9 wt. %). Cell voltage not given.	
4	Nickel foam anode / 5 g L $^{-1}$ kraft lignin dissolved in 1M NaOH / Continuous-flow "swiss-roll" reactor, potentials at 0.8, 2.5, and 3.5 V $^{\odot}$, resulting in the total current densities of 3.6, 8.9 – 17.8, and 44.4 – 67.6 mA cm $^{-2}$,# respectively / Wessling and coauthors (2018) 297	The major monomer generated was vanillin (max yield of 1.25 wt. % after 5 h at 0.8 V $^{\circ}$), but carboxylic acids (oxalic, malonic, succinic, malic, formic, and acetic acids) were the main products, presenting total yield ~ 40 wt. % after 5h at 2.5 V $^{\circ}$.	

	Cu/Ni-Mo-Co cathode and Pb/PbO ₂ anode / 50 g L ⁻¹ corn stover	ECOD reached 93.29% after 6h. Sixteen monomers were	
5	lignin dissolved in 1 M aqueous NaOH / Undivided batch		
	reactor, optimized current density of 25 mA cm ⁻² and	9.17 wt. %. Eight non-identified products were also	
	temperature of 40°C / Li and coauthors (2018) ²⁹⁸	observed. Cell voltage not given.	
	Ni anode / 10 g L ⁻¹ kraft lignin emulsion (H ₂ O: EtGly-	Average total molecular weight decreased 75% and 90%	
6	ChCl&:methyl isobutyl ketone, in volume ratio 1:3:6) / Undivided		
Ū	batch reactor, potentials of 2.5 and 3.5 V [@] / Wessling and	after 1h at 2.5 and 3.5 V [®] . The products were not identified	
	coauthors (2017) ²⁷⁸	and quantified. Current densities not given.	
	RVC electrodes / 10% (w/w) alkali and organosolv lignin	ECOD up to 31 wt. %. Forty-two monomers were identified	
7	dissolved in ILs* / Undivided batch reactor at 2.5 V [®] at 65 °C /	with relative individual yields of up to 34.7 %. Current	
	Volmer and coauthors (2017) ²⁸⁸	densities not given.	
-	, ,	ŭ .	
	Different *DSAs (Ru _{0.4} Ir _{0.6} O _x , Ru _{0.2} Mn _{0.2} Ir _{0.6} O _x , Ru _{0.2} Pd _{0.2} Ir _{0.6} O _x ,	Highest total yield of ECOD products (including oligomers,	
•	$Ru_{0.2}V_{0.2}Ir_{0.6}O_x$, and $Ru_{0.2}Ti_{0.2}Ir_{0.6}O_x$) as anodes / 10 wt. % of kraft	·	
8	lignin in triethylammonium methanesulfonate / Undivided batch	on $Ru_{0.2}Mn_{0.2}Ir_{0.6}O_x$ electrode; 20.5% of these products	
	reactor at 1.8 V [®] and 70 °C / Hempelmann and coauthors	were alkylphenolics. The IL* was fully recovered. Current	
	(2017) ²⁹³	densities not given.	
	Ni electrodes / 5 g L ⁻¹ kraft lignin dissolved in DESs ^{&} / Undivided	Total yield of monomers ~2 wt. % and fourteen monomers	
9	batch reactor at potentials of 0.5 and 1.0 V vs. Ag/AgCl /	were identified (relative yields of up to 38 %). The DESs ^{&}	
	Wessling and coworkers (2016) ²⁹⁴	were fully recovered. Current densities not given.	
	Ni foam electrodes / 5 g L ⁻¹ kraft lignin dissolved in 1 M aqueous	Total lignin denotymerization achieved in 4h. Turchin	
10	NaOH / Applied currents from 35.6 to 142.2 mA cm ⁻² ,# in a	monomers identified, but the individual yield of the	
10	continuous-flow reactor. Continuous separation of the low-		
	molecular-weight compounds and residual lignin done by	quantified compounds was each <0.5%. The continuous	

	polymeric membrane nanofiltration / Wessling and coauthors	s separation of the monomers almost triples the yields. Cell		
	(2016) ²⁷⁵	voltage not given.		
	Ni and stainless steel electrodes / 10 wt. % of kraft lignin in 3M			
	NaOH / Undivided batch reactor at currents density of 38 mA	High selective generation of vanillin was archived with		
11	cm ⁻² and 80 °C. A strongly basic anion exchange resin was used	yields close to 1.0 wt. %. Cell voltage not given.		
	to separate the depolymerization products / Waldvogel and	yields close to 1.0 wt. %. Cell voltage not given.		
	coworkers (2015) ²⁷⁷			

[®]Cell voltage. MWNTs: Multi-walled nanotubes. RVC: reticulated vitreous carbon foam. *1-ethyl-3-methylimidazolium trifluoromethanesulfonate ([emim][OTf]) and triethylammonium methanesulfonate (TMS). [&]Mixtures of choline chloride with urea (urea–ChCl) and with ethylene glycol (EtGly–ChCl) in the proportion of 1:2 (mol/mol). [&]Dimensionally stable anodes. [#]Assuming an electrode geometry area of 56.24 cm². ^{275,297}

3.5.2 Electro-hydrogenation and deoxygenation of lignin-derived aromatics

The depolymerization of lignin produces a variety of oxygenated aromatic molecules (one of the major components of bio-oil, as shown in Scheme 14), which are potential intermediates for fuel and other value-added building blocks. However, the raw form of the bio-oils is highly corrosive, unstable during storage, and highly oxygenated (which means low heating value, c.a. 40% of the heating value of diesel, for example).²⁹⁹

As a method for stabilization and valorization of these lignin-derived bio-oils, electrocatalytic hydrogenation-deoxygenation (ECHDO) has been highlighted, 300–309 since it can be performed at mild conditions. Tables 8 and 9 show noteworthy records for ECHDO of some of these molecules; Table 8 presents routes where the bio-oil-derived molecules were completely hydrogenated (including the aromatic rings), while Table 9 shows methods where ECHDO was specifically performed on side groups. Scheme 15 below shows the main pathways of ECHDO of lignin-derived aromatics. When the molecules have alkenyl, aldehyde, or carbonyl groups, these undergo ECHDO first, while carboxylic and alcohol functions are not easily reduced. In general, the methoxy groups are removed (substituted by hydrogen) under ECHDO conditions, but this mechanism does not happen if the aromatic ring is first hydrogenated.

Scheme 15. Electro-hydrogenation and deoxygenation of some lignin-derived aromatics. A, B, and R groups follow the same structures presented in Scheme 14. The dotted arrow presents a route for a minority product, while arrows marked by an "X" indicate routes that are not presently achievable. These paths are reported as a composite representation of several experimental works. 300–308

Table 8. Record efficiencies* for full electro-hydrogenation and deoxygenation of some lignin-derived aromatics (aromatic ring reduction).

Entry	Reactant	Products / Y% (X%)&	F.E.	Electrochemical parameters#	Ref.
1	Phenol (A, B, and R: -H)	cyclohexanol (A, B, and R: -H / C: -OH) / >80% (>99%)	>90%	200 - 250 mA cm ⁻² (-0.35 V vs. NHE, TOF : 815 - 889 h ⁻¹ , at 55°C) or 500 - 800 mA cm ⁻² (-0.5 0.6 V vs. NHE, TOF : 700 h ⁻¹ , at 35°C) in 0.1 M H ₄ [W ₁₂ SiO ₄₀] + 2% (Pt to substrate ratio) Pt/C, on C electrodes	303
2	p-cresol (A and B: -H / R: -CH ₃)	4-methylcyclohexanol (A and B: -H / C: -OH / R: - CH ₃) / 99% (87%)	39%	100 mA cm ⁻² in 0.2 M HCl at 80 °C on Ru/Zorflex-activated carbon cloth	304
3	Guaiacol (A and R: -H / B: -OCH₃)	cyclohexanol (A, B, and R: -H / C: -OH) / >50% (>90%)	>90%	100 – 200 mA cm ⁻² (-0.27 – -0.35 V vs. NHE, at 35°C) or 250 mA cm ² (-0.37 V vs. NHE, at	303

				55°C) in 0.1 M H ₄ [W ₁₂ SiO ₄₀] + 2% (Pt to	
				substrate ratio) Pt/C, on C electrodes	
4	2-methoxy-4- methylphenol (A: -H / B: -OCH ₃ / R: -CH ₃)	4-methylcyclohexanol (A and B: -H / C: -OH / R: - CH ₃) / 94.4% (77%)	72%	100 mA cm ⁻² in 0.1 M H ₄ [W ₁₂ SiO ₄₀] + 2% (Pt to substrate ratio) Pt/C (suspension) methanol:H ₂ O (1:9, v:v), at 55 °C on C electrodes	303
5	2-methoxy-4- propylphenol (A: -H / B: -OCH ₃ / R: -CH ₂ CH ₂ CH ₃)	2-methoxy-4- propylcyclohexanol (A: -H / B: -OCH ₃ / C: -OH / R: - CH ₂ CH ₂ CH ₃) / 61% (63 %)	29%	100 mA cm ⁻² in 0.2 M HCl at 80 °C on Ru/Zorflex-activated carbon clot	304
6	2-methoxy-4- propylphenol (A: -H / B: -OCH ₃ / R: -CH ₂ CH ₂ CH ₃)	4-propylcyclohexanol (A and B: -H / C: -OH / R: - CH ₂ CH ₂ CH ₃) / 38 % (63 %)	29%	100 mA cm ⁻² in 0.2 M HCl at 80 °C on Ru/Zorflex-activated carbon clot	304
7	4-methylbenzene-1,2- diol (A: -H / B: -OH / R: -CH ₃)	4-methylcyclohexanol (A and B: -H / C: -OH / R: - CH ₃) / 74.8% (>99%)	93%	100 mA cm ⁻² in 0.1 M H ₄ [W ₁₂ SiO ₄₀] + 2% (Pt to substrate ratio) Pt/C, at 55 °C on C electrodes	303

*Record performance for production of a specific compound was chosen based on highest faradaic efficiency (F.E.) to the primary product, followed by selectivity and conversion. Only for products that showed yields higher than 20%. *Yield [Y%] (conversion [X%]). *Reaction carried out at room temperature when it is not specified.

Table 9. Record efficiencies* for partial electro-hydrogenation and deoxygenation of some lignin-derived aromatics (no hydrogenation of aromatic rings).

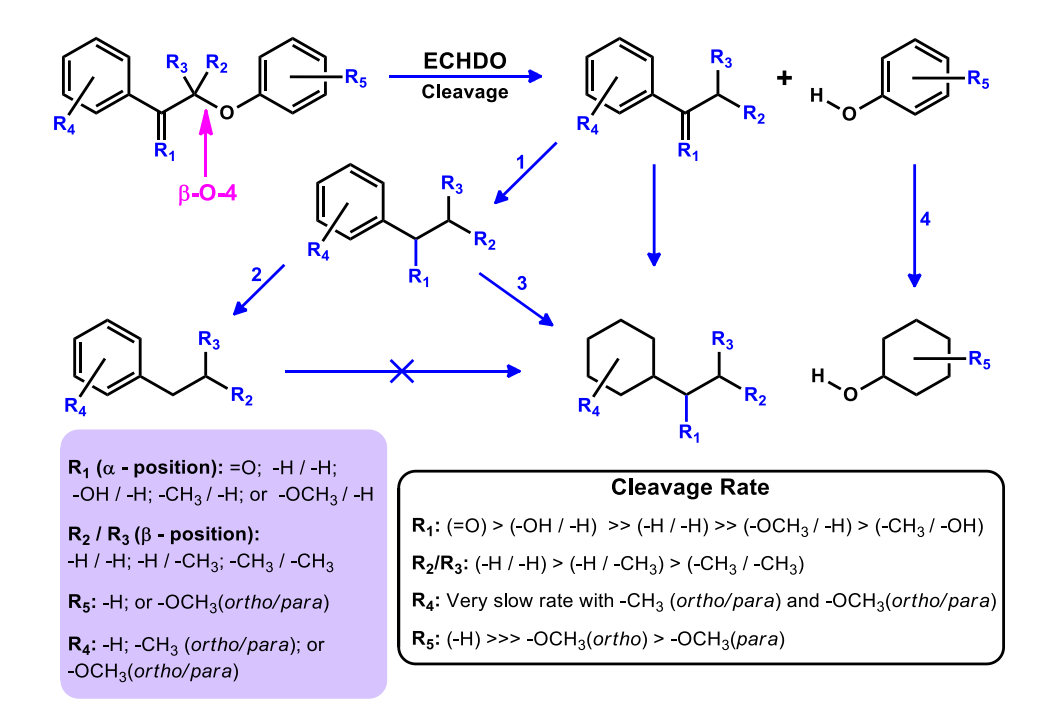
Entry	Reactant	Products / Y% (X%)&	F.E.	Electrochemical parameters#	Ref.
1	1-(4-hydroxy-3-methoxyphenyl)ethanone (A: -H / B: -OCH ₃ / C: -OH / R: -COCH ₃)	4-ethyl-2- methoxyphenol (R was reduced to: - CH ₂ CH ₃) / 91% (91%)	72%	100 mA cm ⁻² in 0.1 M H ₄ [W ₁₂ SiO ₄₀] + 2% (Pt to substrate ratio) Pt/C (suspension) methanol:H ₂ O (1:9, v:v), at 55 °C on C electrodes	303
2	4-hydroxy-3-methoxybenzaldehyde (A: -H / B: -OCH ₃ / C: -OH / R: -CHO)	2-methoxy-4- methylphenol (R was reduced to: - CH ₃) / 83% (95%)	95%	100 mA cm ⁻² in 0.1 M H ₄ [W ₁₂ SiO ₄₀] + 2% (Pt to substrate ratio) Pt/C, at 55 °C on C electrodes	303

		2-methoxy-4-			
	2-methoxy-4-(prop-1-en-1-yl)phenol	propylphenol		100 mA cm ⁻² in 0.1 M H ₄ [W ₁₂ SiO ₄₀] +	
3	(A: -H / B: -OCH ₃ / C: -OH / R: -	(R was reduced to: -	99%	2% (Pt to substrate ratio) Pt/C, at 55 °C	303
	CH=CHCH ₃)	CH ₂ CH ₂ CH ₃) / 95%		on C electrodes	
		(96%)			
4	1-(2-hydroxyphenyl)ethanone A and R: -H / C: -OH / B: -CHO	o-cresol (B was reduced to: -CH ₃) / 99%	94%	100 mA cm ⁻² in 0.1 M H ₄ [W ₁₂ SiO ₄₀] + 2% (Pt to substrate ratio) Pt/C, at 55 °C	303
		(96%)		on C electrodes	
5	Benzaldehyde (A: -CHO / B, C, R: - H)	Benzyl alcohol (A was reduced to: -CH ₂ OH) / >95% (>95%) /	93.4 – 99.7%	0.1 – 0.4 mA cm ⁻² , -0.5 V – -0.9V vs. Ag/AgCl _(KCl sat.)) in acetate buffer solution (pH 5) on Pd/C. TOF: 719 – 3899 h ⁻¹	302

^{*}Record performance for production of a specific compound was chosen based on highest faradaic efficiency (F.E.) to the primary product, followed by selectivity and conversion. Only products with yields higher than 20% shown. *Yield [Y%] (conversion [X%]). *Reaction carried out at room temperature when not specified.

As commented before, various strategies for depolymerization of lignin have been explored. Several harsh methodologies of lignin removal from biomass create new cross-linking, which make the extraction of small building block more difficult. Newer approaches pursue milder cleavage strategies, in particular, for the cleavage of the so-called β-O-4 alkyl aryl ether, the most common of the linking modes present in this bio-polymer.²⁶⁷ In this context, ECH/ECHDO is not only a method that can be used for light lignin monomer hydrogenation and hydrodeoxygenation but can also be applied to structures slightly more complex. Jackson and coauthors showed that ECH/ECHDO is a good method for cleavage of aryl alkyl ether, links very common in lignin structure.³⁰⁰ They used several model structures with different substituents on the aromatic rings and α - and β -positions, demonstrating high conversion (~ 100%) for the cleavage of the C-O-C bonds and hydrogenation of the cleavage products, as can be seen in Scheme 16.300 They proposed that the activation of the α-position (R₁) with a ketone or hydroxyl groups is crucial for the cleavage mechanism of these lignin-models; molecules with R₁ substituted by -H / -H, -H / -OCH₃, or -OH / -CH₃ showed very slower cleavage rates. In contrast, the βsubstituents mostly promote steric effects; the rates for molecules with bulky R₂/R₃ groups are slower than for those with -H β-substituents. After cleavage, the phenolic fragments undergo further ECH into cyclic alcohols, while the fragments with ketone substituent undergo ECH to alcohols (Scheme 16, path 1). These alcohols can be partially (Scheme 16, path 2) or completely (Scheme 16, path 3) reacted by ECHDO. In this last path, the aromatic ring is also hydrogenated and this mechanism involves the participation of α -oxo, making the product of path 2 nearly terminal, hardly reducing into the product of path 3. Donating R₄ or R₅ groups (such as -CH₃ and -OCH₃) on the aromatic rings also make the cleavage very sluggish.

This work shows that ECH / ECHDO can be a promising approach for depolymerization of lignin under milder conditions (aqueous solution, room temperature, *in-situ* generated H₂) than those used in different methodologies; for example, mild thermochemical approaches were reported by Lercher and coworkers (aqueous solution using nickel supported on SiO₂ as the catalyst, at 120 °C and with 6 bar of H₂)³¹⁰ and Dyson and coauthors (Ru-Ni and Rh-Ni alloys as catalysts, at 95°C and 1 bar of H₂).³¹¹ As in all such comparisons, many further considerations must be made for a full techno-economic analysis, but the electrochemical pathways nonetheless present promise to merit further development.



Scheme 16. β-O-4 alkyl aryl ether cleavage via electrochemical hydrodeoxygenation (ECHDO) of various lignin models.

4. Computational methodologies to model electrocatalytic environments

Computational modeling has provided invaluable insights that have advanced the development of many thermocatalytic and electrocatalytic conversion processes, and it can likewise accelerate the pace of process development for the electrocatalytic conversion of biomass-derived feedstocks. However, the complexity of both the reaction networks of biomass-derived species and the electrochemical environment pose unique challenges, particularly given the need to ensure a reasonable computational cost. Herein, we discuss frameworks and recent developments in methodology for simulating (1) electrocatalytic charge-transfer processes (potential and solvation), (2) large molecule reaction networks, and (3) multiscale electrochemical reaction phenomena. In many cases, the highlighted methods are developed for simpler electrochemical reactions or applied to thermal biomass conversion, but these advances are critical first steps to effective modeling of the more complex electrochemical reactions of biomass derivatives.

4.1. Computational frameworks for the electrochemical environment

In this section, we detail recent advances in modeling of electrochemical environments in periodic-density functional theory (DFT) calculations, which currently balance an accurate representation of the electronic structure of the extended solid electrode with computational tractability. A summary of widely applied methodologies and their corresponding computational cost, is provided in Figure 6. First, we survey common methodologies for including the effect of the electrolyte and the applied potential on the thermodynamic properties of electrochemical conversions. Second, we describe recent advances in the calculation of activation

energy barriers for potential-dependent proton-electron transfer steps involved in electrocatalytic reactions.

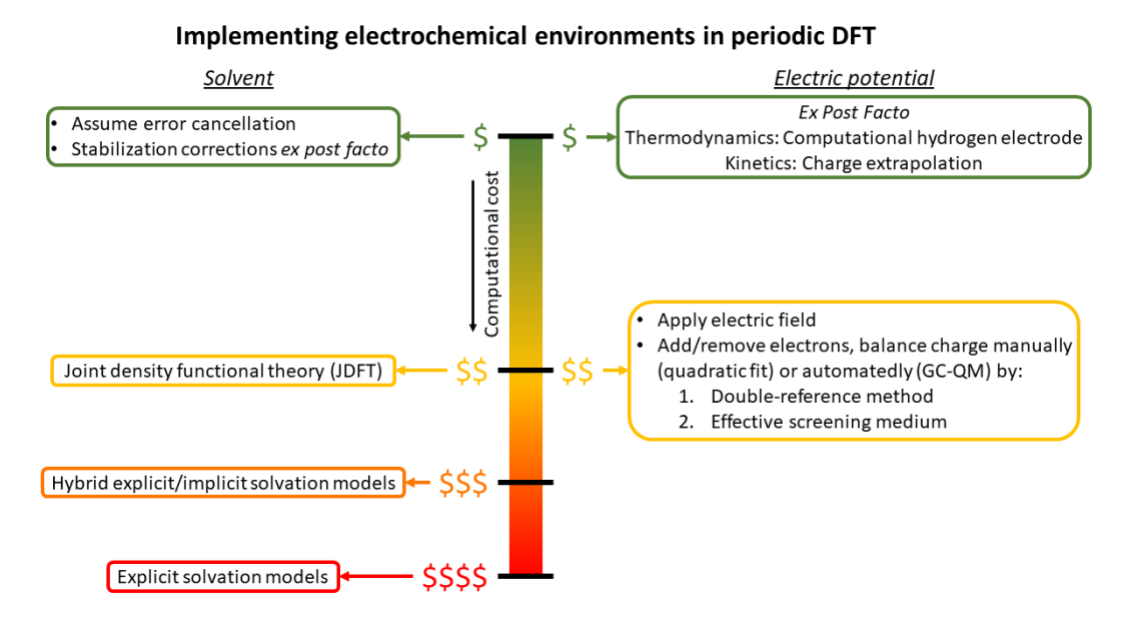


Figure 6. Summary of methodologies to implement solvent and electric potential to simulate electrochemical environments in periodic DFT calculations. The approaches are tiered by their relative computational cost (green – low cost, red – high cost).

4.1.1. Methods to include solvent/electrolyte effects

To capture solvent/electrolyte effects in electrochemical models, both implicit and explicit solvation models are available. There are generally three classes of implicit solvation models that utilize DFT frameworks (example methods in parentheses):³¹² linear solvation (GLSSA13,³¹² SCCS,³¹³ and CANDLE³¹⁴), non-linear solvation (GLSSA13),^{312,315} and non-local solvation (SALSA).³¹⁶ Each of these implicit solvation models seeks to minimize the free energy of the system, including contributions from the electrode surface and surface adsorbates, the implicit solvent, and interactions between these two systems. The primary difference between the

linear and non-linear solvation models pertains to the linear and non-linear treatments of the solvent dielectric response and the response of electrolyte ions.³¹² In contrast, non-local implicit solvation models incorporate non-local dielectric responses using the distribution of solvent molecule centers.³¹⁶ These implicit solvation models are advantageous in that they involve a much lower computational cost than explicit solvation modeling; however, implicit models do not describe direct effects of the applied potential on the hydrogen-bond network, the electrochemical double layer, or interactions between the electrode surface and the electrolyte ions.^{317,318} Commonly used DFT codes for implicit solvation models include VASPsol^{319,320} and JDFTx.^{319–322}

Modeling the solvent molecules explicitly usually requires ca. four water layers above the surface to simulate both the electrochemical double layer and the bulk electrolyte. To obtain meaningful statistical averages for interactions between the metal surface and the solvent, ab initio molecular dynamics (AIMD) simulations are required. Therefore, while this method does allow the user to capture direct information about, e.g., the effect of the solvent's hydrogen-bonding network on intermediate stability, the necessary AIMD simulations require a large computational cost (see Figure 6). Yuk et al. performed AIMD simulations to model and compare benzaldehyde hydrogenation over Pd(111) and Pt(111) under thermocatalytic and electrocatalytic conditions, observing that the presence of solvent reduces C-H and O-H bond-formation barriers.

To overcome the drawbacks of using exclusively implicit or explicit solvent modeling, researchers have developed hybrid approaches.^{325,326} These hybrid methods include a thinner, more computationally tractable explicit solvation layer

above the electrode surface, and an implicit continuum solvation model above this explicit solvation layer to account for bulk solvent/electrolyte.

4.1.2. Computational hydrogen electrode (CHE)

The computational hydrogen electrode (CHE) framework developed by Nørskov et al. has been used extensively to incorporate electric potential effects ex post facto. The CHE approach assumes that, at an electrode potential (U) of 0 V relative to the standard hydrogen electrode (SHE), the reaction of $H_2 \leftrightarrow 2(H^+ + e^-)$ is equilibrated for an electrolyte with 0 pH, 298 K, and 1 bar H_2 in the gas phase. Within the CHE methodology, the DFT-calculated Gibbs free energy (G) is shifted by -eU for each proton-electron pair involved in the reaction step, i.e.:

$$G = E + ZPE - TS - neU$$
 (eq. 1)

where *e* is the electron charge, *E*, *ZPE*, and *S* are the DFT-calculated total energy, zero-point energy, and entropy, respectively, *T* is the absolute temperature, and *n* is the number of proton-electron pairs. Corrections for systems at a pH other than 0 are made by:

$$G(pH) = G(pH=0) - k_B T \cdot pH \cdot ln(10)$$
 (eq. 2)

where k_B is the Boltzmann constant.

The CHE approach works best for reaction mechanisms that can be adequately described by proton-coupled electron transfers, and for which scaling of

activation barriers with reaction energy can be established. Thermodynamic analyses of electrochemical conversion processes via the CHE has seen widespread success in computational catalyst screening through elucidation of reactivity descriptors that reveal volcano-shaped dependence with measured density, overpotential) performance (e.g., current for well-understood electrochemical reactions such as the hydrogen evolution reaction/hydrogen oxidation reaction (HER/HOR) and the oxygen reduction/oxygen evolution reactions (ORR/OER).327-332 For example, Nørskov et al. found a volcano-shaped dependence between the rate of the ORR and the oxygen adsorption energy, and used this insight to identify Pt₃Sc and Pt₃Y catalysts with performances that exceeded pure Pt. 327,332

Recent studies have applied the CHE formalism to study the electrochemical conversion of biomass-derived intermediates. For example, Shan et al. utilized the CHE approach to study Ag, Pb, and Ni as electrocatalysts for furfural reduction to furfuryl alcohol and 2-methylfuran.³³³ Their results suggest that furfuryl alcohol is predicted to be the primary product on Ag and Pb electrocatalysts, while furfuryl alcohol and 2-methylfuran are expected to form from Ni electrocatalysts. In another study, Valter and coworkers modeled glycerol electrooxidation on gold catalysts.¹²⁷ They show through a calculated Pourbaix diagram that the surface is bare under reaction conditions, and that the onset potentials to form a variety of glycerol oxidation products range from 0.39 V to 0.60 V vs. RHE.

4.1.3. Methods to explicitly include electric potential

The CHE formalism presents a highly efficient approach to calculate the effect of an implicit applied electric potential *ex post facto*. However, since the electric potential is only captured implicitly, this methodology does not capture the direct effect of potential on adsorption, reaction, and desorption processes, which may be particularly important when multifunctional surface intermediates with high dipole moments are considered. Possible decoupling of electron transfer and ion (e.g. proton) transfer is also not captured. Several methods have been developed to incorporate an explicit applied electric potential in periodic-DFT calculations, all of which must maintain a net-zero charge for the overall system. The common methodologies described here are to: (a) directly apply an electric field to the system or (b) add/remove charge to/from the system and compensate with either a uniform background charge or sheet of compensating charge away from the catalyst surface.

(i) Directly applying an electric field

In periodic-DFT calculations, the presence of adsorbates on a model catalyst surface induces a dipole resulting in an artificial electric field in the z (surface normal) direction. To account for this artificial electric field, corrections are commonly made by introducing a planar dipole layer to self-consistently compensate for the adsorbate-induced dipole. This dipole layer can be modified (with an appropriately thick vacuum layer) such that it is non-self-consistent and introduces an electric field with a user-specified strength. When the electric field is incorporated in this manner, the presence of the dipole layer results in equal and opposite potentials on both sides of the slab-surface model, giving a sawtooth-shaped external potential profile. Though this method can be used to calculate adsorption properties for

surface intermediates in the presence of an applied electric field, these calculations can suffer from slow convergence due to charge-sloshing effects. Furthermore, this method uses both exposed surfaces of the slab model to screen the potential in the z direction; therefore, it does not utilize a simulated electrolyte to screen the potential, such that electrochemical double layer properties are not captured.

(ii) Add/remove charge to system

Another method to apply an electric potential in the simulation environment is to add/remove charge to/from the system. As mentioned earlier, this charge must be balanced to give a net-zero system charge, which is typically accomplished using one of two methods. The first approach, referred to as the double-reference method, involves a uniform background charge and results in an applied potential due to the difference in charge between the catalyst surface and the background charge. 337,338 Using this method, the electric potential at the slab surface can be calculated for a given charge (q), relative to the standard hydrogen electrode (SHE), as:

$$U_a \text{ (V/SHE)} = -4.6 \text{ V} - \phi_a/e$$
 (eq. 3)

In this equation, ϕ_q is the work function of the slab surface at a charge of q, while 4.6 V is the average value of the work function of the SHE.³³⁸ The work function in this equation must be defined as the energy required to move an electron from the slab surface to the vacuum where the potential is zero. For systems without a vacuum layer that have, e.g., an implicit solvation added, the calculated work function needs

94

to be shifted to account for moving the electron from the bulk electrolyte to the vacuum. This concept is depicted schematically in Figure 7.

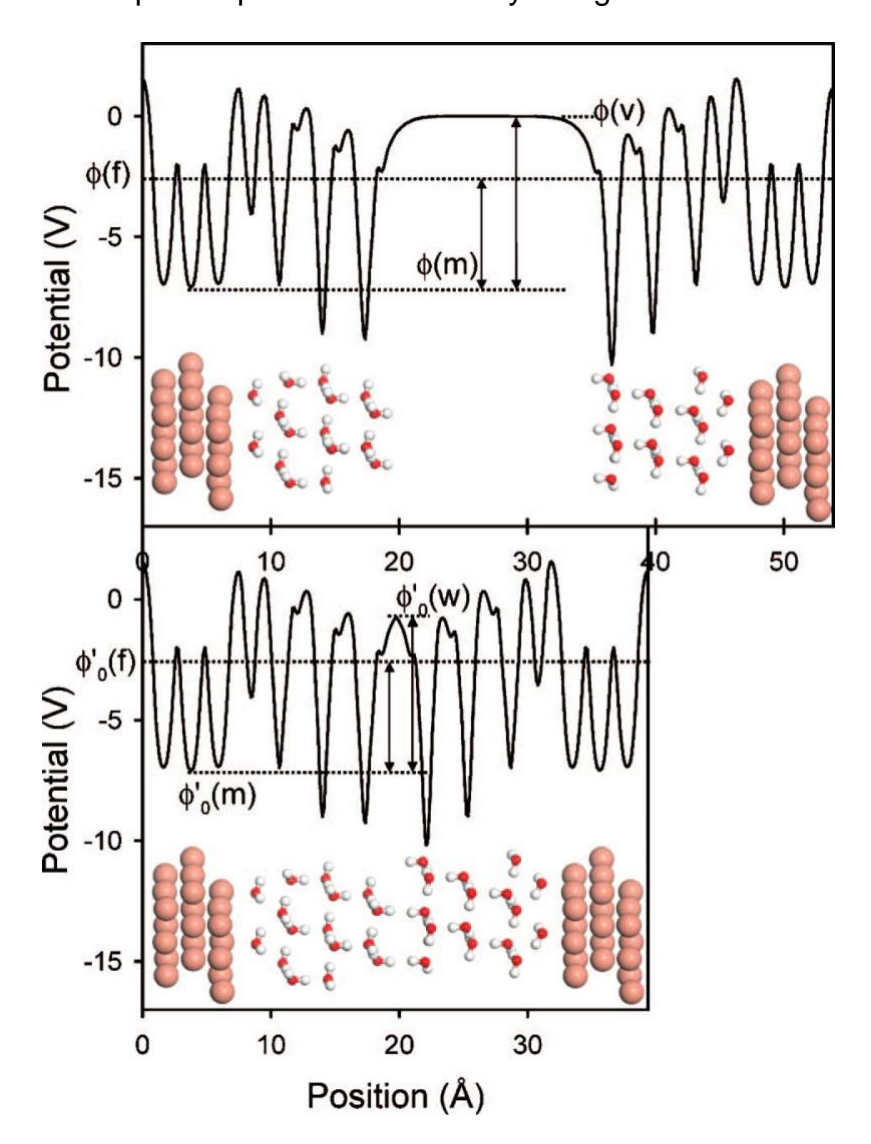


Figure 7. A schematic diagram illustrating the electrostatic potential profile as a function of position across the normal axis of the unit cell. The system shown here contains two symmetric $Cu(111)/H_2O$ slab faces contained within the periodic simulation cell. The variables $\varphi(v)$, $\varphi(m)$, and $\varphi(f)$ denote the position of reference, bulk metal, and Fermi potentials for the double reference model. Top: The slab/water system shown in its elongated form due to the insertion of a vacuum reference electrode $\varphi(v)$. Bottom: The closed unit cell containing the solvent phase reference electrode $\varphi'_0(w)$, the bulk metal

potential $\varphi_0'(m)$, and the Fermi potential $\varphi_0'(f)$. Reprinted figure with permission from Christopher D. Taylor et al. Phys. Rev. B 2006, 73 (16), 165402.³³⁸ Copyright [2006] [American Physical Society].

Applying a uniform background charge to a system requires a correction to the DFT-calculated energy to account for both the energy required to add/remove electrons to/from the system and the interactions of the modeled electrons/ions with the background charge. There are two common routes to implement the doublereference method. The first is to complete the calculations by adding/removing a range of numbers of electrons, with either integer or fractional charges. For each charge value, the corresponding corrected energy and applied potential are calculated. Using this data, the corrected system energy (Ecorrected) is fit as a quadratic function of the applied potential (U). Recent studies have applied this method to study the electrochemical conversion of biomass-derived species. Lopez-Ruiz and coworkers studied the electrochemical hydrogenation of carboxylic acids, ketones, phenolics, and aldehydes on a range of transition-metal surfaces to which they added 1e⁻ charge to simulate reducing conditions.³³⁹ Their analysis showed that the turnover frequency for HER and carbonyl reduction in aldehydes follow a volcano-shaped dependence on the hydrogen and aldehyde adsorption energies, respectively. In another study, Cantu et al. applied the double-reference method in addition to AIMD simulations to study the role of solvent and cathode-surface charge on the adsorption of benzaldehyde and pentanal at Au and graphene cathode surfaces. 340,341 They found that as the cathode surfaces were charged, the presence of organics at the cathode-solvent interface decreased while that of water increased,

negatively influencing the propensity for charge transfer to occur to/from the studied biomass-derived species.

The second route to implement the double-reference method is to perform grand-canonical quantum mechanics (GC-QM) calculations. In this methodology, the user sets a desired applied potential (or Fermi energy based on equation 3) and adjusts the system charge after each ionic step to ensure that the calculation remains at the set applied potential. While there have been successful developments of new, constant-Fermi codes that directly perform GC-QM calculations (e.g., JDFTx),^{321,322} this method has also been successfully implemented in common constant-charge codes (e.g., VASP) using a "computational potentiostat" framework (see Figure 8).^{342–344}

While there have not been, to the best of our knowledge, studies utilizing GC-QM calculations to study biomass-derived intermediates, this is a promising approach that steps beyond ex post facto methods (e.g., CHE) and is increasingly applied to understand the more widely studied electrochemical reactions (e.g., OER, CO2R).³⁴⁵ For example, Garza, Bell, and Head-Gordon calculated the energetics for elementary steps in the electrochemical reduction mechanism for CO₂ to C₂ products on copper surfaces using both the CHE method and the constant-electrode potential (CEP) model.³⁴¹ They found that the rigor of the CEP method is needed to accurately describe adsorbates with high dipole moments and allow their model to predict the formation of all seven experimentally observed C₂ products. GC-QM calculations have been reported to require approximately three times the computational cost as the analogous potential-independent calculations, ³⁴³ indicating that the extension of

these methods to biomass-derived intermediates should be computationally tractable.

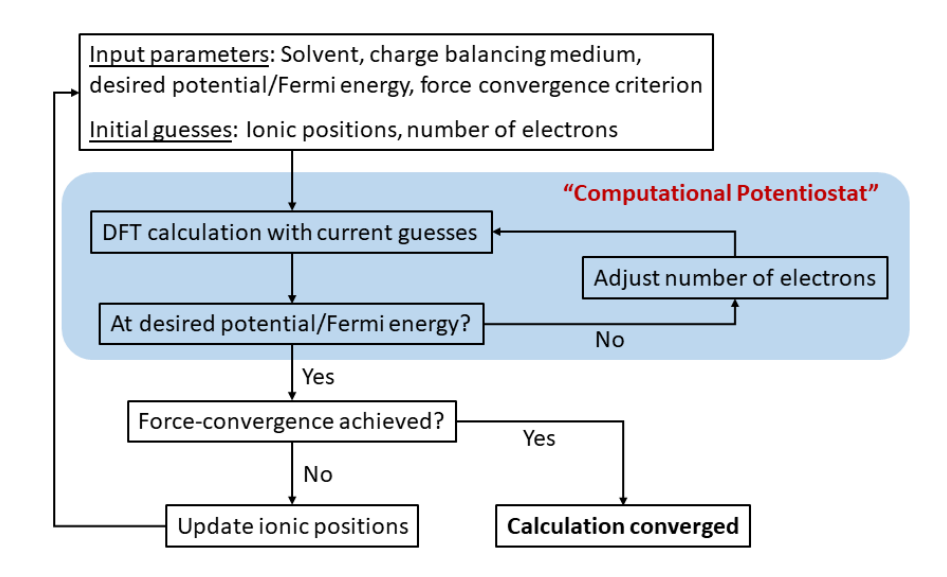


Figure 8. Workflow diagram for the computational potentiostat framework for a grand-canonical quantum mechanics calculation. Adapted from reference ³⁴⁴, (2018) American Chemical Society.

Another approach to balance the added/removed electrons to/from the system is to employ a sheet of semi-infinite uniform electric charge above the slab surface, which both induces a potential between the surface and this sheet and simulates screening of the electric potential by the bulk electrolyte. $^{346-350}$ To determine the operating potential using this framework, the potential-of-zero charge ($U_{\rm pzc}$) potential profile can be used as a reference by comparing the charge-neutral system's potential profile in the z direction to that of the charged system. 351 The user can use this information to tune the applied charge and calculate the corresponding adsorption and reaction energetics under the desired constant-potential conditions.

Herron and coworkers utilized this approach to perform AIMD simulations to study how the presence of an applied potential and explicit solvation model impacts the energetics for the first proton-transfer step in methanol electrooxidation.³²³ Their results showed negative applied biases favored C-H over O-H bond activation, whereas positive applied biases make O-H bond activation more favorable.

4.1.4. Recent Advances in Calculating Electrochemical Activation Barriers

Thermodynamic treatments alone have been widely used to predict the electrocatalytic mechanisms and performance of electrocatalysts, relying on the assumption of Bronsted-Evans-Polyani relationships between reaction kinetics and thermodynamics.^{352–354} However, Exner and Over studied the performance of ab describing electrocatalytic initio thermodynamics calculations in activity. demonstrating that the comparison between thermo- and electrodynamics is only valid when the rate-determining step (RDS) is the same as the potential-determining step (PDS).354 Because this information is not known a priori, caution should be practiced in applying this assumption. For example, the inclusion of applied potential and kinetics to the model developed by Exner showed that volcano plots describing the activity of electrocatalysts toward the HER shifted such that electrocatalysts with endergonic binding of hydrogen, as opposed to thermoneutral adsorption, are predicted to have optimal HER activity.³⁵⁵ In another recent example, Dickens et al. calculated electrochemical OER activation barriers and reaction energetics under an applied potential, resulting in an OER volcano plot that is a function of the current density, as opposed to thermodynamic, limiting-potential volcano plots that are not dependent on the current density.³⁵⁶

In computational thermocatalytic studies, the calculation of activation barriers through DFT is well-established, with a range of possible methods including the climbing-image nudged elastic band (CI-NEB)³⁵⁷ and dimer^{358,359} methods. However, the application of these tools to calculating activation barriers for electron transfer steps requires modifications because electrochemical steps are potential-dependent, and these algorithms were developed primarily for constant-charge codes (e.g., VASP). Therefore, it is imperative that the potential be kept constant throughout the reaction coordinate. Yet, because of limitations in the system size that can be modeled due to the associated computational cost, the operating potential changes across the modeled reaction coordinate (see Figure 9). Here, we provide a summary of recent frameworks to overcome these challenges and accurately calculate potential-dependent activation barriers: first we detail estimation approaches using constant-charge calculations, and then we describe how constant-potential calculations can be extended to calculate activation barriers.

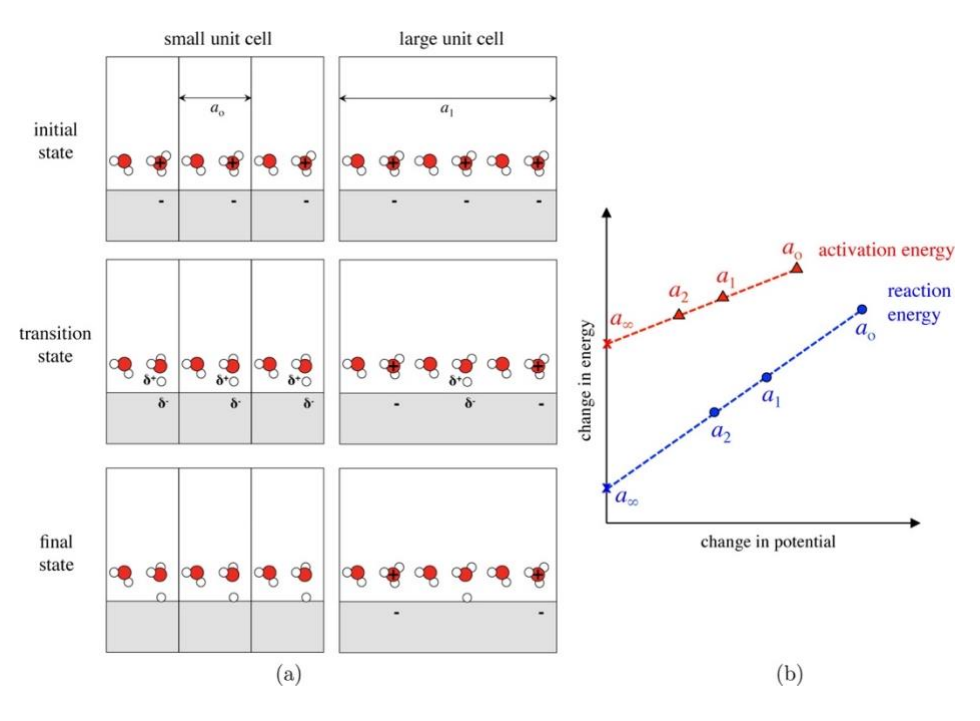


Figure 9. (a) Schematic showing proton transfer to a surface calculated in hypothetical unit cells of different size, a_0 and a_1 . As the unit cell increases in size, the changes in interface charge density and the corresponding potential becomes smaller. (b) Extrapolation of reaction and activation energies calculated at different cell sizes a_i and extrapolated to that at infinite cell size a_∞ , the constant potential limit. Reproduced from reference 360 , (2015) American Chemical Society.

(i) Ex Post Facto Methods

Analogous to the CHE formalism, ex post facto methods have been developed to estimate the potential-dependence of electrochemical activation barriers. Rostamikia et al. developed such a method based on a Butler-Volmer formalism.³⁶¹ In this method, transition states for X-H bond-dissociation or C-OH bond-formation steps are calculated, where this barrier (E_a^0) corresponds to the potential U^0 at which the H or OH species is in equilibrium with the electrolyte. Then, the activation barrier at potential U is calculated as:

$$E_a(U) = E_a^0(U^0) - \beta e(U - U^0)$$
 (eq. 4)

where, e is the electron charge and β is a reaction symmetry term that quantifies the relationship between the activation and reaction energy barriers. Using this approach, Román and coworkers evaluated Au and Pt catalysts for furfural electrooxidation and combined their DFT results with electrochemical reactor measurements to understand the enhanced activity of Au relative to Pt. 186

Another approach, developed by Chan and Nørskov, is the charge-extrapolation method for calculating electrochemical barriers for proton-electron transfer steps. This approach requires a single barrier calculation, as well as the corresponding interfacial charge at the initial, transition, and final states of the pathway. They assume that contributions to the energy change from chemical and electrostatic effects can be separated and derive that the energy change from state 1 to state 2, at a constant potential corresponding to that of state 1, can be calculated as:

$$E_2(\phi_1) - E_1(\phi_1) = E_2(\phi_2) - E_1(\phi_1) + \frac{(q_2 - q_1)(\phi_2 - \phi_1)}{2}$$
 (eq. 5)

where E_i , ϕ_i , and q_i are the DFT-calculated energy, work function (which relates directly to the applied potential, see Equation 3), and interfacial charge of state i, respectively. The interfacial charge can be estimated using well-established methods such as Bader charge analysis. $^{362-365}$ Chan and Nørskov extended upon

this methodology by calculating the activation barrier for an electrochemical step for different unit cell sizes (and therefore different applied potentials). ³⁶⁶ Fitting these activation barriers to the corresponding work function (i.e., applied potential) gives the activation barrier's dependence on the applied potential. From this information, they conclude that the potential-dependence of the activation barrier for the electrochemical steps studied depends on the magnitude of the partial electron transfer that occurs between the initial and transition states.

(ii) Solvated Jellium Method

Kastlunger and co-workers demonstrated an approach for controlled-potential simulations to model elementary electrochemical barriers. He approach, they modeled proton adsorption, in which a proton from the positively charged solvent above the slab surface combines with excess electrons in the metal surface to generate a neutral adsorbed hydrogen atom. This change in metal-surface and solvent charge results in a corresponding change in the work function, and thus the simulated potential, over the reaction coordinate. To overcome this issue, a "solvated jellium" model is employed in which excess electrons are added/removed to/from the system and are compensated by a jellium region of opposite charge in the vacuum layer. To prevent an artificial electric field between the metal surface and this jellium region, a dielectric continuum between the explicitly modeled atoms and the jellium region is introduced, and the jellium slab is immersed in an implicit solvent to better simulate an electrochemical double layer.

For each geometric configuration along the reaction coordinate, an additional check is added between each self-consistent field (SCF) step to ensure that the

added/removed electrons correspond to the target potential (the "computational potentiostat" mentioned above). This approach is like that used for GC-QM calculations outlined in Section 4.1.3 (see Figure 8) but was demonstrated for the calculation of an electrochemical minimum-energy pathway. Similar approaches using a homogeneous background charge through a Poisson-Boltzmann model, with the same updates to the SCF steps to remain at constant potential, have also been used to calculate activation barriers under electrochemical environments.³⁴³

4.2 Modeling large reaction networks

While a handful of studies have used quantum-chemical calculations to model the electrocatalytic conversion of large molecules derived from biomass, 186,367 high computational costs generally restrict the methods to only simple representations of the electrode (e.g., the CHE framework) and reaction pathways that are partially defined by chemical intuition. DFT calculations scale by $O(N^3)$, where N is the number of electrons modeled in the system.³⁶⁸ When considering biomass-derived species, which consist primarily of C₂₊ species, surface unit cells must be enlarged to accommodate intermediates, thereby significantly increasing the computational cost. Adding the electrochemical environment, using the explicit methods described in Section 4.1, further drives up these costs due to the increased system sizes for large molecules, the inclusion of additional electrons in the solvent, as well as the additional equations that must be solved to fully describe the interactions occurring between the surface, adsorbate(s), and electrolyte. Because of these challenges, the methods discussed here for enabling theoretical treatments of large, complex reaction networks have been generally applied to thermal heterogeneous catalysis

and biomass conversion and have not yet been combined with explicit incorporation of electrochemical conditions.

As described for well-understood electrocatalytic reactions in Section 4.1.2., computational modeling has enabled in silico catalyst screening through reactivity descriptors for thermocatalytic reactions involving small reacting species with known reaction mechanisms, such as methanation^{369,370} and ammonia synthesis.³⁷⁰ The descriptor-based approach in computational catalyst screening relies on established linear scaling and transition-state scaling relations.^{371–375} Linear scaling relationships relate the binding energies of reaction intermediates across a range of catalyst surfaces, and are often used to estimate binding energies of adsorbates from that of the atomic species they bind through or the d-band center of the catalyst material. 372,376,377 Transition-state scaling relations connect the thermochemistry of an elementary reaction step with the kinetics by relating the energy of the transitionstate species to the initial- or final-state energy (alternatively, the activation energy barrier can be related to the reaction energy through Bronsted-Evans-Polyani relations).^{373–375} While the error in estimations obtained through these relations can be significant (i.e., 0.2-0.3 eV), limiting their applications in quantitative analyses, their application has been quite successful in predicting qualitative trends across catalytic materials, and even in the design of catalysts with improved performance as demonstrated through experimental tests. 369,371,378

The application of scaling relations in catalyst screening for the conversion of biomass-derived feedstocks could be particularly beneficial, as the reaction networks can be quite large and include many steps and intermediate species that must be computed at a high computational cost. However, establishing and

validating scaling relations and determining appropriate reactivity descriptors requires a set of rigorous first-principles calculations for the intermediates of interest and a clear understanding of the mechanism and rate- or selectivity-controlling step(s). Scaling relations have been reported for some multicenter adsorbates (i.e., intermediates that can bind through more than one atom), such as glycerol and phenol. 376,379 Good agreement between the scaling relation prediction and the rigorous DFT-calculated values (errors of <0.2 eV) was found for many transitionmetal catalysts, but elevated errors were identified in specific cases because of variations in the pi bonds in the intermediate upon adsorption to reactive transition metals and noble metals. This is illustrative of a key challenge in using scaling relations to describe the adsorption and reaction of multicenter adsorbates: as the reacting molecules and catalyst materials become increasingly complex (i.e., multifunctional reactants that can bind through multiple atoms, multifunctional catalyst materials with diverse ensembles of active-site motifs) increased inaccuracies can be expected. For example, variations in adsorption mode, transition-state geometry, or rate-controlling step, across catalytic materials can undermine the applicability of scaling relations in computational studies. 376,379,380 Thus, the use of first-principles-based modeling in catalyst development research for the conversion of biomass-derived feedstocks has primarily focused on earlier stage studies aiming to elucidate reaction mechanisms on a single material or a few similar materials (e.g., reactive transition metals). Examples of such mechanistic studies for the conversion of biomass-derived chemical platforms include the conversion of glycerol on Pt or niobia and the conversion of furfural on Pd, 381-383 as well as thermochemical treatments (i.e., CHE, Section 4.1.2) for the electroreduction

of furfural on Ag, Pb, and Ni catalysts³³³ and the electrooxidation of glycerol on Au catalysts¹²⁷.

Even for studies focusing on a single catalyst material, a full mechanistic analysis can be computationally intensive, because energy minimizations for elementary steps, including consideration of many possible numerous conformations for adsorbed reactants, intermediates, and products are required. To further mitigate the computational cost, semi-empirical approaches, based on group additivity methods for estimating adsorption energies of surface species without requiring a complete quantum-mechanical treatment of the adsorbed state have been used. 383 While the vast majority of contributions in this area have been for gasphase reactions, Gu et. al. recently incorporated an implicit solvent model into their group additivity scheme to describe the Pt/water interface in aqueous phase reforming of ethanol.³⁸⁴ For reaction networks that are highly complex, involving thousands of possible elementary steps, these estimation methods have been combined with rule-based reaction network generation approaches to exhaustively enumerate and describe all possible reaction steps. 385-388 For example, Rangarajan et al. combined (1) automated, rule-based reaction network generation, (2) semiempirical estimation methods, and (3) linear scaling and transition-state scaling to evaluate the relevance of reaction pathways for glycerol conversion on transitionmetal catalysts via microkinetic modeling, for which the total network included 3300 reactions and 500 species.³⁸⁸ Microkinetic models enable extrapolation of theoretical, elementary-step kinetics and thermodynamics to reaction rates under relevant operating temperatures and pressures. 389 A reaction family approach which assumes that reactions with similar chemistry (e.g., protonation, hydride transfer, βscission) can be grouped and parameterized together, is often utilized as a simplifying approach in elementary-step-based microkinetic models of the large reaction networks associated with the conversion of biomass-derived oxygenates. 386,388,390 Current efforts exploring opportunities to leverage machine learning approaches toward both reaction network generation and parameterization (e.g., calculation of elementary step energetics) to further reduce computational costs are ongoing. 391,392 Overall, kinetic studies of large-scale reaction networks can provide important fundamental insight into reaction mechanisms and rate-limiting steps to inform catalyst and process development. An important obstacle lies in the estimation approaches that must be used within these models; errors remain difficult to quantify and can lead to incorrect conclusions when incorporated into the exponential form of reaction rate equations, and therefore careful model validation through microkinetics in combination with experimental data is necessary. 393,394 This will certainly also be the case if such methods are to be extended to the electrochemical conversion of large, biomass-derived molecules.

4.3 Multiscale modeling of electrochemical systems

Our discussion of computational modeling for electrochemical systems thus far has focused on the reactivity of the electrocatalyst as determined by first-principles-based calculations; but, as in thermocatalytic systems, in real electrochemical conversion systems the rates are controlled by both macroscopic kinetics and transport. As described, microkinetic modeling is a commonly used approach for computing reaction rates at physically relevant conditions based on theoretical data for elementary steps (i.e., enthalpy, entropy, activation energy)

computed using either first-principles based calculations on model systems or estimation techniques. For studies of electrochemical reactions, the underlying rate equations in microkinetic models can be parameterized in terms of potential-dependent energetics and used to compute Tafel kinetics for direct comparison with experimentally observed Tafel slopes.^{395–397} This approach has been used to gain insight into the reaction mechanism and effect of the electrochemical environment in widely studied electrochemical reactions including ORR/OER, HOR/HER, CO₂ reduction to CO, among others.

As computational capabilities have increased, recent reports using multiscale modeling have provided unique insight into the interplay between transport and kinetics under electrochemical environments. Nguyen et al. used a combination of DFT calculations and classical MD simulations to demonstrate the effect of the solvent composition and electrode charge on interfacial charge transfer during the electroreduction of benzaldehyde on Au(111).398 In another report, Singh et al. developed a model to describe electrochemical CO₂ reduction on Ag that integrated a continuum model of species transport with a microkinetic model parameterized using DFT calculations (Figure 10) and concluded that the multiscale, multiphysics nature of the model was necessary to determine the physically relevant reaction mechanism, as well as to establish relationships between the product formation rates and the cathode voltage and partial pressure of CO₂ consistent with experimental data.³⁹⁹ Other recent studies report similar conclusions regarding the importance of incorporating both the electrochemical environment and mass transport into model systems aimed at describing electrochemical conversion.³⁹⁷ Notably, there is not yet a standard, off-the-shelf software for generating simulations that integrate transport

and kinetic models. One common approach is to integrate a microkinetic model, written in the numerical programming language of choice, with the COMSOL software package⁴⁰⁰ for transport simulations. For example, the CatINT package offers this approach, and was recently made available as an open source program.³⁹⁷ As with many of the advanced theoretical approaches described throughout this sections, due to the high computational cost, most multiscale studies to date have focused on widely studied electrochemical reactions for relatively small reacting molecules (e.g., CO₂ reduction to CO, HOR/HER, ORR/OER).

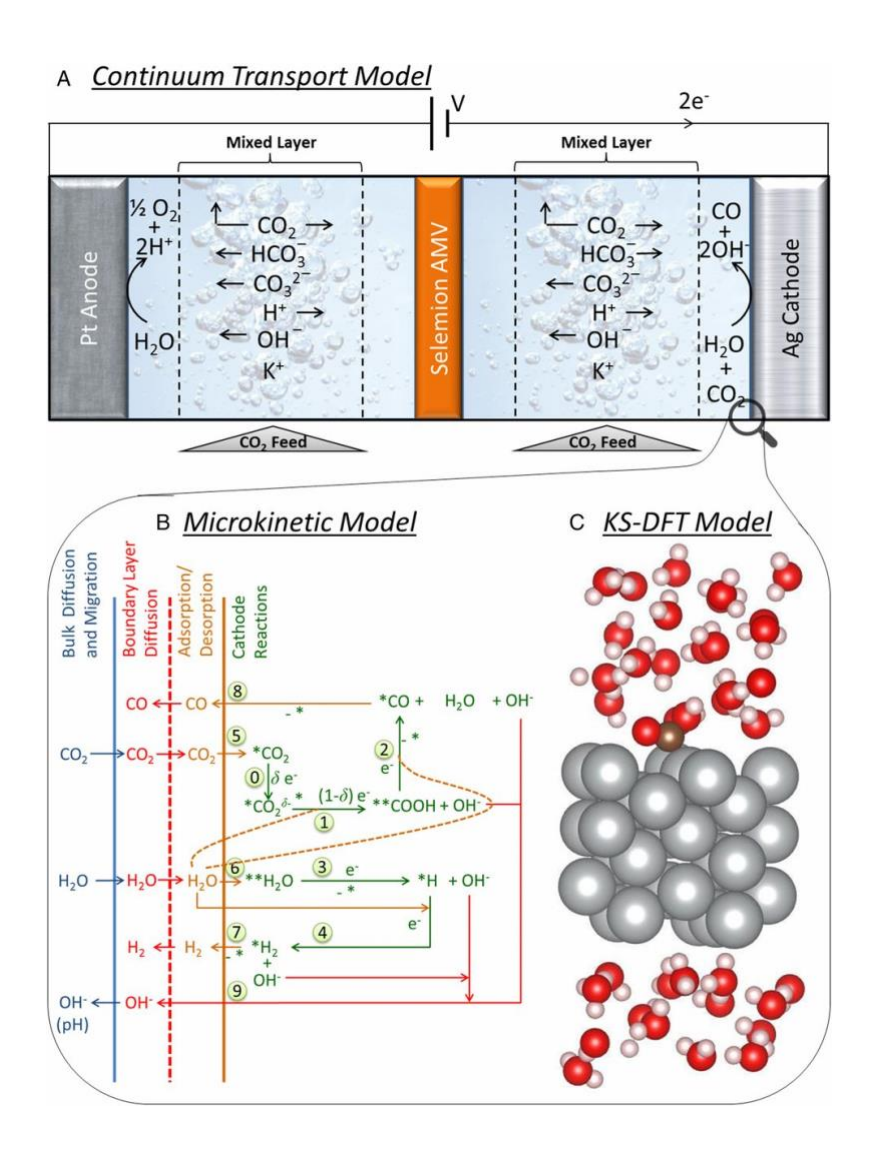


Figure 10. (A) Continuum model for species transport and reaction in a 1D electrochemical cell for CO₂ reduction which is coupled with the (B) microkinetic model showing elementary processes for CO₂R and HER. The microkinetic model is supplied with energetic parameters computed using a (C) DFT model with explicit water layers. Figure reprinted with permission from Proc. Natl. Acad. Sci. 2017, 114 (42), E8812–E8821.³⁹⁹

5. Critical discussions

5.1. Opportunities precedented by electrochemistry of analogues

The aim of this first discussion is to evaluate possible new electrochemical routes that have not been directly demonstrated, but which, by assessment of the authors, seem worthy of investigation based on precedented reactions of chemical analogues. Thus, the specific reactions discussed will not solely involve biomass-derived compounds, but it is attempted throughout to convey the applicability and speculated potential for the suggested pathways. An intended outcome is to move beyond optimization of reactions being currently emphasized and to inspire new efforts to exploit the vast array of functional transformations biomass can offer. Two such avenues include (i) the use of esterification as a preparatory step to permit access to otherwise-challenging transformations, and (ii) coupling chemistries that could fix CO₂ by coupling reactions with common functional groups found in biomass derivatives.

5.1.1 Reduction and oxidation of esters derived from biomolecules

In addition to the shown routes of electrochemical valorization of CAs (such as Kolbe and non-Kolbe electrolysis, and ECH) and ne-AAs, these compounds may

also be converted into bio-esters (by esterification with bio-alcohols) that can be electrochemically reduced to produce alcohols and amino-alcohols, respectively. In this case, the ester function works as an auxiliary group that facilitates the electrochemical reduction of the carbonyl fragment to alcohol. A potential benefit of this approach is that the esterification of the carboxylic function is a good method to permit extraction of these compounds from aqueous solutions (by subsequent distillation); conversion of esters into alcohols and amino-alcohols in a non-aqueous medium can also facilitate the process of extraction of these molecules. Kashimura and coauthors⁴⁰¹ showed several examples of reduction of aliphatic esters on Mg electrodes and in tetrahydrofuran/t-Butanol, as solvent and proton donor respectively, presenting yields of 70 – 90% and F.E. of 40% for production of the respective alcohols. Under similar protocols, the electroreduction of aliphatic esters was used in a convergent paired electrolysis (CPE, paired with the electrooxidation of THF to oxocarbenium ion) to produce 2-alkoxytetrahydrofurans with high yields (77 - 90 %), as can be seen in Scheme 17. It is interesting to note that this CPE is one way to produce protected alcohols that can be used in subsequent reaction steps. 16 Further discussion of paired electrolysis will be provided in Section 5.4.2.

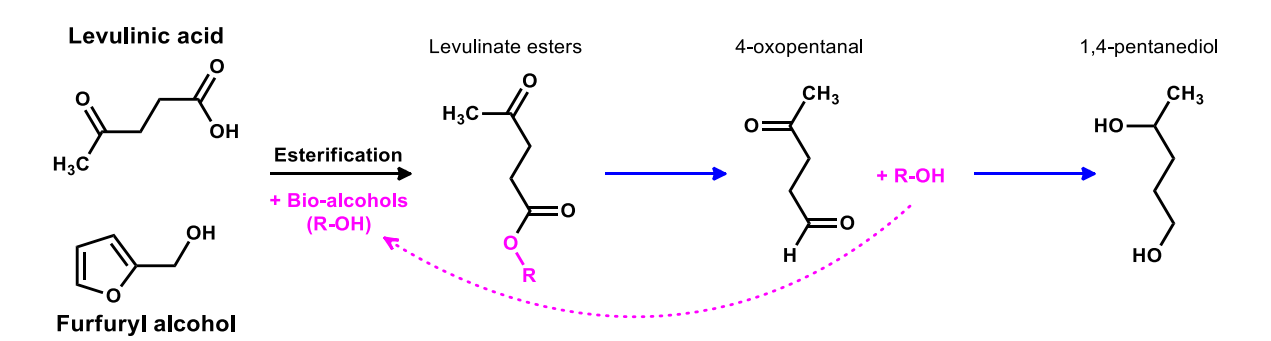
$$\begin{array}{c} & & & & & & \\ & & & & \\ & & & \\ & & & \\ & & & \\ & & & \\ & & & \\ & & & \\$$

Scheme 17. Convergent paired electrolysis to produce 2-alkoxytetrahydrofurans from electroreduction of esters and electrooxidation of THF. Electrolysis performed under a current density of 5 mA cm⁻², 60 - 70% of faradaic efficiency, in 0.01 M LiClO₄ / THF and 6 eq. t-BuOH. The cathode was Mg, anode Pt. Scheme adapted from Murase and coworks⁴⁰², and the general path for electroreduction of esters was also based on several authors.^{401–403}

Based on previous examples, schemes below show some additional electrochemical routes that could reasonably be proposed for the valorization of (i) carboxylic acids (i.e., levulinic, lactic, 3-hydroxypropoic (3-HPA) and malonic acid; succinic and malic acid; fumaric and itaconic acid), and (ii) non-essential amino acids (alanine, glycine, serine, and aspartic acid) *via* esterification (i.e., addition of protecting and/or auxiliary group) followed by electrochemical reduction and/or oxidation. To create these schemes, we are using the well-known paths of oxidation of carboxylic acids (or reduction of esters), and also examples of similar molecules available in the literature. 13,14,16,211,212

i) Carboxylic acids:

The electrochemical valorization of levulinic acid (LA) *via* oxidation of its carboxylic portion and/or reduction of its ketone carbonyl group is well studied, as shown in Section 3.3. Another potential electrochemical route for the production of a diol intermediate from this feedstock is the reduction of levulinate bio-esters. Firstly, the esterification of LA or furfuryl alcohol^{404–406} with bio-alcohols produces levulinate esters, which can then be reduced to 1,4-pentanediol, a building block for the production of high-strength biodegradable polyester polyols, polyurethanes, and other polymeric materials, as well as important fine chemical intermediates. ^{407–409} The conventional thermochemical production of this diol involves the use of noble metal catalysts (such as Rh and Ru)^{410–412} and/or high temperatures (> 150°C) and pressures of H₂ gas (> 6 MPa). ⁴⁰⁷ In contrast, the respective electrochemical route may be performed at ambient conditions. The following scheme shows this proposed route, which is based on the example shown in Scheme 17 and the general path for electroreduction of esters proposed by several authors. ^{401–403}



Scheme 18. Esterification of levulinic acid and furfuryl alcohol followed by electrochemical reduction to produce 1,4-pentanediol.

Following the same trend proposed for levulinate esters, lactate ester, 3-hydroxypropanoate, and malonate esters could also be reduced into valuable diols such as 1,2-propanediol (Scheme 19) and 1,3-propanediol (Scheme 20), respectively. Interestingly, this kind of approach could also be used to convert malonic acid into 3-hydroxypropoic acid (3-HPA), Scheme 20.

Scheme 19. Lactic acid esterification followed by EC-reduction to produce 1,2-propanediol.

Scheme 20. 3-hydroxypropoic acid (3-HPA) and malonic acid esterification followed by electrochemical reduction.

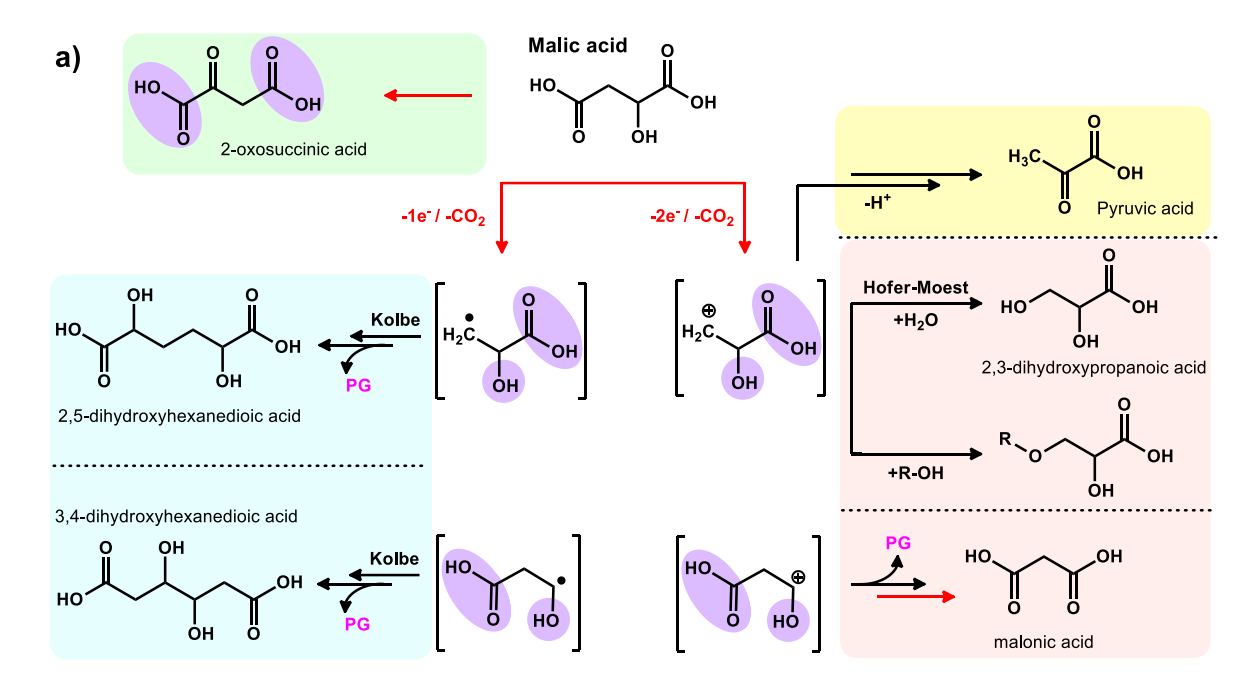
The electrochemical transformation of diacids *via* oxidation is less explored than the respective route for monoacids. This is likely due to the complete combustion of these acids into CO₂ promoted by the oxidation of both carboxylic groups. Protecting one of the groups by esterification or other protecting groups (PG) can be an interesting option to make these molecules more stable towards complete

oxidation and achieve better selectivity toward one specific product.^{218,225,242} A similar approach was previously shown in Scheme 8a, where one of the carboxylic terminations of methyl succinic acid was protected by esterification to specifically produce 2,5-dimethylhexenedioic acid *via* Kolbe electrolysis.²²⁵ Scheme 12 showed another similar protection approach to convert glutamic acid into adiponitrile.²⁴² Therefore, Scheme 21 illustrates potential routes for electrochemical valorization of succinic acid *via* a selective-protection approach, and Kolbe and non-Kolbe paths. Several value-added products can be obtained such as adipic acid, 3-HPA, acrylic acid, and other ether-ester molecules.

Scheme 21. Electro-oxidation of succinic acid. One of the carboxylic acids can be esterified for improving selectivity toward a specific product. ^{218,225,242}

Along the same line of reasoning, Scheme 22a demonstrates that protecting the main carboxylic groups may be a mode for selective electrooxidation of secondary functions—for example, transformation of malic acid into 2-oxosuccinic acid *via* similar routes previously demonstrated for glycerol and other polyol products (*c.f.* Schemes 2 and 3). By protecting the malic acid hydroxyl and one of the

carboxylic groups, the synthesis of a variety of polyfunctional molecules may be achieved. Among those molecules, dihydroxyl-diacids produced *via* Kolbe electrolysis are very interesting; for example, 2,5- and 3,4-dihydroxyhexanedioic acids can be further oxidized to diketones, which are important intermediates for the production of several heterocycles *via* condensation reactions, and other fine chemicals. Scheme 22b shows a likely route where 2,5-dihydroxyhexanedioic acid could be electrooxidized to 2,5-dioxohexanedioic acid, a compound that can be converted into 2,5-furandicarboxylic acid (FDCA, one of the top 12 DOE's value-added chemicals from biomass⁹), *via* Paal-Knorr condensation.⁴¹³ It is also important to comment that, besides furan derivates, these γ-diketones (diketones separated by ethylene group) are also very important intermediates for the synthesis of pyrroles and thiophenes.^{414,415}



Scheme 22. Electrooxidation paths for **(a)** malic acid, and one of the products **(b)** 2,5-dihydroxyhexanedioic acid. Conversion of this dihydroxy-diacid produces a diketone that can be transformed into 2,5-furandicarboxylic acid via Paal-Knorr condensation. For this route, the hydroxyl or/and one of the carboxylic group can be protected (purple shading, PG: protecting group) for improving the selectivity toward one specific product.^{218,225,242}

These diacids may also be electrochemically valorized *via* esterification-reduction routes, following the previous paths presented for levulinate, lactate, 3-hydroxypropanoate, and malic esters (Schemes 17 – 20). As can be seen in Schemes 22 and 23, not only diols/triols (*via* esterification of both carboxylic groups) can be produced from these reactions, but also di/mono-hydroxy-carboxylic acids (*via* selective esterification of one of the carboxylic groups), which are important building blocks.

Scheme 23. Succinic acid esterification followed by electrochemical reduction.

Scheme 24. Malic acid esterification followed by electrochemical reduction.

Unsaturated acids, like fumaric and itaconic acid, not only can undergo ECH as previously shown, but also can be electrochemically hydrodimerized (EHDM reaction). EHDM involves the generation of anion radicals by reduction of electron-deficient double bonds; these reactive species abstract protons from proton-donors (similar to an acid-base reaction) and dimerize *via* radical coupling reactions. Side polymerization paths are a potential drawback of the EHDM reaction because the formed polymers can block the electrode surface. However, these activated alkenes are more easily reduced than the monoacid analogs, and the formed radical anion is less prone to polymerize. HDDM of fumaric and maleic acid derivatives have been studied in the past (in the 1970s and 80s), showing yields higher than 83%. Most of these first studies were performed on Hg electrodes; therefore, the development of new protocols using environmental-friendly conditions would be very interesting for the biomass valorization field. As it was exemplified in Scheme 25 for fumaric acid, another less-evaluated approach arises from the electrochemical transformation of

polycarboxylic acids produced in these routes, where several polyfunctional building blocks can be produced such as branched polyol-polyacid molecules that can be used as monomers for bio-polymer production.

Scheme 25. *a)* Fumaric acid electro-hydrodimerization (EHDM) followed by some examples of electro-oxidation of the polycarboxylic product via Kolbe and non-Kolbe paths. For oxidation paths, some carboxylic groups can be protected (purple shading) for improving the selectivity toward the specific product.^{218,225,242} *b)* Itaconic acid EHDM.

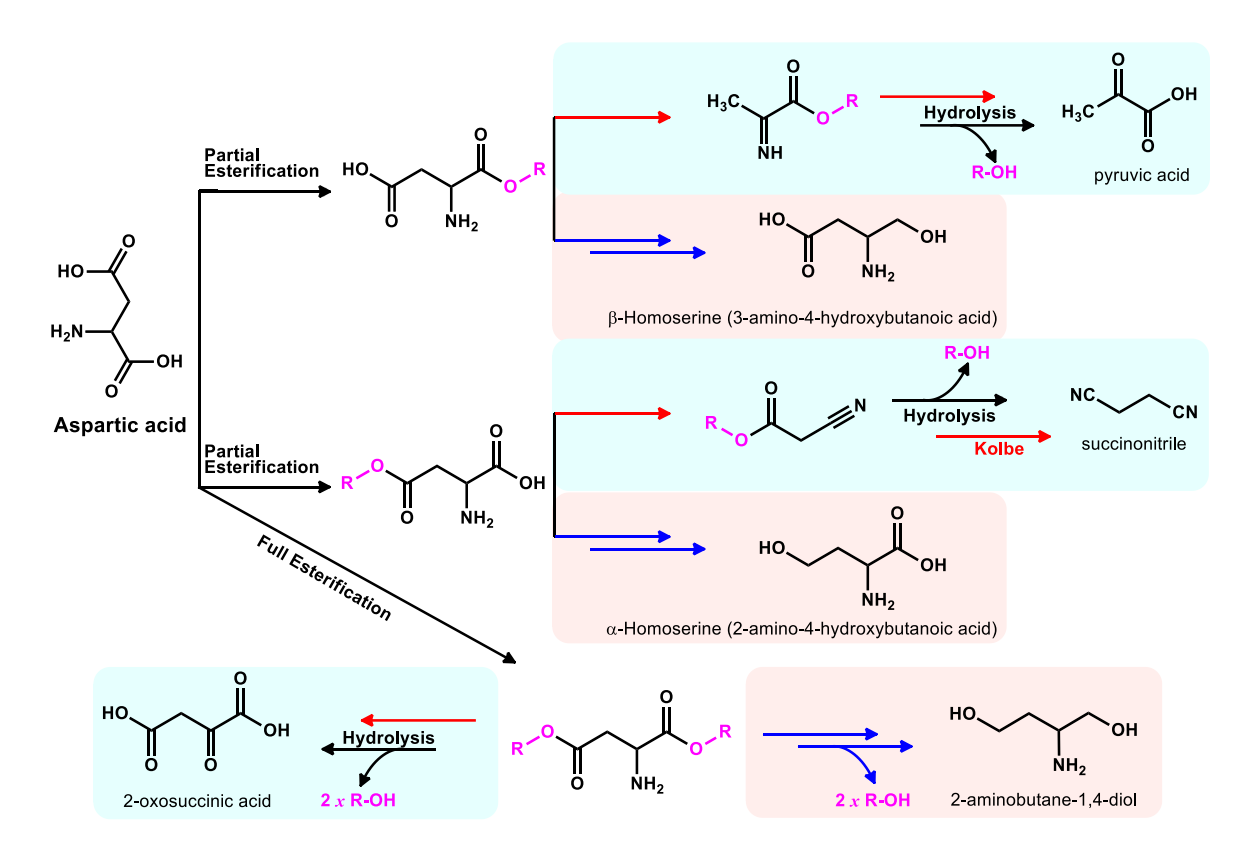
ii) Non-essential amino acids:

As introduced before, the electrochemical valorization of biomass-derived ne-AAs (or AAs from inedible waste proteins) is a potential environmentally friendly strategy for production of N-containing building blocks. In light of this, the following schemes show likely oxidation and reduction paths for conversion of some ne-AA into N-containing building blocks. These routes are based on previous examples,

including the electrochemical paths for glutamic acid and cysteine (shown in Schemes 11 and 12, respectively), as well as paths for carboxylic acids (Section 3.3) and esters (Section 4.1). 13,14,16,211,212 Schemes 25 and 26 show likely paths for production, via esterification-reduction routes, of β-amino-alcohols such as aminopropanol, aminoethanol, aminopropanediol, and aminobutanediol, which are precursors for emulsifiers, food additives, chelating agents, cosmetics, polymers, bioactive molecules, and several other industrially-important compounds.^{237,416} The acarbon of most amino acids found in biomass has L-chirality, and therefore these βamino-alcohols are also chiral. Since electrochemical reactions are performed under mild conditions, it is expected these can retain high enantiomeric excess and may be used as substrates or auxiliaries in asymmetric synthesis. 417 Synthesis of β-aminoalcohols from AAs has generally been performed in hazardous solvents (e.g. tetrahydrofuran) with the use of strong reducing agents (e.g., NaBH₄, 418,419 and LiAlH₄^{420,421}) in large excess–generating a high waste load–or with expensive noble metal catalysts (e.g., Ru-, Rh-, Pt-, Re-based) and high temperatures (80 – 120 °C) and H_2 pressures (40 – 350 bar). 422–425

It is also possible to transform one AA into another through this ester-reduction route, as shown by the transformation of aspartic acid into α - and β -homoserine (Scheme 27). Using the same approach proposed by Fu and coauthors²⁴², aspartic acid can similarly be converted into succinonitrile (Scheme 27). This nitrile is a precursor of 1,4-diaminobutane (DAB, putrescine), which is used in the industrial production of the polyamides such as Stanyl® and EcoPaXX[™]. ⁴²⁶

Scheme 26. Electrochemical conversion routes for **a**) alanine, **b**) glycine, and **c**) serine.



Scheme 27. Electrochemical conversion routes for aspartic acid.

5.1.2. CO₂ coupling to organic functional groups

CO₂ is a ubiquitous carbon feedstock, however, only a small fraction of emitted CO₂ is captured and used. 427 Although CO₂ capture is technologically feasible, the high capture cost and intrinsically low value of CO₂ necessitate the utilization of CO₂ to offset the costs and incentivize capture. Like biomass, CO₂ has been identified as a possible petroleum substitute to produce fuels, chemicals, and materials. CO₂ valorization strategies span from mineral carbonation to produce construction materials to chemical and biological conversion to valuable carbonbased products. 12,24,427,428 Electron-driven utilization of CO₂ has been identified as an important technology in the transition from a linear carbon economy to a circular carbon economy. 12,30,429 This said, direct electrochemical reduction of CO₂ has been extensively reviewed430 and will not be discussed here. However, we discuss possible applications that could merge CO₂ utilization with biomass conversion, based on precedents for electrochemical reactivity between CO2 and various functional groups. In particular, electrocarboxylation (ECC) and heteroatom couplings represent underexplored pathways for fixation of CO2 into organic molecules. The available CO₂ sources that can be leveraged are vast, encompassing the atmospheric supply, to point sources (e.g., biorefineries) and nonpoint sources (transportation). Factors such as purity, supply volume, and proximity to downstream processing (which have been analyzed elsewhere)^{12,427} will inform the utilization pathways of interest, but here we focus on the fundamental chemistries that might be further developed.

CO₂ can be coupled with reactive organic substrates through reduction processes to generate valuable carboxylic acids, which are often precursors to polymers and pharmaceuticals. Reactions of CO₂ with organic molecules can be broadly categorized by two routes: (i) carbon-carbon bond formation to produce carboxylic acids and (ii) carbon-heteroatom bond formation to produce carbonates and carbamates. Functional groups susceptible to ECC that have been demonstrated experimentally to generate carboxylic acids include olefins, alkynes, organic halides, ketones, aldehydes, imines, and alcohols. The corresponding esters are readily available *via* alkylation of the generated carboxylate anion. The electrosynthesis of carbonates and carbamates have been accessed from the coupling of CO₂ and epoxides and amines, respectively. Several reviews have given overviews of all experimentally demonstrated ECC reactions. 431–435 The aim of this discussion is to highlight selected representative examples that transform functional groups that are common in biomass.

The general mechanism of ECC involves the electroreduction of CO₂ and/or an organic substrate leading to formation of the corresponding radical anion (Scheme 28a), which subsequently reacts with the other substrate to generate the carboxylate anion. Most often, this anion is alkylated using ethyl iodide (or another alkylating agent) to form the esters that can be isolated easier than their precursor. Most of the ECC reactions in the literature have utilized sacrificial anodes like magnesium (Mg) or aluminum (Al). In many cases these also play a direct role, for example using the cation (e.g., Mg²⁺) to generate a stabilized metal carboxylate salt.^{432,433} These benefits of sacrificial anodes are married to key disadvantages that hinder industrial-scale application—mainly the cost-ineffective consumption of the

anode, the inability to operate continuously, and the required acid hydrolysis, which increases the purification steps and adds to the waste footprint of the process.

Efforts to replace sacrificial anodes with inert electrodes like platinum and carbon are ongoing with the focus on identifying appropriate counter electrode reactions that deliver stabilizing counter cations to the carboxylate anion. Replacement of sacrificial anodes with inert electrodes will also likely require utilization of a two-chamber electrochemical cell separated by a membrane. Due to the variability in the experimental design for ECC reactions, the key parameters of electrode material, counter electrode reaction, electrolyte, and the type of electrochemical cell will be specified for all reactions discussed.

(i) Olefins

ECC of olefins can result in both mono- and di-carboxylated products (Scheme 28). Carboxylation is possible at the α - and β -positions of the olefin resulting in two possible mono-carboxylated products. For example, ethyl cinnamate was electrocarboyxlated in an undivided cell containing Et₄NBF₄-MeCN and CO₂ with Mg as a sacrificial anode and Ni as the cathode. Global carboxylic acid yield was 78% when the reaction was carried out at -10°C with the low temperature favoring monocarboxylic acid formation. The ratio of β -hydrocarboxylation to α -hydrocarboxylation to dicarboxylation products was 73: 10: 17. The ECC of ethyl cinnamate was also achieved in the room temperature ionic liquid 1-butyl-3-methylimidazolium tetrafluoroborate (BMIMBF₄). Using an undivided cell, Mg as sacrificial anode, and a stainless-steel cathode under a steady stream of CO₂ at 50°C, ethyl cinnamate underwent β -hydrocarboxylation and the corresponding

carboxylic acid was isolated in 41% yield. Hydrogenation of ethyl cinnamate to the saturated ester (yield = 22%) also occurred. Replacement of the ester group of ethyl cinnamate with a nitrile group increased the carboxylation yield to 55% without increasing the hydrogenation yield.

The formation of 2-arylsuccinic acids from aryl-substituted alkenes was accomplished using a Ni cathode and Al sacrificial anode in an undivided cell containing *n*-Bu₄NBr-DMF under 4 MPa CO₂ and applying a constant current density of 10 mA cm⁻² and passing 3 F/mol.⁴³⁸ Styrene was used as a model compound and was successfully dicarboxylated to form 2-phenylsuccinic acid in 87% yield (Scheme 28a). When Ni was replaced with Pt, 89% yield of 2-phenylsuccinic acid was achieved. Expanding the substrate scope, the electrochemical dicarboxylation of αmethylstyrene. 4-methylstyrene. 4-methoxystyrene, 2-vinylnaphthalene, phenylcyclohexene, and 4-fluorostyrene afforded the corresponding dicarboxylic acids in yields of 85%, 82%, 75%, 75%, 50%, and 81%, respectively. Selective βhydrocarboxylation of styrene rather than dicarboxylation to 2-phenylsuccinic acid was pursued using a Ni cathode and Mg sacrificial anode in an undivided cell containing TBABF₄-DMF, 1 atm CO₂, and H₂O as a proton source.⁴³⁹ The concentration of H₂O was critical to changing the selectivity from the dicarboxylation to β-hydrocarboxylation. Without H₂O, the F.E. of dicarboxylation was 89% and upon addition of 0.1 M H₂O, the dicarboxylation yield decreased to 26%, while the F.E. of β-hydrocarboxylation reached a maximum of 65%.

Scheme 28. a) Mechanism of electrocarboxylation of styrene. Path 1 involves the reduction of CO₂ as the first step, while path 2 shows the reduction of styrene as the initial step, and electrocarboxylation of **b)** 1,3-butadiene and **c)** naphthalene.

Unsaturated 1,6-dioic acids have been obtained from 1,3-dienes using AI as sacrificial anode and Ni as the cathode in an undivided cell containing *n*-Bu₄NBr-DMF under 3 MPa CO₂.⁴⁴⁰ The reaction occurred at a constant current density of 10 mA cm⁻² and 4 F/mol of charge passed. Under these conditions, 1,3-butadiene was electrocarboyxlated to 3-hexene-1,6-dioic acid in 84% yield with 42% current efficiency (Scheme 28b).

De Vos et al. expanded the scope of viable conjugated dienes for ECC by demonstrating the dicarboxylation of 1,3-cyclohexadiene, myrcene, and α - and β -farnesene in 96%, 93%, and 72% yield and 64%, 62%, and 48% current efficiency, respectively. This was accomplished in an undivided cell containing TBABr-DMF and 5 bar CO₂ using a Ni cathode and Mg sacrificial anode at a constant current

density of 10 mA cm⁻², passing 2.5 F/mol. Steric bulk and/or electron-donating groups surrounding the conjugated dienes led to decreased carboxylation efficiency. This method was further tailored for the dicarboxylation of conjugated linoleic acid methyl esters (CLAME). Using the optimized conditions of TBABr-MeCN electrolyte, 4 bar CO₂, Ni cathode, Mg sacrificial anode, 3 mA cm⁻², and 3 F/mol, the dicarboxylation of CLAME was achieved with 79% yield and 53% current efficiency. Polycyclic aromatic hydrocarbons also underwent ECC to generate transdicarboxylic acids (Scheme 28c).⁴⁴² In an undivided cell containing *n*-Bu₄NBr-DMF and 4 MPa CO₂ using a Ni cathode and Al sacrificial anode at a constant current density of 15 mA cm⁻² and passing 3 F/mol, naphthalene, 5-methylnapthalene, anthracene, phenanthrene, and 1-H-indene were dicarboxylated to the corresponding trans-dicarboxylic acid on yields of 65%, 55%, 92%, 90%, and 85%, respectively.

(ii) Oxygenates

Oxygenates, such as alcohols, ketones, and aldehydes, are common functional groups in biomass-derived compounds, and ECC has been established as a viable reaction for transforming these functional groups. Ketones are the most extensively explored oxygenate for ECC, while alcohols and aldehydes remain relatively underexplored. ECC of alcohols can produce carbonates^{443–445} or carboxylic acids.⁴⁴⁶ Hu et al. utilized ordered mesoporous carbons embedded with Cu nanoparticles (Cu/OMC) as catalysts for the ECC of benzyl alcohol to benzyl methyl carbonate (Scheme 29a).⁴⁴⁴ The electrochemical reaction was carried out in a two chamber cell using CO₂-saturated TBAI-CH₃CN as the electrolyte, Cu/OMC

deposited on carbon paper as the cathode and graphite as the anode. The electrocatalytic activity was highest for Cu nanoparticles with an average particle size of 31 nm and a maximum yield of 70% was achieved. The yield was only 12% when OMC was utilized as the catalyst without embedded Cu. Senboku et al. demonstrated the ECC of benzyl alcohols containing electron-withdrawing groups on the phenyl rings to the corresponding phenylacetic acid (Scheme 29a). 446 Using an undivided cell containing Bu₄NBF₄-DMF, CO₂, Pt as the cathode, Mg as the anode, *para*-cyanobenzyl alcohol was converted to the corresponding phenylacetic acid in 78% yield. Strong electron-withdrawing groups on the phenyl ring in either the *para* or *ortho* positions was necessary to promote ECC. Production of the carboxylic acid was proposed to occur *via* two possible routes: (1) generation of a carbonate intermediate, or (2) direct reduction of the alcohol to the carboxylate (Scheme 29a). Both paths result in reductive cleavage of the C-O bond followed by CO₂ fixation at the benzylic position.

Scheme 29. a) Proposed mechanism of electrocarboxylation of aromatic alcohols to produce carbonates (path 1) or carboxylates (path 2). **b)** Competing pathways for the electroreduction of benzaldehyde (R = H) or acetophenone ($R = CH_3$) under a CO_2 -saturated electrolyte. **d)** Electrocarboxylation of benzylamine to generate corresponding carbamate.

The ECC of ketones, which generates α-hydroxy acids, was first described by Wawzonek in 1960 through the conversion of benzophenone and acetophenone to benzylic acid and 2-hydroxy-2-phenylpropionic acid, respectively. 447 Reduction of the ketone rather than CO₂ is considered the first step in the ECC mechanism resulting in significant presence of ketyl radical anions in the reaction mixture. Due to this, vicinal diol dimer formation (pinacols) and proton-coupled electron transfer (PCET) reactions to form alcohols are competing pathways during ECC of ketones (Scheme 29b). 432,448 Therefore, careful selection of reaction conditions, such as CO₂ pressure, substrate concentration, cathode material, and solvent, is needed to minimize side reactions and increase the yield of α-hydroxy acids.

Aromatic ketones are the most extensively explored ketone containing substrate for ECC. Using Ni as the cathode and Al as sacrificial anode, Gaoging et al. demonstrated the ECC of acetophenone, benzophenone, 6-methoxy-2acetonapthone, 4-methylacetophenone, and 4-methoxyacetophenone to the corresponding α-hydroxy acids in yields of 80%, 90%, 83%, 56%, and 62%, respectively.449 The experiment was done in an undivided cell containing tetra-nbutyl ammonium (TBA) bromide in dimethylformamide (DMF) electrolyte and 4 MPa CO₂ with the reaction occurring at room temperature at a constant current of 10 mA cm⁻², passing 3 F/mol. The current efficiency reached a maximum of 60% for the conversion of benzophenone. For aromatic ketones containing electron-donating groups (-CH₃ and -OCH₃), yields to the corresponding α-hydroxy acids decreased as pinacol formation increased. The ECC of benzophenone and substituted derivatives of benzophenone was also explored by Zhang et al.450 and Survanarayanan et al.451 The conversion of benzophenone to benzilic acid was accomplished by Zhang et al. using in 95% yield using an undivided cell at room temperature containing Et₄NBF₄-DMF, 1 atm CO₂, Mg as sacrificial anode, and glassy carbon as the cathode. 450 Stainless steel was also identified as viable cathode material when TBAI-DMF was the electrolyte and the reaction occurred at 0°C. Introduction of electron-withdrawing groups to the para position on the phenyl ring in benzophenone resulted in decreased yields of the α-hydroxy acids and was attributed to the lower activity of the ketyl radical anion towards CO₂ activation.

Suryanarayanan et al.⁴⁵¹ demonstrated the ECC of benzophenone to benzilic acid in 87% yield using Ag nanoparticles on boron-doped diamond (Ag-BDD) as the cathode in an undivided cell containing TBABF₄-DMF and a Mg sacrificial anode. *In-*

situ electron spin resonance spectroscopy revealed the formation of stable ketyl radicals on the surface of Ag-BDD. Following this work, Suryanarayanan et al.⁴⁵¹ identified Ag-Cu bimetallic composites as catalysts for the ECC of benzophenone.⁴⁵² Using an undivided cell containing TBABF₄-DMF, CO₂, Mg as sacrificial anode, and Ag-Cu composite electrodeposited on glassy carbon, benzophenone was electrocarboxylated to benzylic acid with a maximum yield of 94% achieved over Ag₇₇Cu₂₃ while passing 2.1F/mol. Increasing the Cu concentration in the composite led to higher yields, reaching a maximum over Ag₇₇Cu₂₃ with further increases in Cu content resulting in decreasing yields.

Zhang et al. explored the impact of ionic liquids on the ECC of aromatic ketones. The ionic liquids (1-butyl-2,3-dimethylimidazolium tetrafluoroborate ([BMMIM][BF4]; $[H_2O] = 9.2$ mM) and 1-butyl-1-methylpyrrolidinium bis-(trifluoromethylsulfonyl)imide ([BMPyrd][TFSI]; $[H_2O] = 1.0$ mM)) were utilized as the electrolyte in an undivided cell with a glassy carbon cathode, Mg sacrificial anode, 453 and a CO_2 atmosphere. Using [BMPyrd][TFSI] as the electrolyte resulted in the conversion of acetophenone to 2-hydroxy-2-phenylpropionic acid with 98% yield while use of [BMMIM][BF4] led to the generation of 2-hydroxy-2-phenylpropionic acid in only 15% yield due to the formation of dimers (25%) and 1-phenylethanol (60%) from competing side reactions. Increasing the H₂O concentration in [BMPyrd][TFSI] from 1.0 to 630.0 mM switched the selectivity of the reaction from ECC to dimerization (100% yield).

Few examples of ECC of aldehydes have been demonstrated in the literature^{454,455} and limited information is provided on the mechanism or impact of reaction conditions on the electrocatalytic performance. One example to note is the

conversion of benzaldehyde and acetaldehyde to the corresponding α-hydroxy acid in yields of 40% and 9%, respectively, using a one chamber cell containing Bu₄NBr-DMF, 1 atm CO₂, Zn as the cathode, and Al as a sacrificial anode.⁴⁵⁵

(iii) Amines

Fixation of CO₂ into amines generates new C-N bonds in the form of carbamates (RNHCO₂⁻). In general, the generated carbamate anion is alkylated using ethyl iodide (or another alkylating agent) to form the carbamate ester that can be isolated easier than its precursor. Casadei et al. established the procedure for the ECC of aliphatic and aromatic amines in a divided cell containing a Cu cathode, Pt anode, and 0.1 M triethylammonium perchlorate (Et₄NClO₄) in MeCN solution continuously bubbled with CO₂. 456 Benzylamine was converted to benzylcarbamate with 92% yield (Scheme 29c).

Feroci et al. expanded on this work and demonstrated the viability of ECC of amines in 1-butyl-3-methylimidazolium tetrafluoroborate (BMIm-BF₄). The experimental set-up used a divided cell with a Pt anode with the reaction occurring at 55°C in the presence of 1 atm CO₂. ⁴⁵⁷ Pt, Cu, and Ni cathodes were evaluated for the ECC of primary and secondary aliphatic amines and the highest yields of the carbamate were achieved for Pt cathodes. Benzylamine undergoes ECC followed by alkylation to form ethyl benzylcarbamate with an 80% yield at an applied charge of 3 F/mol (i.e., faradaic efficiency of 53%). Yields between 76-87% were achieved for other primary and secondary aliphatic amines with the highest yield of 87% achieved for the ECC of *N*-benzylmethylamine.

The established ECC of amines was further expanded to include diamines to generate bis-O-alkylcarbamates. 458 Using an H-cell, Cu cathode, and glassy carbon anode, ECC of the model compound, hexamethylenediamine, was performed in 0.1 M tetetraethylammonium chloride MeCN solution and the bis-carbamate was isolated in > 90% yield. This methodology was expanded to aliphatic diamines and benzyl diamine and the corresponding bis-carbamate were prepared in yields >80%. Aromatic diamines, however, remained unreacted under these reaction conditions. More complex carbamates can be synthesized by replacing the simple electrophilic alkylating agents such as ethyl iodide with arylketones to generate O-β-oxoalkyl carbamates. Wang et al. coupled arylketones, amines, and CO₂ at 40°C in an undivided cell containing tetrabutylammonium iodide (n-Bu₄NI) in MeCN with Pt as the cathode and the anode. 459 Propiophenone and dibutylamine were coupled in the presence of CO₂ to produce the corresponding O-β-oxoalkyl carbamate in 65% yield. The reaction scope was limited to aryl ketones, open-chain secondary amines, and cyclic secondary amines; aliphatic ketones, primary amines, and anilines remained unreacted. Lower yields were observed for cyclic secondary amines, which was attributed to steric hindrance. The proposed mechanism of O-β-oxoalkyl carbamate electrosynthesis proceeds via hydrogen atom abstraction from the arylketone by the in-situ generated iodine radical to form the corresponding radical, which is halogenated by the *in-situ* generated molecular iodine. The electrophilic halogenated derivative of the arylketone is coupled with the ECC formed carbamate anion to produce the desired *O*-β-oxoalkyl carbamate.

Moving Beyond Sacrificial Anodes

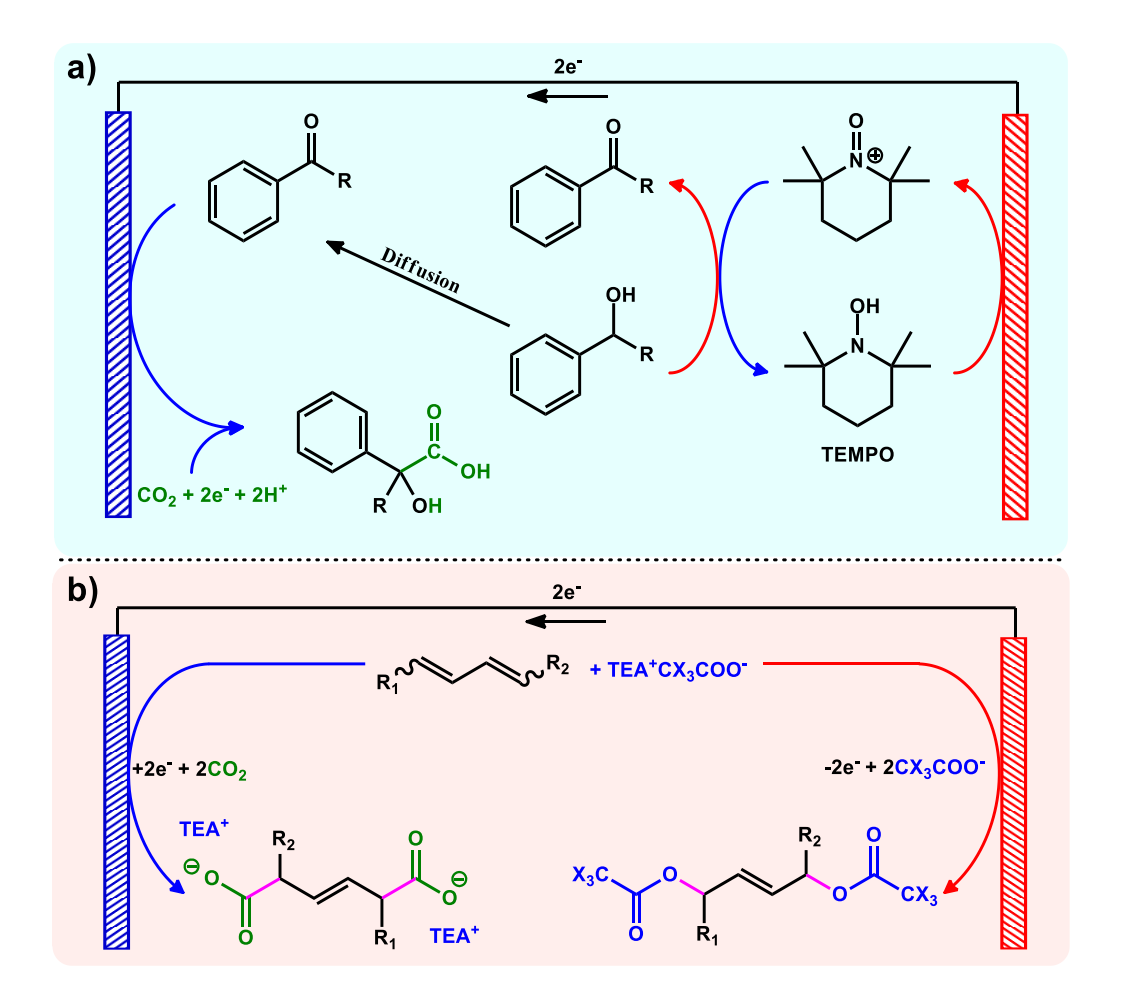
The standard electrochemical configuration employed for ECC reactions is an undivided cell with a sacrificial anode. As outlined previously, industrial-scale ECC will require replacement of sacrificial anodes with inert electrodes. Platinum or carbon electrodes, the most common substitutes, can perform a benign counter reaction and deliver the stabilizing cation to the generated carboxylate anion. There is value to be found, however, by selecting an anodic reaction to further upgrade the organic substrates undergoing ECC at the cathode. Two strategies have been employed to use the anodic reaction to add functionality to the organic substrates:

(1) oxidize the organic substrate at the anode followed by ECC at the cathode to generate one unique product (tandem paired electrosynthesis) and (2) the organic substrate undergoes separate, but simultaneous reactions at the anode and cathode to generate two unique products (divergent paired electrosynthesis). Such paired reactions are discussed further in Section 5.4.2.

Following the first strategy, Muchez et al. used a glassy carbon electrode as the anode to facilitate the TEMPO-mediated oxidation of an aromatic alcohol to the corresponding ketone and aldehyde, which underwent ECC at a Ni foil cathode to α-hydroxy acids (Scheme 30a).⁴⁶⁰ The reaction proceeded in an undivided electrochemical cell using 0.1 M tetraethylammonium acetate (TEAAc) in MeCN at room temperature with 5 bar CO₂. Water (0.03 M) was added to the reaction mixture to facilitate proton transfer from the alcohol to TEMPO during the oxidation. At an applied charge of 3 F/mol, 1-phenylethanol was oxidized with 85% yield and electrocarboyxlated to 2-phenyllactate with a yield of 36%. The scope of the reaction was expanded to include benzyl alcohol conversion to mandelic acid with a yield of 15%, and benzhydrol conversion to benzylic acid with a yield of 59%. Screening Zn,

Sn, Mo, and Ta as cathode materials revealed the yield to 2-pheynllactate increased to 38% over Mo (F.E. = 25%) and benzylic acid yield was 61% over Zn (F.E. = 41%). The low ECC efficiencies are attributed to proton- and water-induced side reactions such as pinacol dimer formation, reduction to alcohols, and disproportionation to ketone and alcohol via α -hydrogen abstraction.

In accordance with the second strategy, Matthesen et al. established a protocol for the simultaneous cathodic carboxylation and anodic acetoxylation of conjugated dienes to dicarboxylate salts and diesters, respectively (Scheme 30b).⁴⁶¹ Using an undivided cell, 1 bar CO₂, 0.15 M tetraethylammonium trifluoroacetate in MeCN, and applying a charge of 1.5 F/mol, 1,3-cyclohexadiene was transformed to tetraethylammonium 2-cyclohexene-1,4-dicarboxylate at the Ni cathode and 2-cyclohexene-1,4-di(trifluoroacetate) at the graphite anode with yields of 35% and 49% respectively. Attempts to expand the scope were challenging, highlighting the limited versatility of this method, as terminal double bonds facilitated ECC, but not acetoxylation, while internal double bonds in aliphatic chains demonstrated the converse reactivity.



Scheme 30. a) Tandem paired electrosynthesis of α -hydroxy acids via electrocatalytic coupling of alcohols and CO_2 without the use of sacrificial anodes. Adapted from Kim and coauthors. b) Paired electrosynthesis of diacid and diester (diol precursor) from conjugated dienes, carbon dioxide, and tetraethylammonium (TEA) acetate salts (with X = H or F). Adapted from De Vos and coauthors. 461

5.2 Benchmarking and protocols for comparing data

Based on the current state-of-the-art, a number of critical needs can be identified in order to facilitate organization, understanding, and advancement in the application of electrochemistry to biomass conversion. First and foremost, review of

the wide range of literature to date makes clear that the conditions under which measurements are recorded are in great need of standardization. Reactions are frequently reported without (i) closure of mass and energy balances, (ii) validation of measured reaction performance and interplay with electrostatic and transport phenomena at the cell-scale, and (iii) uniform rate definitions and reporting conventions. These issues span far beyond the fields being reviewed, and certain aspects have been mentioned in recent perspectives. 462,463 Nevertheless, the complex combination of biomass and electrochemistry amplifies the need for diligence. Thus, the authors suggest the following "best practices" should be observed for various laboratories to improve reproducibility, make direct comparisons of data, and to build on each others' results.

5.2.1 Establishing mass and energy balances

The basic need to fully account for the inputs and outputs of the system is critical —not only so that performance can be compared, but also so that the process can be meaningfully discussed in the context of scale-up and incorporation into larger, integrated networks of unit operations at a plant level. While it is understandable that accounting may be imperfect in new, exploratory studies, the standard for any given new reaction chemistry needs to rapidly move toward closure of mass and energy balances. This is in principle a simple concept, but in practice, several challenges must be overcome.

First, electrochemistry can frequently generate products spanning gas evolution, solid deposition, and both solvated and phase-separating liquids. Consequently, rigorous assays are often a challenge and require a suite of

coordinated analytical techniques. Analysis methods for gases and liquids are generally well established and frequently consist of a chromatographic or other separation, followed by appropriate detection (thermal conductivity, mass spectrometry, flame ionization detection, UV-absorbance, IR-absorbance, refractive index, to name a few). NMR assays can also be invaluable in identifying species present, though extra care must be taken not to miss overlapping peaks due to solvent suppression sequences; isotopically labeled solvents can circumvent some of these concerns for clarifying experiments but are generally not scalable for routine analysis. Solids analysis can present more difficulties, particularly if reactants or products polymerize or deposit on an electrode (and if the electrode contains elements in common such as carbon) or a separating membrane, but an array of elemental analysis methods are available. Basic combustion analysis can provide elemental ratios of organics to close the mass balance, while auxiliary chemical analysis by IR, XPS, or solid NMR can be used to ascertain general characteristics and functionalities present.

An additional source for ambiguity in charge balances can lie in reactions where substantial charging of a mediator species is performed prior to the introduction of target molecules. This can be particularly significant for polymediators, as noted in a recent work where a soluble polyoxometalate (POM) was used as a multi-electron mediator for electrochemical hydrodeoxygenation of bio-phenols into hydrocarbons.³⁰³ The state of charge of the solution species before and after reaction must be included in the final accounting of Faradaic efficiency. Finally, care should also be taken to analyze both working and counter electrode chambers for separated cells, to assess unwanted reactivity at the counter electrode,

and to assay membranes, which not only can be prone to crossover, 464 but can also absorb and act as a sink for certain organic molecules. 465,466

Beyond the "apparent" mass and energy balances of reaction, many reaction pathways may involve a mixture of chemical and electrochemical steps, some of which may even involve homogeneous oxidation/reduction (or disproportionation) such that assigning charge balances (Faradaic efficiency) may not be representative of solely Faradaic processes. Some of these reactions may be intricately coupled to the electrochemistry, while others may manifest due to inadequate purification of starting materials or storage conditions prior to analysis. Trace components can be particularly susceptible to misassignments, as has been often noted in fields such as electrochemical N₂ reduction, where impurities have been found to represent a significant portion of NH₃ identified as "product". 467 Common examples of non-Faradaic interference in the charge balance would be Cannizzaro disproportionation of aldehydes (to carboxylic acid and alcohol) at high pH and concentration. 177 As a specific example, the local pH close to the working electrode under electrochemical reduction of furfural tends to be basic (even for electrolysis in an acid medium because of competing HER), favoring the Cannizzaro reaction to chemically produce furoic acid and furfuryl alcohol, which is also a likely product of electrochemical reduction of this compound. In this example, some of the furfuryl alcohol produced from Cannizzaro could be wrongly counted in the Faradaic efficiency calculation, generating an inflated electrochemical performance. Care must be taken through the application of multiple chemical analysis tools (chromatography, spectroscopy, etc), and these studies must involve control measurements done over variable periods using each detectable species and combinations thereof in representative

environments (electrolyte, solvent, temperature, pH, etc) in order to separate the time scales over which various chemistries are relevant.

Energy balances are also critical to consider, particularly for any process that will be operated on a large scale. The most significant challenge to closing energy balances (besides the need to first close the mass balance) is the limited availability of thermodynamic data. Many structures do not have well-established enthalpies and entropies of formation, and contributions of solvation will also modify equilibrium potentials relative to those calculated from gas-phase thermochemistry. 41,468 Advances in ab-initio methods are a promising avenue to begin closing this gap, and other approaches such as group-additivity methods^{469,470} can also at least provide insight for rough estimates of the energetic practicality of a given transformation. Presuming that reliable thermochemical data is available for all relevant species, the closure of the energy balance then requires computing the heat and electrical work that each (net cell) reaction generates (or consumes), weighting it by the proportion of current passed to each respective reaction, and comparing against the actual energy input (or generation for galvanic cells) to determine the overall efficiency of the process. While there may be a temptation to consider each of these processes in the context that renewable electricity will be abundant and cheap, projections highlighted in Section 5.4 indicate the capital and operating costs for relevant scale processes will remain high for the foreseeable future. Well-informed comparison against efficiency for alternative thermochemical processes will also allow a more informed establishment of benchmarks, such as a maximum acceptable overpotential for a reaction.

5.2.2 Cell validation and consistency of reaction conditions

Coupled to the broad need for mass and energy balances is a need for well-documented reaction conditions to ensure reproducibility. It is well established that many variables in the electrochemical system contribute to its net performance, yet it is a frequent practice to assign performance metrics (rates, product selectivities, etc.) to conditions defined just by a given combination of electrode, electrolyte, potential, current density, temperature, and/or reagent concentrations or pressures. These are all critical variables to record, but in many cases are not (or not fully) documented. For example, galvanostatic electrolysis is often reported with no information on the change in potential vs. time.

In batch cell reactions (as most research studies employ), as the reagent is depleted, the overpotential will rise to maintain the rate, and a portion of this current may correspond to secondary reactions. Some works assume that the chemistry being studied is highly selective and the product is insensitive to potential. However, this must be validated, and such clean selectivity will rarely apply to aqueous chemistry of biomass derivatives. Drifts in potential are also necessary to document in order to close the energy balance. Potential, alongside temperature and concentrations, thermodynamically defines the system. Thus, these are the relevant quantities for interpretation of benchmarks and understanding kinetics; these must be reported at regular intervals within batch reactions and at regular points along flow paths where applicable in reactors with spatial inhomogeneity.

Coupled to the thermodynamic definition of reaction conditions is the determination that these supposed conditions are indeed uniform within a cell. Electroanalytical chemists are trained to construct systems in a manner that permits

several convenient, simplifying assumptions, discussed below. Unfortunately, the common electroanalytical assumptions are often extrapolated—particularly by inexperienced researchers who may specialize in other fields and wish to use electrochemical techniques. Analytical systems are generally designed with the use of large excess of supporting electrolyte, low current density (relative to the supporting electrolyte), oversized counter electrodes, well-defined reference electrode placement, and vigorous mixing; these collectively allow assumptions that the electrochemical processes at the working electrode are solely influenced by the chosen potential and are determinate from a pure reaction-diffusion modeling framework. 471,472 These types of fundamental studies are critical (and still sparse in the area of biomass-derived molecules), but when translating to systems that scale to high current density and bulk conversion of reactants, some parameters are not always practical to control. For example, heterogeneity in local electrolyte concentrations emerging from solution resistance effects can lead to non-uniform distribution of equipotentials (and thus current density) across an electrode surface. When constructing systems aimed at high rates of bulk electrolysis, care must be taken to choose geometries that are well defined and not prone to distortion in anticipated current distributions^{473,474} —e.g. with aligned, macroscopically flat electrodes of the same size, and documented separation. Well-characterized commercial systems may also be a wise choice for reproducibility without creating undue extra work. 475,476 More complex geometries and cell designs might be invoked for practical reasons for specific chemistries, but it is particularly critical to characterize their expected primary, secondary, and tertiary current distributions, as well as correlated temperature and concentration gradients, with multiphysics

simulations. Misunderstandings generated by ill-defined benchtop chemistry will only be exacerbated in scale-up.

5.2.3 Catalyst reporting conventions

Novel catalytic electrode materials and catalytic molecular mediators occupy a wide portion of current research efforts in electrochemical conversion. Presuming the system is well-characterized with respect to the macroscopic inputs, outputs, and defined conditions, materials comparisons can commence. The primary and highly sought figure of merit, relevant to both electrocatalytic surfaces and mediated systems, is the assignment of "activity".

In the case of surface-mediated catalysis, extensive discussions from fuel cell and electrolysis communities reveal lessons that can be heeded.²² Best practice should involve measurement of the electrochemically active surface area (ECSA) of every material and normalization of currents to this area. Additional metrics such as geometric area specific-activity, mass-specific activity, activity normalized to precious metal content, and/or activity normalized to volume in porous catalysts are all relevant, useful, and worth reporting. However, normalization to ECSA is the most directly indicative of the intrinsic material properties. When nanostructured materials with high porosity are implemented, it is further critical to establish that the normalized activity is linearly proportional to the quantity of catalyst on the electrode. If not, there is a strong chance that internal mass transport losses are present within the pore space of the catalyst film. We stress that these losses are distinct from external transport losses (those directly addressable with convection) and can only be verified with changes to the quantity and/or pore structure of the catalyst. This

information can be used to determine a Thiele modulus and effectiveness factor to assess catalyst utilization.^{477–479} In some cases, porous catalysts may exhibit valuable properties due precisely to their impact on mass transport⁴⁸⁰—for example, local depletion of protons has been cited as a factor in reducing lost faradaic efficiency to HER for CO₂ and other organic reduction reactions.^{481,482} However, these scenarios with mixed control between kinetics and transport require even more stringent characterization and modeling to understand the performance, else they become nearly impossible to benchmark.

Thus, it is critical to establish methods for ECSA determination on a multitude of materials classes. Some routes such as underpotential deposition of hydrogen and CO stripping⁴⁸³ or probe metals underpotential deposition⁴⁸⁴ are well established for noble metals, although for alloys can often deviate substantially from estimates based on behavior of the host metal.⁴⁸⁵ In the absence of a validated adsorbing probe molecule, materials are often relegated to surface area estimates by measuring capacitance. While capacitance-based estimates can be informative, they are subject to errors in the assumed value of specific capacitance, which can vary substantially with conditions. Care must be taken to understand the influence of the local environment; for example, some materials show dramatically different capacitance in aqueous vs. organic electrolytes due to ion transfer reactions that cannot be isolated. 486 Materials can also undergo oxidation or reduction-related surface area changes if the potential applied for the electrolysis differs from the potentials where the capacitive surface area was estimated. Additionally, materials with dilute active sites, such as metal-doped-carbons, may require auxiliary measurement to determine the density of active sites per unit of material area. In

these cases, specific chemical probes should be identified, or the information should be obtained through appropriate spectroscopic means—this has recently been shown for Fe sites in doped graphitic catalysts using Mössbauer spectroscopy.⁴⁸⁷

Remaining metrics (such as the macroscopic current density or mass-specific activity) factor heavily into system cost and, again, are important to document, but should only be argued to represent superior performance in cases where concrete and transparent calculation can definitively show this comparison is best. For example, carbon-based fuel cell catalysts have been benchmarked against those made from precious metal particles by direct comparison of turnover frequency per active site coupled to the density of active sites per unit volume achievable within a real cell.⁴⁸⁸ These volumetric-activities were then justified as the most appropriate comparison between such disparate material classes.

In the case of mediated electron transfer or mediated homogeneous catalysis, the turnover rate and turnover number of the mediator molecules should likewise be established. Quantification of the sites for such catalysts should be simple as they relate to homogeneous concentrations, but kinetic experiments should be performed to prove whether rates are limited by (a) the electron-transfer kinetics between electrode and mediator, or mediator and substrate; or by (b) mass transport of mediator to the electrode or substrate molecules. This information can then be used to determine actual turnover frequencies and turnover numbers for the mediator.

Central discussions and ideas on benchmarking and protocols for organic electrocatalytic reactions are organized in a "roadmap" in Figure 11. While it would be premature to establish specific quantitative performance targets for most of the reactions reviewed here, rigorous measurements and documentation as outlined in

the figure will ensure that the literature can be relied upon when establishing these metrics in the future.

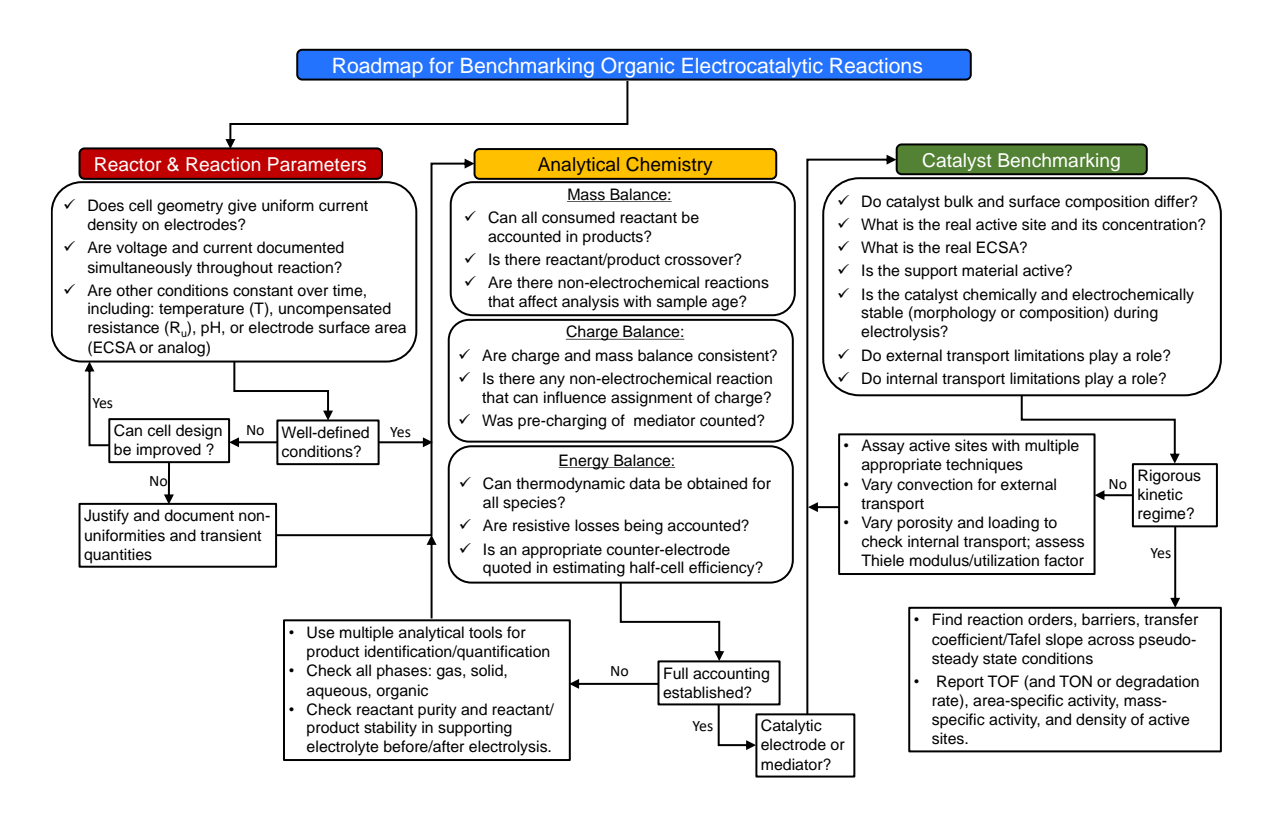


Figure 11. Roadmap for benchmarking organic electrocatalytic reactions

5.3 Fundamental research needs

Once benchmarking efforts are reliable and comparable, work can be done in trying to improve figures of merit for performance through engineering of molecular phenomena. "Best practices" are less defined (or more experiment-specific), but should be directed toward the ideal of full determination of elementary step reaction paths and the roles of local reaction environment, mediator, and/or electrode surface in promoting these reactions. Perhaps in contrast to the prior discussion of Section 5.2, we do not suggest such studies are necessarily expected to be comprehensive

and definitive within single publications. Nonetheless, adherence to aforementioned standards in measurement will permit meaningful focus on these molecular inquiries.

As with most chemical problems, the fundamental challenge lies in gaining a picture of molecular structures and events as they exist during reaction. Great strides have been made in the past several decades in the fields of synthesis, characterization, and simulation. Coupling these fields has led to cases in which relatively simple reactions can be nearly quantitatively modeled on well-defined and well-characterized catalysts. However, with the introduction of increasing molecular complexity, increasingly branched reaction networks, solvation, and field effects, all occurring at the interface between two condensed phases, a full description of the phenomena remains elusive. Biomass conversion and electrochemistry, and their intersection in particular, represent a space in which state-of-the-art methods still require broader adoption and development.

The use of single-crystal electrodes has a rich history in electrochemistry and has led to tremendous insights into small-molecule reactions that are easily interpreted from their electrical signatures (e.g., oxygen reduction). The requirement of product assays for more complex chemistry, coupled to difficulties in synthesizing large single crystal electrodes, adds considerable analytical challenges. Thus, a high barrier to entry has likely contributed to the rarity of such studies. Nevertheless, a number of approaches have been developed to couple single-crystal or thin-film electrochemistry with semi-quantitative analysis, such as by coupling to online electrochemical mass spectrometry (OLEMS)⁴⁹¹ or to liquid chromatography by placement of a probe within a few microns of the surface. Heavy, 492,493

Broader use of *in-situ* spectroscopy will also be critical, and in particular when

combined with surface science of well-defined catalysts. 494 Vibrational spectroscopy will be invaluable to elucidation of organic pathways, as these molecules present numerous IR- and Raman-active functionalities. Thin-film infrared reflection absorption spectroscopy (IRRAS) is particularly suited to studies of molecules on flat surfaces, and the experimental setups are well documented. 495,496 Novel recent approaches to Raman spectroscopy have exploited the concept of "borrowed" resonance from surface-enhanced Raman spectroscopy (SERS) active particles (deposited onto single-crystal surfaces), allowing further characterization of organics by that technique. 497,498

Moving to more practical catalyst formulations, the recent wave of nanoscience and advanced synthesis of facet-controlled particles means that well-defined surfaces can in many instances be scaled up and studied by more traditional reactor kinetics and by spectroscopies that are more suited to probing bulk materials (e.g. *in-situ* X-ray spectroscopies)^{499,500} or which require rough films (such as attenuated total reflectance surface-enhanced infrared absorption spectroscopy, ATR-SEIRAS).^{501,502} At present, the most controlled syntheses are geared to single-metal or single-metal-oxide materials; development of facet control in synthesis of alloys, complex oxides, phosphides, nitrides, and other novel classes of material will prove invaluable in elucidating their activities. Likewise, minimization of defects in framework materials such as those based on graphene, MOFs, or COFs will similarly be critical to understanding their activities. These types of materials, and strong kinetic and spectroscopic studies of their electrocatalytic behavior, will be a key bridge in understanding more heterogeneous and scalable materials.

In tandem with development of experimental approaches, many simulation needs are also pressing. Existing examples of the use of computational modeling in electrocatalyst development clearly demonstrate the additional insight we can gain by incorporating the electrochemical environment into simulations. Still, only very limited examples exist of attempts to apply computational modeling toward informing the development of processes for the electrocatalytic conversion of biomass-derived feedstocks due to the additional complexities outlined here (i.e., size of molecules, complexity of the reaction networks, impurities). A critical need is validation of models developed with varying fidelity by experimental data so that we can establish the rigor in simulating the electrochemical environment required to produce meaningful results. Improved algorithms that enable modeling the full complexity of large species and reaction networks at a reasonable computational cost, or establishment of accurate simplifying relationships relevant to these systems, will also be transformative.

5.4 Economic, logistic, and technical considerations

5.4.1 Production scale and energy needs for biofuels and bioproducts

With the scale of electrochemical biomass conversion currently limited to the lab level, combined with scarce published techno-economic analyses (TEA), near-term research targets should leverage the key learnings of similar, more established, technologies such as CO₂ and H₂O electrolysis where appropriate. While these feedstocks are by comparison less complex than biomass, TEA themes such as the importance of retaining oxygen from the parent compound, minimizing degree of

electron transfer, and emphasizing efficient process integration and separations transcend feedstock choice and will be critical to the development and underlying technical and economic viability of electrochemical biomass conversion. Similarly, many of the key themes from thermochemical and biochemical upgrading of distributed biomass sources also apply, such as minimizing transportation distances from feedstock sources, co-locating with product distribution infrastructure (i.e., refining), and the importance of maximizing conversion efficiency and equipment utilization. 503,504

One of the greatest differences between biomass and petroleum is the elemental composition and oxygen content. Whereas the standard petroleum feedstock is on average 1 wt.% oxygen, 505,506 oxygen accounts for approximately 40 wt.% in biomass.507 With products commonly marketed on a per mass basis, biomass-derived products that retain the greatest amount of oxygen are likely to be better positioned economically to compete with petroleum-based products and may be a target for first-of-a-kind plants. Electrochemical depolymerization reactions that retain the initial mass while targeting otherwise difficult to access bond types with a high selectivity could be one promising example. Conversely, as the degree of deoxygenation is increased, for example if targeting hydrocarbon fuels, process complexity and the number of required electrons per mole of product is increased, driving up the total energy demand and operating costs of the process. It may be recognized that deeply reduced products such as fuels do also represent a higher degree of energy storage, but in the current economic and resource landscape, the value proposition is still a challenge compared to targeting oxygenates.

Process energy demand is known to be a critical operating variable which significantly impacts both operating cost and carbon intensity. With non-renewable energy sources comprising ~75% of global installed electricity capacity in 2019, 508 a high energy (electron) demand is not only more expensive, but depending on the fuel source for electricity generation, can lead to net greenhouse gas emissions that in some cases exceed that of incumbent petrochemical processes. To truly transform the global carbon economy and utilize biomass-derived electrochemical processes with lower net emissions, fully or near-fully renewable energy processes are desired, thereby reducing the load on the existing grid and lowering carbon intensity of the electron generation step. However, the transition to renewable energy comes with challenges of intermittency of supply, power demand, land usage, and upfront capital costs that must be considered, even at smaller scales.

To illustrate the impact of product selection and the number of electrons transferred on these renewable energy generation challenges, in Table 10 we calculate the power demand, land use, and capital cost of energy generation for a hypothetical solar-powered electrochemical process for the reduction of furfural to furfuryl alcohol (FA) and 2-methyl tetrahydrofuran (MTHF) as shown in Scheme 31. Furfural was targeted in this example as it represents a compelling near-term feedstock for electrochemical conversion while FA and MTHF are two promising reductive products requiring two and eight electrons per mole of product, respectively.

Scheme 31. Pathway for the electrochemical reduction of furfural to furfuryl alcohol and 2-methyl tetrahydrofuran.

Power demand is calculated based on Faraday's Law of Electrolysis in Equation 6 where the required charge (Q) in Coulombs is calculated from three variables: molar yield of product (m_i), the number of electrons required per molecule of product (n_i), and the Faradaic efficiency of forming the targeted product (e_f), along with Faraday's constant, F.

$$Q = \frac{n_i m_i F}{e_f} \text{ (eq. 6)}$$

Based on the desired rate of production, charge is converted to current (amps) and multiplied with the whole cell potential (volts) to give total power demand in watts per unit flow rate of product. For this exercise, we study a three order of magnitude range in production of 1, 10, and 100 kmol per hour of product, consistent with smaller distributed processes, at a fixed cell potential of 2.5 V (conservative) and Faradaic efficiency of 100% (theoretical maximum). For perspective on scale, an average 40 million gallon per year bioethanol facility operates at approximately a 340 kmol/h production rate.

In reducing furfural to furfuryl alcohol, the calculated energy demand for this hypothetical case ranges from 0.1 to approximately 13 MW depending on production rate. However, in the case of 2-methyl tetrahydrofuran, since eight electrons are required versus two, the calculated required power demand increases accordingly, ranging from 0.5 to 52 MW for the same production rate(s). Because renewable energy sources experience seasonal and diurnal variations in generation, the actual installed capacity required to power these processes will be higher than the calculated energy demand to account for losses. Applying the 2019 global capacity factor for solar energy of 18%, 18 the actual installed capacity needed ranges from 0.7 to 73 MW and 2.9 to 292 MW for FA and MTHF, respectively. Assuming an output of 320 W per panel, the number of individual solar panels required ranges from ~2,300 in the lowest case (FA, 1 kmol/h) to 913,000 in the highest case (2M-THF, 100 kmol/h). As a point of reference, the Solar Star farm in California (the largest utility scale solar installation in the United States) currently comprises over 1.7 million individual panels generating an estimated 579 MW.⁵⁰⁹However, most utility scale solar installations are significantly smaller, generating on average between 1-5 MW and comprising several thousand to tens of thousands of panels depending on specific power output.⁵¹⁰ With a current installed cost of \$995/kW¹⁸ the total cost for the solar power infrastructure to power a reduction to FA and MTHF would range from \$0.7 million to over \$290 million. Further, based on an average total area use of 0.03 km²/MW solar, the land demand ranges from 0.02 to 9.4 km².⁵¹¹ Note that in the case of wind energy, the footprint increases even further from 0.13 to 50.4 km² to satisfy the same power demands.⁵¹²

Table 10: Calculated power demand, installed cost, and land usage of solar energy required for hypothetical distributed case in the reduction of furfural to furfuryl alcohol (FA) and 2-methyl tetrahydrofuran (MTHF)

Producti on Rate (kmol/h)	Case	Energy Demand (MW)*	Req. Solar Capacity (MW)	Installed Cost Solar (\$M)	# Solar Panels	Land Use (km²)
1	FA	0.1	0.7	0.7	2,300	0.02
	2M-THF	0.5	2.9	2.9	9,100	0.09
10	FA	1.3	7.3	7.3	22,800	0.24
	2M-THF	5.3	29.2	29.1	91,300	0.94
100	FA	13.2	73.1	72.7	228,000	2.35
	2M-THF	52.6	292.2	290.8	913,000	9.41

^{*}Assuming cell potential of 2.5 V and 100% faradaic efficiency for calculations.

This illustrative example highlights that, even for smaller distributed scale systems, the power demand for renewable energy can be substantial, requiring upfront capital costs in electricity generation of up to hundreds of millions of dollars and several square kilometers of physical land usage. These challenges are mitigated as the number of electrons utilized in the electrochemical step are reduced, or alternatively, as the on-purpose energy production for conversion is reduced such as through the use of otherwise curtailed grid electricity. Given the heterogeneity of input conditions experienced world-wide with respect to electricity, feedstock, and infrastructure availability, the true viability of first-of-a-kind adopters should be evaluated on a case-by-case basis under their specific regional constraints. However, in general these data suggest that near-term opportunities lie in molecules requiring transfer of the fewest electrons and those that form or retain oxygenated moieties that are challenging and costly to derive from petrochemical/hydrocarbon feedstocks. However, as the core conversion technology improves over time, and if feedstock and renewable electricity costs continue to fall, species that are more highly reduced and have tighter margins could also conceivably become competitive.

5.4.2 Process intensification and half-reaction pairing

In many ways, optimization of specific electrochemical reaction performance is only the beginning of an equally complex engineering endeavor to couple redox processes. To maximize the economic viability of an electrosynthetic method, it is important that both electrochemical half-reactions produce value-added chemicals. For example, in one of the most well-known electrochemical industrial processes, the chloralkali process, sodium hydroxide and chlorine gas (or sodium hypochlorite) are generated at the cathodic and anodic sides, respectively.⁵¹³ In assessing energy demand during lab-scale tests, it is often assumed that aqueous electrolytic reactions will be performed with the opposite electrode performing water splitting; either oxygen evolution reaction (OER, against reductions) or hydrogen evolution reaction (HER, against oxidations). If an anode potential is not too high (in oxidative direction), pairing against the oxygen reduction reaction (ORR) may also be considered with cogeneration of electricity. However, O₂ generated from the OER of water splitting is not generally a useful coproduct, nor is the water generated by ORR. Hydrogen may be desirable but likely needs to have an outlet for use on-site or locally.

Alternatively, more complex optimization can be considered, in which both electrode reactions are able to generate a useable product. In doing so, a number of questions must be considered: Are the synthetic scales of the two products

compatible? Are the reaction conditions similar enough, and the selectivity of each electrode sufficient that they can be performed in an undivided cell? If divided cells are required, are there ion-exchange membrane compatibility issues and/or do they operate at a compatible pH with a common ion intermediate that can be transferred between compartments? If pH conditions are not compatible, is the chemistry valuable enough to warrant introduction of a bipolar membrane with added voltage drop? Is there homogeneous chemistry or other issues that require stable vs. intermittent power input? Can the pairing generate useful electricity as a galvanic cell? Are there more complex logistical parameters —for example, might differences in scale be surmounted by process modularity, running a larger scale reaction against two different counter-reactions (e.g., HER in cells with two different organic oxidations)? These questions are challenging to address for exploratory chemistries but should be kept in mind as researchers begin to increase focus on seemingly viable reactions.

Beyond the traditional approach in which half-reactions are considered as isolated processes that might be added together, there are a number of more creative approaches to coupled electrosynthesis. Five primary classifications have been made based on the relationship between the reactants and products, and assuming that all products have economical value (i.e., are not sub-product or waste): Parallel (PPE), linear (LPE), convergent (CPE), divergent (DPE), and tandem (TPE), or sequential, paired electrolysis (as illustrated in Figure 12).

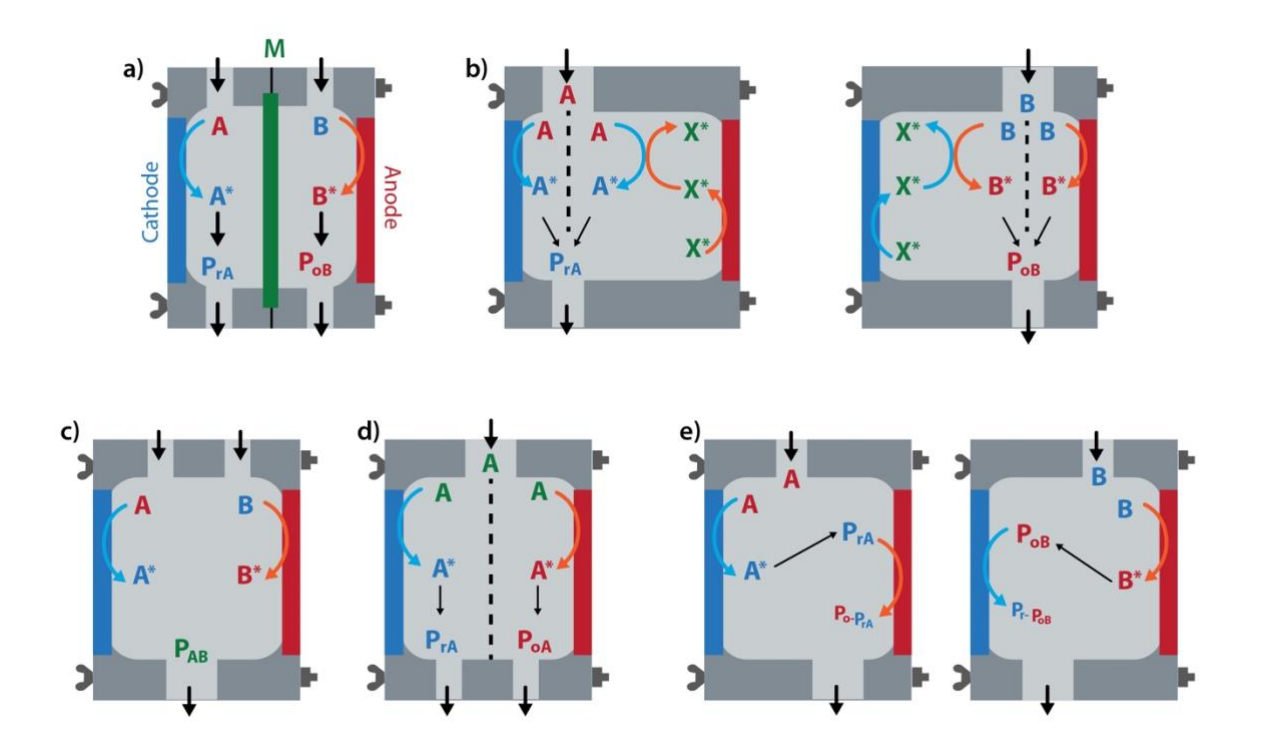
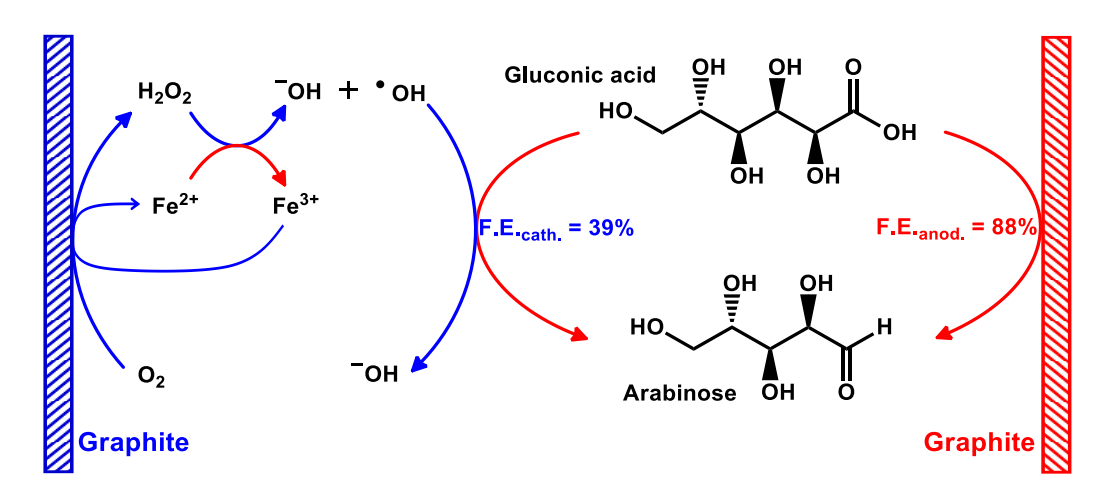


Figure 12. Schematic illustration of the paired electrochemical systems: **a)** Parallel (PPE), **b)** Cathodic (c-LPE, left) and anodic (a-LPE, right) linear, **c)** Convergent (CPE), and **d)** Divergent paired electrolysis (DPE). **e)** Tandem paired electrolysis (TPE).

PPE is the most common example, where different reactants (A and B, Figure 12a) are electrochemically converted (through electroreduction or electrooxidation) into different products (P_{rA} and P_{oB}) such as the coupling of carbon dioxide reduction³³ or hydrogen evolution reaction^{35,514} with organic oxidation previously commented in this review. In LPE, the starting material is converted, in both reactor compartments, into just one product; this product can be more reduced (Figure 12b – left reactor) or oxidized (Figure 12b – right reactor) than the starting material. This kind of system may work in two ways: the reactant can be reduced (right reactor) / oxidized (left reactor) by an electrogenerated auxiliary species (X*), as represented in Figure 12. An example is the LPE of gluconic acid to produce arabinose; gluconic

acid is indirectly oxidized to arabinose in the cathodic compartment by hydroxyl radicals; these auxiliary species are produced from the reaction of H₂O₂ (electrogenerated from O₂ reduction) with iron ions present in the reaction system (Scheme 32).¹⁶⁴ LPE can also be performed when one part of the reactant is oxidized and another part is reduced, generating different intermediates that can react with each other producing a coupling product.



Scheme 32. Linear paired electrolysis of gluconic acid to produce arabinose. 164

Close to this previous example, in CPE, different reactants are electrochemically converted into dissimilar intermediates that react with each other generating a coupling product (Figure 12c), for example, the CPE to produce 2-alkoxytetrahydrofurans from electroreduction of esters and electrooxidation of THF (Scheme 17).⁴⁰² In the opposite case, in DPE, the same starting material can be oxidized and reduced to generate different products (Figure 12d), as exemplified in Scheme 13 by electrochemical conversion of L-cystine into L-cysteic acid (anodic) and L-cysteine (cathodic).²³⁹ Other examples of DPE are the simultaneous electrocatalytic oxidation and electrocatalytic hydrogenation of HMF into 2,5-

furandicarboxylic acid (FDCA) and 2,5-bishydroxymethyl-tetrahydrofuran (DHMTHF);⁵¹⁵ of fructose into gluconic acid, and sorbitol and mannitol;¹⁵⁹ and glucose into gluconic acid and sorbitol.¹⁵⁷

Finally, in TPE (Figure 12e), the substrate molecule can be sequentially anodically and cathodically (or vice versa) transformed in an undivided cell. Scheme 33 below shows the tandem transformation of xylose into δ -valerolactone *via* mediated oxidation followed by reduction. ¹⁶⁰

Scheme 33. Tandem paired electrolysis of xylose into δ -valerolactone. Scheme adapted from Schröder and co-authors. DSA: dimensionally stable anode

All of these reactions can be performed in a batch or a flow electrochemical reactor, and the anodic and cathodic compartments may be divided by ion-exchange membranes (such as Nafion®, Sustainion®, and Fumasep®) or other non-selective physical separators such as porous membranes or sintered glass, amongst others. These membranes may help to decrease the resistive energy losses by permitting the reduction of the distance between anode and cathode without compromising the selectivity of the reaction (preventing competitive reactions of products and reactants in the opposite compartments). They can also enable the cell compartments to work

in a slightly different condition of solvent, supporting electrolyte and pH.¹⁸⁸ Figure 12a represents a divided cell, where "M" (a green separator between cathodic and anodic chambers) signifies an ion-exchange membrane.¹⁸⁸

5.4.3 Top technical challenges

The timeframe from innovation to commercialization for new technologies can be lengthy, often requiring multiple decades. In the case of electricity generation technologies for example, the median time to reach widespread commercialization has been estimated at 43 years. Considering the relative immaturity of electrochemical biomass conversion, there is a need to significantly accelerate the development and deployment timeline of these technologies if they are to play a meaningful role in the mitigation of global carbon emissions as noted in recent IPCC reports. Reaching commercialization in a timely manner will require not only a concerted effort from governments and policymakers, but will also require overcoming a host of technical challenges. In Table 11 and discussion below, we identify top technical challenges as noted in open literature and through subject matter expert interviews.

Table 11. Top Technical Challenges for Electrochemical Biomass Conversion*

Challenges

Low faradaic efficiency due to competition from hydrogen/oxygen evolution reactions 178,518

Costly product separation due to low product concentrations and mixed product streams^{39,169,201}

Slow conversion rates compared to non-electrochemical techniques⁵¹⁹

Low selectivity in targeting specific functionalities / intermediates within real mixtures²⁰¹

Polymerization leading to electrode fouling⁵²⁰

Reaction mechanisms poorly understood 193,201

Impurity-induced fouling on catalyst surface, metal deposition, coking⁵¹⁹

Membrane and catalyst durability in harsh operating conditions⁵¹⁸

Reactor scale-up and moving from half-cell to continuous whole-cell processes⁵¹⁹

Insufficient analytical methods to fully characterize reactant and product streams (e.g., bio-oils)

519

Membrane crossover of chemical species⁵¹⁹

Biomass feedstock variability (H₂O, minerals, high MW components)⁵¹⁹

Calibrating simultaneous tandem electro-catalysis on the anode and cathode in terms of rates,

market sizes, technical variables⁵¹⁹

Establishment of compatibility with intermittent power

Replacing noble metals in electrocatalysts²⁰¹

*The authors would like to acknowledge and thank all subject matter experts who agreed to be interviewed and shared their expertise during the writing of this review.

i) Improving selectivity and suppressing competing reactions

Unlike water electrolysis, which involves the conversion of a simple 3-atom molecule, electrochemistry on biomass and biomass derivatives is significantly more complex. Biomass derivatives span multiple functionalities such as aldehydes, ketones, furanics, alcohols, glycols, carbonyls, ethers, etc., and in the case of raw bio-oils, can exceed over 100 individual components. Consequently, selectively reducing or oxidizing a specific intermediate or functional group represents a major technical challenge in real systems. Polymerization side reactions leading to electrode fouling are also a significant concern for certain classes of biomass derivatives^{14,212}—particularly in the case of reduction of compounds with unsaturated bonds¹⁷⁶ and in oxidation of phenolic compounds.⁵²⁰ Further, cross-reactions between products and reactants inside the reaction compartment can negatively impact product selectivity.

162

The greatest challenge to faradaic efficiency, however, is competition from the hydrogen and oxygen evolution reactions (HER, OER) during reduction and oxidation chemistries, respectively. HER is, in particular, kinetically favored over organic redox reactions and often consumes most of the incoming electrons in aqueous mixtures. Directing product formation towards desired organics during electroreduction and away from H₂/O₂ represents a crucial long-term technical challenge. However, in some cases, H₂ formation as a co-product on the cathode during electro-oxidation reactions may be desired to help offset costs.

ii) Increasing reaction rates

Demonstrated current densities (i.e., rates) for biomass/intermediate redox reactions are up to two orders of magnitude lower than those observed in H₂O or CO₂ electrolysis. Low rates increase the physical footprint of processes, which drives up capital costs and can easily outweigh the benefit of lower feedstock (electricity) costs. Current density can be increased by operating at a higher cell voltage but comes with drawbacks as it lowers energy efficiency and, as noted above, if water is present can often favor HER/OER. Novel biomass-specific reactor designs, improved catalyst selectivity, and non-aqueous electrolytes (if separations can be made practical) represent a few pathways to increase reaction rates warranting more R&D moving forward.

iii) Improving catalyst stability and impurity tolerance

With biomass and its intermediates on average comprised of high molecular weight species, combined with the sulfur, minerals, metals, and other impurities

inherent in the parent biomass feedstock, maintaining sustained electrocatalyst activity over reasonable lifetimes is considered a major technical hurdle to electrochemical conversion. Larger molecules and suspended solids from ash or biochar will likely require dedicated upstream separation prior to conversion to avoid catalyst fouling. After removal of these components, some water-soluble inorganic compounds are still present—e.g., Ca, K, Fe, Al, Zn, and S, usually below the 200 ppm level.^{9,68-72} It may be expected that alkali ions will be inert since they are also components of common supporting electrolytes, although they can introduce variable field effects that impact catalysis in some potential ranges.⁵²¹ Other metallic ions (e.g. Fe, Al, and Zn) can be deleterious to the electrochemical reaction, electrodepositing on surfaces and decreasing activity/selectivity. For example, deposition of Fe and Zn can favor the HER over reduction of organics; in some cases, these metals may also act as electromediators (cf. Scheme 32). Sulfur compounds are mainly concentrated in char (as sulfate or metallic sulfide) and are present in low amounts (compared to coal and crude oil^{9,68–72}), but may also act as poisoning compounds if they are present as thiols or sulfide ions. 13-16 Sulfates are less problematic though can also adsorb under certain conditions. 490 Some small organic components may also interfere with target electrochemical reactions—e.g., molecules such as olefins, furans, and other aromatics may electro-polymerize under some conditions and poison electrodes. With most current research studying single-component model compound systems, a transition to more realistic systems combined with further electrocatalyst and membrane development is needed to improve the long-term stability of these materials.

With regard to the electrode material itself, stability may also be of particular concern under oxidizing conditions, where dissolution, corrosion, and particle ripening can all occur depending on the potential, pH and other conditions. In general, cathodic conditions do not often pose problems, but electrodes can be exposed to undesired conditions while idle and thus care should still be taken to evaluate stability not only under polarization, but also at open-circuit.

iv) Feedstock flexibility and improving analytical methods

Electrochemical catalysts and reactors are in general not feedstock flexible but rather are finely tuned to operate with a well-defined feedstock (e.g., pure water, CO₂) over a specific pre-defined operating range. In contrast, raw bio-oils and other biomass-derived streams are inherently heterogenous, multi-component, and often ill-defined. In a similar vein, the reactors are often operable over a range of potentials, but consequences of true intermittent power supplies and their impact on complex reaction networks is not well-established. Thus, conventional electrochemical systems are likely to perform poorly, and there is a need to develop next-generation electrocatalysts and reactors specifically tailored for organic feedstocks and intermittent power. However, before this rational design process can occur, analytical methods must be improved to allow for multi-phase assays and the complete characterization of all products and functionalities within biorefinery process streams. If the incoming and exiting products cannot be fully quantified, the development of next-generation processes will be slowed. Further considerations on fundamental research needs to enable the above characterizations and improvements have been discussed in Section 5.2-5.3.

6. Conclusions and prospects

Throughout this review, we have highlighted the emerging and clearly immense research space for applications of electrochemical methods in transforming biomass-derived molecules. While the potential opportunities are vast, it is also clear that there remain a wide array of questions to be addressed, ranging from the technical feasibility of achieving selective transformations at high rates to the logistical interdependencies with renewable power. Substantial efforts will be needed spanning fundamental science, applied engineering, economics and policy in order to unravel the ultimate niche for these technologies. In the near term, our analysis suggests that to advance the low TRL and improve the prospects for industrial-scale implementation of electrochemical biomass processing, it will make the most sense to begin with small-scale, high-margin chemicals that will not hinge on small variations in the cost of electricity or require subsidies. These exercises will allow continued development of the technologies in order to permit more realistic techno-economic evaluations and justify attempts to compete with highly-optimized incumbent technologies. The development cycle will be dramatically accelerated if benchmarking standards are adopted and results reported in a manner that all can understand, reproduce, and learn from. In the much longer term, it is conceivable that the combination of diverse feedstocks available, in large part from biomass, combined with abundant renewable electricity, will lead to a re-imagined, but realistic and sustainable chemical supply chain.

AUTHOR INFORMATION

Corresponding Authors

Adam Holewinski – Renewable and Sustainable Energy Institute & Department of Chemical and Biological Engineering, University of Colorado, Boulder, CO 80303, United States; orcid.org/0000-0001-8307-5881; Phone: +1 303 492-3153; e-mail: adam.holewinski@colorado.edu

Joshua A. Schaidle – Catalytic Carbon Transformation and Scale-up Center, National Renewable Energy Laboratory, Golden, CO 80401, United States; orcid.org/0000-0003-2189-5678; Phone: +1 303 384-7823; e-mail: joshua.schaidle@nrel.gov

Authors

Francisco W. S. Lucas – Department of Chemical and Biological Engineering & Renewable and Sustainable Energy Institute, University of Colorado, Boulder, CO 80303, United States; orcid.org/0000-0002-4637-8469.

R. Gary Grim – Catalytic Carbon Transformation and Scale-up Center, National Renewable Energy Laboratory, Golden, CO 80401, United States; orcid.org/0000-0002-1154-7795.

Sean A. Tacey – Catalytic Carbon Transformation and Scale-up Center, National Renewable Energy Laboratory, Golden, CO 80401, United States; orcid.org/0000-0001-7833-6901.

Courtney Downes – Catalytic Carbon Transformation and Scale-up Center, National Renewable Energy Laboratory, Golden, CO 80401, United States; orcid.org/0000-0001-8631-1579.

Joseph Hasse – Department of Chemical and Biological Engineering & Renewable and Sustainable Energy Institute, University of Colorado, Boulder, CO 80303, United States; orcid.org/0000-0002-0580-1355.

Alex M. Roman – Department of Chemical and Biological Engineering & Renewable and Sustainable Energy Institute, University of Colorado, Boulder, CO 80303, United States.

Carrie A. Farberow – Catalytic Carbon Transformation and Scale-up Center, National Renewable Energy Laboratory, Golden, CO 80401, United States; orcid.org/0000-0002-3753-962X.

Biographies

Francisco W. S. Lucas receive his Ph.D. degree in Physical-chemistry from the Federal University of Sao Carlos. His research interests are based on electrochemistry, renewable energy, and green chemistry. He has experience in electrochemical biomass-upgrading, electrocatalysis, organic electrosynthesis, electroanalytical methods, pollutants electro-degradation, and synthesis and characterization of semiconductors for photovoltaic and photoelectrochemical applications.

Webpage: ttps://www.researchgate.net/profile/Francisco_Willian_De_Souza_Lucas **R. Gary Grim** is a staff scientist at the Center for Catalytic Carbon Transformation,

National Renewable Energy Laboratory (NREL). His research interests focus on the

use of low-cost renewable energy for the capture, conversion, and utilization of carbon dioxide to address growing global climate and environmental challenges.

Webpage: https://www.nrel.gov/research/staff/gary-grim.html

Sean A. Tacey is a postdoctoral researcher in the Catalytic Carbon Transformation & Scale-Up Center at the National Renewable Energy Laboratory. He obtained his Ph.D. in 2019 from the University of Wisconsin – Madison, and his research interests include atomic-scale modeling for thermo- and electrocatalytic processes for renewable energy production/upgrading.

Webpage: https://www.nrel.gov/research/staff/sean-tacey.html

Courtney Downes received her Ph.D. in Chemistry from the University of Southern California in 2018. She was a postdoctoral researcher in the Catalytic Carbon Transformation & Scale-Up Center at the National Renewable Energy Laboratory from 2018-2020. Her interests include science policy and energy geopolitics.

Joseph Hasse is a graduate student in the Holewinski Lab in the Chemical Engineering Department at the University of Colorado Boulder. His research interests focus is primarily on using in FTIR SEIRAs in order to characterize catalytically relevant surface species during the electro-oxidation of biomass model compounds.

Alex M. Roman earned his PhD in Chemical Engineering from the University of Colorado-Boulder in 2020, which was funded by an NSF Graduate Research Fellowship and under the joint supervision of J. Will Medlin and Adam Holewinski. He received his Bachelor of Chemical Engineering from Auburn University in 2014. He is currently working as a Research Engineer at Pioneer Astronautics in Lakewood, CO.

169

Carrie A. Farberow is a Research Engineer and Group Manager in the Catalytic

Carbon Transformation & Scale-up Center at NREL, where she leads research in

catalyst design to produce fuels and chemicals from biomass and waste resources.

She received a Ph.D. in Chemical Engineering from the University of Wisconsin –

Madison.

Webpage: https://www.nrel.gov/research/staff/carrie-farberow.html

Joshua A. Schaidle is the director of the Chemical Catalysis for Bioenergy

(ChemCatBio) Consortium and is the lead for the Catalytic Carbon Transformation

platform at the National Renewable Energy Laboratory. He seeks to advance the

catalysis and bioenergy fields by working at the interface of foundational science and

applied engineering, leveraging a combined experimental and computational

approach.

Webpage: https://www.nrel.gov/research/staff/joshua-schaidle.html

Adam Holewinski is an Assistant Professor of Chemical and Biological Engineering

at the University of Colorado Boulder and a Fellow of the CU-NREL Renewable and

Sustainable Energy Institute. His research interests lie in heterogeneous catalysis

and electrochemistry for sustainable production of energy and chemicals,

emphasizing characterization through kinetics, spectroscopy, and modeling.

Webpage: https://www.colorado.edu/chbe/adam-holewinski

170

ACKNOWLEDGMENT

Partial support of this work was provided by NSF CBET grant 1665176. This work was also authored in part by the National Renewable Energy Laboratory, operated by Alliance for Sustainable Energy, LLC, for the U.S. Department of Energy (DOE) under Contract No. DE-AC36-08GO28308. Funding provided by U.S. Department of Energy Office of Energy Efficiency and Renewable Energy Bioenergy Technologies Office. This work was also supported by the Laboratory Directed Research and Development (LDRD) Program at NREL. The views expressed in the article do not necessarily represent the views of the DOE or the U.S. Government. The U.S. Government retains and the publisher, by accepting the article for publication, acknowledges that the U.S. Government retains a nonexclusive, paid-up, irrevocable, worldwide license to publish or reproduce the published form of this work, or allow others to do so, for U.S. Government purposes.

References

- (1) The National Renewable Energy Laboratory. Renewable Electricity Futures Study https://www.nrel.gov/analysis/re-futures.html. Last accessed date was January 2020.
- (2) Lemmon, J. P. Energy: Reimagine Fuel Cells. *Nature* **2015**, *525* (7570), 447–449. https://doi.org/10.1038/525447a.
- (3) Tripathi, N.; Hills, C. D.; Singh, R. S.; Atkinson, C. J. Biomass Waste Utilisation in Low-Carbon Products: Harnessing a Major Potential Resource. *npj Clim. Atmos. Sci.* **2019**, *2* (1), 35. https://doi.org/10.1038/s41612-019-0093-5.
- (4) Serrano-Ruiz, J. C.; Luque, R.; Sepúlveda-Escribano, A. Transformations of Biomass-Derived Platform Molecules: From High Added-Value Chemicals to Fuels via Aqueous-Phase Processing. *Chem. Soc. Rev.* **2011**, *40* (11), 5266. https://doi.org/10.1039/c1cs15131b.
- (5) Ragauskas, A. J. The Path Forward for Biofuels and Biomaterials. *Science*. **2006**, *311* (5760), 484–489. https://doi.org/10.1126/science.1114736.
- (6) U.S. Department of Energy. 2016 Billion-ton Report: Advancing Domestic Resources for a Thriving Bioeconomy https://www.energy.gov/sites/prod/files/2016/12/f34/2016_billion_ton_report_ 12.2.16 0.pdf. Last accessed date was January 2020.
- (7) Andrade, D. S.; Gavilanes, F. Z.; Silva, H. R.; Henrique Leite Castro, G.; Telles, T. S. Sustainable Bioenergy Production. In *Recent Developments in Bioenergy Research*; Elsevier, 2020; pp 363–391. https://doi.org/10.1016/B978-0-12-819597-0.00019-2.
- (8) Muscat, A.; de Olde, E. M.; de Boer, I. J. M.; Ripoll-Bosch, R. The Battle for Biomass: A Systematic Review of Food-Feed-Fuel Competition. *Glob. Food Sec.* **2019**, 100330. https://doi.org/10.1016/j.gfs.2019.100330.
- (9) Cho, E. J.; Trinh, L. T. P.; Song, Y.; Lee, Y. G.; Bae, H.-J. Bioconversion of Biomass Waste into High Value Chemicals. *Bioresour. Technol.* **2020**, *298*, 122386. https://doi.org/10.1016/j.biortech.2019.122386.
- (10) The U.S. Energy Information Administration's (EIA). Short-term energy outlook https://www.eia.gov/outlooks/steo/report/global_oil.php. Last accessed date was January 2020.
- (11) The U.S. Energy Information Administration's (EIA). Oil and petroleum products explained: Refining crude oil https://www.eia.gov/energyexplained/oil-and-petroleum-products/refining-crude-oil.php. Last accessed date was January 2020.
- (12) Grim, R. G.; Huang, Z.; Guarnieri, M. T.; Ferrell, J. R.; Tao, L.; Schaidle, J. A. Transforming the Carbon Economy: Challenges and Opportunities in the Convergence of Low-Cost Electricity and Reductive CO2 Utilization. *Energy Environ. Sci.* **2020**, *13* (2), 472–494. https://doi.org/10.1039/C9EE02410G.
- (13) Frontana-Uribe, B. A.; Little, R. D.; Ibanez, J. G.; Palma, A.; Vasquez-Medrano, R. Organic Electrosynthesis: A Promising Green Methodology in Organic Chemistry. *Green Chem.* **2010**, *12* (12), 2099. https://doi.org/10.1039/c0gc00382d.
- (14) Hammerich, O.; Speiser, B.; Editors. *Organic Electrochemistry: Revised and Expanded, Fifth Edition.*, 5th ed.; CRC Press: Boca Raton, FL, 2016.

- (15) James Grimshaw. *Electrochemical Reactions and Mechanisms in Organic Chemistry*; Elsevier: Belfast, 2000; Vol. 124. https://doi.org/10.1021/ja015344j.
- (16) Yan, M.; Kawamata, Y.; Baran, P. S. Synthetic Organic Electrochemical Methods Since 2000: On the Verge of a Renaissance. *Chem. Rev.* 2017, 117 (21), 13230–13319. https://doi.org/10.1021/acs.chemrev.7b00397.
- (17) Botte, G. G. Electrochemical Manufacturing in the Chemical Industry. *Interface Mag.* **2014**, *23* (3), 49–55. https://doi.org/10.1149/2.F04143if.
- (18) The International Renewable Energy Agency (IRENA). Renewable Power Generation Costs in 2019 https://www.irena.org/publications/2020/Jun/Renewable-Power-Costs-in-2019. Last accessed date was January 2020.
- (19) Dominic Dudley. Renewable Energy Will Be Consistently Cheaper Than Fossil Fuels By 2020, Report Claims https://www.forbes.com/sites/dominicdudley/2018/01/13/renewable-energy-cost-effective-fossil-fuels-2020/?sh=48fd0d444ff2. Last accessed date was January 2020.
- (20) Electricity Markets & Policy. Wind Technologies Market Report https://emp.lbl.gov/wind-technologies-market-report/. Last accessed date was January 2020.
- (21) Akhade, S. A.; Singh, N.; Gutiérrez, O. Y.; Lopez-Ruiz, J.; Wang, H.; Holladay, J. D.; Liu, Y.; Karkamkar, A.; Weber, R. S.; Padmaperuma, A. B.; et al. Electrocatalytic Hydrogenation of Biomass-Derived Organics: A Review. *Chem. Rev.* **2020**, 120 (20), 11370–11419. https://doi.org/10.1021/acs.chemrev.0c00158.
- (22) Borup, R.; Meyers, J.; Pivovar, B.; Kim, Y. S.; Mukundan, R.; Garland, N.; Myers, D.; Wilson, M.; Garzon, F.; Wood, D.; et al. Scientific Aspects of Polymer Electrolyte Fuel Cell Durability and Degradation. *Chem. Rev.* **2007**, 107 (10), 3904–3951. https://doi.org/10.1021/cr050182I.
- (23) McCrory, C. C. L.; Jung, S.; Ferrer, I. M.; Chatman, S. M.; Peters, J. C.; Jaramillo, T. F. Benchmarking Hydrogen Evolving Reaction and Oxygen Evolving Reaction Electrocatalysts for Solar Water Splitting Devices. *J. Am. Chem. Soc.* **2015**, *137* (13), 4347–4357. https://doi.org/10.1021/ja510442p.
- (24) Chauvy, R.; Meunier, N.; Thomas, D.; De Weireld, G. Selecting Emerging CO2 Utilization Products for Short- to Mid-Term Deployment. *Appl. Energy* **2019**, 236, 662–680. https://doi.org/10.1016/j.apenergy.2018.11.096.
- (25) Yaashikaa, P. R.; Senthil Kumar, P.; Varjani, S. J.; Saravanan, A. A Review on Photochemical, Biochemical and Electrochemical Transformation of CO2 into Value-Added Products. *J. CO2 Util.* **2019**, 33, 131–147. https://doi.org/10.1016/j.jcou.2019.05.017.
- (26) Roh, K.; Bardow, A.; Bongartz, D.; Burre, J.; Chung, W.; Deutz, S.; Han, D.; Heßelmann, M.; Kohlhaas, Y.; König, A.; et al. Early-Stage Evaluation of Emerging CO 2 Utilization Technologies at Low Technology Readiness Levels. *Green Chem.* **2020**, 22 (12), 3842–3859. https://doi.org/10.1039/C9GC04440J.
- (27) Liu, Q.; Wu, L.; Jackstell, R.; Beller, M. Using Carbon Dioxide as a Building Block in Organic Synthesis. *Nat. Commun.* **2015**, *6*, 5933.

- https://doi.org/10.1038/ncomms6933.
- (28) Verma, S.; Kim, B.; Jhong, H.-R. "Molly"; Ma, S.; Kenis, P. J. A. A Gross-Margin Model for Defining Technoeconomic Benchmarks in the Electroreduction of CO 2. *ChemSusChem* **2016**, *9* (15), 1972–1979. https://doi.org/10.1002/cssc.201600394.
- (29) Jouny, M.; Luc, W.; Jiao, F. General Techno-Economic Analysis of CO 2 Electrolysis Systems. *Ind. Eng. Chem. Res.* **2018**, *57* (6), 2165–2177. https://doi.org/10.1021/acs.iecr.7b03514.
- (30) Bushuyev, O. S.; De Luna, P.; Dinh, C. T.; Tao, L.; Saur, G.; van de Lagemaat, J.; Kelley, S. O.; Sargent, E. H. What Should We Make with CO2 and How Can We Make It? *Joule* **2018**, *2* (5), 825–832. https://doi.org/10.1016/j.joule.2017.09.003.
- (31) Herron, J. A.; Kim, J.; Upadhye, A. A.; Huber, G. W.; Maravelias, C. T. A General Framework for the Assessment of Solar Fuel Technologies. *Energy Environ. Sci.* **2015**, *8* (1), 126–157. https://doi.org/10.1039/C4EE01958J.
- (32) Palmer, C.; Saadi, F.; McFarland, E. W. Technoeconomics of Commodity Chemical Production Using Sunlight. *ACS Sustain. Chem. Eng.* **2018**, *6* (5), 7003–7009. https://doi.org/10.1021/acssuschemeng.8b00830.
- (33) Na, J.; Seo, B.; Kim, J.; Lee, C. W.; Lee, H.; Hwang, Y. J.; Min, B. K.; Lee, D. K.; Oh, H.-S.; Lee, U. General Technoeconomic Analysis for Electrochemical Coproduction Coupling Carbon Dioxide Reduction with Organic Oxidation. *Nat. Commun.* **2019**, *10* (1), 5193. https://doi.org/10.1038/s41467-019-12744-y.
- (34) Anson, C. W.; Stahl, S. S. Mediated Fuel Cells: Soluble Redox Mediators and Their Applications to Electrochemical Reduction of O 2 and Oxidation of H 2, Alcohols, Biomass, and Complex Fuels. *Chem. Rev.* **2020**, *120* (8), 3749–3786. https://doi.org/10.1021/acs.chemrev.9b00717.
- (35) Holade, Y.; Tuleushova, N.; Tingry, S.; Servat, K.; Napporn, T. W.; Guesmi, H.; Cornu, D.; Kokoh, K. B. Recent Advances in the Electrooxidation of Biomass-Based Organic Molecules for Energy, Chemicals and Hydrogen Production. *Catal. Sci. Technol.* **2020**, *10* (10), 3071–3112. https://doi.org/10.1039/C9CY02446H.
- (36) Bocci, E.; Di Carlo, A.; McPhail, S. J.; Gallucci, K.; Foscolo, P. U.; Moneti, M.; Villarini, M.; Carlini, M. Biomass to Fuel Cells State of the Art: A Review of the Most Innovative Technology Solutions. *Int. J. Hydrogen Energy* **2014**, *39* (36), 21876–21895. https://doi.org/10.1016/j.ijhydene.2014.09.022.
- (37) Lu, L.; Ren, Z. J. Microbial Electrolysis Cells for Waste Biorefinery: A State of the Art Review. *Bioresour. Technol.* **2016**, *215*, 254–264. https://doi.org/10.1016/j.biortech.2016.03.034.
- (38) Carneiro, J.; Nikolla, E. Electrochemical Conversion of Biomass-Based Oxygenated Compounds. *Annu. Rev. Chem. Biomol. Eng.* **2019**, *10* (1), 85–104. https://doi.org/10.1146/annurev-chembioeng-060718-030148.
- (39) Du, L.; Shao, Y.; Sun, J.; Yin, G.; Du, C.; Wang, Y. Electrocatalytic Valorisation of Biomass Derived Chemicals. *Catal. Sci. Technol.* **2018**, *8* (13), 3216–3232. https://doi.org/10.1039/C8CY00533H.
- (40) Lam, C. H.; Deng, W.; Lang, L.; Jin, X.; Hu, X.; Wang, Y. Minireview on Bio-Oil Upgrading via Electrocatalytic Hydrogenation: Connecting Biofuel

- Production with Renewable Power. *Energy & Fuels* **2020**, *34* (7), 7915–7928. https://doi.org/10.1021/acs.energyfuels.0c01380.
- (41) Peduzzi, E.; Boissonnet, G.; Maréchal, F. Biomass Modelling: Estimating Thermodynamic Properties from the Elemental Composition. *Fuel* **2016**, *181*, 207–217. https://doi.org/10.1016/j.fuel.2016.04.111.
- (42) Dupont, C.; Rougé, S.; Berthelot, A.; Da Silva Perez, D.; Graffin, A.; Labalette, F.; Laboubée, C.; Mithouard, J.-C.; Pitocchi, S. Bioenergy II: Suitability of Wood Chips and Various Biomass Types for Use in Plant of BtL Production by Gasification. *Int. J. Chem. React. Eng.* 2010, 8 (1), 1–21. https://doi.org/10.2202/1542-6580.1949.
- (43) Al-Hamamre, Z.; Saidan, M.; Hararah, M.; Rawajfeh, K.; Alkhasawneh, H. E.; Al-Shannag, M. Wastes and Biomass Materials as Sustainable-Renewable Energy Resources for Jordan. *Renew. Sustain. Energy Rev.* **2017**, *67*, 295–314. https://doi.org/10.1016/j.rser.2016.09.035.
- (44) Isikgor, F. H.; Becer, C. R. Lignocellulosic Biomass: A Sustainable Platform for the Production of Bio-Based Chemicals and Polymers. *Polym. Chem.* **2015**, 6 (25), 4497–4559. https://doi.org/10.1039/C5PY00263J.
- (45) Mettler, M. S.; Vlachos, D. G.; Dauenhauer, P. J. Top Ten Fundamental Challenges of Biomass Pyrolysis for Biofuels. *Energy Environ. Sci.* **2012**, *5* (7), 7797. https://doi.org/10.1039/c2ee21679e.
- (46) Alishah Aratboni, H.; Rafiei, N.; Garcia-Granados, R.; Alemzadeh, A.; Morones-Ramírez, J. R. Biomass and Lipid Induction Strategies in Microalgae for Biofuel Production and Other Applications. *Microb. Cell Fact.* **2019**, *18* (1), 178. https://doi.org/10.1186/s12934-019-1228-4.
- (47) Sajjadi, B.; Chen, W.-Y.; Raman, A. A. A.; Ibrahim, S. Microalgae Lipid and Biomass for Biofuel Production: A Comprehensive Review on Lipid Enhancement Strategies and Their Effects on Fatty Acid Composition. *Renew. Sustain. Energy Rev.* **2018**, 97, 200–232. https://doi.org/10.1016/j.rser.2018.07.050.
- (48) Forde, C. J.; Meaney, M.; Carrigan, J. B.; Mills, C.; Boland, S.; Hernon, A. Biobased Fats (Lipids) and Oils from Biomass as a Source of Bioenergy. In *Bioenergy Research: Advances and Applications*; Elsevier, 2014; pp 185–201. https://doi.org/10.1016/B978-0-444-59561-4.00012-7.
- (49) Lee, K. T.; Ofori-Boateng, C. Biofuels: Production Technologies, Global Profile, and Market Potentials; 2013; pp 31–74. https://doi.org/10.1007/978-981-4451-70-3 2.
- (50) Alaswad, A.; Dassisti, M.; Prescott, T.; Olabi, A. G. Technologies and Developments of Third Generation Biofuel Production. *Renew. Sustain. Energy Rev.* **2015**, *51*, 1446–1460. https://doi.org/10.1016/j.rser.2015.07.058.
- (51) Sari, Y. W. Biomass and Its Potential for Protein and Amino Acids; Valorizing Agricultural by-Products, Wageningen University, 2015.
- (52) Tuck, C. O.; Perez, E.; Horvath, I. T.; Sheldon, R. A.; Poliakoff, M. Valorization of Biomass: Deriving More Value from Waste. *Science.* **2012**, 337 (6095), 695–699. https://doi.org/10.1126/science.1218930.
- (53) De Schouwer, F.; Claes, L.; Vandekerkhove, A.; Verduyckt, J.; De Vos, D. E. Protein-Rich Biomass Waste as a Resource for Future Biorefineries: State of the Art, Challenges, and Opportunities. *ChemSusChem* **2019**, *12* (7), 1272–

- 1303. https://doi.org/10.1002/cssc.201802418.
- (54) Sharma, P.; Gaur, V. K.; Kim, S.-H.; Pandey, A. Microbial Strategies for Bio-Transforming Food Waste into Resources. *Bioresour. Technol.* **2020**, *299*, 122580. https://doi.org/10.1016/j.biortech.2019.122580.
- (55) Michels, J. The Use of Biomass for the Production of Fuel and Chemicals. In *Bioeconomy for Beginners*; Springer Berlin Heidelberg: Berlin, Heidelberg, 2020; pp 77–103. https://doi.org/10.1007/978-3-662-60390-1_4.
- (56) Ranganathan, S.; Dutta, S.; Moses, J. A.; Anandharamakrishnan, C. Utilization of Food Waste Streams for the Production of Biopolymers. *Heliyon* **2020**, *6* (9), e04891. https://doi.org/10.1016/j.heliyon.2020.e04891.
- (57) Capezza, A. J.; Newson, W. R.; Olsson, R. T.; Hedenqvist, M. S.; Johansson, E. Advances in the Use of Protein-Based Materials: Toward Sustainable Naturally Sourced Absorbent Materials. *ACS Sustain. Chem. Eng.* **2019**, *7*(5), 4532–4547. https://doi.org/10.1021/acssuschemeng.8b05400.
- (58) Xue, Y.; Lofland, S.; Hu, X. Thermal Conductivity of Protein-Based Materials: A Review. *Polymers (Basel).* **2019**, *11* (3), 456. https://doi.org/10.3390/polym11030456.
- (59) Gustavsson, J.; Cederberg, C.; Sonesson, U.; Otterdijk, R. van; Meybeck, A. Global food losses and food waste Extent, causes and prevention http://www.fao.org/3/a-i2697e.pdf. Last accessed date was January 2020.
- (60) Joffres, B.; Lorentz, C.; Vidalie, M.; Laurenti, D.; Quoineaud, A.-A.; Charon, N.; Daudin, A.; Quignard, A.; Geantet, C. Catalytic Hydroconversion of a Wheat Straw Soda Lignin: Characterization of the Products and the Lignin Residue. *Appl. Catal. B Environ.* 2014, 145, 167–176. https://doi.org/10.1016/j.apcatb.2013.01.039.
- (61) Holladay, J. E.; White, J. F.; Bozell, J. J.; Johnson, D. *Top Value-Added Chemicals from Biomass, Volume II Results of Screening for Potential Candidates From Biorefinery Lignin*; 2007.
- (62) Gui, M. M.; Lee, K. T.; Bhatia, S. Feasibility of Edible Oil vs. Non-Edible Oil vs. Waste Edible Oil as Biodiesel Feedstock. *Energy* **2008**, *33* (11), 1646–1653. https://doi.org/10.1016/j.energy.2008.06.002.
- (63) Hoarau, J.; Caro, Y.; Grondin, I.; Petit, T. Sugarcane Vinasse Processing: Toward a Status Shift from Waste to Valuable Resource. A Review. *J. Water Process Eng.* **2018**, *24*, 11–25. https://doi.org/10.1016/j.jwpe.2018.05.003.
- (64) Lammens, T. M.; Franssen, M. C. R.; Scott, E. L.; Sanders, J. P. M. Availability of Protein-Derived Amino Acids as Feedstock for the Production of Bio-Based Chemicals. *Biomass and Bioenergy* **2012**, *44*, 168–181. https://doi.org/10.1016/j.biombioe.2012.04.021.
- (65) Iram, A.; Cekmecelioglu, D.; Demirci, A. Distillers' Dried Grains with Solubles (DDGS) and Its Potential as Fermentation Feedstock. *Appl. Microbiol. Biotechnol.* **2020**, *104* (14), 6115–6128. https://doi.org/10.1007/s00253-020-10682-0.
- (66) Zhang, C.; Sanders, J. P. M.; Bruins, M. E. Critical Parameters in Cost-Effective Alkaline Extraction for High Protein Yield from Leaves. *Biomass and Bioenergy* **2014**, 67, 466–472. https://doi.org/10.1016/j.biombioe.2014.05.020.
- (67) Callegaro, K.; Brandelli, A.; Daroit, D. J. Beyond Plucking: Feathers

- Bioprocessing into Valuable Protein Hydrolysates. *Waste Manag.* **2019**, *95*, 399–415. https://doi.org/10.1016/j.wasman.2019.06.040.
- (68) Selective Catalysis for Renewable Feedstocks and Chemicals; Nicholas, K. M., Ed.; Topics in Current Chemistry; Springer International Publishing: Cham, 2014; Vol. 353. https://doi.org/10.1007/978-3-319-08654-5.
- (69) Kobayashi, H.; Fukuoka, A. Synthesis and Utilisation of Sugar Compounds Derived from Lignocellulosic Biomass. *Green Chem.* **2013**, *15* (7), 1740. https://doi.org/10.1039/c3gc00060e.
- (70) Biorefinery of Alternative Resources: Targeting Green Fuels and Platform Chemicals; Nanda, S., N. Vo, D.-V., Sarangi, P. K., Eds.; Springer Singapore: Singapore, 2020. https://doi.org/10.1007/978-981-15-1804-1.
- (71) Lin, Y.-C.; Huber, G. W. The Critical Role of Heterogeneous Catalysis in Lignocellulosic Biomass Conversion. *Energy Environ. Sci.* **2009**, *2* (1), 68–80. https://doi.org/10.1039/B814955K.
- (72) Huber, G. W.; Iborra, S.; Corma, A. Synthesis of Transportation Fuels from Biomass: Chemistry, Catalysts, and Engineering. *Chem. Rev.* **2006**, *106* (9), 4044–4098. https://doi.org/10.1021/cr068360d.
- (73) Collard, F. X.; Blin, J. A Review on Pyrolysis of Biomass Constituents: Mechanisms and Composition of the Products Obtained from the Conversion of Cellulose, Hemicelluloses and Lignin. *Renew. Sustain. Energy Rev.* **2014**, 38, 594–608. https://doi.org/10.1016/j.rser.2014.06.013.
- (74) Bridgwater, A. V. Review of Fast Pyrolysis of Biomass and Product Upgrading. *Biomass and Bioenergy* **2012**, 38, 68–94. https://doi.org/10.1016/j.biombioe.2011.01.048.
- (75) Mu, W.; Ben, H.; Ragauskas, A.; Deng, Y. Lignin Pyrolysis Components and Upgrading-Technology Review. *Bioenergy Res.* **2013**, *6* (4), 1183–1204. https://doi.org/10.1007/s12155-013-9314-7.
- (76) Mohan, D.; Pittman, C. U.; Steele, P. H. Pyrolysis of Wood/Biomass for Bio-Oil: A Critical Review. *Energy & Fuels* **2006**, *20* (3), 848–889. https://doi.org/10.1021/ef0502397.
- (77) Molino, A.; Chianese, S.; Musmarra, D. Biomass Gasification Technology: The State of the Art Overview. *J. Energy Chem.* **2016**, *25* (1), 10–25. https://doi.org/10.1016/j.jechem.2015.11.005.
- (78) Kirubakaran, V.; Sivaramakrishnan, V.; Nalini, R.; Sekar, T.; Premalatha, M.; Subramanian, P. A Review on Gasification of Biomass. *Renew. Sustain. Energy Rev.* **2009**, *13* (1), 179–186. https://doi.org/10.1016/j.rser.2007.07.001.
- (79) Axelsson, L.; Franzén, M.; Ostwald, M.; Berndes, G.; Lakshmi, G.; Ravindranath, N. H. Perspective: Jatropha Cultivation in Southern India: Assessing Farmers' Experiences. *Biofuels, Bioprod. Biorefining* **2012**, *6* (3), 246–256. https://doi.org/10.1002/bbb.
- (80) Elliott, D. C.; Biller, P.; Ross, A. B.; Schmidt, A. J.; Jones, S. B. Hydrothermal Liquefaction of Biomass: Developments from Batch to Continuous Process. *Bioresour. Technol.* **2015**, 178, 147–156. https://doi.org/10.1016/j.biortech.2014.09.132.
- (81) Toor, S. S.; Rosendahl, L.; Rudolf, A. Hydrothermal Liquefaction of Biomass: A Review of Subcritical Water Technologies. *Energy* **2011**, *36* (5), 2328–2342.

- https://doi.org/10.1016/j.energy.2011.03.013.
- (82) Gollakota, A. R. K.; Kishore, N.; Gu, S. A Review on Hydrothermal Liquefaction of Biomass. *Renew. Sustain. Energy Rev.* **2018**, *81* (August 2016), 1378–1392. https://doi.org/10.1016/j.rser.2017.05.178.
- (83) Coronado, I.; Stekrova, M.; Reinikainen, M.; Simell, P.; Lefferts, L.; Lehtonen, J. A Review of Catalytic Aqueous-Phase Reforming of Oxygenated Hydrocarbons Derived from Biorefinery Water Fractions. *Int. J. Hydrogen Energy* **2016**, *41* (26), 11003–11032. https://doi.org/10.1016/j.ijhydene.2016.05.032.
- (84) Knez; Markočič, E.; Hrnčič, M. K.; Ravber, M.; Škerget, M. High Pressure Water Reforming of Biomass for Energy and Chemicals: A Short Review. *J. Supercrit. Fluids* **2015**, *96*, 46–52. https://doi.org/10.1016/j.supflu.2014.06.008.
- (85) Davda, R. R.; Shabaker, J. W.; Huber, G. W.; Cortright, R. D.; Dumesic, J. A. A Review of Catalytic Issues and Process Conditions for Renewable Hydrogen and Alkanes by Aqueous-Phase Reforming of Oxygenated Hydrocarbons over Supported Metal Catalysts. *Appl. Catal. B Environ.* 2005, 56 (1-2 SPEC. ISS.), 171–186. https://doi.org/10.1016/j.apcatb.2004.04.027.
- (86) Moreno, A. D.; Alvira, P.; Ibarra, D.; Tomás-pejó, E. *Production of Platform Chemicals from Sustainable Resources*; 2017. https://doi.org/10.1007/978-981-10-4172-3.
- (87) Kang, S.; Fu, J.; Zhang, G. From Lignocellulosic Biomass to Levulinic Acid: A Review on Acid-Catalyzed Hydrolysis. *Renew. Sustain. Energy Rev.* **2018**, *94* (March 2017), 340–362. https://doi.org/10.1016/j.rser.2018.06.016.
- (88) Yu, I. K. M.; Tsang, D. C. W. Conversion of Biomass to Hydroxymethylfurfural: A Review of Catalytic Systems and Underlying Mechanisms. *Bioresour. Technol.* **2017**, *238*, 716–732. https://doi.org/10.1016/j.biortech.2017.04.026.
- (89) Chheda, J. N.; Huber, G. W.; Dumesic, J. A. Liquid-Phase Catalytic Processing of Biomass-Derived Oxygenated Hydrocarbons to Fuels and Chemicals. *Angew. Chemie Int. Ed.* **2007**, *46* (38), 7164–7183. https://doi.org/10.1002/anie.200604274.
- (90) Verardi, A.; De, I.; Ricca, E.; Calabr, V. Hydrolysis of Lignocellulosic Biomass: Current Status of Processes and Technologies and Future Perspectives. In *Bioethanol*; InTech, 2012; pp 95–122. https://doi.org/10.5772/23987.
- (91) Cherubini, F.; Strømman, A. H. Chemicals from Lignocellulosic Biomass: Opportunities, Perspectives, and Potential of Biorefinery Systems. *Biofuels, Bioprod. Biorefining* **2011**, *5* (5), 548–561. https://doi.org/10.1002/bbb.297.
- (92) Delidovich, I.; Leonhard, K.; Palkovits, R. Cellulose and Hemicellulose Valorisation: An Integrated Challenge of Catalysis and Reaction Engineering. *Energy Environ. Sci.* **2014**, *7* (9), 2803. https://doi.org/10.1039/C4EE01067A.
- (93) Marcet, I.; Álvarez, C.; Paredes, B.; Díaz, M. The Use of Sub-Critical Water Hydrolysis for the Recovery of Peptides and Free Amino Acids from Food Processing Wastes. Review of Sources and Main Parameters. *Waste Manag.* **2016**, *49*, 364–371. https://doi.org/10.1016/j.wasman.2016.01.009.
- (94) Carvalheiro, F.; Duarte, L. C.; Gírio, F. M. Hemicellulose Biorefineries: A Review on Biomass Pretreatments. *J. Sci. Ind. Res. (India).* **2008**, *67* (11), 849–864.

- (95) Varadarajan, S.; Miller, D. J. Catalytic Upgrading of Fermentation-Derived Organic Acids. *Biotechnol. Prog.* **1999**, *15* (5), 845–854. https://doi.org/10.1021/bp9900965.
- (96) Brethauer, S.; Studer, M. H. Biochemical Conversion Processes of Lignocellulosic Biomass to Fuels and Chemicals A Review. *Chimia (Aarau)*. **2015**, *69* (10), 572–581. https://doi.org/10.2533/chimia.2015.572.
- (97) Fillat, Ú.; Ibarra, D.; Eugenio, M. E.; Moreno, A. D.; Tomás-Pejó, E.; Martín-Sampedro, R. Laccases as a Potential Tool for the Efficient Conversion of Lignocellulosic Biomass: A Review. *Fermentation* **2017**, 3 (2), 1–30. https://doi.org/10.3390/fermentation3020017.
- (98) Wang, C.; Thygesen, A.; Liu, Y.; Li, Q.; Yang, M.; Dang, D.; Wang, Z.; Wan, Y.; Lin, W.; Xing, J. Bio-Oil Based Biorefinery Strategy for the Production of Succinic Acid. *Biotechnol. Biofuels* **2013**, *6* (1), 74. https://doi.org/10.1186/1754-6834-6-74.
- (99) Dusselier, M.; Mascal, M.; Sels, B. F. Top Chemical Opportunities from Carbohydrate Biomass: A Chemist's View of the Biorefinery; 2014; pp 1–40. https://doi.org/10.1007/128 2014 544.
- (100) Tan, H. W.; Abdul Aziz, A. R.; Aroua, M. K. Glycerol Production and Its Applications as a Raw Material: A Review. *Renew. Sustain. Energy Rev.* **2013**, 27, 118–127. https://doi.org/10.1016/j.rser.2013.06.035.
- (101) Quispe, C. A. G.; Coronado, C. J. R.; Carvalho Jr., J. A. Glycerol: Production, Consumption, Prices, Characterization and New Trends in Combustion. *Renew. Sustain. Energy Rev.* 2013, 27, 475–493. https://doi.org/10.1016/j.rser.2013.06.017.
- (102) Chong, C. C.; Aqsha, A.; Ayoub, M.; Sajid, M.; Abdullah, A. Z.; Yusup, S.; Abdullah, B. A Review over the Role of Catalysts for Selective Short-Chain Polyglycerol Production from Biodiesel Derived Waste Glycerol. *Environ. Technol. Innov.* 2020, 19, 100859. https://doi.org/10.1016/j.eti.2020.100859.
- (103) Simões, M.; Baranton, S.; Coutanceau, C. Electrochemical Valorisation of Glycerol. *ChemSusChem* **2012**, *5* (11), 2106–2124. https://doi.org/10.1002/cssc.201200335.
- (104) Kwon, Y.; Schouten, K. J. P.; Koper, M. T. M. Mechanism of the Catalytic Oxidation of Glycerol on Polycrystalline Gold and Platinum Electrodes. *ChemCatChem* **2011**, 3 (7), 1176–1185. https://doi.org/10.1002/cctc.201100023.
- (105) Dai, C.; Sun, L.; Liao, H.; Khezri, B.; Webster, R. D.; Fisher, A. C.; Xu, Z. J. Electrochemical Production of Lactic Acid from Glycerol Oxidation Catalyzed by AuPt Nanoparticles. *J. Catal.* **2017**, 356, 14–21. https://doi.org/10.1016/j.jcat.2017.10.010.
- (106) Kwon, Y.; Birdja, Y.; Spanos, I.; Rodriguez, P.; Koper, M. T. M. Highly Selective Electro-Oxidation of Glycerol to Dihydroxyacetone on Platinum in the Presence of Bismuth. *ACS Catal.* **2012**, *2* (5), 759–764. https://doi.org/10.1021/cs200599g.
- (107) Kim, H. J.; Lee, J.; Green, S. K.; Huber, G. W.; Kim, W. B. Selective Glycerol Oxidation by Electrocatalytic Dehydrogenation. *ChemSusChem* **2014**, *7* (4), 1051–1056. https://doi.org/10.1002/cssc.201301218.
- (108) Zhang, Z.; Xin, L.; Qi, J.; Chadderdon, D. J.; Sun, K.; Warsko, K. M.; Li, W.

- Selective Electro-Oxidation of Glycerol to Tartronate or Mesoxalate on Au Nanoparticle Catalyst via Electrode Potential Tuning in Anion-Exchange Membrane Electro-Catalytic Flow Reactor. *Appl. Catal. B Environ.* **2014**, *147*, 871–878. https://doi.org/10.1016/j.apcatb.2013.10.018.
- (109) Coutanceau, C.; Baranton, S.; Kouamé, R. S. B. Selective Electrooxidation of Glycerol Into Value-Added Chemicals: A Short Overview. *Front. Chem.* **2019**, 7 (100), 1–15. https://doi.org/10.3389/fchem.2019.00100.
- (110) Zhang, Z.; Xin, L.; Qi, J.; Wang, Z.; Li, W. Selective Electro-Conversion of Glycerol to Glycolate on Carbon Nanotube Supported Gold Catalyst. *Green Chem.* **2012**, *14* (8), 2150. https://doi.org/10.1039/c2gc35505a.
- (111) Lee, S.; Kim, H. J.; Lim, E. J.; Kim, Y.; Noh, Y.; Huber, G. W.; Kim, W. B. Highly Selective Transformation of Glycerol to Dihydroxyacetone without Using Oxidants by a PtSb/C-Catalyzed Electrooxidation Process. *Green Chem.* **2016**, *18* (9), 2877–2887. https://doi.org/10.1039/C5GC02865E.
- (112) Antolini, E. Glycerol Electro-Oxidation in Alkaline Media and Alkaline Direct Glycerol Fuel Cells. *Catalysts* **2019**, 9 (12), 980. https://doi.org/10.3390/catal9120980.
- (113) Houache, M. S. E.; Hughes, K.; Safari, R.; Botton, G. A.; Baranova, E. A. Modification of Nickel Surfaces by Bismuth: Effect on Electrochemical Activity and Selectivity toward Glycerol. ACS Appl. Mater. Interfaces 2020, 12 (13), 15095–15107. https://doi.org/10.1021/acsami.9b22378.
- (114) Zhou, Y.; Shen, Y.; Xi, J.; Luo, X. Selective Electro-Oxidation of Glycerol to Dihydroxyacetone by PtAg Skeletons. ACS Appl. Mater. Interfaces 2019, 11 (32), 28953–28959. https://doi.org/10.1021/acsami.9b09431.
- (115) Ahmad, M. S.; Cheng, C. K.; Ong, H. R.; Abdullah, H.; Hong, C. S.; Chua, G. K.; Mishra, P.; Rahman Khan, M. M. Electro-Oxidation of Waste Glycerol to Tartronic Acid over Pt/CNT Nanocatalyst: Study of Effect of Reaction Time on Product Distribution. *Energy Sources, Part A Recover. Util. Environ. Eff.* 2019, 1–17. https://doi.org/10.1080/15567036.2019.1683099.
- (116) Alaba, P. A.; Lee, C. S.; Abnisa, F.; Aroua, M. K.; Cognet, P.; Pérès, Y.; Wan Daud, W. M. A. A Review of Recent Progress on Electrocatalysts toward Efficient Glycerol Electrooxidation. *Rev. Chem. Eng.* **2020**, 1–33. https://doi.org/10.1515/revce-2019-0013.
- (117) James, O. O.; Sauter, W.; Schröder, U. Towards Selective Electrochemical Conversion of Glycerol to 1,3-Propanediol. *RSC Adv.* **2018**, *8* (20), 10818–10827. https://doi.org/10.1039/C8RA00711J.
- (118) Rahim, S. A. N. M.; Lee, C. S.; Abnisa, F.; Aroua, M. K.; Daud, W. A. W.; Cognet, P.; Pérès, Y. A Review of Recent Developments on Kinetics Parameters for Glycerol Electrochemical Conversion A by-Product of Biodiesel. *Sci. Total Environ.* **2020**, *705*, 135137. https://doi.org/10.1016/j.scitotenv.2019.135137.
- (119) Ahmad, M. S.; Singh, S.; Cheng, C. K.; Ong, H. R.; Abdullah, H.; Khan, M. R.; Wongsakulphasatch, S. Glycerol Electro-Oxidation to Dihydroxyacetone on Phosphorous-Doped Pd/CNT Nanoparticles in Alkaline Medium. *Catal. Commun.* 2020, 139, 105964. https://doi.org/10.1016/j.catcom.2020.105964.
- (120) Ciriminna, R.; Palmisano, G.; Pina, C. Della; Rossi, M.; Pagliaro, M. One-Pot Electrocatalytic Oxidation of Glycerol to DHA. *Tetrahedron Lett.* **2006**, *47* (39),

- 6993-6995. https://doi.org/10.1016/j.tetlet.2006.07.123.
- (121) Nutting, J. E.; Rafiee, M.; Stahl, S. S. Tetramethylpiperidine N -Oxyl (TEMPO), Phthalimide N -Oxyl (PINO), and Related N -Oxyl Species: Electrochemical Properties and Their Use in Electrocatalytic Reactions. *Chem. Rev.* **2018**, *118* (9), 4834–4885. https://doi.org/10.1021/acs.chemrev.7b00763.
- (122) Liu, D.; Liu, J.-C.; Cai, W.; Ma, J.; Yang, H. Bin; Xiao, H.; Li, J.; Xiong, Y.; Huang, Y.; Liu, B. Selective Photoelectrochemical Oxidation of Glycerol to High Value-Added Dihydroxyacetone. *Nat. Commun.* **2019**, *10* (1), 1779. https://doi.org/10.1038/s41467-019-09788-5.
- (123) Lam, C. H.; Bloomfield, A. J.; Anastas, P. T. A Switchable Route to Valuable Commodity Chemicals from Glycerol via Electrocatalytic Oxidation with an Earth Abundant Metal Oxidation Catalyst. *Green Chem.* **2017**, *19* (8), 1958–1968. https://doi.org/10.1039/C7GC00371D.
- (124) Dodekatos, G.; Schünemann, S.; Tüysüz, H. Recent Advances in Thermo-, Photo-, and Electrocatalytic Glycerol Oxidation. *ACS Catal.* **2018**, *8* (7), 6301–6333. https://doi.org/10.1021/acscatal.8b01317.
- (125) Velázquez-Hernández, I.; Zamudio, E.; Rodríguez-Valadez, F. J.; García-Gómez, N. A.; Álvarez-Contreras, L.; Guerra-Balcázar, M.; Arjona, N. Electrochemical Valorization of Crude Glycerol in Alkaline Medium for Energy Conversion Using Pd, Au and PdAu Nanomaterials. *Fuel* **2020**, *262*, 116556. https://doi.org/10.1016/j.fuel.2019.116556.
- (126) Huang, L.; Sun, J.-Y.; Cao, S.-H.; Zhan, M.; Ni, Z.-R.; Sun, H.-J.; Chen, Z.; Zhou, Z.-Y.; Sorte, E. G.; Tong, Y. J.; et al. Combined EC-NMR and In Situ FTIR Spectroscopic Studies of Glycerol Electrooxidation on Pt/C, PtRu/C, and PtRh/C. *ACS Catal.* **2016**, *6* (11), 7686–7695. https://doi.org/10.1021/acscatal.6b02097.
- (127) Valter, M.; Busch, M.; Wickman, B.; Grönbeck, H.; Baltrusaitis, J.; Hellman, A. Electrooxidation of Glycerol on Gold in Acidic Medium: A Combined Experimental and DFT Study. *J. Phys. Chem. C* **2018**, *122* (19), 10489–10494. https://doi.org/10.1021/acs.jpcc.8b02685.
- (128) Benipal, N.; Qi, J.; Liu, Q.; Li, W. Carbon Nanotube Supported PdAg Nanoparticles for Electrocatalytic Oxidation of Glycerol in Anion Exchange Membrane Fuel Cells. *Appl. Catal. B Environ.* **2017**, *210*, 121–130. https://doi.org/10.1016/j.apcatb.2017.02.082.
- (129) Costa Santos, J. B.; Vieira, C.; Crisafulli, R.; Linares, J. J. Promotional Effect of Auxiliary Metals Bi on Pt, Pd, and Ag on Au, for Glycerol Electrolysis. *Int. J. Hydrogen Energy* **2020**, *45* (47), 25658–25671. https://doi.org/10.1016/j.ijhydene.2019.11.225.
- (130) Grand View Research. Acetic Acid Market Size, Share & Trends Analysis Report By Application (Vinyl Acetate Monomer, Purified Terephthalic Acid, Acetate Esters, Ethanol), By Region, And Segment Forecasts, 2020 2027 https://www.grandviewresearch.com/industry-analysis/acetic-acid-market. Last accessed date was January 2020.
- (131) Expert Market Research. Global Acetic Acid Market to Reach 11.85 Million Tons by 2026 https://www.expertmarketresearch.com/pressrelease/global-acetic-acid-market. Last accessed date was January 2020.
- (132) Sauter, W.; Bergmann, O. L.; Schröder, U. Hydroxyacetone: A Glycerol-Based

- Platform for Electrocatalytic Hydrogenation and Hydrodeoxygenation Processes. *ChemSusChem* **2017**, *10* (15), 3105–3110. https://doi.org/10.1002/cssc.201700996.
- (133) Chiu, C.-W.; Dasari, M. A.; Suppes, G. J.; Sutterlin, W. R. Dehydration of Glycerol to Acetol via Catalytic Reactive Distillation. *AIChE J.* **2006**, *52* (10), 3543–3548. https://doi.org/10.1002/aic.10951.
- (134) Basu, S.; Sen, A. K.; Mukherjee, M. Synthesis and Performance Evaluation of Silica-Supported Copper Chromite Catalyst for Glycerol Dehydration to Acetol. *J. Chem. Sci.* **2019**, *131* (8), 82. https://doi.org/10.1007/s12039-019-1662-1.
- (135) Basu, S.; Sen, A. K. Dehydration of Glycerol with Silica—Phosphate-Supported Copper Catalyst. Res. Chem. Intermed. 2020. https://doi.org/10.1007/s11164-020-04161-4.
- (136) Braga, T. P.; Essayem, N.; Valentini, A. Non-Crystalline Copper Oxide Highly Dispersed on Mesoporous Alumina: Synthesis, Characterization and Catalytic Activity in Glycerol Conversion to Acetol. *Quim. Nova* **2016**. https://doi.org/10.5935/0100-4042.20160074.
- (137) Dasari, M. A.; Kiatsimkul, P.-P.; Sutterlin, W. R.; Suppes, G. J. Low-Pressure Hydrogenolysis of Glycerol to Propylene Glycol. *Appl. Catal. A Gen.* **2005**, *281* (1–2), 225–231. https://doi.org/10.1016/j.apcata.2004.11.033.
- (138) Guo, X.; Guan, J.; Li, B.; Wang, X.; Mu, X.; Liu, H. Conversion of Biomass-Derived Sorbitol to Glycols over Carbon-Materials Supported Ru-Based Catalysts. *Sci. Rep.* **2015**, *5* (1), 16451. https://doi.org/10.1038/srep16451.
- (139) Habibi, E.; Razmi, H. Glycerol Electrooxidation on Pd, Pt and Au Nanoparticles Supported on Carbon Ceramic Electrode in Alkaline Media. *Int. J. Hydrogen Energy* **2012**, 37 (22), 16800–16809. https://doi.org/10.1016/j.ijhydene.2012.08.127.
- (140) Sandrini, R. M. L. M.; Sempionatto, J. R.; Herrero, E.; Feliu, J. M.; Souza-Garcia, J.; Angelucci, C. A. Mechanistic Aspects of Glycerol Electrooxidation on Pt(111) Electrode in Alkaline Media. *Electrochem. commun.* **2018**, *86*, 149–152. https://doi.org/10.1016/j.elecom.2017.11.027.
- (141) Antolini, E.; Salgado, J. R. C.; Gonzalez, E. R. The Methanol Oxidation Reaction on Platinum Alloys with the First Row Transition Metals. *Appl. Catal. B Environ.* **2006**, 63 (1–2), 137–149. https://doi.org/10.1016/j.apcatb.2005.09.014.
- (142) Valério Neto, E. S.; Gomes, M. A.; Salazar-Banda, G. R.; Eguiluz, K. I. B. Pt and Pt–Rh Nanowires Supported on Carbon and SnO2:Sb Nanoparticles for Ethanol Electrochemical Oxidation in Acidic Media. *Int. J. Hydrogen Energy* 2018, 43 (1), 178–188. https://doi.org/10.1016/j.ijhydene.2017.11.014.
- (143) Wang, P.; Yin, S.; Wen, Y.; Tian, Z.; Wang, N.; Key, J.; Wang, S.; Shen, P. K. Ternary Pt 9 RhFe x Nanoscale Alloys as Highly Efficient Catalysts with Enhanced Activity and Excellent CO-Poisoning Tolerance for Ethanol Oxidation. ACS Appl. Mater. Interfaces 2017, 9 (11), 9584–9591. https://doi.org/10.1021/acsami.6b14947.
- (144) Jokic, A.; Ristic, N.; Jaksic, M. M.; Spasojevic, M.; Krstajic, N. Simultaneous Electrolytic Production of Xylitol and Xylonic Acid from Xylose. *J. Appl. Electrochem.* **1991**, *21* (4), 321–326. https://doi.org/10.1007/BF01020216.
- (145) Governo, A. T.; Proença, L.; Parpot, P.; Lopes, M. I. S.; Fonseca, I. T. E.

- Electro-Oxidation of d-Xylose on Platinum and Gold Electrodes in Alkaline Medium. *Electrochim. Acta* **2004**, *49* (9–10), 1535–1545. https://doi.org/10.1016/j.electacta.2003.11.013.
- (146) Liu, W.-J.; Xu, Z.; Zhao, D.; Pan, X.-Q.; Li, H.-C.; Hu, X.; Fan, Z.-Y.; Wang, W.-K.; Zhao, G.-H.; Jin, S.; et al. Efficient Electrochemical Production of Glucaric Acid and H2 via Glucose Electrolysis. *Nat. Commun.* **2020**, *11* (1), 265. https://doi.org/10.1038/s41467-019-14157-3.
- (147) Parpot, P.; Pires, S. G.; Bettencourt, A. P. Electrocatalytic Oxidation of D-Galactose in Alkaline Medium. *J. Electroanal. Chem.* **2004**, *566* (2), 401–408. https://doi.org/10.1016/j.jelechem.2003.11.053.
- (148) Parpot, P.; Santos, P. R. B.; Bettencourt, A. P. Electro-Oxidation of d-Mannose on Platinum, Gold and Nickel Electrodes in Aqueous Medium. *J. Electroanal. Chem.* 2007, 610 (2), 154–162. https://doi.org/10.1016/j.jelechem.2007.07.011.
- (149) Matos, J. P. F.; Proença, L.; Lopes, M. I. S.; Fonseca, I. T. E. The Electrochemical Oxidation of Xylitol on Pt (111) in Acid Medium. *J. Electroanal. Chem.* **2004**, *571* (1), 111–117. https://doi.org/10.1016/j.jelechem.2004.04.016.
- (150) Proença, L.; Lopes, M. I. .; Fonseca, I.; Rodes, A.; Gómez, R.; Aldaz, A. On the Oxidation of D-Sorbitol on Platinum Single Crystal Electrodes: A Voltammetric and in Situ FTIRS Study. *Electrochim. Acta* **1998**, *44* (5), 735–743. https://doi.org/10.1016/S0013-4686(98)00219-9.
- (151) Matos, J. P. F.; Proença, L. F. A.; Lopes, M. I. S.; Fonseca, I. T. E.; Rodes, A.; Aldaz, A. Electrooxidation of Xylitol on Platinum Single Crystal Electrodes: A Voltammetric and in Situ FTIRS Study. *J. Electroanal. Chem.* 2007, 609 (1), 42–50. https://doi.org/10.1016/j.jelechem.2007.06.005.
- (152) Silva, A. .; Proença, L.; Lopes, M. I. .; Fonseca, I.; Rodes, A.; Aldaz, A. Electro-Oxidation of d-Mannitol on Platinum Single Crystal Surfaces. *Electrochim. Acta* **2001**, *46* (20–21), 3147–3155. https://doi.org/10.1016/S0013-4686(01)00606-5.
- (153) Chen, S. G.; Wen, T.; Utley, J. H. P. The Use of a Porous Hydrogen Diffusion Anode in the Electrochemical Reduction of Glucose to Sorbitol. *J. Appl. Electrochem.* **1992**, *22* (1), 43–47. https://doi.org/10.1007/BF01093010.
- (154) Proença, L.; Lopes, M. I. S.; Fonseca, I.; Kokoh, K. B.; Léger, J.-M.; Lamy, C. Electrocatalytic Oxidation of D-Sorbitol on Platinum in Acid Medium: Analysis of the Reaction Products. *J. Electroanal. Chem.* **1997**, *432* (1–2), 237–242. https://doi.org/10.1016/S0022-0728(97)00221-0.
- (155) Parpot, P.; Servat, K.; Bettencourt, A. P.; Huser, H.; Kokoh, K. B. TEMPO Mediated Oxidation of Carbohydrates Using Electrochemical Methods. *Cellulose* **2010**, *17* (4), 815–824. https://doi.org/10.1007/s10570-010-9417-7.
- (156) Kwon, Y.; Koper, M. T. M. Electrocatalytic Hydrogenation and Deoxygenation of Glucose on Solid Metal Electrodes. *ChemSusChem* **2013**, *6* (3), 455–462. https://doi.org/10.1002/cssc.201200722.
- (157) Park, K. Flow Reactor Studies of the Paired Electro-Oxidation and Electroreduction of Glucose. *J. Electrochem. Soc.* **1985**, *132* (8), 1850. https://doi.org/10.1149/1.2114229.
- (158) bin Kassim, A.; Rice, C. L.; Kuhn, A. T. Cathodic Reduction of Glucose. J.

- Chem. Soc. Faraday Trans. 1 Phys. Chem. Condens. Phases **1981**, 77 (3), 683. https://doi.org/10.1039/f19817700683.
- (159) Owobi-Andely, Y.; Fiaty, K.; Laurent, P.; Bardot, C. Use of Electrocatalytic Membrane Reactor for Synthesis of Sorbitol. *Catal. Today* **2000**, *56* (1–3), 173–178. https://doi.org/10.1016/S0920-5861(99)00274-6.
- (160) James, O. O.; Sauter, W.; Schröder, U. Electrochemistry for the Generation of Renewable Chemicals: One-Pot Electrochemical Deoxygenation of Xylose to Δ-Valerolactone. *ChemSusChem* **2017**, *10* (9), 2015–2022. https://doi.org/10.1002/cssc.201700209.
- (161) Neha, N.; Islam, M. H.; Baranton, S.; Coutanceau, C.; Pollet, B. G. Assessment of the Beneficial Combination of Electrochemical and Ultrasonic Activation of Compounds Originating from Biomass. *Ultrason. Sonochem.* **2020**, *63*, 104934. https://doi.org/10.1016/j.ultsonch.2019.104934.
- (162) Torto, N. Recent Progress in Electrochemical Oxidation of Saccharides at Gold and Copper Electrodes in Alkaline Solutions. *Bioelectrochemistry* **2009**, 76 (1–2), 195–200. https://doi.org/10.1016/j.bioelechem.2009.06.009.
- (163) Rafaïdeen, T.; Baranton, S.; Coutanceau, C. Highly Efficient and Selective Electrooxidation of Glucose and Xylose in Alkaline Medium at Carbon Supported Alloyed PdAu Nanocatalysts. *Appl. Catal. B Environ.* **2019**, *243*, 641–656. https://doi.org/10.1016/j.apcatb.2018.11.006.
- (164) Chou, C.-F.; Chou, T.-C. Paired Electrooxidation IV. Decarboxylation of Sodium Gluconate to D-Arabinose. *J. Appl. Electrochem.* **2003**, 33, 741–745. https://doi.org/10.1023/A:1025005832155.
- (165) Mariscal, R.; Maireles-Torres, P.; Ojeda, M.; Sádaba, I.; López Granados, M. Furfural: A Renewable and Versatile Platform Molecule for the Synthesis of Chemicals and Fuels. *Energy Environ. Sci.* 2016, 9 (4), 1144–1189. https://doi.org/10.1039/C5EE02666K.
- (166) Chen, B.; Li, F.; Yuan, G. Selective Hydrodeoxygenation of 5-Hydroxy-2(5H)-Furanone to γ-Butyrolactone over Pt/Mesoporous Solid Acid Bifunctional Catalyst. *RSC Adv.* **2017**, 7 (34), 21145–21152. https://doi.org/10.1039/c7ra03205f.
- (167) Eerhart, A. J. J. E.; Faaij, A. P. C.; Patel, M. K. Replacing Fossil Based PET with Biobased PEF; Process Analysis, Energy and GHG Balance. *Energy Environ. Sci.* **2012**, *5* (4), 6407. https://doi.org/10.1039/c2ee02480b.
- (168) Barwe, S.; Weidner, J.; Cychy, S.; Morales, D. M.; Dieckhöfer, S.; Hiltrop, D.; Masa, J.; Muhler, M.; Schuhmann, W. Electrocatalytic Oxidation of 5-(Hydroxymethyl)Furfural Using High-Surface-Area Nickel Boride. *Angew. Chemie Int. Ed.* **2018**, *57* (35), 11460–11464. https://doi.org/10.1002/anie.201806298.
- (169) Kwon, Y.; Schouten, K. J. P.; van der Waal, J. C.; de Jong, E.; Koper, M. T. M. Electrocatalytic Conversion of Furanic Compounds. ACS Catal. 2016, 6 (10), 6704–6717. https://doi.org/10.1021/acscatal.6b01861.
- (170) Liu, W.-J.; Dang, L.; Xu, Z.; Yu, H.-Q.; Jin, S.; Huber, G. W. Electrochemical Oxidation of 5-Hydroxymethylfurfural with NiFe Layered Double Hydroxide (LDH) Nanosheet Catalysts. *ACS Catal.* **2018**, *8* (6), 5533–5541. https://doi.org/10.1021/acscatal.8b01017.
- (171) You, B.; Liu, X.; Liu, X.; Sun, Y. Efficient H 2 Evolution Coupled with Oxidative

- Refining of Alcohols via A Hierarchically Porous Nickel Bifunctional Electrocatalyst. *ACS Catal.* **2017**, *7* (7), 4564–4570. https://doi.org/10.1021/acscatal.7b00876.
- (172) You, B.; Liu, X.; Jiang, N.; Sun, Y. A General Strategy for Decoupled Hydrogen Production from Water Splitting by Integrating Oxidative Biomass Valorization. *J. Am. Chem. Soc.* **2016**, *138* (41), 13639–13646. https://doi.org/10.1021/jacs.6b07127.
- (173) You, B.; Jiang, N.; Liu, X.; Sun, Y. Simultaneous H2Generation and Biomass Upgrading in Water by an Efficient Noble-Metal-Free Bifunctional Electrocatalyst. *Angew. Chemie Int. Ed.* **2016**, *55* (34), 9913–9917. https://doi.org/10.1002/anie.201603798.
- (174) Kashparova, V. P.; Klushin, V. A.; Leontyeva, D. V.; Smirnova, N. V.; Chernyshev, V. M.; Ananikov, V. P. Selective Synthesis of 2,5-Diformylfuran by Sustainable 4-Acetamido-TEMPO/Halogen-Mediated Electrooxidation of 5-Hydroxymethylfurfural. *Chem. An Asian J.* 2016, 11 (18), 2578–2585. https://doi.org/10.1002/asia.201600801.
- (175) Kubota, S. R.; Choi, K.-S. Electrochemical Oxidation of 5-Hydroxymethylfurfural to 2,5-Furandicarboxylic Acid (FDCA) in Acidic Media Enabling Spontaneous FDCA Separation. *ChemSusChem* **2018**, *11* (13), 2138–2145. https://doi.org/10.1002/cssc.201800532.
- (176) Shi, N.; Liu, Q.; Ju, R.; He, X.; Zhang, Y.; Tang, S.; Ma, L. Condensation of α-Carbonyl Aldehydes Leads to the Formation of Solid Humins during the Hydrothermal Degradation of Carbohydrates. *ACS Omega* **2019**, *4* (4), 7330–7343. https://doi.org/10.1021/acsomega.9b00508.
- (177) Geissman, T. A. The Cannizzaro Reaction. In *Organic Reactions*; John Wiley & Sons, Inc.: Hoboken, NJ, USA, 2011; Vol. 88, pp 94–113. https://doi.org/10.1002/0471264180.or002.03.
- (178) Roylance, J. J.; Kim, T. W.; Choi, K.-S. S. Efficient and Selective Electrochemical and Photoelectrochemical Reduction of 5-Hydroxymethylfurfural to 2,5-Bis(Hydroxymethyl)Furan Using Water as the Hydrogen Source. ACS Catal. 2016. 6 (3),1840–1847. https://doi.org/10.1021/acscatal.5b02586.
- (179) Roylance, J. J.; Choi, K.-S. S. Electrochemical Reductive Biomass Conversion: Direct Conversion of 5-Hydroxymethylfurfural (HMF) to 2,5-Hexanedione (HD) via Reductive Ring-Opening. *Green Chem.* **2016**, *18* (10), 2956–2960. https://doi.org/10.1039/C6GC00533K.
- (180) Sacia, E. R.; Deaner, M. H.; Louie, Y. "Lin"; Bell, A. T. Synthesis of Biomass-Derived Methylcyclopentane as a Gasoline Additive via Aldol Condensation/Hydrodeoxygenation of 2,5-Hexanedione. *Green Chem.* **2015**, 17 (4), 2393–2397. https://doi.org/10.1039/C4GC02292K.
- (181) Buntara, T.; Noel, S.; Phua, P. H.; Melián-Cabrera, I.; De Vries, J. G.; Heeres, H. J. Caprolactam from Renewable Resources: Catalytic Conversion of 5-Hydroxymethylfurfural into Caprolactone. *Angew. Chemie Int. Ed.* **2011**, *50* (31), 7083–7087. https://doi.org/10.1002/anie.201102156.
- (182) Chadderdon, X. H.; Chadderdon, D. J.; Pfennig, T.; Shanks, B. H.; Li, W. Paired Electrocatalytic Hydrogenation and Oxidation of 5-(Hydroxymethyl)Furfural for Efficient Production of Biomass-Derived

- Monomers. *Green Chem.* **2019**, *21* (22), 6210–6219. https://doi.org/10.1039/C9GC02264C.
- (183) Banerjee, A.; Dick, G. R.; Yoshino, T.; Kanan, M. W. Carbon Dioxide Utilization via Carbonate-Promoted C–H Carboxylation. *Nature* **2016**, *531* (7593), 215–219. https://doi.org/10.1038/nature17185.
- (184) Corma, A.; Iborra, S.; Velty, A. Chemical Routes for the Transformation of Biomass into Chemicals. *Chem. Rev.* **2007**, *107* (6), 2411–2502. https://doi.org/10.1021/cr050989d.
- (185) Parpot, P.; Bettencourt, A. P.; Chamoulaud, G.; Kokoh, K. B.; Belgsir, E. M. Electrochemical Investigations of the Oxidation-Reduction of Furfural in Aqueous Medium Application to Electrosynthesis. *Electrochim. Acta* **2004**, *49* (3), 397–403. https://doi.org/10.1016/j.electacta.2003.08.021.
- (186) Román, A. M.; Agrawal, N.; Hasse, J. C.; Janik, M. J.; Medlin, J. W.; Holewinski, A. Electro-Oxidation of Furfural on Gold Is Limited by Furoate Self-Assembly. *J. Catal.* **2020**, 391, 327–335. https://doi.org/10.1016/j.jcat.2020.08.034.
- (187) Román, A. M.; Hasse, J. C.; Medlin, J. W.; Holewinski, A. Elucidating Acidic Electro-Oxidation Pathways of Furfural on Platinum. *ACS Catal.* **2019**, *9* (11), 10305–10316. https://doi.org/10.1021/acscatal.9b02656.
- (188) Payne, K. A. P.; Marshall, S. A.; Fisher, K.; Cliff, M. J.; Cannas, D. M.; Yan, C.; Heyes, D. J.; Parker, D. A.; Larrosa, I.; Leys, D. Enzymatic Carboxylation of 2-Furoic Acid Yields 2,5-Furandicarboxylic Acid (FDCA). *ACS Catal.* **2019**, 9 (4), 2854–2865. https://doi.org/10.1021/acscatal.8b04862.
- (189) Shen, G.; Zhang, S.; Lei, Y.; Chen, Z.; Yin, G. Synthesis of 2,5-Furandicarboxylic Acid by Catalytic Carbonylation of Renewable Furfural Derived 5-Bromofuroic Acid. *Mol. Catal.* **2018**, *455* (June), 204–209. https://doi.org/10.1016/j.mcat.2018.06.015.
- (190) Kubota, S. R.; Choi, K.-S. S. Electrochemical Valorization of Furfural to Maleic Acid. *ACS Sustain. Chem. Eng.* **2018**, *6* (8), 9596–9600. https://doi.org/10.1021/acssuschemeng.8b02698.
- (191) Thiyagarajan, S.; Franciolus, D.; Bisselink, R. J. M.; Ewing, T. A.; Boeriu, C. G.; van Haveren, J. Selective Production of Maleic Acid from Furfural via a Cascade Approach Combining Photochemistry and Electro- or Biochemistry. ACS Sustain. Chem. Eng. 2020, 8 (29), 10626–10632. https://doi.org/10.1021/acssuschemeng.0c02833.
- (192) Li, X.; Jia, P.; Wang, T. Furfural: A Promising Platform Compound for Sustainable Production of C 4 and C 5 Chemicals. *ACS Catal.* **2016**, *6* (11), 7621–7640. https://doi.org/10.1021/acscatal.6b01838.
- (193) Chadderdon, X. H.; Chadderdon, D. J.; Matthiesen, J. E.; Qiu, Y.; Carraher, J. M.; Tessonnier, J.-P.; Li, W. Mechanisms of Furfural Reduction on Metal Electrodes: Distinguishing Pathways for Selective Hydrogenation of Bioderived Oxygenates. *J. Am. Chem. Soc.* 2017, 139 (40), 14120–14128. https://doi.org/10.1021/jacs.7b06331.
- (194) Wang, F.; Xu, M.; Wei, L.; Wei, Y.; Hu, Y.; Fang, W.; Zhu, C. G. Fabrication of La-Doped TiO2 Film Electrode and Investigation of Its Electrocatalytic Activity for Furfural Reduction. *Electrochim. Acta* **2015**, *153*, 170–174. https://doi.org/10.1016/j.electacta.2014.11.203.

- (195) Jung, S.; Biddinger, E. J. Electrocatalytic Hydrogenation and Hydrogenolysis of Furfural and the Impact of Homogeneous Side Reactions of Furanic Compounds in Acidic Electrolytes. *ACS Sustain. Chem. Eng.* **2016**, *4* (12), 6500–6508. https://doi.org/10.1021/acssuschemeng.6b01314.
- (196) Jung, S.; Karaiskakis, A. N.; Biddinger, E. J. Enhanced Activity for Electrochemical Hydrogenation and Hydrogenolysis of Furfural to Biofuel Using Electrodeposited Cu Catalysts. *Catal. Today* **2019**, 323, 26–34. https://doi.org/10.1016/j.cattod.2018.09.011.
- (197) Parpot, P.; Bettencourt, A. .; Chamoulaud, G.; Kokoh, K. .; Belgsir, E. . Electrochemical Investigations of the Oxidation–Reduction of Furfural in Aqueous Medium. *Electrochim. Acta* **2004**, *49* (3), 397–403. https://doi.org/10.1016/j.electacta.2003.08.021.
- (198) zhao, B.; Chen, M.; Guo, Q.; Fu, Y. Electrocatalytic Hydrogenation of Furfural to Furfuryl Alcohol Using Platinum Supported on Activated Carbon Fibers. *Electrochim. Acta* **2014**, *135*, 139–146. https://doi.org/10.1016/j.electacta.2014.04.164.
- (199) Chen, S.; Wojcieszak, R.; Dumeignil, F.; Marceau, E.; Royer, S. How Catalysts and Experimental Conditions Determine the Selective Hydroconversion of Furfural and 5-Hydroxymethylfurfural. *Chem. Rev.* **2018**, *118* (22), 11023–11117. https://doi.org/10.1021/acs.chemrev.8b00134.
- (200) da Silva, E. D.; Gonzalez, W. A.; Fraga, M. A. Aqueous-Phase Oxidation of 5-Hydroxymethylfurfural over Pt/ZrO2 Catalysts: Exploiting the Alkalinity of the Reaction Medium and Catalyst Basicity. *Green Process. Synth.* **2016**, *5* (4). https://doi.org/10.1515/gps-2016-0010.
- (201) Li, K.; Sun, Y. Electrocatalytic Upgrading of Biomass-Derived Intermediate Compounds to Value-Added Products. *Chem. A Eur. J.* **2018**, *24* (69), 18258–18270. https://doi.org/10.1002/chem.201803319.
- (202) Bababrik, R.; Santhanaraj, D.; Resasco, D. E.; Wang, B. A Comparative Study of Thermal- and Electrocatalytic Conversion of Furfural: Methylfuran as a Primary and Major Product. *J. Appl. Electrochem.* **2020**. https://doi.org/10.1007/s10800-020-01427-y.
- (203) Troiano, D.; Orsat, V.; Dumont, M.-J. Status of Biocatalysis in the Production of 2,5-Furandicarboxylic Acid. *ACS Catal.* **2020**, *10* (16), 9145–9169. https://doi.org/10.1021/acscatal.0c02378.
- (204) Gupta, K.; Rai, R. K.; Singh, S. K. Metal Catalysts for the Efficient Transformation of Biomass-Derived HMF and Furfural to Value Added Chemicals. *ChemCatChem* **2018**, *10* (11), 2326–2349. https://doi.org/10.1002/cctc.201701754.
- (205) Xu, C.; Paone, E.; Rodríguez-Padrón, D.; Luque, R.; Mauriello, F. Recent Catalytic Routes for the Preparation and the Upgrading of Biomass Derived Furfural and 5-Hydroxymethylfurfural. *Chem. Soc. Rev.* **2020**, *49* (13), 4273–4306. https://doi.org/10.1039/D0CS00041H.
- (206) Wojcieszak, R.; Santarelli, F.; Paul, S.; Dumeignil, F.; Cavani, F.; Gonçalves, R. V. Recent Developments in Maleic Acid Synthesis from Bio-Based Chemicals. *Sustain. Chem. Process.* **2015**, 3 (1), 9. https://doi.org/10.1186/s40508-015-0034-5.
- (207) Nilges, P.; Schröder, U. Electrochemistry for Biofuel Generation: Production

- of Furans by Electrocatalytic Hydrogenation of Furfurals. *Energy Environ. Sci.* **2013**, *6* (10), 2925–2931. https://doi.org/10.1039/c3ee41857j.
- (208) Wu, Q.; Bao, X.; Guo, W.; Wang, B.; Li, Y.; Luo, H.; Wang, H.; Ren, N. Medium Chain Carboxylic Acids Production from Waste Biomass: Current Advances and Perspectives. *Biotechnol. Adv.* **2019**, *37* (5), 599–615. https://doi.org/10.1016/j.biotechadv.2019.03.003.
- (209) Lange, J.-P.; Price, R.; Ayoub, P. M.; Louis, J.; Petrus, L.; Clarke, L.; Gosselink, H. Valeric Biofuels: A Platform of Cellulosic Transportation Fuels. *Angew. Chemie Int. Ed.* **2010**, *49* (26), 4479–4483. https://doi.org/10.1002/anie.201000655.
- (210) Xin, L.; Zhang, Z.; Qi, J.; Chadderdon, D. J.; Qiu, Y.; Warsko, K. M.; Li, W. Electricity Storage in Biofuels: Selective Electrocatalytic Reduction of Levulinic Acid to Valeric Acid or γ-Valerolactone. *ChemSusChem* **2013**, *6* (4), 674–686. https://doi.org/10.1002/cssc.201200765.
- (211) Nelsen, S. F. Electrochemical Reactions and Mechanisms in Organic Chemistry By James Grimshaw (The Queen's University of Belfast). Elsevier: Amsterdam and New York. 2000. Xii + 401 Pp. \$251.50. ISBN 0-444-72007-3., 1st ed.; Elsevier Science: Belfast, Northern Ireland, 2002; Vol. 124. https://doi.org/10.1021/ja015344j.
- (212) Fleischmann, M.; Pletcher, D. *Organic Electrochemistry*, 4th ed.; Lund, H., Hammerich, O., Eds.; Marcel Dekker: New York, 1969; Vol. 2. https://doi.org/10.1039/rr9690200087.
- (213) Stang, C.; Harnisch, F. The Dilemma of Supporting Electrolytes for Electroorganic Synthesis: A Case Study on Kolbe Electrolysis. *ChemSusChem* **2016**, *9* (1), 50–60. https://doi.org/10.1002/cssc.201501407.
- (214) Martin, C.; Huser, H.; Servat, K.; Kokoh, K. B. Selective Electroreduction of Pyruvic Acid on Lead Electrode in Acid Medium. *Electrochim. Acta* **2005**, *50* (12), 2431–2435. https://doi.org/10.1016/j.electacta.2004.10.065.
- (215) Rorrer, J. E.; Bell, A. T.; Toste, F. D. Synthesis of Biomass-Derived Ethers for Use as Fuels and Lubricants. *ChemSusChem* **2019**, *12* (13), 2835–2858. https://doi.org/10.1002/cssc.201900535.
- (216) dos Santos, T. R.; Nilges, P.; Sauter, W.; Harnisch, F.; Schröder, U. Electrochemistry for the Generation of Renewable Chemicals: Electrochemical Conversion of Levulinic Acid. *RSC Adv.* **2015**, *5* (34), 26634–26643. https://doi.org/10.1039/C4RA16303F.
- (217) Nilges, P.; dos Santos, T. R.; Harnisch, F.; Schröder, U. Electrochemistry for Biofuel Generation: Electrochemical Conversion of Levulinic Acid to Octane. *Energy Environ. Sci.* **2012**, *5* (1), 5231–5235. https://doi.org/10.1039/C1EE02685B.
- (218) Holzhäuser, F. J.; Creusen, G.; Moos, G.; Dahmen, M.; König, A.; Artz, J.; Palkovits, S.; Palkovits, R. Electrochemical Cross-Coupling of Biogenic Di-Acids for Sustainable Fuel Production. *Green Chem.* **2019**, *21* (9), 2334–2344. https://doi.org/10.1039/C8GC03745K.
- (219) Wu, L.; Mascal, M.; Farmer, T. J.; Arnaud, S. P.; Wong Chang, M.-A. Electrochemical Coupling of Biomass-Derived Acids: New C 8 Platforms for Renewable Polymers and Fuels. *ChemSusChem* **2017**, *10* (1), 166–170. https://doi.org/10.1002/cssc.201601271.

- (220) Sadakiyo, M.; Hata, S.; Fukushima, T.; Juhász, G.; Yamauchi, M. Electrochemical Hydrogenation of Non-Aromatic Carboxylic Acid Derivatives as a Sustainable Synthesis Process: From Catalyst Design to Device Construction. *Phys. Chem. Chem. Phys.* **2019**, *21* (11), 5882–5889. https://doi.org/10.1039/C8CP07445C.
- (221) Qiu, Y.; Xin, L.; Chadderdon, D. J.; Qi, J.; Liang, C.; Li, W. Integrated Electrocatalytic Processing of Levulinic Acid and Formic Acid to Produce Biofuel Intermediate Valeric Acid. *Green Chem.* **2014**, *16* (3), 1305–1315. https://doi.org/10.1039/C3GC42254B.
- (222) Bisselink, R. J. M.; Crockatt, M.; Zijlstra, M.; Bakker, I. J.; Goetheer, E.; Slaghek, T. M.; van Es, D. S. Identification of More Benign Cathode Materials for the Electrochemical Reduction of Levulinic Acid to Valeric Acid. ChemElectroChem 2019, 6 (13), 3285–3290. https://doi.org/10.1002/celc.201900734.
- (223) Serrano-Ruiz, J. C.; Wang, D.; Dumesic, J. A. Catalytic Upgrading of Levulinic Acid to 5-Nonanone. *Green Chem.* **2010**, *12* (4), 574. https://doi.org/10.1039/b923907c.
- (224) Holzhäuser, F. J.; Artz, J.; Palkovits, S.; Kreyenschulte, D.; Büchs, J.; Palkovits, R. Electrocatalytic Upgrading of Itaconic Acid to Methylsuccinic Acid Using Fermentation Broth as a Substrate Solution. *Green Chem.* **2017**, *19* (10), 2390–2397. https://doi.org/10.1039/C6GC03153F.
- (225) Hancock, J. E. H.; Linstead, R. P. 702. 1: 2-Dicarboxylic Acids. Part I. Positional Isomerides Derived from Methylsuccinic Acid; with a Note on the Rearrangement of Unsymmetrical Compounds of This Type. *J. Chem. Soc.* **1953**, 3490–3496. https://doi.org/10.1039/jr9530003490.
- (226) Gao, Y. Method for Production of Succinic Acid and Sulfuric Acid by Paired Electrosynthesis. US20130134047A1, 2012.
- (227) Ma, C.; Zhao, F.; Hou, Q. Method for Electrolytic Synthesis of Butanedioic Acid and Fixed Bed Electrochemical Reaction Device. CN 201510256796, 2015.
- (228) Zhao, F.; Ma, C. In-Situ Electrochemistry Preparation for Ti/TiO2 Membrane Electrode. CN 200810122146, 2009.
- (229) Zheng, X.; Chen, Z.; Chen, R.; Chen, X. Method for Producing Butanedioic Acid Based on Serial Overflowing Method of Bipolar Membrane Electrolytic Cell. CN102899680A, 2013.
- (230) Shen, H.; Zhao, F.; Ma, C. Method for Electrolytic Synthesis of Amber Acid by Using Electrochemistry Pipe Reactor. CN101407923A, 2009.
- (231) Zhang, X.; Zhang, X. Method for Maleic Anhydride Electroreduction to Produce Succinic Acid. CN101008085A, 2007.
- (232) Matthiesen, J. E.; Carraher, J. M.; Vasiliu, M.; Dixon, D. A.; Tessonnier, J.-P. Electrochemical Conversion of Muconic Acid to Biobased Diacid Monomers. *ACS Sustain. Chem. Eng.* **2016**, *4* (6), 3575–3585. https://doi.org/10.1021/acssuschemeng.6b00679.
- (233) Meyers, J.; Mensah, J. B.; Holzhäuser, F. J.; Omari, A.; Blesken, C. C.; Tiso, T.; Palkovits, S.; Blank, L. M.; Pischinger, S.; Palkovits, R. Electrochemical Conversion of a Bio-Derivable Hydroxy Acid to a Drop-in Oxygenate Diesel Fuel. *Energy Environ. Sci.* **2019**, *12* (8), 2406–2411. https://doi.org/10.1039/C9EE01485C.

- (234) Wu, H.; Song, J.; Xie, C.; Hu, Y.; Zhang, P.; Yang, G.; Han, B. Surface Engineering in PbS via Partial Oxidation: Towards an Advanced Electrocatalyst for Reduction of Levulinic Acid to γ-Valerolactone. *Chem. Sci.* **2019**, *10* (6), 1754–1759. https://doi.org/10.1039/C8SC03161D.
- (235) Cabasso, I.; Li, M.; Yuan, Y. Electrochemical Synthesis of a Novel Compound, 5-Acetyl-2,9-Decanedione, and Theoretical Analysis of Its Lithium Ion Complex. *RSC Adv.* **2012**, *2* (26), 9998. https://doi.org/10.1039/c2ra21328a.
- (236) Dalavoy, T.; Jackson, J.; Swain, G.; Miller, D.; Li, J.; Lipkowshi, J. Mild Electrocatalytic Hydrogenation of Lactic Acid to Lactaldehyde and Propylene Glycol. *J. Catal.* **2007**, 246 (1), 15–28. https://doi.org/10.1016/j.jcat.2006.11.009.
- (237) Amines Market Size Worth \$29.3 Billion By 2025. Grand View Research. 2017.
- (238) Hayes, K. S. Industrial Processes for Manufacturing Amines. *Appl. Catal. A Gen.* **2001**, 221 (1–2), 187–195. https://doi.org/10.1016/S0926-860X(01)00813-4.
- (239) Wang, X.; Zhao, J. Synthesis of L-Cysteine and L-Cysteic Acid by Paired Electrolysis Method. *Chem. Lett.* **2004**, 33 (3), 332–333. https://doi.org/10.1246/cl.2004.332.
- (240) Ogura, K.; Kobayashi, M.; Nakayama, M.; Miho, Y. In-Situ FTIR Studies on the Electrochemical Oxidation of Histidine and Tyrosine. *J. Electroanal. Chem.* **1999**, *463* (2), 218–223. https://doi.org/10.1016/S0022-0728(98)00458-6.
- (241) Ogura, K.; Kobayashi, M.; Nakayama, M.; Miho, Y. Electrochemical and in Situ FTIR Studies on the Adsorption and Oxidation of Glycine and Lysine in Alkaline Medium. *J. Electroanal. Chem.* **1998**, *449* (1–2), 101–109. https://doi.org/10.1016/S0022-0728(98)00015-1.
- (242) Dai, J.-J.; Huang, Y.-B.; Fang, C.; Guo, Q.-X.; Fu, Y. Electrochemical Synthesis of Adiponitrile from the Renewable Raw Material Glutamic Acid. *ChemSusChem* **2012**, 5 (4), 617–620. https://doi.org/10.1002/cssc.201100776.
- (243) Kuleshova, N. E.; Vvedenskii, A. V.; Bobrinskaya, E. V. Anodic Oxidation of Serine Anion on Smooth and Platinized Platinum. *Russ. J. Electrochem.* **2018**, *54* (7), 592–597. https://doi.org/10.1134/S1023193518070042.
- (244) McGregor, W. H.; Carpenter, F. H. Alkaline Bromine Oxidation of Amino Acids and Peptides: Formation of α-Ketoacyl Peptides and Their Cleavage by Hydrogen Peroxide *. Biochemistry 1962, 1 (1), 53–60. https://doi.org/10.1021/bi00907a009.
- (245) Bellale, E. V.; Huddar, S. N.; Mahajan, U. S.; Akamanchi, K. G. Oxidative Decarboxylation of α-Amino Acids to Nitriles Using o-lodoxybenzoic Acid in Aqueous Ammonia. *Pure Appl. Chem.* **2011**, 83 (3), 607–612. https://doi.org/10.1351/PAC-CON-10-09-15.
- (246) Hiegel, G. A.; Lewis, J. C.; Bae, J. W. Conversion of A-Amino Acids into Nitriles by Oxidative Decarboxylation with Trichloroisocyanuric Acid. *Synth. Commun.* **2004**, *34* (19), 3449–3453. https://doi.org/10.1081/SCC-200030958.
- (247) Laval, G.; Golding, B. T. One-Pot Sequence for the Decarboxylation of α-Amino Acids. *Synlett* **2003**, No. 4, 0542–0546. https://doi.org/10.1055/s-2003-37512.
- (248) Dakin, H. D. On the Oxidation of Amino-Acids and of Related Substances with

- Chloramine-T. *Biochem. J.* **1917**, *11* (2), 79–95. https://doi.org/10.1042/bj0110079.
- (249) Claes, L.; Verduyckt, J.; Stassen, I.; Lagrain, B.; De Vos, D. E. Ruthenium-Catalyzed Aerobic Oxidative Decarboxylation of Amino Acids: A Green, Zero-Waste Route to Biobased Nitriles. *Chem. Commun.* **2015**, *51* (30), 6528–6531. https://doi.org/10.1039/C5CC00181A.
- (250) Kourist, R.; Guterl, J.-K.; Miyamoto, K.; Sieber, V. Enzymatic Decarboxylation-An Emerging Reaction for Chemicals Production from Renewable Resources. *ChemCatChem* **2014**, 6 (3), 689–701. https://doi.org/10.1002/cctc.201300881.
- (251) Wang, J.; Mao, J.; Tian, W.; Wei, G.; Xu, S.; Ma, W.; Chen, K.; Jiang, M.; Ouyang, P. Coproduction of Succinic Acid and Cadaverine Using Lysine as a Neutralizer and CO 2 Donor with I -Lysine Decarboxylase Overexpressed Escherichia Coli AFP111. *Green Chem.* **2018**, *20* (12), 2880–2887. https://doi.org/10.1039/C8GC00224J.
- (252) Dose, K. Eine Neue Darstellungsweise von Aminen Aus Aminocarbonsäuren. Chem. Ber. 1957. 90 (7),1251-1258. https://doi.org/10.1002/cber.19570900712.
- (253) Cassani, C.; Bergonzini, G.; Wallentin, C.-J. Photocatalytic Decarboxylative Reduction of Carboxylic Acids and Its Application in Asymmetric Synthesis. *Org. Lett.* **2014**, *16* (16), 4228–4231. https://doi.org/10.1021/ol5019294.
- (254) Jackson, D. M.; Ashley, R. L.; Brownfield, C. B.; Morrison, D. R.; Morrison, R. W. Rapid Conventional and Microwave-Assisted Decarboxylation of L-Histidine and Other Amino Acids via Organocatalysis with R-Carvone Under Superheated Conditions. *Synth. Commun.* **2015**, *45* (23), 2691–2700. https://doi.org/10.1080/00397911.2015.1100745.
- (255) De Schouwer, F.; Claes, L.; Claes, N.; Bals, S.; Degrève, J.; De Vos, D. E. Pd-Catalyzed Decarboxylation of Glutamic Acid and Pyroglutamic Acid to Bio-Based 2-Pyrrolidone. *Green Chem.* **2015**, *17* (4), 2263–2270. https://doi.org/10.1039/C4GC02194K.
- (256) Verduyckt, J.; Van Hoof, M.; De Schouwer, F.; Wolberg, M.; Kurttepeli, M.; Eloy, P.; Gaigneaux, E. M.; Bals, S.; Kirschhock, C. E. A.; De Vos, D. E. PdPb-Catalyzed Decarboxylation of Proline to Pyrrolidine: Highly Selective Formation of a Biobased Amine in Water. *ACS Catal.* **2016**, *6* (11), 7303–7310. https://doi.org/10.1021/acscatal.6b02561.
- (257) Huang, W.; Zheng, J.; Li, Z. New Oscillatory Electrocatalytic Oxidation of Amino Compounds on a Nanoporous Film Electrode of Electrodeposited Nickel Hydroxide Nanoflakes. *J. Phys. Chem. C* **2007**, *111* (45), 16902–16908. https://doi.org/10.1021/jp0738980.
- (258) Matthessen, R.; Claes, L.; Fransaer, J.; Binnemans, K.; De Vos, D. E. Decarboxylation of a Wide Range of Amino Acids with Electrogenerated Hypobromite. *European J. Org. Chem.* **2014**, *2014* (30), 6649–6652. https://doi.org/10.1002/ejoc.201403112.
- (259) Blanco, D. E.; Dookhith, A. Z.; Modestino, M. A. Controlling Selectivity in the Electrocatalytic Hydrogenation of Adiponitrile through Electrolyte Design. *ACS Sustain. Chem. Eng.* **2020**, 8 (24), 9027–9034. https://doi.org/10.1021/acssuschemeng.0c01789.

- (260) Roeser, J.; Permentier, H. P.; Bruins, A. P.; Bischoff, R. Electrochemical Oxidation and Cleavage of Tyrosine- and Tryptophan-Containing Tripeptides. *Anal. Chem.* **2010**, *82* (18), 7556–7565. https://doi.org/10.1021/ac101086w.
- (261) Permentier, H. P.; Jurva, U.; Barroso, B.; Bruins, A. P. Electrochemical Oxidation and Cleavage of Peptides Analyzed with On-Line Mass Spectrometric Detection. *Rapid Commun. Mass Spectrom.* **2003**, *17* (14), 1585–1592. https://doi.org/10.1002/rcm.1090.
- (262) Ralph, T. R.; Hitchman, M. L.; Millington, J. P.; Walsh, F. C. The Electrochemistry of L-Cystine and I-Cysteine Part 2: Electrosynthesis of I-Cysteine at Solid Electrodes. *J. Electroanal. Chem.* **1994**, *375* (1–2), 17–27. https://doi.org/10.1016/0022-0728(94)03408-7.
- (263) Babu, K. F.; Sivasubramanian, R.; Noel, M.; Kulandainathan, M. A. A Homogeneous Redox Catalytic Process for the Paired Synthesis of L-Cysteine and I-Cysteic Acid from I-Cystine. *Electrochim. Acta* **2011**, *56* (27), 9797–9801. https://doi.org/10.1016/j.electacta.2011.08.052.
- (264) Foo, T.; Panova, A. Process for the Synthesis of Glycolonitrile. US 7,368,492 B2.
- (265) Scott, E.; Peter, F.; Sanders, J. Biomass in the Manufacture of Industrial Products—the Use of Proteins and Amino Acids. *Appl. Microbiol. Biotechnol.* **2007**, *75* (4), 751–762. https://doi.org/10.1007/s00253-007-0932-x.
- (266) Sanchez-Cano, G.; Montiel, V.; Aldaz, A. Synthesis of L-Cysteic Acid by Indirect Electrooxidation and an Example of Paired Synthesis: L-Cysteic and I-Cysteine from I-Cystine. *Tetrahedron* **1991**, *47* (4–5), 877–886. https://doi.org/10.1016/S0040-4020(01)87076-9.
- (267) Agarwal, A.; Rana, M.; Park, J.-H. Advancement in Technologies for the Depolymerization of Lignin. *Fuel Process. Technol.* **2018**, *181*, 115–132. https://doi.org/10.1016/j.fuproc.2018.09.017.
- (268) Asina, F.; Brzonova, I.; Voeller, K.; Kozliak, E.; Kubátová, A.; Yao, B.; Ji, Y. Biodegradation of Lignin by Fungi, Bacteria and Laccases. *Bioresour. Technol.* **2016**, *220*, 414–424. https://doi.org/10.1016/j.biortech.2016.08.016.
- (269) Elfadly, A. M.; Zeid, I. F.; Yehia, F. Z.; Rabie, A. M.; Aboualala, M. M.; Park, S.-E. Highly Selective BTX from Catalytic Fast Pyrolysis of Lignin over Supported Mesoporous Silica. *Int. J. Biol. Macromol.* **2016**, *91*, 278–293. https://doi.org/10.1016/j.ijbiomac.2016.05.053.
- (270) Yang, S.; Yuan, T.-Q.; Li, M.-F.; Sun, R.-C. Hydrothermal Degradation of Lignin: Products Analysis for Phenol Formaldehyde Adhesive Synthesis. *Int. J. Biol. Macromol.* **2015**, 72, 54–62. https://doi.org/10.1016/j.ijbiomac.2014.07.048.
- (271) Yunpu, W.; Leilei, D.; Liangliang, F.; Shaoqi, S.; Yuhuan, L.; Roger, R. Review of Microwave-Assisted Lignin Conversion for Renewable Fuels and Chemicals. *J. Anal. Appl. Pyrolysis* **2016**, *119*, 104–113. https://doi.org/10.1016/j.jaap.2016.03.011.
- (272) Zhou, M.; Xu, J.; Jiang, J.; Sharma, B. A Review of Microwave Assisted Liquefaction of Ligninin Hydrogen Donor Solvents: Effect of Solvents and Catalysts. *Energies* **2018**, *11* (11), 2877. https://doi.org/10.3390/en11112877.
- (273) Gazi, S. Valorization of Wood Biomass-Lignin via Selective Bond Scission: A Minireview. *Appl. Catal. B Environ.* **2019**, *257*, 117936.

- https://doi.org/10.1016/j.apcatb.2019.117936.
- (274) Nguyen, S. T.; Murray, P. R. D.; Knowles, R. R. Light-Driven Depolymerization of Native Lignin Enabled by Proton-Coupled Electron Transfer. *ACS Catal.* **2020**, *10* (1), 800–805. https://doi.org/10.1021/acscatal.9b04813.
- (275) Stiefel, S.; Schmitz, A.; Peters, J.; Di Marino, D.; Wessling, M. An Integrated Electrochemical Process to Convert Lignin to Value-Added Products under Mild Conditions. *Green Chem.* **2016**, *18* (18), 4999–5007. https://doi.org/10.1039/C6GC00878J.
- (276) Stiefel, S.; Lölsberg, J.; Kipshagen, L.; Möller-Gulland, R.; Wessling, M. Controlled Depolymerization of Lignin in an Electrochemical Membrane Reactor. *Electrochem. commun.* **2015**, *61*, 49–52. https://doi.org/10.1016/j.elecom.2015.09.028.
- (277) Schmitt, D.; Regenbrecht, C.; Hartmer, M.; Stecker, F.; Waldvogel, S. R. Highly Selective Generation of Vanillin by Anodic Degradation of Lignin: A Combined Approach of Electrochemistry and Product Isolation by Adsorption. *Beilstein J. Org. Chem.* 2015, 11, 473–480. https://doi.org/10.3762/bjoc.11.53.
- (278) Di Marino, D.; Aniko, V.; Stocco, A.; Kriescher, S.; Wessling, M. Emulsion Electro-Oxidation of Kraft Lignin. *Green Chem.* **2017**, *19* (20), 4778–4784. https://doi.org/10.1039/C7GC02115A.
- (279) Zirbes, M.; Waldvogel, S. R. Electro-Conversion as Sustainable Method for the Fine Chemical Production from the Biopolymer Lignin. *Curr. Opin. Green Sustain. Chem.* **2018**, *14*, 19–25. https://doi.org/10.1016/j.cogsc.2018.05.001.
- (280) Bateni, F.; Ghahremani, R.; Staser, J. A. Electrochemical Oxidative Valorization of Lignin by the Nanostructured PbO2/MWNTs Electrocatalyst in a Low-Energy Depolymerization Process. *J. Appl. Electrochem.* **2020**, 1–14. https://doi.org/10.1007/s10800-020-01451-y.
- (281) Movil, O.; Garlock, M.; Staser, J. A. Non-Precious Metal Nanoparticle Electrocatalysts for Electrochemical Modification of Lignin for Low-Energy and Cost-Effective Production of Hydrogen. *Int. J. Hydrogen Energy* **2015**, *40* (13), 4519–4530. https://doi.org/10.1016/j.ijhydene.2015.02.023.
- (282) Ghahremani, R.; Farales, F.; Bateni, F.; Staser, J. A. Simultaneous Hydrogen Evolution and Lignin Depolymerization Using NiSn Electrocatalysts in a Biomass-Depolarized Electrolyzer. *J. Electrochem. Soc.* **2020**, *167* (4), 043502. https://doi.org/10.1149/1945-7111/ab7179.
- (283) Bawareth, B.; Di Marino, D.; Nijhuis, T. A.; Wessling, M. Unravelling Electrochemical Lignin Depolymerization. *ACS Sustain. Chem. Eng.* **2018**, 6 (6), 7565–7573. https://doi.org/10.1021/acssuschemeng.8b00335.
- (284) Movil-Cabrera, O.; Rodriguez-Silva, A.; Arroyo-Torres, C.; Staser, J. A. Electrochemical Conversion of Lignin to Useful Chemicals. *Biomass and Bioenergy* **2016**, *88*, 89–96. https://doi.org/10.1016/j.biombioe.2016.03.014.
- (285) Chen, A.; Wen, Y.; Han, X.; Qi, J.; Liu, Z.; Zhang, S.; Li, G. Electrochemical Decomposition of Wheat Straw Lignin into Guaiacyl-, Syringyl-, and Phenol-Type Compounds Using Pb/PbO 2 Anode and Alloyed Steel Cathode in Alkaline Solution. *Environ. Prog. Sustain. Energy* **2019**, *38* (4), 13117. https://doi.org/10.1002/ep.13117.
- (286) Bosque, I.; Magallanes, G.; Rigoulet, M.; Kärkäs, M. D.; Stephenson, C. R. J. Redox Catalysis Facilitates Lignin Depolymerization. *ACS Cent. Sci.* **2017**, 3

- (6), 621–628. https://doi.org/10.1021/acscentsci.7b00140.
- (287) Chio, C.; Sain, M.; Qin, W. Lignin Utilization: A Review of Lignin Depolymerization from Various Aspects. *Renew. Sustain. Energy Rev.* **2019**, 107, 232–249. https://doi.org/10.1016/j.rser.2019.03.008.
- (288) Dier, T. K. F.; Rauber, D.; Durneata, D.; Hempelmann, R.; Volmer, D. A. Sustainable Electrochemical Depolymerization of Lignin in Reusable Ionic Liquids. *Sci. Rep.* **2017**, *7* (1), 5041. https://doi.org/10.1038/s41598-017-05316-x.
- (289) Zhu, H.; Wang, L.; Chen, Y.; Li, G.; Li, H.; Tang, Y.; Wan, P. Electrochemical Depolymerization of Lignin into Renewable Aromatic Compounds in a Non-Diaphragm Electrolytic Cell. *RSC Adv.* **2014**, *4* (56), 29917. https://doi.org/10.1039/C4RA03793F.
- (290) Wang, L.; Liu, S.; Jiang, H.; Chen, Y.; Wang, L.; Duan, G.; Sun, Y.; Chen, Y.; Wan, P. Electrochemical Generation of ROS in Ionic Liquid for the Degradation of Lignin Model Compound. *J. Electrochem. Soc.* **2018**, *165* (11), H705–H710. https://doi.org/10.1149/2.0801811jes.
- (291) Zhu, H.; Chen, Y.; Qin, T.; Wang, L.; Tang, Y.; Sun, Y.; Wan, P. Lignin Depolymerization via an Integrated Approach of Anode Oxidation and Electro-Generated H2O2 Oxidation. *RSC Adv.* **2014**, *4* (12), 6232. https://doi.org/10.1039/c3ra47516f.
- (292) Wang, L.; Chen, Y.; Liu, S.; Jiang, H.; Wang, L.; Sun, Y.; Wan, P. Study on the Cleavage of Alkyl-O-Aryl Bonds by in Situ Generated Hydroxyl Radicals on an ORR Cathode. *RSC Adv.* **2017**, *7* (81), 51419–51425. https://doi.org/10.1039/C7RA11236J.
- (293) Rauber, D.; Dier, T. K. F.; Volmer, D. A.; Hempelmann, R. Electrochemical Lignin Degradation in Ionic Liquids on Ternary Mixed Metal Electrodes. *Zeitschrift für Phys. Chemie* **2018**, *232* (2), 189–208. https://doi.org/10.1515/zpch-2017-0951.
- (294) Di Marino, D.; Stöckmann, D.; Kriescher, S.; Stiefel, S.; Wessling, M. Electrochemical Depolymerisation of Lignin in a Deep Eutectic Solvent. *Green Chem.* **2016**, *18* (22), 6021–6028. https://doi.org/10.1039/C6GC01353H.
- (295) Lan, C.; Fan, H.; Shang, Y.; Shen, D.; Li, G. Electrochemically Catalyzed Conversion of Cornstalk Lignin to Aromatic Compounds: An Integrated Process of Anodic Oxidation of a Pb/PbO 2 Electrode and Hydrogenation of a Nickel Cathode in Sodium Hydroxide Solution. Sustain. Energy Fuels 2020, 4 (4), 1828–1836. https://doi.org/10.1039/C9SE00942F.
- (296) Jia, Y.; Wen, Y.; Han, X.; Qi, J.; Liu, Z.; Zhang, S.; Li, G. Electrocatalytic Degradation of Rice Straw Lignin in Alkaline Solution through Oxidation on a Ti/SnO 2 –Sb 2 O 3 /α-PbO 2 /β-PbO 2 Anode and Reduction on an Iron or Tin Doped Titanium Cathode. *Catal. Sci. Technol.* **2018**, *8* (18), 4665–4677. https://doi.org/10.1039/C8CY00307F.
- (297) Di Marino, D.; Jestel, T.; Marks, C.; Viell, J.; Blindert, M.; Kriescher, S. M. A.; Spiess, A. C.; Wessling, M. Carboxylic Acids Production via Electrochemical Depolymerization of Lignin. *ChemElectroChem* **2019**, *6* (5), 1434–1442. https://doi.org/10.1002/celc.201801676.
- (298) Cai, P.; Fan, H.; Cao, S.; Qi, J.; Zhang, S.; Li, G. Electrochemical Conversion of Corn Stover Lignin to Biomass-Based Chemicals between Cu/Ni Mo Co

- Cathode and Pb/PbO 2 Anode in Alkali Solution. *Electrochim. Acta* **2018**, *264*, 128–139. https://doi.org/10.1016/j.electacta.2018.01.111.
- (299) Tumbalam Gooty, A.; Li, D.; Berruti, F.; Briens, C. Kraft-Lignin Pyrolysis and Fractional Condensation of Its Bio-Oil Vapors. *J. Anal. Appl. Pyrolysis* **2014**, *106*, 33–40. https://doi.org/10.1016/j.jaap.2013.12.006.
- (300) Zhou, Y.; Klinger, G. E.; Hegg, E. L.; Saffron, C. M.; Jackson, J. E. Multiple Mechanisms Mapped in Aryl Alkyl Ether Cleavage via Aqueous Electrocatalytic Hydrogenation over Skeletal Nickel. *J. Am. Chem. Soc.* **2020**, 142 (8), 4037–4050. https://doi.org/10.1021/jacs.0c00199.
- (301) Li, Z.; Garedew, M.; Lam, C. H.; Jackson, J. E.; Miller, D. J.; Saffron, C. M. Mild Electrocatalytic Hydrogenation and Hydrodeoxygenation of Bio-Oil Derived Phenolic Compounds Using Ruthenium Supported on Activated Carbon Cloth. Green Chem. 2012, 14 (9), 2540. https://doi.org/10.1039/c2gc35552c.
- (302) Song, Y.; Sanyal, U.; Pangotra, D.; Holladay, J. D.; Camaioni, D. M.; Gutiérrez, O. Y.; Lercher, J. A. Hydrogenation of Benzaldehyde via Electrocatalysis and Thermal Catalysis on Carbon-Supported Metals. *J. Catal.* **2018**, *359*, 68–75. https://doi.org/10.1016/j.jcat.2017.12.026.
- (303) Liu, W.; You, W.; Gong, Y.; Deng, Y. High-Efficiency Electrochemical Hydrodeoxygenation of Bio-Phenols to Hydrocarbon Fuels by a Superacid-Noble Metal Particle Dual-Catalyst System. *Energy Environ. Sci.* **2020**, *13* (3), 917–927. https://doi.org/10.1039/C9EE02783A.
- (304) Garedew, M.; Young-Farhat, D.; Jackson, J. E.; Saffron, C. M. Electrocatalytic Upgrading of Phenolic Compounds Observed after Lignin Pyrolysis. *ACS Sustain. Chem. Eng.* **2019**, *7* (9), 8375–8386. https://doi.org/10.1021/acssuschemeng.9b00019.
- (305) Lam, C. H.; Lowe, C. B.; Li, Z.; Longe, K. N.; Rayburn, J. T.; Caldwell, M. A.; Houdek, C. E.; Maguire, J. B.; Saffron, C. M.; Miller, D. J.; et al. Electrocatalytic Upgrading of Model Lignin Monomers with Earth Abundant Metal Electrodes. *Green Chem.* **2015**, *17* (1), 601–609. https://doi.org/10.1039/C4GC01632G.
- (306) Wijaya, Y. P.; Grossmann-Neuhaeusler, T.; Dhewangga Putra, R. D.; Smith, K. J.; Kim, C. S.; Gyenge, E. L. Electrocatalytic Hydrogenation of Guaiacol in Diverse Electrolytes Using a Stirred Slurry Reactor. *ChemSusChem* 2020, 13 (3), 629–639. https://doi.org/10.1002/cssc.201902611.
- (307) Garedew, M.; Young-Farhat, D.; Bhatia, S.; Hao, P.; Jackson, J. E.; Saffron, C. M. Electrocatalytic Cleavage of Lignin Model Dimers Using Ruthenium Supported on Activated Carbon Cloth. *Sustain. Energy Fuels* **2020**, *4* (3), 1340–1350. https://doi.org/10.1039/C9SE00912D.
- (308) Sanyal, U.; Lopez-Ruiz, J.; Padmaperuma, A. B.; Holladay, J.; Gutiérrez, O. Y. Electrocatalytic Hydrogenation of Oxygenated Compounds in Aqueous Phase. *Org. Process Res. Dev.* **2018**, 22 (12), 1590–1598. https://doi.org/10.1021/acs.oprd.8b00236.
- (309) Wu, W.-B.; Huang, J.-M. Electrochemical Cleavage of Aryl Ethers Promoted by Sodium Borohydride. *J. Org. Chem.* **2014**, *79* (21), 10189–10195. https://doi.org/10.1021/jo5018537.
- (310) He, J.; Zhao, C.; Lercher, J. A. Ni-Catalyzed Cleavage of Aryl Ethers in the Aqueous Phase. J. Am. Chem. Soc. 2012, 134 (51), 20768–20775.

- https://doi.org/10.1021/ja309915e.
- (311) Bulut, S.; Siankevich, S.; van Muyden, A. P.; Alexander, D. T. L.; Savoglidis, G.; Zhang, J.; Hatzimanikatis, V.; Yan, N.; Dyson, P. J. Efficient Cleavage of Aryl Ether C–O Linkages by Rh–Ni and Ru–Ni Nanoscale Catalysts Operating in Water. *Chem. Sci.* **2018**, *9* (25), 5530–5535. https://doi.org/10.1039/C8SC00742J.
- (312) Gunceler, D.; Letchworth-Weaver, K.; Sundararaman, R.; Schwarz, K. A.; Arias, T. A. The Importance of Nonlinear Fluid Response in Joint Density-Functional Theory Studies of Battery Systems. *Model. Simul. Mater. Sci. Eng.* **2013**, *21* (7), 074005. https://doi.org/10.1088/0965-0393/21/7/074005.
- (313) Andreussi, O.; Dabo, I.; Marzari, N. Revised Self-Consistent Continuum Solvation in Electronic-Structure Calculations. *J. Chem. Phys.* **2012**, *136* (6), 064102. https://doi.org/10.1063/1.3676407.
- (314) Sundararaman, R.; Goddard, W. A. The Charge-Asymmetric Nonlocally Determined Local-Electric (CANDLE) Solvation Model. *J. Chem. Phys.* **2015**, *142* (6), 064107. https://doi.org/10.1063/1.4907731.
- (315) Sundararaman, R.; Gunceler, D.; Arias, T. A. Weighted-Density Functionals for Cavity Formation and Dispersion Energies in Continuum Solvation Models. *J. Chem. Phys.* **2014**, *141* (13), 134105. https://doi.org/10.1063/1.4896827.
- (316) Sundararaman, R.; Schwarz, K. A.; Letchworth-Weaver, K.; Arias, T. A. Spicing up Continuum Solvation Models with SaLSA: The Spherically Averaged Liquid Susceptibility Ansatz. *J. Chem. Phys.* **2015**, *142* (5), 054102. https://doi.org/10.1063/1.4906828.
- (317) Duan, Z.; Henkelman, G. Calculations of the PH-Dependent Onset Potential for CO Electrooxidation on Au(111). *Langmuir* **2018**, *34* (50), 15268–15275. https://doi.org/10.1021/acs.langmuir.8b03644.
- (318) Collinge, G.; Yuk, S. F.; Nguyen, M.-T.; Lee, M.-S.; Glezakou, V.-A.; Rousseau, R. Effect of Collective Dynamics and Anharmonicity on Entropy in Heterogenous Catalysis: Building the Case for Advanced Molecular Simulations. *ACS Catal.* **2020**, *10* (16), 9236–9260. https://doi.org/10.1021/acscatal.0c01501.
- (319) Mathew, K.; Sundararaman, R.; Letchworth-Weaver, K.; Arias, T. A.; Hennig, R. G. Implicit Solvation Model for Density-Functional Study of Nanocrystal Surfaces and Reaction Pathways. *J. Chem. Phys.* **2014**, *140* (8), 084106. https://doi.org/10.1063/1.4865107.
- (320) Mathew, K.; Kolluru, V. S. C.; Mula, S.; Steinmann, S. N.; Hennig, R. G. Implicit Self-Consistent Electrolyte Model in Plane-Wave Density-Functional Theory. **2016**.
- (321) Sundararaman, R.; Letchworth-Weaver, K.; Schwarz, K. A.; Gunceler, D.; Ozhabes, Y.; Arias, T. A. JDFTx: Software for Joint Density-Functional Theory. *SoftwareX* **2017**, *6*, 278–284. https://doi.org/10.1016/j.softx.2017.10.006.
- (322) Sundararaman, R.; Goddard, W. A.; Arias, T. A. Grand Canonical Electronic Density-Functional Theory: Algorithms and Applications to Electrochemistry. *J. Chem. Phys.* **2017**, *146* (11), 114104. https://doi.org/10.1063/1.4978411.
- (323) Herron, J. A.; Morikawa, Y.; Mavrikakis, M. Ab Initio Molecular Dynamics of Solvation Effects on Reactivity at Electrified Interfaces. *Proc. Natl. Acad. Sci.* **2016**, *113* (34), E4937–E4945. https://doi.org/10.1073/pnas.1604590113.

- (324) Yuk, S. F.; Lee, M.-S.; Akhade, S. A.; Nguyen, M.-T.; Glezakou, V.-A.; Rousseau, R. First-Principle Investigation on Catalytic Hydrogenation of Benzaldehyde over Pt-Group Metals. *Catal. Today* **2020**. https://doi.org/10.1016/j.cattod.2020.07.039.
- (325) Gauthier, J. A.; Dickens, C. F.; Heenen, H. H.; Vijay, S.; Ringe, S.; Chan, K. Unified Approach to Implicit and Explicit Solvent Simulations of Electrochemical Reaction Energetics. *J. Chem. Theory Comput.* **2019**, *15* (12), 6895–6906. https://doi.org/10.1021/acs.jctc.9b00717.
- (326) Gauthier, J. A.; Ringe, S.; Dickens, C. F.; Garza, A. J.; Bell, A. T.; Head-Gordon, M.; Nørskov, J. K.; Chan, K. Challenges in Modeling Electrochemical Reaction Energetics with Polarizable Continuum Models. *ACS Catal.* **2019**, *9* (2), 920–931. https://doi.org/10.1021/acscatal.8b02793.
- (327) Nørskov, J. K. K.; Rossmeisl, J.; Logadottir, A.; Lindqvist, L.; Kitchin, J. R.; Bligaard, T.; Jónsson, H.; Loagdottir, A.; Lindqvist, L.; Kitchin, J. R.; et al. Origin of the Overpotential for Oxygen Reduction at a Fuel-Cell Cathode. *J. Phys. Chem. B* 2004, 108 (46), 17886–17892. https://doi.org/10.1021/jp047349j.
- (328) Nørskov, J. K.; Bligaard, T.; Logadottir, A.; Kitchin, J. R.; Chen, J. G.; Pandelov, S.; Stimming, U. Trends in the Exchange Current for Hydrogen Evolution. *J. Electrochem. Soc.* **2005**, *152* (3), J23. https://doi.org/10.1149/1.1856988.
- (329) Greeley, J.; Jaramillo, T. F.; Bonde, J.; Chorkendorff, I.; Nørskov, J. K. Computational High-Throughput Screening of Electrocatalytic Materials for Hydrogen Evolution. *Nat. Mater.* **2006**, *5* (11), 909–913. https://doi.org/10.1038/nmat1752.
- (330) Stamenkovic, V. R.; Mun, B. S.; Arenz, M.; Mayrhofer, K. J. J.; Lucas, C. A.; Wang, G.; Ross, P. N.; Markovic, N. M. Trends in Electrocatalysis on Extended and Nanoscale Pt-Bimetallic Alloy Surfaces. *Nat. Mater.* **2007**, *6* (3), 241–247. https://doi.org/10.1038/nmat1840.
- (331) Jiao, Y.; Zheng, Y.; Jaroniec, M.; Qiao, S. Z. Design of Electrocatalysts for Oxygen- and Hydrogen-Involving Energy Conversion Reactions. *Chem. Soc. Rev.* **2015**, *44* (8), 2060–2086. https://doi.org/10.1039/C4CS00470A.
- (332) Greeley, J.; Stephens, I. E. L.; Bondarenko, A. S.; Johansson, T. P.; Hansen, H. A.; Jaramillo, T. F.; Rossmeisl, J.; Chorkendorff, I.; Nørskov, J. K. Alloys of Platinum and Early Transition Metals as Oxygen Reduction Electrocatalysts. *Nat. Chem.* **2009**, *1* (7), 552–556. https://doi.org/10.1038/nchem.367.
- (333) Shan, N.; Hanchett, M. K.; Liu, B. Mechanistic Insights Evaluating Ag, Pb, and Ni as Electrocatalysts for Furfural Reduction from First-Principles Methods. *J. Phys. Chem. C* **2017**, 121 (46), 25768–25777. https://doi.org/10.1021/acs.jpcc.7b06778.
- (334) Neugebauer, J.; Scheffler, M. Adsorbate-Substrate and Adsorbate-Adsorbate Interactions of Na and K Adlayers on Al(111). *Phys. Rev. B* **1992**, *46* (24), 16067–16080. https://doi.org/10.1103/PhysRevB.46.16067.
- (335) Feibelman, P. J. Surface-Diffusion Mechanism versus Electric Field: Pt/Pt(001). *Phys. Rev. B* **2001**, *64* (12), 125403. https://doi.org/10.1103/PhysRevB.64.125403.
- (336) Skúlason, E.; Jónsson, H. Atomic Scale Simulations of Heterogeneous

- Electrocatalysis: Recent Advances. *Adv. Phys. X* **2017**, *2* (3), 481–495. https://doi.org/10.1080/23746149.2017.1308230.
- (337) Filhol, J.-S.; Neurock, M. Elucidation of the Electrochemical Activation of Water over Pd by First Principles. *Angew. Chemie Int. Ed.* **2006**, *45* (3), 402–406. https://doi.org/10.1002/anie.200502540.
- (338) Taylor, C. D.; Wasileski, S. A.; Filhol, J.-S.; Neurock, M. First Principles Reaction Modeling of the Electrochemical Interface: Consideration and Calculation of a Tunable Surface Potential from Atomic and Electronic Structure. *Phys. Rev. B* **2006**, 73 (16), 165402. https://doi.org/10.1103/PhysRevB.73.165402.
- (339) Lopez-Ruiz, J. A.; Andrews, E.; Akhade, S. A.; Lee, M.-S.; Koh, K.; Sanyal, U.; Yuk, S. F.; Karkamkar, A. J.; Derewinski, M. A.; Holladay, J.; et al. Understanding the Role of Metal and Molecular Structure on the Electrocatalytic Hydrogenation of Oxygenated Organic Compounds. *ACS Catal.* **2019**, *9* (11), 9964–9972. https://doi.org/10.1021/acscatal.9b02921.
- (340) Cantu, D. C.; Padmaperuma, A. B.; Nguyen, M.-T.; Akhade, S. A.; Yoon, Y.; Wang, Y.-G.; Lee, M.-S.; Glezakou, V.-A.; Rousseau, R.; Lilga, M. A. A Combined Experimental and Theoretical Study on the Activity and Selectivity of the Electrocatalytic Hydrogenation of Aldehydes. *ACS Catal.* **2018**, *8* (8), 7645–7658. https://doi.org/10.1021/acscatal.8b00858.
- (341) Garza, A. J.; Bell, A. T.; Head-Gordon, M. Mechanism of CO 2 Reduction at Copper Surfaces: Pathways to C 2 Products. *ACS Catal.* **2018**, *8* (2), 1490–1499. https://doi.org/10.1021/acscatal.7b03477.
- (342) Zhang, H.; Goddard, W. A.; Lu, Q.; Cheng, M.-J. The Importance of Grand-Canonical Quantum Mechanical Methods to Describe the Effect of Electrode Potential on the Stability of Intermediates Involved in Both Electrochemical CO 2 Reduction and Hydrogen Evolution. *Phys. Chem. Chem. Phys.* **2018**, *20* (4), 2549–2557. https://doi.org/10.1039/C7CP08153G.
- (343) Goodpaster, J. D.; Bell, A. T.; Head-Gordon, M. Identification of Possible Pathways for C–C Bond Formation during Electrochemical Reduction of CO 2: New Theoretical Insights from an Improved Electrochemical Model. *J. Phys. Chem. Lett.* **2016**, *7* (8), 1471–1477. https://doi.org/10.1021/acs.jpclett.6b00358.
- (344) Kastlunger, G.; Lindgren, P.; Peterson, A. A. Controlled-Potential Simulation of Elementary Electrochemical Reactions: Proton Discharge on Metal Surfaces. *J. Phys. Chem. C* **2018**, *122* (24), 12771–12781. https://doi.org/10.1021/acs.jpcc.8b02465.
- (345) Xiao, H.; Shin, H.; Goddard, W. A. Synergy between Fe and Ni in the Optimal Performance of (Ni,Fe)OOH Catalysts for the Oxygen Evolution Reaction. *Proc. Natl. Acad. Sci.* **2018**, *115* (23), 5872–5877. https://doi.org/10.1073/pnas.1722034115.
- (346) Lozovoi, A. Y.; Alavi, A. Vibrational Frequencies of CO on Pt(111) in Electric Field: A Periodic DFT Study. *J. Electroanal. Chem.* **2007**, *607* (1–2), 140–146. https://doi.org/10.1016/j.jelechem.2007.02.030.
- (347) He, Y.; Wei, X. Y.; Chan, C. T.; Che, J. G. Effect of External Electric Field on the Surface Energetics of Ag/Si(111). *Phys. Rev. B* **2005**, *71* (4), 045401. https://doi.org/10.1103/PhysRevB.71.045401.

- (348) Hamada, I.; Otani, M.; Sugino, O.; Morikawa, Y. Green's Function Method for Elimination of the Spurious Multipole Interaction in the Surface/Interface Slab Model. *Phys. Rev. B* **2009**, *80* (16), 165411. https://doi.org/10.1103/PhysRevB.80.165411.
- (349) Otani, M.; Sugino, O. First-Principles Calculations of Charged Surfaces and Interfaces: A Plane-Wave Nonrepeated Slab Approach. *Phys. Rev. B* **2006**, 73 (11), 115407. https://doi.org/10.1103/PhysRevB.73.115407.
- (350) Lozovoi, A. Y.; Alavi, A. Reconstruction of Charged Surfaces: General Trends and a Case Study of Pt(110) and Au(110). *Phys. Rev. B* **2003**, *68* (24), 245416. https://doi.org/10.1103/PhysRevB.68.245416.
- (351) Otani, M.; Hamada, I.; Sugino, O.; Morikawa, Y.; Okamoto, Y.; Ikeshoji, T. Structure of the Water/Platinum Interface—a First Principles Simulation under Bias Potential. *Phys. Chem. Chem. Phys.* **2008**, *10* (25), 3609. https://doi.org/10.1039/b803541e.
- (352) Calle-Vallejo, F.; Martínez, J. I.; García-Lastra, J. M.; Rossmeisl, J.; Koper, M. T. M. Physical and Chemical Nature of the Scaling Relations between Adsorption Energies of Atoms on Metal Surfaces. *Phys. Rev. Lett.* 2012, 108 (11), 116103. https://doi.org/10.1103/PhysRevLett.108.116103.
- (353) Montemore, M. M.; Medlin, J. W. Scaling Relations between Adsorption Energies for Computational Screening and Design of Catalysts. *Catal. Sci. Technol.* **2014**, *4* (11), 3748–3761. https://doi.org/10.1039/C4CY00335G.
- (354) Greeley, J. Theoretical Heterogeneous Catalysis: Scaling Relationships and Computational Catalyst Design. *Annu. Rev. Chem. Biomol. Eng.* **2016**, *7* (1), 605–635. https://doi.org/10.1146/annurev-chembioeng-080615-034413.
- (355) Exner, K. S. Does a Thermoneutral Electrocatalyst Correspond to the Apex of a Volcano Plot for a Simple Two-Electron Process? *Angew. Chemie* **2020**, *132* (26), 10320–10324. https://doi.org/10.1002/ange.202003688.
- (356) Dickens, C. F.; Kirk, C.; Nørskov, J. K. Insights into the Electrochemical Oxygen Evolution Reaction with Ab Initio Calculations and Microkinetic Modeling: Beyond the Limiting Potential Volcano. *J. Phys. Chem. C* **2019**, *123* (31), 18960–18977. https://doi.org/10.1021/acs.jpcc.9b03830.
- (357) Henkelman, G.; Jónsson, H. Improved Tangent Estimate in the Nudged Elastic Band Method for Finding Minimum Energy Paths and Saddle Points. *J. Chem. Phys.* **2000**, *113* (22), 9978–9985. https://doi.org/10.1063/1.1323224.
- (358) Henkelman, G.; Jónsson, H. A Dimer Method for Finding Saddle Points on High Dimensional Potential Surfaces Using Only First Derivatives. *J. Chem. Phys.* **1999**, *111* (15), 7010–7022. https://doi.org/10.1063/1.480097.
- (359) Heyden, A.; Bell, A. T.; Keil, F. J. Efficient Methods for Finding Transition States in Chemical Reactions: Comparison of Improved Dimer Method and Partitioned Rational Function Optimization Method. *J. Chem. Phys.* **2005**, *123* (22), 224101. https://doi.org/10.1063/1.2104507.
- (360) Chan, K.; Nørskov, J. K. Electrochemical Barriers Made Simple. *J. Phys. Chem. Lett.* **2015**, 6 (14), 2663–2668. https://doi.org/10.1021/acs.jpclett.5b01043.
- (361) Rostamikia, G.; Mendoza, A. J.; Hickner, M. A.; Janik, M. J. First-Principles Based Microkinetic Modeling of Borohydride Oxidation on a Au(111) Electrode. *J. Power Sources* **2011**, *196* (22), 9228–9237.

- https://doi.org/10.1016/j.jpowsour.2011.07.042.
- (362) Tang, W.; Sanville, E.; Henkelman, G. A Grid-Based Bader Analysis Algorithm without Lattice Bias. *J. Phys. Condens. Matter* **2009**, *21* (8), 084204. https://doi.org/10.1088/0953-8984/21/8/084204.
- (363) Sanville, E.; Kenny, S. D.; Smith, R.; Henkelman, G. Improved Grid-Based Algorithm for Bader Charge Allocation. *J. Comput. Chem.* **2007**, *28* (5), 899–908. https://doi.org/10.1002/jcc.20575.
- (364) Henkelman, G.; Arnaldsson, A.; Jónsson, H. A Fast and Robust Algorithm for Bader Decomposition of Charge Density. *Comput. Mater. Sci.* **2006**, *36* (3), 354–360. https://doi.org/10.1016/j.commatsci.2005.04.010.
- (365) Yu, M.; Trinkle, D. R. Accurate and Efficient Algorithm for Bader Charge Integration. *J. Chem. Phys.* **2011**, 134 (6), 064111. https://doi.org/10.1063/1.3553716.
- (366) Chan, K.; Nørskov, J. K. Potential Dependence of Electrochemical Barriers from Ab Initio Calculations. *J. Phys. Chem. Lett.* **2016**, *7* (9), 1686–1690. https://doi.org/10.1021/acs.jpclett.6b00382.
- (367) Gong, L.; Agrawal, N.; Roman, A.; Holewinski, A.; Janik, M. J. Density Functional Theory Study of Furfural Electrochemical Oxidation on the Pt (1 1 1) Surface. *J. Catal.* **2019**, 373, 322–335. https://doi.org/10.1016/j.jcat.2019.04.012.
- (368) Sholl, D.; Steckel, J. A. *Density Functional Theory: A Practical Introduction.*; John Wiley & Sons, Inc.: Hoboken, New Jersey, 2011.
- (369) Andersson, M.; Bligaard, T.; Kustov, A.; Larsen, K.; Greeley, J.; Johannessen, T.; Christensen, C.; Norskov, J. Toward Computational Screening in Heterogeneous Catalysis: Pareto-Optimal Methanation Catalysts. *J. Catal.* **2006**, 239 (2), 501–506. https://doi.org/10.1016/j.jcat.2006.02.016.
- (370) Kustov, A. L.; Frey, A. M.; Larsen, K. E.; Johannessen, T.; Nørskov, J. K.; Christensen, C. H. CO Methanation over Supported Bimetallic Ni–Fe Catalysts: From Computational Studies towards Catalyst Optimization. *Appl. Catal. A Gen.* **2007**, 320, 98–104. https://doi.org/10.1016/j.apcata.2006.12.017.
- (371) Grabow, L. C. Chapter 1. Computational Catalyst Screening; pp 1–58. https://doi.org/10.1039/9781849734905-00001.
- (372) Abild-Pedersen, F.; Greeley, J.; Studt, F.; Rossmeisl, J.; Munter, T. R.; Moses, P. G.; Skúlason, E.; Bligaard, T.; Nørskov, J. K. Scaling Properties of Adsorption Energies for Hydrogen-Containing Molecules on Transition-Metal Surfaces. *Phys. Rev. Lett.* **2007**, *99* (1), 016105. https://doi.org/10.1103/PhysRevLett.99.016105.
- (373) Nørskov, J. K.; Bligaard, T.; Logadottir, A.; Bahn, S.; Hansen, L. B.; Bollinger, M.; Bengaard, H.; Hammer, B.; Sljivancanin, Z.; Mavrikakis, M.; et al. Universality in Heterogeneous Catalysis. *J. Catal.* **2002**, *209* (2), 275–278. https://doi.org/10.1006/jcat.2002.3615.
- (374) van Santen, R. A.; Neurock, M.; Shetty, S. G. Reactivity Theory of Transition-Metal Surfaces: A Brønsted-Evans-Polanyi Linear Activation Energy-Free-Energy Analysis. *Chem. Rev.* **2010**, *110* (4), 2005–2048. https://doi.org/10.1021/cr9001808.
- (375) Evans, M. G.; Polanyi, M. Inertia and Driving Force of Chemical Reactions.

- Trans. Faraday Soc. 1938, 34, 11. https://doi.org/10.1039/tf9383400011.
- (376) Liu, B.; Greeley, J. Density Functional Theory Study of Selectivity Considerations for C–C Versus C–O Bond Scission in Glycerol Decomposition on Pt(111). *Top. Catal.* **2012**, *55* (5–6), 280–289. https://doi.org/10.1007/s11244-012-9806-2.
- (377) Norskov, J. K.; Abild-Pedersen, F.; Studt, F.; Bligaard, T. Density Functional Theory in Surface Chemistry and Catalysis. *Proc. Natl. Acad. Sci.* **2011**, *108* (3), 937–943. https://doi.org/10.1073/pnas.1006652108.
- (378) Studt, F.; Abild-Pedersen, F.; Bligaard, T.; Sorensen, R. Z.; Christensen, C. H.; Norskov, J. K. Identification of Non-Precious Metal Alloy Catalysts for Selective Hydrogenation of Acetylene. *Science.* **2008**, *320* (5881), 1320–1322. https://doi.org/10.1126/science.1156660.
- (379) Liu, X.; An, W.; Wang, Y.; Turner, C. H.; Resasco, D. E. Hydrodeoxygenation of Guaiacol over Bimetallic Fe-Alloyed (Ni, Pt) Surfaces: Reaction Mechanism, Transition-State Scaling Relations and Descriptor for Predicting C–O Bond Scission Reactivity. *Catal. Sci. Technol.* **2018**, *8* (8), 2146–2158. https://doi.org/10.1039/C8CY00282G.
- (380) Lee, K.; Gu, G. H.; Mullen, C. A.; Boateng, A. A.; Vlachos, D. G. Guaiacol Hydrodeoxygenation Mechanism on Pt(111): Insights from Density Functional Theory and Linear Free Energy Relations. *ChemSusChem* **2015**, *8* (2), 315–322. https://doi.org/10.1002/cssc.201402940.
- (381) Vorotnikov, V.; Mpourmpakis, G.; Vlachos, D. G. DFT Study of Furfural Conversion to Furan, Furfuryl Alcohol, and 2-Methylfuran on Pd(111). ACS Catal. 2012, 2 (12), 2496–2504. https://doi.org/10.1021/cs300395a.
- (382) Liu, B.; Greeley, J. Decomposition Pathways of Glycerol via C–H, O–H, and C–C Bond Scission on Pt(111): A Density Functional Theory Study. *J. Phys. Chem. C* **2011**, *115* (40), 19702–19709. https://doi.org/10.1021/jp202923w.
- (383) Foo, G. S.; Wei, D.; Sholl, D. S.; Sievers, C. Role of Lewis and Brønsted Acid Sites in the Dehydration of Glycerol over Niobia. *ACS Catal.* **2014**, *4*(9), 3180–3192. https://doi.org/10.1021/cs5006376.
- (384) Gu, G. H.; Schweitzer, B.; Michel, C.; Steinmann, S. N.; Sautet, P.; Vlachos, D. G. Group Additivity for Aqueous Phase Thermochemical Properties of Alcohols on Pt(111). *J. Phys. Chem. C* **2017**, *121* (39), 21510–21519. https://doi.org/10.1021/acs.jpcc.7b07340.
- (385) Rangarajan, S.; Bhan, A.; Daoutidis, P. Rule-Based Generation of Thermochemical Routes to Biomass Conversion. *Ind. Eng. Chem. Res.* **2010**, 49 (21), 10459–10470. https://doi.org/10.1021/ie100546t.
- (386) Vinu, R.; Broadbelt, L. J. Unraveling Reaction Pathways and Specifying Reaction Kinetics for Complex Systems. *Annu. Rev. Chem. Biomol. Eng.* **2012**, 3 (1), 29–54. https://doi.org/10.1146/annurev-chembioeng-062011-081108.
- (387) Rangarajan, S.; R. O. Brydon, R.; Bhan, A.; Daoutidis, P. Automated Identification of Energetically Feasible Mechanisms of Complex Reaction Networks in Heterogeneous Catalysis: Application to Glycerol Conversion on Transition Metals. *Green Chem.* **2014**, *16* (2), 813–823. https://doi.org/10.1039/C3GC41386A.
- (388) Goldsmith, C. F.; West, R. H. Automatic Generation of Microkinetic

- Mechanisms for Heterogeneous Catalysis. *J. Phys. Chem. C* **2017**, *121* (18), 9970–9981. https://doi.org/10.1021/acs.jpcc.7b02133.
- (389) Gokhale, A. A.; Kandoi, S.; Greeley, J. P.; Mavrikakis, M.; Dumesic, J. A. Molecular-Level Descriptions of Surface Chemistry in Kinetic Models Using Density Functional Theory. *Chem. Eng. Sci.* **2004**, *59* (22–23), 4679–4691. https://doi.org/10.1016/j.ces.2004.09.038.
- (390) Dellon, L. D.; Sung, C.-Y.; Robichaud, D. J.; Broadbelt, L. J. 110th Anniversary: Microkinetic Modeling of the Vapor Phase Upgrading of Biomass-Derived Oxygenates. *Ind. Eng. Chem. Res.* **2019**, *58* (33), 15173–15189. https://doi.org/10.1021/acs.iecr.9b03242.
- (391) Ulissi, Z. W.; Medford, A. J.; Bligaard, T.; Nørskov, J. K. To Address Surface Reaction Network Complexity Using Scaling Relations Machine Learning and DFT Calculations. *Nat. Commun.* **2017**, 8 (1), 14621. https://doi.org/10.1038/ncomms14621.
- (392) Kitchin, J. R. Machine Learning in Catalysis. *Nat. Catal.* **2018**, *1* (4), 230–232. https://doi.org/10.1038/s41929-018-0056-y.
- (393) Medford, A. J.; Wellendorff, J.; Vojvodic, A.; Studt, F.; Abild-Pedersen, F.; Jacobsen, K. W.; Bligaard, T.; Norskov, J. K. Assessing the Reliability of Calculated Catalytic Ammonia Synthesis Rates. *Science.* **2014**, *345* (6193), 197–200. https://doi.org/10.1126/science.1253486.
- (394) Sutton, J. E.; Guo, W.; Katsoulakis, M. A.; Vlachos, D. G. Effects of Correlated Parameters and Uncertainty in Electronic-Structure-Based Chemical Kinetic Modelling. *Nat. Chem.* **2016**, *8* (4), 331–337. https://doi.org/10.1038/nchem.2454.
- (395) Holewinski, A.; Linic, S. Elementary Mechanisms in Electrocatalysis: Revisiting the ORR Tafel Slope. *J. Electrochem. Soc.* **2012**, *159* (11), H864–H870. https://doi.org/10.1149/2.022211jes.
- (396) Shinagawa, T.; Garcia-Esparza, A. T.; Takanabe, K. Insight on Tafel Slopes from a Microkinetic Analysis of Aqueous Electrocatalysis for Energy Conversion. *Sci. Rep.* **2015**, *5* (1), 13801. https://doi.org/10.1038/srep13801.
- (397) Ringe, S.; Morales-Guio, C. G.; Chen, L. D.; Fields, M.; Jaramillo, T. F.; Hahn, C.; Chan, K. Double Layer Charging Driven Carbon Dioxide Adsorption Limits the Rate of Electrochemical Carbon Dioxide Reduction on Gold. *Nat. Commun.* **2020**, *11* (1), 33. https://doi.org/10.1038/s41467-019-13777-z.
- (398) Nguyen, M.-T.; Akhade, S. A.; Cantu, D. C.; Lee, M.-S.; Glezakou, V.-A.; Rousseau, R. Electro-Reduction of Organics on Metal Cathodes: A Multiscale-Modeling Study of Benzaldehyde on Au (111). *Catal. Today* **2020**, *350*, 39–46. https://doi.org/10.1016/j.cattod.2019.05.067.
- (399) Singh, M. R.; Goodpaster, J. D.; Weber, A. Z.; Head-Gordon, M.; Bell, A. T. Mechanistic Insights into Electrochemical Reduction of CO 2 over Ag Using Density Functional Theory and Transport Models. *Proc. Natl. Acad. Sci.* **2017**, 114 (42), E8812–E8821. https://doi.org/10.1073/pnas.1713164114.
- (400) COMSOL Multiphysics® https://www.comsol.com/. Last accessed date was January 2020.
- (401) Shono, T.; Masuda, H.; Murase, H.; Shimomura, M.; Kashimura, S. Electroorganic Chemistry. 134. Facile Electroreduction of Methyl Esters and N,N-Dimethylamides of Aliphatic Carboxylic Acids to Primary Alcohols. *J. Org.*

- Chem. 1992, 57 (4), 1061–1063. https://doi.org/10.1021/jo00030a003.
- (402) Ishifune, M.; Yamashita, H.; Matsuda, M.; Ishida, H.; Yamashita, N.; Kera, Y.; Kashimura, S.; Masuda, H.; Murase, H. Electroreduction of Aliphatic Esters Using New Paired Electrolysis Systems. *Electrochim. Acta* **2001**, *46* (20–21), 3259–3264. https://doi.org/10.1016/S0013-4686(01)00617-X.
- (403) Kashimura, S.; Murai, Y.; Ishifune, M.; Masuda, H.; Shimomura, M.; Murase, H.; Shono, T.; Toftlund, H. Electroreductive Intramolecular Cyclization of Olefinic Esters and Its Application to the Synthesis of Muscone. *Acta Chem. Scand.* **1999**, *53*, 949–951. https://doi.org/10.3891/acta.chem.scand.53-0949.
- (404) Lange, J.-P.; van de Graaf, W. D.; Haan, R. J. Conversion of Furfuryl Alcohol into Ethyl Levulinate Using Solid Acid Catalysts. *ChemSusChem* **2009**, *2* (5), 437–441. https://doi.org/10.1002/cssc.200800216.
- (405) Chen, B.; Li, F.; Huang, Z.; Lu, T.; Yuan, Y.; Yuan, G. Integrated Catalytic Process to Directly Convert Furfural to Levulinate Ester with High Selectivity. *ChemSusChem* **2014**, 7 (1), 202–209. https://doi.org/10.1002/cssc.201300542.
- (406) Tiwari, M. S.; Dicks, J. S.; Keogh, J.; Ranade, V. V.; Manyar, H. G. Direct Conversion of Furfuryl Alcohol to Butyl Levulinate Using Tin Exchanged Tungstophosphoric Acid Catalysts. *Mol. Catal.* **2020**, *488*, 110918. https://doi.org/10.1016/j.mcat.2020.110918.
- (407) Du, X.-L.; Bi, Q.-Y.; Liu, Y.-M.; Cao, Y.; He, H.-Y.; Fan, K.-N. Tunable Copper-Catalyzed Chemoselective Hydrogenolysis of Biomass-Derived γ-Valerolactone into 1,4-Pentanediol or 2-Methyltetrahydrofuran. *Green Chem.* **2012**, *14* (4), 935. https://doi.org/10.1039/c2gc16599f.
- (408) Deng, T.; Yan, L.; Li, X.; Fu, Y. Continuous Hydrogenation of Ethyl Levulinate to 1,4-Pentanediol over 2.8Cu-3.5Fe/SBA-15 Catalyst at Low Loading: The Effect of Fe Doping. *ChemSusChem* **2019**, *12* (16), 3837–3848. https://doi.org/10.1002/cssc.201901198.
- (409) Ahn, Y.-C.; Han, J. Catalytic Production of 1,4-Pentanediol from Corn Stover. *Bioresour. Technol.* **2017**, 245, 442–448. https://doi.org/10.1016/j.biortech.2017.09.007.
- (410) Li, M.; Li, G.; Li, N.; Wang, A.; Dong, W.; Wang, X.; Cong, Y. Aqueous Phase Hydrogenation of Levulinic Acid to 1,4-Pentanediol. *Chem. Commun.* **2014**, 50 (12), 1414. https://doi.org/10.1039/c3cc48236g.
- (411) Stones, M. K.; Banz Chung, E. M.-J.; da Cunha, I. T.; Sullivan, R. J.; Soltanipanah, P.; Magee, M.; Umphrey, G. J.; Moore, C. M.; Sutton, A. D.; Schlaf, M. Conversion of Furfural Derivatives to 1,4-Pentanediol and Cyclopentanol in Aqueous Medium Catalyzed by Trans -[(2,9-Dipyridyl-1,10-Phenanthroline)(CH 3 CN) 2 Ru](OTf) 2. ACS Catal. 2020, 10 (4), 2667–2683. https://doi.org/10.1021/acscatal.9b05055.
- (412) Liu, Q.; Qiao, B.; Liu, F.; Zhang, L.; Su, Y.; Wang, A.; Zhang, T. Catalytic Production of 1,4-Pentanediol from Furfural in a Fixed-Bed System under Mild Conditions. *Green Chem.* **2020**, *22* (11), 3532–3538. https://doi.org/10.1039/D0GC00233J.
- (413) Li, Xinglong; Zhang, Kun; Xu, Hai; Xu, Qiang; Jiang, N. Method for Preparing 2,5-Furandicarboxylic Acid and Its Derivatives. CN 2017-10469754, 2017.
- (414) Minetto, G.; Raveglia, L. F.; Sega, A.; Taddei, M. Microwave-Assisted Paal-

- Knorr Reaction Three-Step Regiocontrolled Synthesis of Polysubstituted Furans, Pyrroles and Thiophenes. *European J. Org. Chem.* **2005**, *2005* (24), 5277–5288. https://doi.org/10.1002/ejoc.200500387.
- (415) Khaghaninejad, S.; Heravi, M. M. Paal–Knorr Reaction in the Synthesis of Heterocyclic Compounds; 2014; pp 95–146. https://doi.org/10.1016/B978-0-12-420160-6.00003-3.
- (416) Bergmeier, S. C. The Synthesis of Vicinal Amino Alcohols. *Tetrahedron* **2000**, *56* (17), 2561–2576. https://doi.org/10.1016/S0040-4020(00)00149-6.
- (417) Ager, D. J.; Prakash, I.; Schaad, D. R. 1,2-Amino Alcohols and Their Heterocyclic Derivatives as Chiral Auxiliaries in Asymmetric Synthesis. *Chem. Rev.* **1996**, *96* (2), 835–876. https://doi.org/10.1021/cr9500038.
- (418) Seki, H.; Koga, K.; Matsuo, H.; Ohki, S.; Matsuo, I.; Yamada, S. Studies on Optically Active Amino Acids. V. Synthesis of Optically Active α-Aminoalcohols by the Reduction of α-Amino Acid Esters with Sodium Borohydride. *Chem. Pharm. Bull. (Tokyo).* 1965, 13 (8), 995–1000. https://doi.org/10.1248/cpb.13.995.
- (419) Gonçalves, R. S. B.; Pinheiro, A. C.; da Silva, E. T.; da Costa, J. C. S.; Kaiser, C. R.; de Souza, M. V. N. Simple Methodology for the Preparation of Amino Alcohols from Amino Acid Esters Using NaBH 4 –Methanol in THF. Synth. Commun. 2011, 41 (9), 1276–1281. https://doi.org/10.1080/00397911.2010.481747.
- (420) Karrer, P.; Portmann, P.; Suter, M. L-Valinol UndL-Tyrosinol. *Helv. Chim. Acta* **1949**, 32 (3), 1156–1157. https://doi.org/10.1002/hlca.19490320374.
- (421) Karrer, P.; Nicolaus, B. J. R. Reduktionen Einiger Einfacher Peptide Mit Lithiumaluminiumhydrid. *Helv. Chim. Acta* **1952**, 35 (5), 1581–1585. https://doi.org/10.1002/hlca.19520350520.
- (422) Kuriyama, W.; Ino, Y.; Ogata, O.; Sayo, N.; Saito, T. A Homogeneous Catalyst for Reduction of Optically Active Esters to the Corresponding Chiral Alcohols without Loss of Optical Purities. Adv. Synth. Catal. 2010, 352 (1), 92–96. https://doi.org/10.1002/adsc.200900114.
- (423) Studer, M.; Burkhardt, S.; Blaser, H.-U. Catalytic Hydrogenation of Chiral α-Amino and α-Hydroxy Esters at Room Temperature with Nishimura Catalyst without Racemization. *Adv. Synth. Catal.* **2001**, 343 (8), 802–808. https://doi.org/10.1002/1615-4169(20011231)343:8<802::AID-ADSC802>3.0.CO;2-T.
- (424) Mägerlein, W.; Dreisbach, C.; Hugl, H.; Tse, M. K.; Klawonn, M.; Bhor, S.; Beller, M. Homogeneous and Heterogeneous Ruthenium Catalysts in the Synthesis of Fine Chemicals. *Catal. Today* **2007**, *121* (1–2), 140–150. https://doi.org/10.1016/j.cattod.2006.11.024.
- (425) Tamura, M.; Tamura, R.; Takeda, Y.; Nakagawa, Y.; Tomishige, K. Insight into the Mechanism of Hydrogenation of Amino Acids to Amino Alcohols Catalyzed by a Heterogeneous MoO x -Modified Rh Catalyst. *Chem. A Eur. J.* **2015**, *21* (7), 3097–3107. https://doi.org/10.1002/chem.201405769.
- (426) Lammens, T. M.; Le Nôtre, J.; Franssen, M. C. R.; Scott, E. L.; Sanders, J. P. M. Synthesis of Biobased Succinonitrile from Glutamic Acid and Glutamine. ChemSusChem 2011, 4 (6), 785–791. https://doi.org/10.1002/cssc.201100030.

- (427) National-Academies-of-Sciences,-Engineering, A.-M. *Gaseous Carbon Waste Streams Utilization*; National Academies Press: Washington, D.C., 2019. https://doi.org/10.17226/25232.
- (428) Kätelhön, A.; Meys, R.; Deutz, S.; Suh, S.; Bardow, A. Climate Change Mitigation Potential of Carbon Capture and Utilization in the Chemical Industry. *Proc. Natl. Acad. Sci.* **2019**, *116* (23), 11187–11194. https://doi.org/10.1073/pnas.1821029116.
- (429) De Luna, P.; Hahn, C.; Higgins, D.; Jaffer, S. A.; Jaramillo, T. F.; Sargent, E. H. What Would It Take for Renewably Powered Electrosynthesis to Displace Petrochemical Processes? *Science*. **2019**, *364* (6438), eaav3506. https://doi.org/10.1126/science.aav3506.
- (430) Gao, D.; Arán-Ais, R. M.; Jeon, H. S.; Roldan Cuenya, B. Rational Catalyst and Electrolyte Design for CO2 Electroreduction towards Multicarbon Products. *Nat. Catal.* **2019**, *2* (3), 198–210. https://doi.org/10.1038/s41929-019-0235-5.
- (431) Cherubini-Celli, A.; Mateos, J.; Bonchio, M.; Dell'Amico, L.; Companyó, X. Transition Metal-Free CO 2 Fixation into New Carbon-Carbon Bonds. *ChemSusChem* **2018**, *11* (18), 3056–3070. https://doi.org/10.1002/cssc.201801063.
- (432) Matthessen, R.; Fransaer, J.; Binnemans, K.; De Vos, D. E. Electrocarboxylation: Towards Sustainable and Efficient Synthesis of Valuable Carboxylic Acids. *Beilstein J. Org. Chem.* **2014**, *10*, 2484–2500. https://doi.org/10.3762/bjoc.10.260.
- (433) Senboku, H.; Katayama, A. Electrochemical Carboxylation with Carbon Dioxide. *Curr. Opin. Green Sustain. Chem.* **2017**, 3, 50–54. https://doi.org/10.1016/j.cogsc.2016.10.003.
- (434) Cao, Y.; He, X.; Wang, N.; Li, H.-R.; He, L.-N. Photochemical and Electrochemical Carbon Dioxide Utilization with Organic Compounds. *Chinese J. Chem.* **2018**, *36* (7), 644–659. https://doi.org/10.1002/cjoc.201700742.
- (435) Lu, Y.; Zou, Y.; Zhao, W.; Wang, M.; Li, C.; Liu, S.; Wang, S. Nanostructured Electrocatalysts for Electrochemical Carboxylation with CO 2. *Nano Sel.* **2020**, *1* (2), 135–151. https://doi.org/10.1002/nano.202000001.
- (436) Wang, H.; Du, Y.-F.; Lin, M.-Y.; Zhang, K.; Lu, J.-X. Electrochemical Reduction and Carboxylation of Ethyl Cinnamate in MeCN. *Chinese J. Chem.* **2008**, *26* (9), 1745–1748. https://doi.org/10.1002/cjoc.200890316.
- (437) Wang, H.; Zhang, G.; Liu, Y.; Luo, Y.; Lu, J. Electrocarboxylation of Activated Olefins in Ionic Liquid BMIMBF4. *Electrochem. commun.* **2007**, *9* (9), 2235–2239. https://doi.org/10.1016/j.elecom.2007.06.031.
- (438) Yuan, G.-Q.; Jiang, H.-F.; Lin, C.; Liao, S.-J. Efficient Electrochemical Synthesis of 2-Arylsuccinic Acids from CO2 and Aryl-Substituted Alkenes with Nickel as the Cathode. *Electrochim. Acta* **2008**, *53* (5), 2170–2176. https://doi.org/10.1016/j.electacta.2007.09.023.
- (439) Kim, Y.; Park, G. Do; Balamurugan, M.; Seo, J.; Min, B. K.; Nam, K. T. Electrochemical B-Selective Hydrocarboxylation of Styrene Using CO 2 and Water. *Adv. Sci.* **2020**, *7* (3), 1900137. https://doi.org/10.1002/advs.201900137.
- (440) Li, C.-H.; Yuan, G.-Q.; Ji, X.-C.; Wang, X.-J.; Ye, J.-S.; Jiang, H.-F. Highly

- Regioselective Electrochemical Synthesis of Dioic Acids from Dienes and Carbon Dioxide. *Electrochim. Acta* **2011**, *56* (3), 1529–1534. https://doi.org/10.1016/j.electacta.2010.06.057.
- (441) Matthessen, R.; Fransaer, J.; Binnemans, K.; Vos, D. E. De. Electrochemical Dicarboxylation of Conjugated Fatty Acids as an Efficient Valorization of Carbon Dioxide. RSC Adv. 2013, 3 (14), 4634. https://doi.org/10.1039/c3ra00129f.
- (442) Yuan, G.; Li, L.; Jiang, H.; Qi, C.; Xie, F. Electrocarboxylation of Carbon Dioxide with Polycyclic Aromatic Hydrocarbons Using Ni as the Cathode. *Chinese J. Chem.* **2010**, *28* (10), 1983–1988. https://doi.org/10.1002/cjoc.201090331.
- (443) Zhang, L.; Niu, D.; Zhang, K.; Zhang, G.; Luo, Y.; Lu, J. Electrochemical Activation of CO 2 in Ionic Liquid (BMIMBF 4): Synthesis of Organic Carbonates under Mild Conditions. *Green Chem.* **2008**, *10* (2), 202–206. https://doi.org/10.1039/B711981J.
- (444) Hu, Q.-L.; Zhang, Z.-X.; Zhang, J.-J.; Li, S.-M.; Wang, H.; Lu, J.-X. Ordered Mesoporous Carbon Embedded with Cu Nanoparticle Materials for Electrocatalytic Synthesis of Benzyl Methyl Carbonate from Benzyl Alcohol and Carbon Dioxide. *ACS Omega* **2020**, *5* (7), 3498–3503. https://doi.org/10.1021/acsomega.9b03651.
- (445) Wu, L.-X.; Wang, H.; Xiao, Y.; Tu, Z.-Y.; Ding, B.-B.; Lu, J.-X. Synthesis of Dialkyl Carbonates from CO2 and Alcohols via Electrogenerated N-Heterocyclic Carbenes. *Electrochem. commun.* **2012**, *25*, 116–118. https://doi.org/10.1016/j.elecom.2012.09.028.
- (446) Senboku, H.; Yoneda, K.; Hara, S. Electrochemical Direct Carboxylation of Benzyl Alcohols Having an Electron-Withdrawing Group on the Phenyl Ring: One-Step Formation of Phenylacetic Acids from Benzyl Alcohols under Mild Conditions. *Tetrahedron Lett.* 2015, 56 (48), 6772–6776. https://doi.org/10.1016/j.tetlet.2015.10.068.
- (447) Wawzonek, S.; Gundersen, A. Polarographic Studies in Acetonitrile and Dimethylformamide. *J. Electrochem. Soc.* **1960**, *107* (6), 537. https://doi.org/10.1149/1.2427738.
- (448) Zhao, S.-F.; Horne, M.; Bond, A. M.; Zhang, J. Electrochemical Reduction of Aromatic Ketones in 1-Butyl-3-Methylimidazolium-Based Ionic Liquids in the Presence of Carbon Dioxide: The Influence of the Ketone Substituent and the Ionic Liquid Anion on Bulk Electrolysis Product Distribution. *Phys. Chem. Chem. Phys.* 2015, 17 (29), 19247–19254. https://doi.org/10.1039/C5CP00095E.
- (449) Yuan, G.; Li, Z.; Jiang, H. Electrosyntheses of α -Hydroxycarboxylic Acids from Carbon Dioxide and Aromatic Ketones Using Nickel as the Cathode. *Chinese J. Chem.* **2009**, *27* (8), 1464–1470. https://doi.org/10.1002/cjoc.200990246.
- (450) Zhao, S.-F.; Wang, H.; Lan, Y.-C.; Liu, X.; Lu, J.-X.; Zhang, J. Influences of the Operative Parameters and the Nature of the Substrate on the Electrocarboxylation of Benzophenones. *J. Electroanal. Chem.* **2012**, *664*, 105–110. https://doi.org/10.1016/j.jelechem.2011.11.001.
- (451) Saravanan, K. R.; Chandrasekaran, M.; Suryanarayanan, V. Efficient Electrocarboxylation of Benzophenone on Silver Nanoparticles Deposited

- Boron Doped Diamond Electrode. *J. Electroanal. Chem.* **2015**, 757, 18–22. https://doi.org/10.1016/j.jelechem.2015.08.033.
- (452) Rajagopal, V.; Velayutham, D.; Suryanarayanan, V.; Kathiresan, M.; Ho, K. C. Electrochemical Fabrication of Dendritic Silver–Copper Bimetallic Nanomaterials in Protic Ionic Liquid for Electrocarboxylation. *J. Taiwan Inst. Chem. Eng.* **2018**, *87*, 158–164. https://doi.org/10.1016/j.jtice.2018.03.030.
- (453) Zhao, S.-F.; Horne, M.; Bond, A. M.; Zhang, J. Electrocarboxylation of Acetophenone in Ionic Liquids: The Influence of Proton Availability on Product Distribution. *Green Chem.* **2014**, *16* (4), 2242–2251. https://doi.org/10.1039/C3GC42404A.
- (454) Doherty, A. Electrochemical Reduction of Butyraldehyde in the Presence of CO2. *Electrochim. Acta* **2002**, *47* (18), 2963–2967. https://doi.org/10.1016/S0013-4686(02)00196-2.
- (455) Silvestri, G.; Gambino, S.; Filardo, G. Electrochemical Carboxylation of Aldehydes and Ketones with Sacrificial Aluminum Anodes. *Tetrahedron Lett.* **1986**, *27* (29), 3429–3430. https://doi.org/10.1016/S0040-4039(00)84814-5.
- (456) Casadei, M. A.; Inesi, A.; Moracci, F. M.; Rossi, L. Electrochemical Activation of Carbon Dioxide: Synthesis of Carbamates. *Chem. Commun.* **1996**, No. 22, 2575. https://doi.org/10.1039/cc9960002575.
- (457) Feroci, M.; Orsini, M.; Rossi, L.; Sotgiu, G.; Inesi, A. Electrochemically Promoted C-N Bond Formation from Amines and CO 2 in Ionic Liquid BMIm-BF 4: Synthesis of Carbamates. *J. Org. Chem.* **2007**, *72* (1), 200–203. https://doi.org/10.1021/jo061997c.
- (458) Forte, G.; Chiarotto, I.; Richter, F.; Trieu, V.; Feroci, M. Towards a Sustainable Electrochemical Activation for Recycling CO 2: Synthesis of Bis-O-Alkylcarbamates from Aliphatic and Benzyl Diamines. *React. Chem. Eng.* **2017**, 2 (5), 646–649. https://doi.org/10.1039/C7RE00101K.
- (459) Wang, J.; Qian, P.; Hu, K.; Zha, Z.; Wang, Z. Electrocatalytic Fixation of Carbon Dioxide with Amines and Arylketones. *ChemElectroChem* **2019**, 6 (16), 4292–4296. https://doi.org/10.1002/celc.201801724.
- (460) Muchez, L.; De Vos, D. E.; Kim, M. Sacrificial Anode-Free Electrosynthesis of α-Hydroxy Acids via Electrocatalytic Coupling of Carbon Dioxide to Aromatic Alcohols. ACS Sustain. Chem. Eng. 2019, 7 (19), 15860–15864. https://doi.org/10.1021/acssuschemeng.9b04612.
- (461) Matthessen, R.; Fransaer, J.; Binnemans, K.; De Vos, D. E. Paired Electrosynthesis of Diacid and Diol Precursors Using Dienes and CO 2 as the Carbon Source. *ChemElectroChem* **2015**, *2* (1), 73–76. https://doi.org/10.1002/celc.201402299.
- (462) Bligaard, T.; Bullock, R. M.; Campbell, C. T.; Chen, J. G.; Gates, B. C.; Gorte, R. J.; Jones, C. W.; Jones, W. D.; Kitchin, J. R.; Scott, S. L. Toward Benchmarking in Catalysis Science: Best Practices, Challenges, and Opportunities. *ACS Catal.* **2016**, *6* (4), 2590–2602. https://doi.org/10.1021/acscatal.6b00183.
- (463) Schüth, F.; Ward, M. D.; Buriak, J. M. Common Pitfalls of Catalysis Manuscripts Submitted to Chemistry of Materials. *Chem. Mater.* **2018**, *30* (11), 3599–3600. https://doi.org/10.1021/acs.chemmater.8b01831.
- (464) Heinzel, A.; Barragán, V. M. A Review of the State-of-the-Art of the Methanol

- Crossover in Direct Methanol Fuel Cells. *J. Power Sources* **1999**, *84* (1), 70–74. https://doi.org/10.1016/S0378-7753(99)00302-X.
- (465) Barton, Z. J.; Garrett, G. H.; Kurtyka, N.; Spivey, T. D.; Schaidle, J. A.; Holewinski, A. Electrochemical Reduction Selectivity of Crotonaldehyde on Copper. J. Appl. Electrochem. 2020. https://doi.org/10.1007/s10800-020-01415-2.
- (466) Ren, Y.; Yu, C.; Tan, X.; Han, X.; Huang, H.; Huang, H.; Qiu, J. Is It Appropriate to Use the Nafion Membrane in Electrocatalytic N 2 Reduction? *Small Methods* **2019**, 3 (12), 1900474. https://doi.org/10.1002/smtd.201900474.
- (467) Andersen, S. Z.; Čolić, V.; Yang, S.; Schwalbe, J. A.; Nielander, A. C.; McEnaney, J. M.; Enemark-Rasmussen, K.; Baker, J. G.; Singh, A. R.; Rohr, B. A.; et al. A Rigorous Electrochemical Ammonia Synthesis Protocol with Quantitative Isotope Measurements. *Nature* **2019**, *570* (7762), 504–508. https://doi.org/10.1038/s41586-019-1260-x.
- (468) Catoire, L.; Yahyaoui, M.; Osmont, A.; Gökalp, I.; Brothier, M.; Lorcet, H.; Guénadou, D. Thermochemistry of Compounds Formed during Fast Pyrolysis of Lignocellulosic Biomass. *Energy & Fuels* **2008**, *22* (6), 4265–4273. https://doi.org/10.1021/ef800418z.
- (469) JOBACK, K. G.; REID, R. C. ESTIMATION OF PURE-COMPONENT PROPERTIES FROM GROUP-CONTRIBUTIONS. *Chem. Eng. Commun.* **1987**, *57* (1–6), 233–243. https://doi.org/10.1080/00986448708960487.
- (470) Constantinou, L.; Gani, R. New Group Contribution Method for Estimating Properties of Pure Compounds. *AIChE J.* **1994**, *40* (10), 1697–1710. https://doi.org/10.1002/aic.690401011.
- (471) Allen J. Bard, L. R. F. *Electrochemical Methods: Fundamentals and Applications*, 2nd ed.; Wiley & Sons Ltd, 2000.
- (472) Dickinson, E. J. F.; Limon-Petersen, J. G.; Rees, N. V.; Compton, R. G. How Much Supporting Electrolyte Is Required to Make a Cyclic Voltammetry Experiment Quantitatively "Diffusional"? A Theoretical and Experimental Investigation. *J. Phys. Chem. C* **2009**, *113* (25), 11157–11171. https://doi.org/10.1021/jp901628h.
- (473) Oldham, K. B.; Stevens, N. P. C. Uncompensated Resistance. 2. The Effect of Reference Electrode Nonideality. *Anal. Chem.* **2000**, *72* (17), 3981–3988. https://doi.org/10.1021/ac000154x.
- (474) Myland, J. C.; Oldham, K. B. Uncompensated Resistance. 1. The Effect of Cell Geometry. Anal. Chem. 2000, 72 (17), 3972–3980. https://doi.org/10.1021/ac0001535.
- (475) Gütz, C.; Stenglein, A.; Waldvogel, S. R. Highly Modular Flow Cell for Electroorganic Synthesis. *Org. Process Res. Dev.* **2017**, *21* (5), 771–778. https://doi.org/10.1021/acs.oprd.7b00123.
- (476) Gütz, C.; Klöckner, B.; Waldvogel, S. R. Electrochemical Screening for Electroorganic Synthesis. *Org. Process Res. Dev.* **2016**, *20* (1), 26–32. https://doi.org/10.1021/acs.oprd.5b00377.
- (477) Haverkort, J. W. A Theoretical Analysis of the Optimal Electrode Thickness and Porosity. *Electrochim. Acta* **2019**, 295, 846–860. https://doi.org/10.1016/j.electacta.2018.10.065.
- (478) Gloaguen, F.; Andolfatto, F.; Durand, R.; Ozil, P. Kinetic Study of

- Electrochemical Reactions at Catalyst-Recast Ionomer Interfaces from Thin Active Layer Modelling. *J. Appl. Electrochem.* **1994**, *24* (9), 863–869. https://doi.org/10.1007/BF00348773.
- (479) Gloaguen, F.; Convert, P.; Gamburzev, S.; Velev, O. A.; Srinivasan, S. An Evaluation of the Macro-Homogeneous and Agglomerate Model for Oxygen Reduction in PEMFCs. *Electrochim. Acta* **1998**, *43* (24), 3767–3772. https://doi.org/10.1016/S0013-4686(98)00136-4.
- (480) Bae, J. H.; Han, J.-H.; Chung, T. D. Electrochemistry at Nanoporous Interfaces: New Opportunity for Electrocatalysis. *Phys. Chem. Chem. Phys.* **2012**, *14* (2), 448–463. https://doi.org/10.1039/C1CP22927C.
- (481) Larrazábal, G. O.; Martín, A. J.; Pérez-Ramírez, J. Building Blocks for High Performance in Electrocatalytic CO 2 Reduction: Materials, Optimization Strategies, and Device Engineering. *J. Phys. Chem. Lett.* **2017**, *8* (16), 3933–3944. https://doi.org/10.1021/acs.jpclett.7b01380.
- (482) Lucas, F. W. S.; Lima, F. H. B. Electrodeposited Tin-Antimony Alloys as Novel Electrocatalysts for Selective and Stable Carbon Dioxide Reduction to Formate. *ChemElectroChem* **2020**, *7* (18), 3733–3742. https://doi.org/10.1002/celc.202000769.
- (483) Moniri, S.; Van Cleve, T.; Linic, S. Pitfalls and Best Practices in Measurements of the Electrochemical Surface Area of Platinum-Based Nanostructured Electro-Catalysts. *J. Catal.* **2017**, 345, 1–10. https://doi.org/10.1016/j.jcat.2016.11.018.
- (484) Herrero, E.; Buller, L. J.; Abruña, H. D. Underpotential Deposition at Single Crystal Surfaces of Au, Pt, Ag and Other Materials. *Chem. Rev.* **2001**, *101* (7), 1897–1930. https://doi.org/10.1021/cr9600363.
- (485) Shao, M.; Odell, J. H.; Choi, S.-I.; Xia, Y. Electrochemical Surface Area Measurements of Platinum- and Palladium-Based Nanoparticles. *Electrochem. commun.* **2013**, 31, 46–48. https://doi.org/10.1016/j.elecom.2013.03.011.
- (486) Yoon, Y.; Yan, B.; Surendranath, Y. Suppressing Ion Transfer Enables Versatile Measurements of Electrochemical Surface Area for Intrinsic Activity Comparisons. *J. Am. Chem. Soc.* **2018**, *140* (7), 2397–2400. https://doi.org/10.1021/jacs.7b10966.
- (487) Sahraie, N. R.; Kramm, U. I.; Steinberg, J.; Zhang, Y.; Thomas, A.; Reier, T.; Paraknowitsch, J.-P.; Strasser, P. Quantifying the Density and Utilization of Active Sites in Non-Precious Metal Oxygen Electroreduction Catalysts. *Nat. Commun.* **2015**, *6* (1), 8618. https://doi.org/10.1038/ncomms9618.
- (488) Lefèvre, M.; Proietti, E.; Jaouen, F.; Dodelet, J.-P. Iron-Based Catalysts with Improved Oxygen Reduction Activity in Polymer Electrolyte Fuel Cells. *Science*. **2009**, *324* (5923), 71–74. https://doi.org/10.1126/science.1170051.
- (489) Honkala, K. Ammonia Synthesis from First-Principles Calculations. *Science*. **2005**, *307* (5709), 555–558. https://doi.org/10.1126/science.1106435.
- (490) Markovic, N. Surface Science Studies of Model Fuel Cell Electrocatalysts. *Surf. Sci. Rep.* **2002**, *45* (4–6), 117–229. https://doi.org/10.1016/S0167-5729(01)00022-X.
- (491) Schouten, K. J. P.; Pérez Gallent, E.; Koper, M. T. M. Structure Sensitivity of the Electrochemical Reduction of Carbon Monoxide on Copper Single

- Crystals. *ACS Catal.* **2013**, 3 (6), 1292–1295. https://doi.org/10.1021/cs4002404.
- (492) Kwon, Y.; Koper, M. T. M. M. Combining Voltammetry with HPLC: Application to Electro-Oxidation of Glycerol. *Anal. Chem.* **2010**, *82* (13), 5420–5424. https://doi.org/10.1021/ac101058t.
- (493) Rodriguez, P.; Kwon, Y.; Koper, M. T. M. The Promoting Effect of Adsorbed Carbon Monoxide on the Oxidation of Alcohols on a Gold Catalyst. *Nat. Chem.* **2012**, *4* (3), 177–182. https://doi.org/10.1038/nchem.1221.
- (494) Zaera, F. Probing Liquid/Solid Interfaces at the Molecular Level. *Chem. Rev.* **2012**, *112* (5), 2920–2986. https://doi.org/10.1021/cr2002068.
- (495) Bewick, A.; Kunimatsu, K.; Stanley Pons, B. Infra Red Spectroscopy of the Electrode-Electrolyte Interphase. *Electrochim. Acta* **1980**, *25* (4), 465–468. https://doi.org/10.1016/0013-4686(80)87039-3.
- (496) Iwasita, T. Electrocatalysis of Methanol Oxidation. *Electrochim. Acta* **2002**, *47* (22–23), 3663–3674. https://doi.org/10.1016/S0013-4686(02)00336-5.
- (497) Li, J.-F.; Rudnev, A.; Fu, Y.; Bodappa, N.; Wandlowski, T. In Situ SHINERS at Electrochemical Single-Crystal Electrode/Electrolyte Interfaces: Tuning Preparation Strategies and Selected Applications. *ACS Nano* **2013**, *7* (10), 8940–8952. https://doi.org/10.1021/nn403444j.
- (498) Guan, S.; Donovan-Sheppard, O.; Reece, C.; Willock, D. J.; Wain, A. J.; Attard, G. A. Structure Sensitivity in Catalytic Hydrogenation at Platinum Surfaces Measured by Shell-Isolated Nanoparticle Enhanced Raman Spectroscopy (SHINERS). *ACS Catal.* **2016**, *6* (3), 1822–1832. https://doi.org/10.1021/acscatal.5b02872.
- (499) Pelliccione, C. J.; Timofeeva, E. V.; Katsoudas, J. P.; Segre, C. U. In Situ Ru K-Edge X-Ray Absorption Spectroscopy Study of Methanol Oxidation Mechanisms on Model Submonolayer Ru on Pt Nanoparticle Electrocatalyst. J. Phys. Chem. C 2013, 117 (37), 18904–18912. https://doi.org/10.1021/jp404342z.
- (500) Subbaraman, R.; Tripkovic, D.; Chang, K.-C.; Strmcnik, D.; Paulikas, A. P.; Hirunsit, P.; Chan, M.; Greeley, J.; Stamenkovic, V.; Markovic, N. M. Trends in Activity for the Water Electrolyser Reactions on 3d M(Ni,Co,Fe,Mn) Hydr(Oxy)Oxide Catalysts. *Nat. Mater.* **2012**, *11* (6), 550–557. https://doi.org/10.1038/nmat3313.
- (501) Osawa, M.; Ikeda, M. Surface-Enhanced Infrared Absorption of p-Nitrobenzoic Acid Deposited on Silver Island Films: Contributions of Electromagnetic and Chemical Mechanisms. *J. Phys. Chem.* **1991**, *95* (24), 9914–9919. https://doi.org/10.1021/j100177a056.
- (502) Chen, Y. X.; Miki, A.; Ye, S.; Sakai, H.; Osawa, M. Formate, an Active Intermediate for Direct Oxidation of Methanol on Pt Electrode. *J. Am. Chem. Soc.* **2003**, *125* (13), 3680–3681. https://doi.org/10.1021/ja029044t.
- (503) You, F.; Wang, B. Life Cycle Optimization of Biomass-to-Liquid Supply Chains with Distributed–Centralized Processing Networks. *Ind. Eng. Chem. Res.* **2011**, *50* (17), 10102–10127. https://doi.org/10.1021/ie200850t.
- (504) Resasco, D. E.; Wang, B.; Sabatini, D. Distributed Processes for Biomass Conversion Could Aid UN Sustainable Development Goals. *Nat. Catal.* **2018**, *1* (10), 731–735. https://doi.org/10.1038/s41929-018-0166-6.

- (505) Strel'nikova, E. B.; Goncharov, I. V.; Serebrennikova, O. V. Concentration and Distribution of Oxygen-Containing Compounds in Crude Oils from the Southeastern Part of Western Siberia. *Pet. Chem.* **2012**, *52* (4), 278–283. https://doi.org/10.1134/S096554411204010X.
- (506) Petroleum Composition http://www.petroleum.co.uk/composition. Last accessed date was January 2020.
- (507) Vassilev, S. V.; Baxter, D.; Andersen, L. K.; Vassileva, C. G. An Overview of the Chemical Composition of Biomass. *Fuel* **2010**, *89* (5), 913–933. https://doi.org/10.1016/j.fuel.2009.10.022.
- (508) The International Renewable Energy Agency (IRENA). Global Renewables Outlook: Energy transformation 2050 https://www.irena.org/publications/2020/Apr/Global-Renewables-Outlook-2020. Last accessed date was January 2020.
- (509) The California Energy Commission (CEC). The world's largest utility scale solar project is located in California https://ww2.energy.ca.gov/title24/tour/solarstar/index.html. Last accessed date was January 2020.
- (510) The U.S. Energy Information Administration (EIA). Most U.S. utility-scale solar photovoltaic power plants are 5 megawatts or smaller https://www.eia.gov/todayinenergy/detail.php?id=38272. Last accessed date was January 2020.
- (511) Sean Ong, Clinton Campbell, P. D.; Robert Margolis, G. H. Land-Use Requirements for Solar Power Plants in the United States https://www.nrel.gov/docs/fy13osti/56290.pdf. Last accessed date was January 2020.
- (512) Paul Denholm, M. H.; Maddalena Jackson, and S. O. Land-Use Requirements of Modern Wind Power Plants in the United States https://www.nrel.gov/docs/fy09osti/45834.pdf. Last accessed date was January 2020.
- (513) Karlsson, R. K. B.; Cornell, A. Selectivity between Oxygen and Chlorine Evolution in the Chlor-Alkali and Chlorate Processes. *Chem. Rev.* **2016**, *116* (5), 2982–3028. https://doi.org/10.1021/acs.chemrev.5b00389.
- (514) Sherbo, R. S.; Delima, R. S.; Chiykowski, V. A.; MacLeod, B. P.; Berlinguette, C. P. Complete Electron Economy by Pairing Electrolysis with Hydrogenation. *Nat. Catal.* 2018, 1 (7), 501–507. https://doi.org/10.1038/s41929-018-0083-8.
- (515) Li, S.; Sun, X.; Yao, Z.; Zhong, X.; Cao, Y.; Liang, Y.; Wei, Z.; Deng, S.; Zhuang, G.; Li, X.; et al. Biomass Valorization via Paired Electrosynthesis Over Vanadium Nitride-Based Electrocatalysts. *Adv. Funct. Mater.* **2019**, *29* (42), 1904780. https://doi.org/10.1002/adfm.201904780.
- (516) Gross, R.; Hanna, R.; Gambhir, A.; Heptonstall, P.; Speirs, J. How Long Does Innovation and Commercialisation in the Energy Sectors Take? Historical Case Studies of the Timescale from Invention to Widespread Commercialisation in Energy Supply and End Use Technology. *Energy Policy* **2018**, *123*, 682–699. https://doi.org/10.1016/j.enpol.2018.08.061.
- (517) Editors. Edenhofer, O.; Pichs-Madruga, R.; Sokona, Y.; Minx, J. C.; Farahani, E.; Kadner, S.; Seyboth, K.; Adler, A.; Baum, I.; Brunner, S.; et al. AR5 Climate Change 2014: Mitigation of Climate Change

- https://www.ipcc.ch/report/ar5/wg3/. Last accessed date was January 2020.
- (518) Diaz, L. A.; Lister, T. E.; Rae, C.; Wood, N. D. Anion Exchange Membrane Electrolyzers as Alternative for Upgrading of Biomass-Derived Molecules. *ACS Sustain. Chem. Eng.* **2018**, *6* (7), 8458–8467. https://doi.org/10.1021/acssuschemeng.8b00650.
- (519) Grim, G. Personal Communication with Some Researchers from This Field. 2020.
- (520) Yang, X.; Kirsch, J.; Fergus, J.; Simonian, A. Modeling Analysis of Electrode Fouling during Electrolysis of Phenolic Compounds. *Electrochim. Acta* **2013**, *94*, 259–268. https://doi.org/10.1016/j.electacta.2013.01.019.
- (521) Resasco, J.; Chen, L. D.; Clark, E.; Tsai, C.; Hahn, C.; Jaramillo, T. F.; Chan, K.; Bell, A. T. Promoter Effects of Alkali Metal Cations on the Electrochemical Reduction of Carbon Dioxide. *J. Am. Chem. Soc.* **2017**, *139* (32), 11277–11287. https://doi.org/10.1021/jacs.7b06765.

Highlight Quotes

Given the length and likely desire to distribute these evenly, we have listed 10 selections but marked our 'top 4' preferred with asterisks (**** "Quote" *****):

Top 4 Quotes:

***** "Electrochemistry poses a number of possible advantages for chemical conversion, and biomass valorization in particular. These include (i) amenability to operate directly on aqueous feedstocks, (ii) generation of oxidative or reducing equivalents without external (wasteful, possibly toxic) reagents, and (iii) operability near ambient conditions, which also facilitates (iv) smaller (possibly highly distributed) scale, intermittent processing with diminished reliance on heat recovery." Page 10 *****

***** "The challenges in drawing comparison on equal bases in some cases underscores the need for improved benchmarking and motivates the critical discussion on best practices, which need to become standardized in a manner similar to what has been established for simpler systems such as water electrolyzers or fuel cells." Page 12/13 *****

***** "First and foremost, review of the wide range of literature to date makes clear that the conditions under which measurements are recorded are in great need of standardization. Reactions are frequently reported without (i) closure of mass and energy balances, (ii) validation of measured reaction performance and interplay with electrostatic and transport phenomena at the cell-scale, and (iii) uniform rate definitions and reporting conventions."

Page 138/139 *****

***** "Considering the relative immaturity of electrochemical biomass conversion, there is a need to significantly accelerate the development and deployment timeline of these technologies if they are to play a meaningful role in the mitigation of global carbon emissions" Page 162 *****

A few more quotes, any of which could be added if the editors would like:

"In some cases, polymerization may even occur, and this can represent a particular challenge for sustained direct CT processes and heterogeneous catalysis. " Page 27

"Environmentally-friendly routes for the production of N-containing building blocks from protein-rich biomass wastes (which are often unsuitable for food/feed production due to poor nutritional quality, biologic contamination, toxicity, or legislative issues) are desirable." Page 64

"Overoxidation and repolymerization of monomers are some of the main problems found in lignin ECOD ... To overcome these issues, some authors have proposed methodologies to remove the low molecular weight depolymerization products from the reaction medium as soon as they are formed" Page 74

"Because of these challenges, the [computational] methods discussed here for enabling theoretical treatments of large, complex reaction networks have been generally applied to thermal heterogeneous catalysis and biomass conversion and have not yet been combined with explicit incorporation of electrochemical conditions." Page 105/106

Beyond the "apparent" mass and energy balances of reaction, many reaction pathways may involve a mixture of chemical and electrochemical steps, some of

which may even involve homogeneous oxidation/reduction (or disproportionation) such that assigning charge balances (Faradaic efficiency) may not be representative of solely Faradaic processes.

Page 141

"Best practices" are less defined (or more experiment-specific), but should be directed toward the ideal of full determination of elementary step reaction paths and the roles of local reaction environment, mediator, and/or electrode surface in promoting these reactions." Page 148